

This item was submitted to Loughborough's Institutional Repository (<https://dspace.lboro.ac.uk/>) by the author and is made available under the following Creative Commons Licence conditions.



For the full text of this licence, please go to:  
<http://creativecommons.org/licenses/by-nc-nd/2.5/>

# **AN EXPERIMENTAL STUDY OF LOW TEMPERATURE COMBUSTION IN A DIESEL ENGINE**

by

Shenghui Cong

B.Eng., Tianjin University 2001

M.Sc., Tianjin University 2005

A Doctoral Thesis

Submitted in partial fulfilment of the requirements

for the award of

Doctor of Philosophy of Loughborough University

December 2010

LOUGHBOROUGH UNIVERSITY

© Shenghui Cong 2010

## **Certificate of Originality**

This is to certify that I am responsible for the work submitted in this thesis, that the original work is my own except as specified in the acknowledgements or in footnotes, and that neither the thesis nor the original work contained therein has been submitted to this or any other institution for a higher degree.

.....(Signed)

.....(Date)

## Abstract

Increased efficiency and reduced emissions demands from users and legislative organisations have led to the development of advanced combustion technologies for diesel engines. Exhaust gas recirculation (EGR) is a widely used technology to control diesel combustion and emissions, primarily to reduce emissions of oxides of nitrogen (NO<sub>x</sub>). Implementation of high levels of EGR (> 50%) is able to simultaneously reduce both emissions of NO<sub>x</sub> and particulate matter (PM) to ultra low levels. However, high EGR combustion is subject to reduced combustion efficiency and stability with increased total hydrocarbon (THC) and carbon monoxide (CO) emissions. This thesis presents research into low temperature diesel combustion (LTC) operation and the effects on combustion and emissions when the engine is operated under air, fuel and EGR rates encountered during transitions between LTC and conventional diesel operation modes. This has resulted in an improved understanding of the diesel combustion process and pollutant emissions with high rates of EGR, different fuel injection pressures and timings, post fuel injection and exhaust back pressures. The sensitivity of LTC to variations in engine speed, fuel injection quantity, and EGR rate and intake manifold temperature were investigated. Pseudo-transient operation of the engine was studied to interpret the transient performance of a diesel engine during transients within LTC and from LTC to conventional diesel combustion in a new European driving-cycle (NEDC) test.

Experimental investigations were conducted on a single cylinder research diesel engine. Cylinder pressure, fuel consumption and gaseous and particulate emissions (filter smoke number, size distribution, and total number) were measured. The results showed that an increase in EGR rate can realise LTC on the research engine. Fuel injection parameters influenced the combustion phasing, and control of this was able to improve the combustion stability and to reduce the THC and CO emissions. The low smoke number for the LTC diesel combustion was a result of reduced mean particle size with possible changes in particulate composition. EGR is the most critical parameter influencing the LTC combustion and emissions. Transient simulation of an engine exhibits significant discrepancies in EGR rate and boost pressure. Pseudo-transient points at intermediate load condition showed significantly increased emissions, particularly smoke number. Retarded fuel injection timing and increased boost pressure were demonstrated to be an effective strategy to reduce smoke emissions for these pseudo-transient operating points.



## Acknowledgements

The work described in this thesis could not have been completed without the support of the exemplary colleagues with whom I was fortunate to work. First, I would like to thank my supervisors, Dr. Gordon McTaggart-Cowan and Professor Colin Garner, for their unending support, patience, and advice during my PhD study at Loughborough University. The development of both my technical proficiency and my abilities as an independent researcher is a direct result of their guidance and tutelage. I also want to extend special recognition to Adrian Broster, Steve Horner, Steve Taylor and Graham Smith for their technical support on the experimental system setup and operation. Special thanks also go to Edward Winward for his help conducting the engine experiments. His willingness to share his engine testing experiences and knowledge is greatly appreciated.

I also want to acknowledge Asish Sarangi and Antonis Michailids for the friendly research environment they have created. Their teamwork, collaboration and enthusiasm towards research have cheered me up whenever I have had difficulties in my study. I would like to thank Dr. Andy Williams and Alan Baker for their valuable advice on engine modelling. I also thank the graduate students who I have been honoured to work with, in particular, Jugraj Atwal, Aaron Snapes and James Shrubbs, for their valuable contributions to the setup of the experimental system. Special thanks go to Stephen Johnson for his help on proof reading of this thesis.

Special acknowledge goes to Dr. Emad Wahab, Andy Scarisbrick, Dr. Zulshan Mahmood and Tim Morris from Ford Motor Company for their valuable suggestions and guidance on the research. I would like to acknowledge Dr. Mark Peckham and Chris Nickolaus from Cambustion for their technical support and comprehensive advice on the emissions measurement equipment.

Finally, I want to thank my family, especially my parents, for their endless love and support during my pursuit of education. My brother and sister, they took most of the family responsibility and gave me unconditional support during my study.

## Nomenclature

°CA	=	Crank angle degree	
ANOVA	=	Analysis of variance	
ATDC	=	After top-dead-centre	
AGTDC	=	After gas exchange top dead centre	
BGTDC	=	Before gas exchange top dead centre	
CA5	=	5% total heat release point	°CA ATDC
CA50	=	Mid-point of integrated heat-release rate	°CA ATDC
CA90	=	90% total heat release point	°CA ATDC
CLD	=	Chemiluminescent detection	
CMD	=	Count median diameter	nm
CO	=	Carbon monoxide	
CO <sub>2</sub>	=	Carbon dioxide	
CoV	=	Coefficient of variation (standard deviation / mean)	%
DMS	=	Differential mobility analyzer	
DOC	=	Diesel oxidation catalyst	
DoE	=	Design of experiments	
DPF	=	Diesel particulate filter	
DurL	=	Duration of low temperature reactions	°CA
DurF	=	Duration of the 1 <sup>st</sup> half high temperature combustion	
DurP	=	Duration of the 2 <sup>nd</sup> half high temperature combustion	
EBP	=	Exhaust back pressure	Pa
ECE	=	Urban driving cycle	
EGR	=	Exhaust gas recirculation	%
EMS	=	Engine management system	
EUDC	=	Extra-urban driving cycle	
EVC	=	Exhaust valve close	°CA ATDC
EVO	=	Exhaust valve open	°CA ATDC
f	=	Degrees-of-freedom	
FID	=	Flame ionisation detection	
FSN	=	Filter smoke number	
HCCI	=	Homogeneous charge compression ignition	
HSDI	=	High speed direct injection	
HRR	=	Heat-release rate	J/°CA
ID	=	Ignition delay	°CA
IDL	=	Ignition delay of low temperature reaction	°CA
IMEP <sub>g</sub>	=	Gross indicated mean effective pressure	Pa
IHR	=	Integrated heat-release rate	J
ISF	=	Insoluble fraction	
IVC	=	Intake valve close	°CA ATDC
IVO	=	Intake valve open	°CA ATDC
LHV	=	Lower heating value	MJ/kg
LNT	=	Lean NO <sub>x</sub> trap	
LTC	=	Low temperature diesel combustion	
LTR	=	Low temperature reaction	J/°CA

MK	=	Modulated kinetics	
MPA	=	Magnetopneumatic condenser microphone detection	
NDIR	=	Non-dispersive infra-red	
NEDC	=	New European driving cycle	
NO <sub>x</sub>	=	Oxides of nitrogen (include NO, NO <sub>2</sub> )	
NTC	=	Negative temperature coefficient	
P	=	Percentage contribution	%
p	=	Pressure	Pa
PAH	=	Polycyclic aromatic hydrocarbon	
PCCI	=	Premixed charge compression ignition	
P <sub>inj</sub>	=	Fuel injection pressure	Pa
PID	=	Proportional–integral–derivative controller	
PLC	=	Programmable logic controller	
PM	=	Particulate matter	
PN	=	Particle number	
PPCI	=	Partial premixed compression ignition	
RGF	=	Residual gas fraction	%
SCR	=	Selective catalyst reduction	
SI	=	Spark ignition	
SoC	=	Start of combustion	°CA ATDC
SoCH	=	Start of high temperature combustion	°CA ATDC
SoCL	=	Start of low temperature combustion	°CA ATDC
SOF	=	Soluble organic fraction	
SoI	=	Start of fuel injection	°CA ATDC
T	=	Temperature	K
THC	=	Hydrocarbons (total)	
UNIBUS	=	Uniform bulky combustion system	
VGT	=	Variable geometry turbocharger	
VNT	=	Variable nozzle turbine	

## **Co-Authorship Statement**

The work presented in this thesis was conceived, conducted, and disseminated by the doctoral candidate. The co-authors of the manuscripts that comprise part of this thesis made contributions only as is commensurate with a thesis committee or as experts in a specific area as it pertains to the work. The co-authors provided direction and support. The co-authors reviewed each manuscript prior to submission for publication and offered critical evaluations; however, the candidate was responsible for the writing and the final content of these manuscripts.

# Table of Contents

<b>ABSTRACT</b> .....	<b>I</b>
<b>ACKNOWLEDGEMENTS</b> .....	<b>II</b>
<b>NOMENCLATURE</b> .....	<b>III</b>
<b>CO-AUTHORSHIP STATEMENT</b> .....	<b>V</b>
<b>TABLE OF CONTENTS</b> .....	<b>VI</b>
<b>LIST OF TABLES</b> .....	<b>X</b>
<b>LIST OF FIGURES</b> .....	<b>XII</b>
<b>CHAPTER 1 INTRODUCTION</b> .....	<b>- 1 -</b>
1.1 DIESEL ENGINE EMISSION LEGISLATIONS .....	- 2 -
1.2 CONVENTIONAL DIESEL AND LOW TEMPERATURE COMBUSTION.....	- 3 -
1.3 OBJECTIVES AND SCOPE.....	- 5 -
1.4 THESIS STRUCTURE .....	- 6 -
1.5 CONTRIBUTIONS TO THE BODY OF KNOWLEDGE.....	- 7 -
1.6 PUBLICATIONS ARISING FROM THIS RESEARCH.....	- 8 -
<b>CHAPTER 2 LITERATURE REVIEW</b> .....	<b>- 9 -</b>
2.1 DIESEL ENGINE EMISSIONS .....	- 9 -
2.1.1 <i>CO<sub>2</sub> emission and fuel consumption</i> .....	- 10 -
2.1.2 <i>NO<sub>x</sub> formation and reduction</i> .....	- 10 -
2.1.3 <i>Particulate matter (PM)</i> .....	- 12 -
2.1.4 <i>NO<sub>x</sub>-PM trade-off</i> .....	- 14 -
2.1.5 <i>THC and CO formation and control</i> .....	- 15 -
2.1.6 <i>Combustion noise</i> .....	- 16 -
2.2 DIESEL AFTERTREATMENT SYSTEMS .....	- 17 -
2.3 MODERN DIESEL ENGINE TECHNOLOGIES.....	- 19 -
2.3.1 <i>Advanced fuel injection systems</i> .....	- 20 -
2.3.2 <i>Turbocharging</i> .....	- 21 -
2.3.3 <i>Exhaust gas recirculation (EGR)</i> .....	- 22 -
2.4 LOW TEMPERATURE DIESEL COMBUSTION .....	- 24 -
2.4.1 <i>Low temperature combustion strategies</i> .....	- 26 -
2.4.2 <i>Technologies with LTC</i> .....	- 32 -
2.5 DIESEL ENGINE TRANSIENT OPERATION .....	- 32 -
2.5.1 <i>Dynamic behaviour of engine sub-systems during transients</i> .....	- 33 -
2.5.2 <i>Effects of engine thermal conditions during a transient</i> .....	- 34 -
2.5.3 <i>Transient combustion behaviour during LTC</i> .....	- 34 -
2.5.4 <i>Diesel engine combustion characteristics during mode shifts</i> .....	- 35 -
2.5.5 <i>Transient EGR control</i> .....	- 36 -

2.6 1D SIMULATION OF DIESEL TRANSIENT OPERATION .....	- 36 -
2.7 IDENTIFICATION OF KEY KNOWLEDGE GAPS .....	- 37 -
<b>CHAPTER 3 RESEARCH APPARATUS AND PROCEDURES .....</b>	<b>- 39 -</b>
3.1 TEST ENGINE SPECIFICATION.....	- 39 -
3.1.1 <i>Research engine systems</i> .....	- 41 -
3.1.2 <i>Instrumentation and data acquisition</i> .....	- 44 -
3.2 EMISSIONS MEASUREMENT SYSTEM .....	- 47 -
3.2.1 <i>Gaseous emissions measurement</i> .....	- 47 -
3.2.2 <i>Smoke/particulate measurement</i> .....	- 49 -
3.3 EXPERIMENTAL PARAMETERS.....	- 49 -
3.4 1D ENGINE SIMULATION .....	- 53 -
3.5 DESIGN OF EXPERIMENTS.....	- 55 -
3.5.1 <i>Operating conditions</i> .....	- 56 -
3.5.2 <i>Analysis of variance (ANOVA)</i> .....	- 56 -
<b>CHAPTER 4 HIGH EGR DIESEL COMBUSTION .....</b>	<b>- 59 -</b>
4.1 INTRODUCTION .....	- 59 -
4.2 EXPERIMENTAL METHODOLOGY .....	- 60 -
4.3 RESULTS .....	- 63 -
4.3.1 <i>EGR rate test</i> .....	- 63 -
4.3.2 <i>Particle number and size distribution</i> .....	- 72 -
4.3.3 <i>Effects of fuel injection parameters on LTC</i> .....	- 79 -
4.3.4 <i>Effects of post fuel injection</i> .....	- 90 -
4.4 DISCUSSION .....	- 95 -
4.5 CONCLUSIONS.....	- 98 -
<b>CHAPTER 5 LOW TEMPERATURE DIESEL COMBUSTION .....</b>	<b>- 100 -</b>
5.1 INTRODUCTION .....	- 100 -
5.2 LOW TEMPERATURE OXIDATION OF HYDROCARBONS .....	- 100 -
5.3 RESEARCH METHODOLOGY .....	- 102 -
5.4 RESULTS .....	- 105 -
5.4.1 <i>Effects of EGR rate</i> .....	- 105 -
5.4.2 <i>Intake charge temperature</i> .....	- 110 -
5.4.3 <i>Fuel injection pressure</i> .....	- 114 -
5.4.4 <i>Fuel injection timing</i> .....	- 118 -
5.5 DISCUSSION .....	- 121 -
5.6 CONCLUSIONS.....	- 122 -
<b>CHAPTER 6 EFFECTS OF EXHAUST BACK PRESSURE ON CONVENTIONAL AND LOW TEMPERATURE DIESEL COMBUSTION .....</b>	<b>- 126 -</b>
6.1 INTRODUCTION .....	- 126 -

6.2 RESEARCH METHODOLOGY .....	- 127 -
6.2.1 Measurement of RGF.....	- 127 -
6.2.2 Engine operating conditions.....	- 129 -
6.2.3 Engine modelling.....	- 131 -
6.3 RESULTS .....	- 131 -
6.3.1 Simulated RGF results.....	- 131 -
6.3.2 Conventional diesel combustion.....	- 132 -
6.3.3 Low temperature diesel combustion .....	- 135 -
6.3.4 Effective EGR .....	- 140 -
6.4 CONCLUSIONS.....	- 142 -
<b>CHAPTER 7 SENSITIVITY OF LTC TO ENGINE OPERATING PARAMETERS .....</b>	<b>- 144 -</b>
7.1 INTRODUCTION .....	- 144 -
7.2 DESIGN OF EXPERIMENTS AND ANOVA .....	- 145 -
7.2.1 Selection of the factors.....	- 145 -
7.2.2 Observations/responses .....	- 147 -
7.2.3 DoE methods .....	- 147 -
7.2.4 ANOVA.....	- 149 -
7.3 RESULTS .....	- 150 -
7.3.1 Fractional factorial test .....	- 150 -
7.3.2 Taguchi L9 test result.....	- 155 -
7.3.3 Taguchi method for different load and speed conditions.....	- 157 -
7.4 DISCUSSION .....	- 160 -
7.5 CONCLUSIONS.....	- 162 -
<b>CHAPTER 8 PSEUDO-TRANSIENT OPERATION OF AN LTC DIESEL ENGINE.....</b>	<b>- 164 -</b>
8.1 INTRODUCTION .....	- 164 -
8.2 RESEARCH METHODOLOGY .....	- 165 -
8.2.1 Engine modelling.....	- 168 -
8.2.2 Pseudo-transient operating points.....	- 169 -
8.2.3 Engine experiments .....	- 171 -
8.3 RESULTS .....	- 172 -
8.3.1 Transient within LTC.....	- 172 -
8.3.2 Transient during combustion mode shifting.....	- 176 -
8.3.3 Effects of fuel injection parameters on high-EGR pseudo-transient points.....	- 181 -
8.3.4 Effects of fuel injection parameters on low-EGR pseudo-transient point.....	- 187 -
8.4 DISCUSSION .....	- 191 -
8.5 CONCLUSIONS.....	- 194 -
<b>CHAPTER 9 CONCLUSIONS AND FURTHER WORK .....</b>	<b>- 197 -</b>
9.1 DISCUSSION OF OVERALL RESULTS .....	- 197 -

9.2 CONCLUSIONS.....	- 200 -
9.3 IMPLICATIONS FOR ENGINE DEVELOPERS.....	- 203 -
9.4 FURTHER WORK.....	- 205 -
9.5 CLOSING COMMENTS.....	- 206 -
<b>REFERENCES .....</b>	<b>- 207 -</b>
<b>APPENDICES .....</b>	<b>- 219 -</b>
APPENDIX A1 DESIGN OF INTAKE AND EXHAUST SURGE TANKS.....	- 219 -
APPENDIX A2 ENGINE INSTRUMENTATION .....	- 222 -
APPENDIX A3 EMISSIONS MEASUREMENT EQUIPMENT .....	- 223 -
APPENDIX A4 RESIDUAL GAS FRACTION MEASUREMENT AND PREDICTION.....	- 224 -



## List of Tables

Table 1.1 EU emission standards for diesel passenger cars (g/km).....	- 2 -
Table 3.1 Engine specifications .....	- 39 -
Table 3.2 Fuel injection equipment system specifications .....	- 40 -
Table 3.3 Example of ANOVA routine.....	- 57 -
Table 4.1 Operating conditions for EGR test.....	- 61 -
Table 4.2 Operating conditions for fuel injection parameters test.....	- 61 -
Table 4.3 Operating conditions for post fuel injection test.....	- 62 -
Table 5.1 Engine operating conditions.....	- 103 -
Table 6.1 Engine Operating Conditions (conventional diesel*).....	- 130 -
Table 6.2 Engine Operating Conditions (LTC) .....	- 130 -
Table 7.1 Factors investigated and the other engine operating parameters.....	- 146 -
Table 7.2 Aliasing in half fractional factorial design.....	- 148 -
Table 7.3 Half fractional factorial design ( $2 * 3 * 3 * 3$ ).....	- 148 -
Table 7.4 Taguchi $3^4$ L9 design.....	- 149 -
Table 7.5 Half fractional factorial test results (1500 rpm 8 mg/cycle) .....	- 150 -
Table 7.6 ANOVA table of fractional factorial test results on THC (1500 rpm 8 mg/cycle).....	- 151 -
Table 7.7 Summary of the ANOVA for the half fractional factorial test results on the observations (1500 rpm 8 mg/cycle case).....	- 152 -
Table 7.8 Taguchi L9 test results (1500 rpm 8 mg/cycle).....	- 155 -
Table 7.9 ANOVA table for Taguchi L9 test results on THC (1500 rpm 8 mg/cycle, non-pooled) .....	- 156 -
Table 7.10 ANOVA table for Taguchi L9 test results on THC (1500 rpm 8 mg/cycle, pooled) .....	- 156 -
Table 7.11 Summary of the ANOVA for the Taguchi L9 test results on the observations (1500 rpm 8 mg/cycle).....	- 157 -
Table 7.12 Summary of the ANOVA for the Taguchi L9 test results on the observations (2500 rpm 8 mg/cycle).....	- 158 -
Table 7.13 Summary of the ANOVA for the Taguchi L9 test results on the observations (1500 rpm 16 mg/cycle).....	- 159 -
Table 7.14 Summary of the ANOVA for the Taguchi L9 test results on the observations (2500 rpm 16 mg/cycle).....	- 159 -
Table 8.1 Representative transient routes .....	- 167 -
Table 8.2 Selected pseudo-transient points from load transient within LTC [1] ..	- 169 -

Table 8.3 Selected pseudo-transient points from load transient crossing combustion modes [3].....	- 170 -
Table 8.4 Selected pseudo-transient points from load transient crossing combustion modes [3] with high EGR rate for conventional diesel combustion .....	- 171 -
Table 8.5 Effects of fuel injection parameters over individual pseudo-transient operating point.....	- 172 -
Table A2.1 Engine instrumentation list.....	- 222 -
Table A3.1 Emissions measurement equipment specifications.....	- 223 -
Table A4. 1 Engine operating conditions .....	- 226 -

## List of Figures

Figure 2.1 Local fuel-air equivalence ratio, $\Phi$ , versus temperature showing contours of high soot and NO <sub>x</sub> formation regions.....	26 -
Figure 3.1 Combustion chamber piston bowl geometry.....	40 -
Figure 3.2 Schematic of gases flow in the research engine.....	41 -
Figure 3.3 Schematic of experimental system.....	43 -
Figure 3.4 1D single-cylinder research engine WAVE model.....	54 -
Figure 4.1 Effects of EGR rate on diesel engine emissions at 8 mg/cycle fuelling conditions.....	64 -
Figure 4.2 Effects of EGR rate on diesel engine emissions at 16 mg/cycle fuelling conditions.....	65 -
Figure 4.3 Effects of EGR rate on diesel engine combustion process at 8 mg/cycle fuelling conditions.....	67 -
Figure 4.4 Effects of EGR rate on diesel engine combustion process at 16 mg/cycle fuelling conditions.....	68 -
Figure 4.5 Effects of EGR rate on diesel engine combustion at 8 mg/cycle fuelling conditions.....	70 -
Figure 4.6 Effects of EGR rate on diesel engine combustion at 16 mg/cycle fuelling conditions.....	70 -
Figure 4.7 Effects of EGR rate on CoV(IMEP) and THC emissions...-	71 -
Figure 4.8 1500 rpm 8 mg/cycle particle size distribution with EGR sweep.....-	73 -
Figure 4.9 1500 rpm 16 mg/cycle particle size distribution with EGR sweep...-	74 -
Figure 4.10 2500 rpm 16 mg/cycle particle size distribution with EGR sweep.-	75 -
Figure 4.11 Total particle number and volume vs. filter smoke number...-	77 -
Figure 4.12 Particulate CMD vs. EGR rate for the three operating conditions.....-	78 -
Figure 4.13 Effects of Sol on 8 mg/cycle LTC heat release rate, needle lift (not to scale) also shown.....	80 -
Figure 4.14 Effects of fuel injection pressure on low load LTC heat release rate.-	81 -
Figure 4.15 Effects of fuel injection pressure and Sol on CoV(IMEP) and THC emissions (1500 rpm 8 mg/cycle).....	81 -
Figure 4.16 Effects of fuel injection pressure and Sol on CoV(IMEP) and THC emissions (2500 rpm 8 mg/cycle).....	82 -
Figure 4.17 Effects of combustion phasing (CA50) on CoV(IMEP) and THC emissions for 8 mg/cycle LTC conditions.....	83 -

Figure 4.18 Effects of combustion phasing (CA50) on indicated thermal efficiency for 8 mg/cycle LTC conditions.....	84 -
Figure 4.19 Effects of Sol on intermediate load (16 mg/cycle) LTC heat release rate and cylinder pressure.....	86 -
Figure 4.20 Details of cool flame reaction heat release of Figure 4.19.....	86 -
Figure 4.21 Effects of Sol on CoV(IMEP) and THC emissions for intermediate load LTC conditions.....	87 -
Figure 4.22 Effects of fuel injection pressure on intermediate load (16 mg/cycle) LTC heat release rate and cylinder pressure.....	87 -
Figure 4.23 Details of cool flame reaction heat release rate of Figure 4.22.....	88 -
Figure 4.24 Effects of fuel injection pressure on CoV(IMEP) and THC emissions for 16 mg/cycle load LTC.....	88 -
Figure 4.25 Effects of combustion phasing (CA50) on CoV(IMEP) and THC emissions for 16 mg/cycle LTC conditions.....	89 -
Figure 4.26 Effects of combustion phasing (CA50) on indicated thermal efficiency for 16 mg/cycle LTC conditions.....	90 -
Figure 4.27 Effects of post fuel injection quantity on emissions.....	91 -
Figure 4.28 Effects of post fuel injection quantity on emissions.....	92 -
Figure 4.29 Effects of post fuel injection quantity engine on thermal efficiency....	92 -
Figure 4.30 Effects of post fuel injection quantity on heat release rate.....	93 -
Figure 4.31 Effects of post fuel injection timing on emissions.....	94 -
Figure 4.32 Effects of post fuel injection timing on heat release rate.....	95 -
Figure 4.33 Local fuel-air equivalence ratio, $\Phi$ , versus temperature (T) showing contours of soot and NOx formation .....	96 -
Figure 5.1 Typical low temperature diesel combustion cylinder pressure and heat release curves.....	104 -
Figure 5.2 Effects of EGR rate on LTC heat release.....	106 -
Figure 5.3 Effects of EGR rate on LTC combustion phasing.....	108 -
Figure 5.4 Effects of EGR rate on LTC stability and emissions.....	109 -
Figure 5.5 Effects of intake manifold temperature on LTC heat release.....	111 -
Figure 5.6 Effects of intake manifold temperature on LTC combustion phasing.-	112 -
Figure 5.7 Effects of intake manifold temperature on LTC combustion stability and emissions.....	113 -
Figure 5.8 Effects of fuel injection pressure on LTC heat release.....	115 -
Figure 5.9 Effects of fuel injection pressure on LTC combustion phasing.....	116 -
Figure 5.10 Effects of fuel injection pressure on LTC combustion stability and emissions.....	117 -

Figure 5.11 Effects of Sol on LTC heat release.....	118 -
Figure 5.12 Effects of Sol on LTC combustion phasing.....	119 -
Figure 5.13 Effects of Sol on LTC combustion stability and emissions.....	120 -
Figure 6.1 Concept of the RGF measurement.....	128 -
Figure 6.2 CO <sub>2</sub> concentration and absolute exhaust manifold pressure measurement during a skip-firing event.....	129 -
Figure 6.3 Simulation results of RGF vs. EBP for conventional and LTC diesel combustion.....	132 -
Figure 6.4 Simulation results of equivalence ratio over RGF for conventional and LTC diesel combustion.....	132 -
Figure 6.5 Effects of EBP on conventional diesel combustion heat release rate.....	134 -
Figure 6.6 Effects of EBP on conventional diesel combustion emissions.....	135 -
Figure 6.7 Effects of EBP on LTC heat release rate.....	136 -
Figure 6.8 Effect of EBP on LTC combustion phasing.....	138 -
Figure 6.9 Effects of EBP on combustion stability represented by CoV of IMEP.....	139 -
Figure 6.10 Effects of EBP on LTC smoke and THC emissions.....	139 -
Figure 6.11 Effective EGR vs. external EGR on LTC emissions.....	141 -
Figure 7.1 Plots of the THC and CO emissions over the main factors and the interactive influence of EGR rate with other parameters.....	153 -
Figure 7.2 Plots of CA <sub>50</sub> and CoV(IMEP) over the main factors and the interactive influence of EGR rate with other parameters.....	154 -
Figure 7.3 Effects of intake oxygen concentration on LTC THC, CO emissions, and CA <sub>50</sub> and CoV(IMEP) (1500 rpm 8 mg/cycle, half fractional factorial test).....	162 -
Figure 8.1 NEDC driving-cycle vehicle speed profile.....	165 -
Figure 8.2 Engine fuel injection quantity and speed profile during a NEDC urban and extra urban driving-cycle test.....	166 -
Figure 8.3 Engine operating command parameters and performance for the pseudo-transient operating points during a load transient within LTC mode.....	173 -
Figure 8.4 Emissions and efficiency of the pseudo-transient operating points during a load transient within LTC mode.....	174 -
Figure 8.5 Effect of boost pressure on heat release rate for the pseudo-transient operating points of LTC transient.....	175 -
Figure 8.6 Engine operating parameters and performance for the pseudo-transient operating points during a load transient crossing combustion mode.....	177 -

Figure 8.7 Emissions and efficiency of the pseudo-transient operating points during a load transient crossing combustion mode.....- 178 -

Figure 8.8 Effect of boost pressure on engine emissions and performance for the pseudo-transient points during a combustion mode shifting transient.....- 180 -

Figure 8.9 Effect of boost pressure on heat release rate for the pseudo-transient points of combustion mode shifting transient.....- 180 -

Figure 8.10 Effect of Sol and boost pressure on the pseudo-transient point emissions.....- 182 -

Figure 8.11 Effect of Sol and boost pressure on the pseudo-transient point ignition delay and CA50.....- 182 -

Figure 8.12 Effect of Sol and boost pressure on the pseudo-transient point indicated thermal efficiency.....- 183 -

Figure 8.13 Effect of Sol and boost pressure on the pseudo-transient point heat release rate.....- 184 -

Figure 8.14 Effect of fuel injection pressure and boost pressure on the pseudo-transient point emissions .....- 185 -

Figure 8.15 Effect of fuel injection pressure and boost pressure on the pseudo-transient point ignition delay and CA50.....- 186 -

Figure 8.16 Effect of fuel injection pressure and boost pressure on the pseudo-transient point indicated thermal efficiency.....- 186 -

Figure 8.17 Effect of fuel injection pressure and boost pressure on the pseudo-transient point heat release rate.....- 187 -

Figure 8.18 Effect of Sol on the low EGR pseudo-transient point emissions.....- 188 -

Figure 8.19 Effect of Sol on the low EGR pseudo-transient point ignition delay and CA50.....- 188 -

Figure 8.20 Effect of Sol on the low EGR pseudo-transient point indicated thermal efficiency.....- 189 -

Figure 8.21 Effect of fuel injection pressure on the low EGR pseudo-transient point emissions.....- 190 -

Figure 8.22 Effect of fuel injection pressure on the low EGR pseudo-transient point ignition delay and CA50.....- 190 -

Figure 8.23 Effect of fuel injection pressure on the Low EGR pseudo-transient point indicated thermal efficiency.....- 190 -

Figure 8.24 Effect of Sol and fuel injection pressure on the low EGR pseudo-transient point heat release rate.....- 191 -

Figure 8.25 Local fuel-air equivalence ratio,  $\Phi$ , versus temperature (T) showing contours of soot and NOx formation .....- 193 -

Figure 9.1 Local fuel-air equivalence ratio,  $\Phi$ , versus temperature (T) showing contours of soot and NOx formation .....- 198 -

Figure A1.1 Simulation results of the effects of surge tanks size on the pressure pulsations in the intake and exhaust system.....- 220 -

Figure A1.2 Effects of surge tanks on the pressure pulsations in the intake and exhaust manifolds.....- 221 -

Figure A4.1 RGF measurement results without throttling in the exhaust system vs. exhaust back pressure.....- 227 -

Figure A4.2 Exhaust back pressure vs. throttle diameter.....- 228 -

Figure A4.3 RGF vs. exhaust back pressure.....- 229 -

Figure A4.4 Effect of exhaust throttling on intake manifold (top), in-cylinder (middle) and exhaust manifold (bottom) pressures (absolute) during the intake valve opening period at 3000 rpm, 6 bar IMEP.....- 230 -

Figure A4.5 Comparison of intake manifold pressure between engine model prediction and measurement at 3000 rpm 6 bar IMEP condition with 12 mm orifice diameter throttling in exhaust.....- 231 -

Figure A4.6 Comparison of RGFs between model predictions and measurement results at 3000 rpm cases.....- 232 -

Figure A4.7 Breakup of the sources of RGF for 3000 rpm 6 bar IMEP operating condition.....- 232 -

## Chapter 1 Introduction

The diesel engine is one of the most efficient types of internal combustion engine, offering good fuel economy and low carbon dioxide (CO<sub>2</sub>) emissions. Diesel engine powered cars account for more than half of total new car registrations in the European Union (EU) (ACEA, 2010). However, the diesel engine is also a source of particulate matter (PM) and nitrogen oxide (NO<sub>x</sub>) emissions, both of which are subject to legislative limits because of their adverse effects on the environment and human health. Traditional diesel engines release less unburned hydrocarbons (THC) and carbon monoxide (CO) than typical spark ignition engines due to their overall lean burn characteristics. A number of technologies have been proposed for the reduction of the PM and NO<sub>x</sub> emissions from diesel engines. Low temperature combustion (LTC) is especially promising because, when done correctly, emissions of NO<sub>x</sub> and PM are reduced to near-zero levels at the engine's exhaust port. As a result, expensive and complicated NO<sub>x</sub> and PM aftertreatment systems would not be required. However, LTC causes reduced combustion efficiency, leading to higher fuel consumption and increased greenhouse gas emissions, as well as significant increases in THC and CO concentrations in the exhaust gas compared to conventional diesel combustion (Ogawa *et al.*, 2007). To simultaneously reduce emissions of these species and improve the efficiency of a diesel engine operating with LTC under real-world conditions while maintaining near-zero NO<sub>x</sub> and PM emissions is a great technical challenge.

The power and speed demanded from automotive diesel engines varies rapidly during a driving-cycle, either for certification or in real-world use. Engine efficiency and emissions are generally inferior under transient operation compared to steady-state conditions (Black *et al.*, 2007; Galindo *et al.*, 2001; Wijetunge *et al.*, 1999). Since an engine in a vehicle runs primarily in transient conditions, the engine transient operation contributes significantly more to the total amount of emissions over a driving-cycle than the steady-state engine operation (Hagena *et al.*, 2006). Hence, new engine combustion technologies need to be evaluated in both steady-state and transient operating conditions, so that their full impact and potential can be established.

Many techniques that are used to reduce emissions are sensitive to transient operation. Exhaust gas recirculation (EGR), which is one of the main techniques used to control diesel combustion temperatures and heat release rates (Ladommatos



*et al.*, 1998a; Ladommatos *et al.*, 1998b; Ladommatos *et al.*, 2000), leads to increased complications in the combustion process and in the air-path dynamics (Langridge *et al.*, 2002). For example, the inertia of EGR gas flow can cause higher or lower concentrations of EGR than desired in the combustion chamber during transients. This fluctuation in EGR rate has a significant impact on the engine combustion and emissions (Hagena *et al.*, 2006; Payri *et al.*, 2010). It is reasonable to expect that diesel engine combustion with high EGR rates is more sensitive to transient operation.

This thesis presents research into LTC diesel operation and the effects on combustion and emissions when the engine is operated under air, fuel and EGR rates encountered during transitions between LTC and conventional diesel operation modes. Experimental work is conducted to improve understanding of the sensitivity of LTC diesel combustion to changes in operating conditions that could be encountered during in-vehicle engine operation, including during mode-shifts between LTC and conventional diesel combustion.

## 1.1 Diesel Engine Emission Legislations

Emission legislations for engines are becoming more stringent. Table 1.1 lists the trends of diesel passenger car emissions standards in Europe since 1992. Both NO<sub>x</sub> and PM permitted emissions are reduced in successive stages of legislation. For the current Euro V standard, diesel engine PM emissions face a mass reduction of 80% and NO<sub>x</sub> emissions face a reduction of 30% from the Euro IV standard. The test cycle has also been changed; more realistic driving-cycles have been adopted, which means more transient operations during the engine tests and more challenges for the engines to meet the required emission standards.

Table 1.1 EU emission standards for diesel passenger cars (g/km)

Tier	Introduction Date	CO	HC+NO <sub>x</sub>	NO <sub>x</sub>	PM	PN*
Euro I	1992.07	2.72	0.97	-	0.14	-
Euro II	1996.01	1.00	0.90	-	0.10	-
Euro III	2000.01	0.64	0.56	0.50	0.05	-
Euro IV	2005.01	0.50	0.30	0.25	0.025	-
Euro V	2009.09	0.50	0.23	0.18	0.005	-
Euro VI	2014.09	0.50	0.17	0.08	0.005	6.0*10 <sup>11</sup>

\* Particle number in #/km

Particle number has also attracted increasing attention. Even with low PM mass emissions, a very large number of nano-particles are still being released from the engines, which are considered by some to be harmful for the human health (Choe *et*

*al.*, 2008; Oberdorster *et al.*, 1994; Oberdorster *et al.*, 2002). A total particle number limit of  $6 \cdot 10^{11} \#/\text{km}$  has been introduced for the Euro VI legislation (EU, 2007).

## 1.2 Conventional Diesel and Low Temperature Combustion

There are three main combustion phases for a conventional diesel engine: ignition delay; premixed combustion; and mixing controlled combustion (Heywood, 1988). Ignition delay is the period between the start of fuel injection into the combustion chamber and the start of combustion. It is determined by the physical and chemical properties of the fuel and charge gas (comprising a mixture of air, EGR and residual burned gas) in the combustion chamber, such as fuel droplet break-up and atomization, air motion, air temperature, oxygen concentration, cylinder wall temperature and fuel properties. The combustion of the flammable fuel-air mixture formed during this period is the premixed combustion. In this stage, the combustion is fast and the heat release rate is high. After this stage, the remaining fuel that has not yet burned and the fuel subsequently injected will burn after a process of liquid fuel atomization, vaporization, mixing of fuel vapour with air, and pre-flame chemical reactions. It is primarily controlled by the fuel-air mixing process.

Hsu (2002) divides the mixing controlled combustion phase into a diffusion burning period and a post-burning period. The post-burning period starts by the end of the fuel injection. In this period, the reducing cylinder pressure in the expansion stroke results in a slower combustion rate. If the temperature in this stage is too low to support the oxidation of PM, THC and CO, these emissions will be emitted from the engine. The low temperature during this phase is also considered to be the main cause of bulk quenching (Han *et al.*, 2009; Mendez *et al.*, 2009).

EGR is often used as a method to reduce NO<sub>x</sub> emissions. It consists of introducing exhaust gas back into the combustion chamber and it has the effect of slowing reactions and reducing the combustion temperatures. Traditionally, EGR is used to reduce NO<sub>x</sub> emissions, although it normally also increases PM emissions. However, when increasing the EGR rate to very high levels (i.e. > 50%), a very significant reduction in both PM and NO<sub>x</sub> can be achieved simultaneously. Low combustion temperatures and long ignition delays are the main contributors to the reductions in these emissions (Bobba *et al.*, 2009; Yun *et al.*, 2008).

Local equivalence ratio and flame temperature are the main control variables to the engine-out PM and NO<sub>x</sub> emissions. Diesel combustion concepts, such as homogeneous charge compression ignition (HCCI), premixed charge compression

ignition (PCCI), and partial premixed compression ignition (PPCI) and low temperature combustion (LTC) have been studied by different researchers e.g. including (Aronsson *et al.*, 2009; Beatrice *et al.*, 2007b; Hasegawa *et al.*, 2003; Laguitton *et al.*, 2007; Ogawa *et al.*, 2007; Simescu *et al.*, 2003; Yao *et al.*, 2009) to achieve low NO<sub>x</sub> and PM emissions. LTC follows a broad approach similar as other of these combustion concepts listed above, i.e. to reduce the combustion temperatures through improved fuel-air mixing. The distinctive aspect of LTC, however, is that it employs conventional diesel combustion system with high levels of EGR, which reduces the combustion temperature to the soot formation temperature lower limit. Timing of the combustion process is controlled by the fuel injection event. Even for fuel-rich operating conditions, smoke formation can be suppressed very effectively by the low temperatures. Details of these combustion regimes will be discussed in Chapter 2.

LTC provides significant diesel engine emissions reduction at low and intermediate engine loads. This combustion regime effectively suppresses both the NO<sub>x</sub> and PM favoured formation conditions by keeping local temperatures below the levels required to form either NO<sub>x</sub> or PM. However, the low oxygen concentrations caused by high EGR rates restrict the fuel injection quantity permitted (Ogawa *et al.*, 2007), which in turn limits the engine load. To run the engine at LTC mode for low to medium engine loads and conventional diesel combustion for high load engine operation could be a strategy to meet both the future emissions regulations and the engine performance requirements (Wang, 2007). To successfully accomplish this strategy, the transition between LTC and conventional diesel combustion ('mode shifting') needs to be carefully managed. There is a current lack of fundamental understanding of the engine conditions that might be encountered during such a transition.

Engine transients, such as start-up and rapid changes in speeds and loads, are a very significant cause of pollutant emissions from direct injection diesel engines (Hagena *et al.*, 2006). The interactions between EGR and other sub-systems such as air-exchange and fuel injection systems during transients are complex. The deviations of fuel-air ratio and EGR rate from their equivalent steady-state operation conditions affect the combustion behaviour, influencing emissions, fuel consumption and performance (Hagena *et al.*, 2006; Wijetunge *et al.*, 1999). In particular, engines equipped with turbochargers typically suffer from an inherent "turbo-lag" effect as the engine speed and load are rapidly changed. Turbo-lag results in a relatively lower

level of trapped air charge in the cylinder for a transient operation from low to high load or speed conditions compared to their equivalent steady-state operation conditions. This effect is exacerbated in the presence of an EGR system, which adds an extra level of complexity to the response of the air-exchange process to engine transients. The mismatch of the fuel delivery and inducted air mass causes an overshoot of equivalence ratio (Galindo *et al.*, 2001; Hagen *et al.*, 2006). Due to the unsteady air exchange processes, the optimised EGR rate during transient operation is different from the steady-state conditions and is difficult to control. Hence, the cycle-by-cycle air-fuel-ratio and EGR rate changes cause a deterioration in engine emissions (Yokomura *et al.*, 2004).

### **1.3 Objectives and Scope**

The overall objective of the research reported in this thesis was to improve the understanding of diesel combustion and emissions behaviour during high EGR operating conditions in a high speed direct injection (HSDI) single cylinder research diesel engine. Specific interest was placed on the low temperature diesel combustion (LTC) characteristics expected during steady-state and transient operation. The research uses a single-cylinder research engine to investigate the following specific objectives:

- 1) to understand the engine combustion behaviour and emissions characteristics under LTC mode realised through introducing of high levels of EGR;
- 2) to improve the understanding of LTC, specifically to identify the distinctive features of LTC compared to conventional diesel combustion;
- 3) to investigate the LTC sensitivity to engine fuel injection strategies and air-path parameters. The key parameters being investigated are EGR rate, intake charge temperature, fuel injection quantity, fuel injection pressure and timing, exhaust back pressure and engine speed;
- 4) to investigate the diesel engine combustion behaviour during transient operation conditions within LTC mode identified by a 1D engine transient simulation model; and
- 5) to investigate diesel engine combustion behaviour during engine combustion mode shifting between LTC and conventional diesel combustion.

These objectives were expected to provide a better understanding of the diesel LTC behaviour and emissions, especially during transient operation conditions. From this

study, improved operation modes have been found to optimise the LTC process, with the goal of reducing the influence of the transients on the engine efficiency and emissions.

## **1.4 Thesis Structure**

The thesis is structured as follows: Chapter 1 has provided the background and motivations for the research. Chapter 2 gives a review of the modern diesel engine combustion and emissions control techniques, and the current state of the understanding of the diesel engine combustion and pollutant formation mechanisms. It reviews the techniques to achieve LTC with high rates of EGR, and diesel engine transient operation characteristics. In Chapter 3, the experimental system setup and engine 1D modelling are described.

Chapter 4 presents the implementation of LTC on the research engine by introduction of high rates of EGR. The influence of fuel injection parameters on LTC combustion and emissions are evaluated. The effects of EGR rate on particle size distribution and numbers are also introduced.

Chapter 5 explains some of the characteristics of LTC. The low temperature reactions and negative temperature coefficient (NTC) phenomena are observed with variations of engine operating parameters. Their correlation with the main combustion and emissions are also evaluated.

Chapter 6 discusses the influence of exhaust back pressure on LTC combustion. The residual gas fraction rise caused by increased exhaust back pressure lead to increased effective EGR rate and temperature. The influences of these factors on LTC combustion and emissions are investigated.

Chapter 7 introduces the LTC sensitivity to the small variations of the engine operating parameters, such as EGR rate, intake charge temperature, fuel injection quantity and engine speed. Design of experiments and statistical analysis of variables are implemented in the study to elucidate the sensitivity of LTC to the variations of these parameters.

Chapter 8 evaluates the engine combustion and emissions during simulated transient operating conditions with different engine combustion control strategies. The selected in-transient operating points are studied experimentally in detail to identify the potential transient control strategies which could reduce transient emissions and

improve transient performance for LTC engines. Fuel injection parameters and boost pressure are evaluated on the in-transient operating points in emissions and efficiency.

Finally, Chapter 9 summarizes the research, providing the main conclusions from the research and presents suggestions for future work.

## **1.5 Contributions to the Body of Knowledge**

The major contributions to knowledge resulting from this research are listed below:

1) EGR has been found to be the most critical control parameter for a stable LTC diesel combustion. Improvement in EGR rate control accuracy is essential for the practical implementation of LTC.

2) There is a linear relation between LTC combustion stability and combustion phasing, with more advanced combustion increasing combustion stability when there is no fuel impingement occurring.

3) Fuel injection timing has the most significant influence on LTC combustion and emissions. Fuel injection pressure shows marginal effects on LTC combustion. Post fuel injection was shown to have generally detrimental effects on LTC emissions.

4) EGR rate affects PM emissions in terms of filter smoke number (FSN), particle number (PN) and size distribution. An increase in EGR rate from zero to high level (i.e. for LTC, > ~50%) reduces the total PN per cycle. However, the lowest total PN is found at the intermediate EGR rate condition where the smoke number is at the peak. The count median diameter of the particle size distribution is increased for intermediate EGR rate conditions and is reduced in the LTC mode.

5) Exhaust back pressure increases the trapped residual gas fraction, increasing the 'effective' EGR rate; this has a discernable influence on LTC combustion and emissions which is similar, but not identical, to the effect of an equivalent increase in EGR.

6) Transient simulation of a diesel engine is used to identify the critical operating points which have significant influences on engine performance and emissions during a transient process. The chosen 'pseudo-transient points' are experimentally studied on the single-cylinder research engine running under steady-state condition.

7) Retarding the fuel injection timing effectively delays the combustion phasing. This is used to reduce smoke emissions for the pseudo-transient points which normally have high smoke emissions. An increase in boost pressure at the same time reduces the fuel consumption penalty caused by the late combustion.

8) The low temperature reactions and negative temperature coefficient (NTC) phases of the LTC process are influenced by the composition and temperature of the charge.

## **1.6 Publications Arising from this Research**

This research has led to the following publications:

S. Cong, G. P. McTaggart-Cowan and C. P. Garner, The Effects of Exhaust Back Pressure on Conventional and Low Temperature Diesel Combustion, IMechE part D: J. Automobile Engineering, accepted.

S. Cong, G. P. McTaggart-Cowan and C. P. Garner, Effects of Fuel Injection Parameters on Low Temperature Diesel Combustion Stability, SAE 2010-01-0611

S. Cong, G. P. McTaggart-Cowan and C. P. Garner, The Effects of Exhaust Back Pressure on Conventional and Low Temperature Diesel Combustion, Internal Combustion Engines: Performance, Fuel Economy and Emissions Conference, Institution of Mechanical Engineers, December 2009, London.

S. Cong, G. P. McTaggart-Cowan and C. P. Garner, Measurement of Residual Gas Fraction in a Single Cylinder HSDI Diesel Engine through Skip-firing, SAE 2009-01-1961.

## **Chapter 2 Literature Review**

Understanding pollutant formation mechanisms in diesel engines provides an opportunity for engine developers to control emissions by optimising the combustion process. In-cylinder conditions such as charge temperature, EGR rate and fuel-air distribution are critical parameters that substantially influence the combustion event. Therefore, knowledge of their influence on emissions is essential in minimising engine-out emissions. The engine operating parameters which most influence diesel combustion and their implementations for pollutant formation and consumption will be discussed in this chapter.

A number of advanced diesel engine technologies have been developed or are under development to help meet the future stringent emission legislations while satisfying the increasing demands for high performance and low fuel consumption. These technologies include sophisticated fuel injection systems and air exchange systems, which control the fuel mixing and charge composition and temperature during engine operation. These technologies can be used to optimise the combustion process, reducing both the fuel consumption and emissions. Exhaust gas after-treatment systems are effective on reducing tail-pipe emissions. However, for the more stringent future emission legislation, a significant reduction in engine-out emissions is of significant value since it helps reduce the demands on exhaust aftertreatment systems, and hence efficiency, cost, size and durability.

This chapter focuses on reviewing current and near-future technologies that aim to significantly reduce engine-out emissions from diesel engines, with a focus on LTC techniques. This chapter will also identify where there are gaps in the current state of knowledge relating to high-EGR diesel combustion in light duty diesel engines during both steady-state and transient operation.

### **2.1 Diesel Engine Emissions**

The regulated pollutants in the exhaust of internal combustion engines consist of oxides of nitrogen (mainly NO and NO<sub>2</sub>, commonly referred to as NO<sub>x</sub>), particulate matter (PM, mainly comprising solid carbon with absorbed hydrocarbon compounds), carbon monoxide (CO) and unburned hydrocarbons (THC). In addition, internal combustion engines are also a significant source of carbon dioxide (CO<sub>2</sub>) emissions, and hence are attracting increasing attention due to their contribution to global CO<sub>2</sub>



levels. Engine noise is another concern for diesel engines due to its effect on vehicle refinement and comfort.

### **2.1.1 CO<sub>2</sub> emission and fuel consumption**

CO<sub>2</sub> is a gas that has been identified by climate scientists as the main contributor to climate change (EU, 2006; IPCC, 2007). After power generation, road transport is the second biggest source of man-made greenhouse gas emissions in the EU. It contributes about one quarter of the EU's total man-made emissions of carbon dioxide (CO<sub>2</sub>), and it is one of the few sectors where emissions are still rising rapidly. As a result, the European Parliament has enacted legislation to require automotive manufacturers to meet fleet-average CO<sub>2</sub> emissions of 120 g/km by 2015 and 95 g/km by 2020 (EU, 2009).

Along with CO<sub>2</sub> emissions, the consumption of liquid hydrocarbons for transportation applications is also increasing. Since the fossil fuel (from which most diesel fuel is made) is a finite resource whose amount and stability of supply is unknown, there is a need for ever-increasing efficiency. Therefore, the reduction in fuel consumption of engines is an important fundamental goal as directly helping with reduced greenhouse gases.

The diesel engine has a lower fuel consumption and hence lower CO<sub>2</sub> emissions than a similar power gasoline engine due to its higher compression ratio and throttle-less design. Any improvement in engine efficiency will lead to a reduction in CO<sub>2</sub> emissions and fuel consumption. However, in general, steps that improve engine efficiency will tend to increase emissions; as a result, meeting both CO<sub>2</sub> and air pollutant emissions standards at the same time poses a significant challenge.

### **2.1.2 NO<sub>x</sub> formation and reduction**

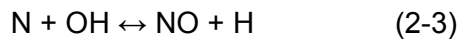
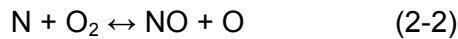
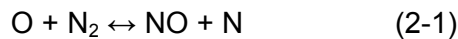
NO<sub>x</sub> is one of the principal pollutants emitted by combustion processes (Kuo, 2005). They damage human health and the environment severely (APIS, 2010); thus, government agencies are passing stringent laws to control the emissions of these pollutants. Understanding the NO<sub>x</sub> formation mechanism is essential when developing combustion strategies to control the amount of NO<sub>x</sub> generated from combustion.

The formation of NO<sub>x</sub> is a complex process that involves many elementary chemical reactions. The primary pollutant, directly emitted, is nitric oxide (NO), together with a small proportion of nitrogen dioxide (NO<sub>2</sub>). NO is oxidised by ozone in the atmosphere, on a time scale of tens of minutes, to give NO<sub>2</sub>. In rural air, away from sources of NO, most of the nitrogen oxides in the atmosphere are in the form of NO<sub>2</sub>. The major NO<sub>x</sub> formation routes in internal combustion engines are categorized below (Kuo, 2005):

- 1) Thermal NO route, also known as the Zel'dovich mechanism;
- 2) Prompt NO route, also known as the Fenimore NO mechanism;
- 3) Fuel-bound nitrogen route.

### **Thermal NO mechanism (Zel'dovich mechanism)**

In a diesel engine, NO<sub>x</sub> formation is driven primarily by the oxidation of atmospheric nitrogen via the extended Zel'dovich mechanism (Heywood, 1988):



This NO formation mechanism is highly temperature dependent due to the large activation energies required to generate free N atoms (i.e. to break the triple bond of N<sub>2</sub>, the dissociation energy is 946 kJ/mol). The reaction rates become high when temperatures exceed 1900 K and the NO remains during cooling since the reverse reaction rate is very slow.

The main controlling factors for the thermal NO formation are: the temperature of the mixture; the concentration of oxygen; and the time in the high temperature environment. These factors are reached in the post flame zones in the combustion chamber. Thus, NO formation in the post flame gases is almost always dominant (Heywood, 1988; Kitamura *et al.*, 2005). A combustion process with the post flame gases fuel-air equivalence ratio near unit (~0.8-1.0) has the highest temperature and the peak initial NO formation rate (Dec, 1997; Kuo, 2005).

### **Prompt NO mechanism (Fenimore mechanism)**

Fenimore (Kuo, 2005) discovered that some NO was promptly produced in the flame zone of laminar premixed flames long before there would be time to form NO by the

thermal mechanism. Prompt NO in hydrocarbon flames is formed primarily by a reaction sequence that is indicated by the rapid reaction of hydrocarbon radicals (i.e. CH, CH<sub>2</sub>, C<sub>2</sub>, C<sub>2</sub>H, C) with molecular nitrogen, leading to formation of amines or hydrocyanic acid (HCN) that subsequently reacts to form NO. Therefore, the prompt NO mechanism is of significant importance with hydrocarbon fuels when the thermal mechanism is greatly reduced, especially under fuel rich conditions where temperatures are so low that the first step of the thermal mechanism does not occur.

At low temperatures (i.e.  $T < 2000\text{K}$ ), and with rich ( $\Phi > 1.0$ ) mixtures, the prompt NO mechanism dominates the rate of NO formation (Kuo, 2005). Under this low temperature condition, the thermal NO formation rate is insignificant. A diesel engine operating in LTC mode features a low combustion temperature and a lower overall air-fuel-ratio. Both these effects tend to favour prompt NO formation as the dominant mechanism; thus, in this combustion regime the prompt NO needs to be taken into consideration for LTC emissions analysis.

### **NO production from fuel-bound nitrogen**

Fuel-bound nitrogen is another potential source of NO during combustion (Kuo, 2005). The conversion of fuel-bound nitrogen into NO is strongly dependent on the local combustion environment (e.g. temperature and fuel-air ratio) and on the initial level of nitrogen compounds in the fuel-air mixture. The fuel nitrogen reaction is initiated by a rapid conversion of the fuel nitrogen compounds to hydrogen cyanide (HCN) and ammonia (NH<sub>3</sub>). The oxidation of HCN and NH<sub>3</sub> into NO is favoured by fuel-rich conditions. However, the fuel bound NO formation in typical diesel engines is insignificant since standard diesel fuel contains only very small quantities of nitrogen. The NO<sub>x</sub> recycled from the previous cycle through EGR system may play another role on the engine out emissions. However, in a steady-stage operating condition, this part of NO<sub>x</sub> will not be emitted.

### **2.1.3 Particulate matter (PM)**

The PM emitted from a conventional diesel engine is a combination of an insoluble fraction (ISF) and a soluble organic fraction (SOF). Carbonaceous particles (soot) are the main component in ISF; it typically consists of approximately eight carbon atoms per hydrogen atom (Xi *et al.*, 2006). The fraction of soot in PM emissions from diesel

engines vary, but is typically higher than 50% (Tan *et al.*, 2004; Tree *et al.*, 2007), even with the most modern (advanced) engine systems.

The soot formation processes include five commonly identified steps: pyrolysis; nucleation; coalescence; surface growth; and coagulation and agglomeration (Smith, 1981; Tree *et al.*, 2007). The decomposition and atomic rearrangement of a fuel molecule into smaller hydrocarbon molecules occurs primarily in a region with both a shortage of oxygen and relatively high temperatures ( $> 750\text{K}$ ) (Aizawa *et al.*, 2008). In this region, the fuel molecules begin to decompose and form cyclic PAHs. Then, with increased temperature, the radical additions of small hydrocarbons to larger aromatic molecules occur. This nucleation process is heavily dependent on the abstraction of hydrogen atoms from the precursors. Since the abstraction of hydrogen atoms is an endothermic reaction, the nucleation process is temperature dependent ( $1300\text{K} - 1600\text{K}$ ) (Tree *et al.*, 2007). Surface growth is the process of adding mass to the surface of a nucleated soot particle. During surface growth, the hot reactive surface of the soot particles accepts gas-phase hydrocarbons. This leads to an increase in soot mass, while the number of particles remains constant (Kitamura *et al.*, 2002). Coagulation and agglomeration are processes for particle combination. During coagulation, two roughly spherically shaped particles combine to form a single spherically shaped particle. Agglomeration occurs when individual particles stick together to form groups of particles. The primary particles retain their original shapes during this process (Tree *et al.*, 2007).

Soot oxidation which leads to the consumption of previously formed particles and precursors, can take place at any time when both soot and oxidising species are present at temperatures above  $1300\text{K}$  (Dec, 1997). Temperature, pressure and local equivalence ratio have fundamental effects on the soot formation and oxidation rates. High temperature enhances both soot formation and oxidation. It is found that soot oxidation will cease when the temperature falls below  $1300\text{K}$  and the soot formation favoured temperature is over  $1500\text{K}$  (Tree *et al.*, 2007). Combustion with a high local equivalence ratio at high temperatures favours every stage of soot formation; it is the main contributor for soot formation in a diesel engine. High pressure is another accelerator for the soot formation. An increase in combustion pressure ( $p$ ) increases soot formation at a rate which could be as high as proportional to  $p^2$  (Tree *et al.*, 2007).

In conventional diesel combustion, both the soot formation and oxidation during combustion process are substantial. The engine-out soot emissions are a result of

combination of these two reactions (Bockhorn *et al.*, 2002). Enhanced fuel mixing can significantly reduce the fuel-air equivalence ratio and reduce the soot formation rate. A longer ignition delay and a higher intensity of premixed combustion can both reduce the local fuel-air equivalence ratios, leading to lower soot formation rate (Crua *et al.*, 2003; Tree *et al.*, 2007). Temperature has a complex effect on soot formation and oxidation and is dependent on fuel-air equivalence ratio. Higher charge temperatures and sufficient oxidizers in the later part of the combustion process can improve the soot oxidation and significantly reduce the engine-out soot emissions (Tree *et al.*, 2007). However, combustion under these conditions leads to significantly increased post-flame thermal NO formation as describe in Section 2.1.2. A reduction in combustion temperatures to below the soot formation temperature thresholds at specific fuel-air equivalence ratios can reduce the soot formed and reduce the soot oxidation demands to lower engine-out soot emissions.

#### **2.1.4 NO<sub>x</sub>-PM trade-off**

According to the mechanisms of NO<sub>x</sub> and PM formation, technologies which can reduce NO<sub>x</sub> emissions usually have negative effects on PM emissions, and *vice versa*. Decreased combustion temperatures with, for example, EGR or retarded fuel injection can effectively reduce NO<sub>x</sub> formation. However, the lower combustion temperatures in the later part of the combustion process result in slow PM oxidation reactions and the slower combustion process reduces the time for oxidising the PM. By advancing the fuel injection timing, the PM can be reduced due to increased premixed combustion and longer oxidation duration in the cycle (Lee *et al.*, 2004). Increased fuel injection pressure is an effective method to reduce the PM formation due to the enhanced fuel-air mixing and reduced local equivalence ratios. However, fast premixed combustion and accelerated overall combustion processes result in higher overall combustion temperatures and increased NO<sub>x</sub> formation (Fang *et al.*, 2010; Fischer *et al.*, 2009).

To reduce PM and NO<sub>x</sub> emissions simultaneously, different methods can to be considered. One of the options is to manage very lean and homogeneous fuel-air mixture combustion (e.g. homogeneous charge compressions ignition, HCCI); or to restrict the combustion temperature below the threshold, which is favoured by soot and NO<sub>x</sub> formation (e.g. low temperature combustion, LTC) (Neely *et al.*, 2005). Another way is to use separate techniques to control the two emissions. For example, an intermediate temperature combustion process could effectively

suppress NO formation. Techniques to reduce PM without significantly impacting NO<sub>x</sub> could include improving fuel-air mixing (i.e. high swirl ratio) (Henein *et al.*, 2006) to reduce PM formation or increasing the turbulence of the combustion during later stage of the combustion process (i.e. post fuel injection) (Bobba *et al.*, 2010; Chen, 2000; Yun *et al.*, 2005a) to enhance the PM oxidation can all reduce the engine-out PM emissions.

### **2.1.5 THC and CO formation and control**

Total hydrocarbons (THC) are the consequence of local flame extinction of the hydrocarbon fuel combustion. THC are composed of either volatile components of diesel fuel which have not participated in the combustion or hydrocarbons which are formed during combustion but which are not completely converted into carbon or hydrogen oxides. Formation of THC are mainly due to two main effects: flame extinction by strain; and flame extinction at walls and crevices (Warnatz *et al.*, 1999). Bulk and wall flame quenching are the sources of THC emissions in a diesel combustion process. Improper fuel-air mixing reinforces the quenching effects and leads to increased THC emissions. Over-mixing causes leaner mixture than the flammable fuel-air mixture. This leads to termination of flame propagation in the zone. Local under-mixing of fuel results in an over-rich mixture during the combustion period, which leads to an oxygen deficit combustion and formation of THC (Heywood, 1988; Mendez *et al.*, 2009).

Like THCs, emissions of carbon monoxide (CO) are primarily a result of incomplete combustion. CO is almost exclusively generated by oxygen-deficient combustion of hydrocarbons. CO emissions from internal combustion engines are controlled primarily by the fuel-air equivalence ratio (Heywood, 1988). Typical diesel engines have insignificant CO emissions due to their overall lean combustion. However, at locally rich regions in the combustion chamber, CO formation can occur since there is insufficient oxygen to oxidise it. For some new combustion concepts such as high EGR diesel combustion, the oxygen-fuel ratio is sometimes too low to achieve complete combustion, and hence CO emissions become substantial.

THC and CO are intermediate products of diesel engine combustion, and, given a high enough in-cylinder temperature and oxygen concentration and sufficient mixing, most of these species should be oxidised before they are emitted from the engine. As a result, they are not a significant concern for traditional diesel engine combustion. However, combustion strategies that reduce the in-cylinder temperature or

equivalence ratio, for example HCCI or LTC, may not be able to fully oxidise all these species.

For the high EGR operation of diesel engines, a significant quantity of THC is formed due to bulk quenching and wall quenching (Mendez *et al.*, 2009). High intake charge dilution (high rate of EGR) leads to reduced oxygen-fuel ratios and lower combustion temperatures. These increase bulk quenching and result in high rates of combustion by-product emissions. In high-EGR combustion, fuel injection timing is normally advanced to increase the fuel mixing time and maintain the combustion phasing for high EGR operation of diesel engines. However, this earlier injection leads to greater fuel jet penetration, resulting in fuel vapour approaching the walls of the combustion chamber. The cooling due to the proximity of the walls may be sufficient to quench the combustion reactions before completion. Lower global in-cylinder temperatures will exacerbate this effect and will also make it more difficult for these species to be oxidised later in the combustion process. Incomplete combustion of the fuel-air mixture trapped in the crevice volume is also one of the sources of THC and CO (Ekoto *et al.*, 2009; Heywood, 1988).

The fuel in the sac volume of injector nozzle is another potential source of partially oxidised fuels (Koci *et al.*, 2009). Oxidation of this sac fuel is low during combustion and it leaves the sac in the later part of the combustion process in the expansion stroke. The low oxygen concentration and reducing temperature under high EGR rate operating conditions make it even more difficult for the oxidation of any fuel vapour emitted from the nozzle sac (Ekoto *et al.*, 2009; Mendez *et al.*, 2009).

### **2.1.6 Combustion noise**

Diesel engines have higher combustion noise compared to equivalent spark ignited (SI) engines due to their higher compression ratio and rapid initial combustion processes. It is one of the concerns for the application of direct injection diesel engine on vehicles because of its impact on vehicle refinement (Costa *et al.*, 2009). Diesel combustion noise is generally caused by the initial rapid combustion of premixed fuel-air mixture in the cylinder. This large pressure gradient results in the so-called “diesel knock”, which is a very strong excitation source that forces the in-cylinder charge to oscillate. In addition, the maximum cylinder pressure rise rate is the constraint parameter for diesel engine operation (Beatrice *et al.*, 2007a; Yun *et al.*, 2008).

The intensity of the premixed combustion has a dominant effect on both the cylinder peak pressure and the pressure rise rate. As mentioned in Chapter 1, the ignition delay influences the premixed combustion stage by affecting the availability of flammable fuel-air mixture (Heywood, 1988; Hsu, 2002). Longer ignition delays often result in a higher premixed combustion rate due to the longer time available for fuel and air to mix to a combustible stoichiometry. Technologies such as pilot fuel injection and retarded fuel injection are effective in reducing the ignition delay and promoting smoother overall combustion processes (Badami *et al.*, 2003).

## **2.2 Diesel Aftertreatment Systems**

Most diesel engine manufactures recognise that in-cylinder combustion control will not ensure that their engines meet the stringent new emissions regulations. As a result, it has become necessary to employ aftertreatment equipment to remove pollutants from the exhaust stream. These techniques have focused on reducing emissions of PM, NO<sub>x</sub>, THC and CO.

### **Diesel particulate filter (DPF)**

The DPF is a device designed to remove the carbonaceous component of PM from the exhaust gas of a diesel engine. These filters have a cellular structure where the exhaust gases flow through the pores of the cell walls. Soot particles are too large to flow through the pores, and they are trapped on the ceramic walls. Periodically the filter is regenerated to consume (oxidise) the soot into CO<sub>2</sub> and clean the filter. It can remove up to 98% per cent of the particles by mass in the exhaust gas (Williams *et al.*, 2008). However, the loading of PM within the DPF increases the exhaust back pressure (a  $\Delta p$  from 5 kPa to 60 kPa depends on soot load and exhaust flow rate) (Boger *et al.*, 2008) which leads to increased pumping work for the engine.

Complex regeneration strategies are needed for removing the particles filtered by the DPF. Most current DPFs use 'active' regeneration techniques that force the DPF into a regime where the collected soot is oxidized. Exhaust manifold fuel injection, post fuel injection and retarded fuel injection are used to increase the exhaust temperature and to introduce reactive oxidizers (e.g. NO<sub>2</sub>) for promoting trapped PM oxidation within the DPF (Florchinger *et al.*, 2004; Gardner *et al.*, 2009; Zhan *et al.*, 2006). 'Passive' regeneration, which can be achieved without needing to adjust the combustion process, is promising but tends to be limited to lower PM loadings. It also normally requires more expensive catalyst loads and specific vehicle duty cycles.



New techniques that are under development would use external energy resources, such as electric-discharge generated plasmas or microwave energy resources, to regenerate the DPF without interacting with the diesel combustion processes (Williams *et al.*, 2009). While these technologies are attracting more interests due to their flexibility in DPF regeneration control, they are not currently commercially available. Johnson Matthey Company has introduced catalysed DPF systems, which can reduce PM by over 85% and THC and CO by over 90% passively.

### **Diesel oxidation catalysts (DOCs)**

In the exhaust streams, the THC and CO emissions can be removed by catalysed oxidations through a DOC. On the catalyst bed, the emissions react with oxygen in the exhaust and produce CO<sub>2</sub> and water. More specifically, a regular DOC can reduce the PM by up to 30%, hydrocarbon based soluble organic fraction (SOF) by around 70%, and THC and CO by over 80% content of diesel exhaust by simple oxidation. However, during converting the THC and CO, NO<sub>2</sub> is formed as a by-product (Johnson, 2008; MECA, 2001). Also, the DOC is an important tool in preparing the exhaust stream to have the 'right' composition and temperature before entering the DPF. For example, the NO<sub>2</sub> formed in the DOC can react with the soot trapped in the DPF and produce NO and CO<sub>2</sub>. Hence, most DPFs are built in combination with a DOC upstream.

One of the main challenges for DOCs is that a reasonable exhaust temperature (typically 200-250°C) (Han *et al.*, 2008) is needed for the catalyst to light off to get an acceptable THC and CO conversion rate. For techniques such as low temperature diesel combustion, low exhaust temperatures may introduce difficulty in the implementation of DOC systems. New DOC systems are under development to cope with the lower diesel exhaust gas temperatures as low as 150°C (Holroyd, 2008; Johnson, 2009; Johnson, 2010).

### **Lean NOx trap (LNT)**

An LNT stores NO<sub>x</sub> under lean conditions and reduces it under rich conditions using precious metals such as Barium and Platinum plated on the surface of the substrate. It uses CO and THC as reductants to convert the NO<sub>x</sub> into N<sub>2</sub>, CO<sub>2</sub> and water during fuel-rich operation. It has a deNO<sub>x</sub> efficiency of up to 70-80%. The trapping capacity depends on the deactivation level of the device and the operating point of the engine. LNT operation and durability is subject to catalyst deactivations due to the high

exhaust temperature and sulphur content in the fuel (Theis *et al.*, 2010; Xu *et al.*, 2008).

### **Selective catalytic reduction (SCR)**

Selective catalytic reduction (SCR) systems use a wash-coated or homogeneous extruded catalyst and a chemical reagent to convert NO<sub>x</sub> to molecular nitrogen and oxygen in the exhaust stream (Muench *et al.*, 2008; Tao *et al.*, 2004). In mobile source applications, an aqueous urea solution is usually the preferred reductant (Tennison *et al.*, 2004). The SCR system can reduce NO<sub>x</sub> emissions by 75 to 90%, (Johnson, 2009; MECA, 2001). Estimation of NO<sub>x</sub> concentration in the exhaust gas, precise control of urea injection to ensure that there is just enough NH<sub>3</sub> to reduce the NO<sub>x</sub> and good distribution within the catalyst are the main challenges for the application of SCR technology.

## **2.3 Modern Diesel Engine Technologies**

To take advantage of diesel engines' high efficiency and to simultaneously reduce its drawbacks, technologies have been developed to achieve cleaner and more efficient diesel combustion strategies. For example, fuel injection systems have been improved significantly from the traditional in-line pump-pipe-injector systems to electrically controlled systems such as common rail fuel injection systems and electric unit injector systems. Complete flexibility in fuel injection pressure, timing, and rate control at varying operating conditions permits optimization of the diesel engine combustion control for higher efficiency and lower emissions. To enhance the air-exchange process, variable geometry turbochargers (VGT) and variable nozzle turbines (VNT) have been developed to optimize boost pressures over the engine load-speed map. These technologies allow better control over fuel-air ratios over a wider range of engine operating conditions than traditional fixed geometry turbochargers could achieve. Electrically controlled EGR systems have also been developed to control the diesel engine combustion process and to reduce the combustion temperature. With improved EGR rate and temperature control accuracy, these systems can reduce NO<sub>x</sub> emissions while retaining a robust combustion process.

### 2.3.1 Advanced fuel injection systems

High pressure fuel injection and multiple-injection are the main features of the advanced fuel injection systems such as common rail systems and electric unit injectors. High-pressure fuel injection has been investigated and recognized as an essential tool for lowering emissions, especially PM. Multiple-injection with high pressure has been attempted to further reduce NO<sub>x</sub> and PM. These flexible fuel injection systems improve the fuel-air mixing and generate more uniform fuel distribution and controllable ignition delay. These features are effective for reducing the engine fuel consumption and emissions (Park *et al.*, 2004). It is also one of the important enablers for new combustion systems such as HCCI and LTC, since these combustion systems need more flexible fuel injection strategies to control the combustion processes.

High pressure fuel injection forms finer droplets and produces locally leaner mixtures (Minami *et al.*, 1990). It improves the fuel-air mixing in the combustion chamber, which reduces the local fuel rich zones and hence PM formation rates. For global high fuel-air ratio combustion, the high-pressure injection enables better air utilization and thus improved combustion efficiency. It also increases the injection rate and reduces combustion duration which permits more retarded injection timing for a given combustion phasing. This lowers peak cylinder pressures and NO<sub>x</sub> emissions without a significant loss in engine thermal efficiency (Bauer *et al.*, 2007). It can also shift the NO<sub>x</sub>-PM trade-off towards lower PM; however, in general injection pressure does not 'break' the inherent trade-off relation (Hountalas *et al.*, 2003; Morgan *et al.*, 2003; Woods *et al.*, 2000).

Multiple-injection strategies, where the injector is opened and closed more than once during the cycle, offer many potential benefits for diesel engine combustion. Bauer *et al.* (2007) suggested a range of multiple injection strategies across the engine operating map. The split injections can be controlled separately both on timing and injection quantity to control engine combustion processes for high efficiency and low emissions (Ehleskog *et al.*, 2007). However, the injection event usually imparts pressure fluctuations in the high pressure fuel pipe upstream of the injector. These pressure pulsations influence the subsequent fuel injection events substantially (Michailidis *et al.*, 2010).

Pilot fuel injection has a significant effect on the reduction of combustion noise (Badami *et al.*, 2003). It reduces the ignition delay of the main injection, which affects

engine performance and emissions strongly at some operating conditions (Carlucci *et al.*, 2003). The reduced ignition delay produces a low intensity of premixed diesel combustion and thus a lower pressure rise rate and lower peak cylinder pressure. However, pilot injection itself has a negative effect on PM emissions, since it reduces the ignition delay for the main fuel injection and leads to more locally fuel-rich combustion points in the main combustion event (Eastwood *et al.*, 2007; Zhang, 1999).

Another form of multiple-injection is post injection, where a small volume of fuel is injected into the cylinder late in the combustion, creating extra turbulence and flow energy. With the improved late-cycle mixing and combustion of this volume of fuel, the combustion in the after burn period (Hsu, 2002) is improved. Also, PM oxidation is enhanced without increasing NO<sub>x</sub> emissions since NO<sub>x</sub> formation mainly occurs earlier in the combustion at higher temperatures (Desantes *et al.*, 2007; Park *et al.*, 2004). Research has shown that the timing of the post injection has a more significant influence on PM reduction than the mass of fuel injection (Yun *et al.*, 2007). However, the optimisation for the number of injections, relative injection timing and relative injection quantities increase the complexity and cost for the application of multiple fuel injection strategies. The multiple fuel injection strategies could increase the injector wear as well.

### **2.3.2 Turbocharging**

The principal objective of a diesel turbocharger system is to increase the engine power density. The turbocharger increases the mass of air in the cylinder and consequently allows more fuel to be burned at a given fuel-air equivalence ratio. The main motivations for engine turbocharging (Taylor, 1985) include:

- 1) Increasing the maximum power/torque output of a given engine;
- 2) Maintaining sea-level power at higher altitudes;
- 3) Reducing the size of an engine required for a given duty; and
- 4) Improving fuel economy for engines used mostly at or near full load.

When a basic turbocharger with a fixed geometry is used to provide boost for an engine, a compromise must be made between maximum power and a suitable shaped torque-speed curve. For example, if a turbocharger is matched with a four stroke automotive engine to get higher torque at low engine speed, the turbocharger would likely over-speed at higher engine speeds at high load. To avoid this risk, an

exhaust waste gate can be used to by-pass some of the exhaust gas around the turbocharger turbine at high speeds, thus reducing turbine speed and also avoiding excessive intake manifold pressure (over-boost). A drawback of the waste-gate is that the by-passed gas reduces the enthalpy extracted from the exhaust stream, and hence the overall efficiency of the turbocharger at high speeds. The use of a variable geometry turbocharger removes this inherent compromise by providing a wider range of control (Hiereth *et al.*, 2006; Watson *et al.*, 1984). The exhaust back pressure caused by the turbocharger can also be reduced for the VGT systems.

Currently, variable geometry turbocharging systems are not only used to increase the power density of an engine but also to control the engine combustion processes. A variable boost system allows flexible control, and thus optimisation of the boost pressure for different load and speed conditions. In addition to the original power and fuel economy goals of variable boost systems, these systems have been proven to also reduce emissions and improve engine transient response (Arnold *et al.*, 2002; Filipi *et al.*, 2001). The implementation of EGR systems in diesel engine applications introduces extra requirements for the VGT/VNT system, as it needs to simultaneously maintain the exhaust back pressure for the desired exhaust gas flow in the EGR system while also trying to maximize the air-handling system response during engine transient operation (Buchwald *et al.*, 2006).

### **2.3.3 Exhaust gas recirculation (EGR)**

EGR has been used to control automotive spark-ignition engine combustion behaviour for decades (Heywood, 1988). EGR reduces NO<sub>x</sub> formation in both diesel and gasoline-fuelled spark ignition combustion processes. However, in diesels, it increases engine-out PM emissions in conventional diesel combustion (Heywood, 1988). Achieving high levels of EGR (> 50% depending on operating conditions) can lead to the low temperature combustion regime, where PM emissions are reduced to levels even lower than those with no EGR. When high EGR is combined with other technologies such as high pressure fuel injection and high swirl ratio which can improve the in-cylinder charge mixing, diesel engines can achieve very low engine-out NO<sub>x</sub> and PM emissions (Henein *et al.*, 2006). How the EGR and other technologies can be used to control the combustion and emissions under LTC will be discussed in Section 2.4. However, a review of the fundamental mechanisms of how EGR influences diesel combustion is required.

The main mechanisms by which EGR influences diesel engine combustion and emissions (Ladommatos *et al.*, 1998a; Ladommatos *et al.*, 1998b; Ladommatos *et al.*, 2000; Ladommatos *et al.*, 1998c; Nitu *et al.*, 2002) are:

1) Reduction in the in-cylinder oxygen concentration. The oxidation rate of fuel is decreased by the reduced oxygen concentration. The slower combustion process reduces the local peak combustion temperature, reducing the NO formation rate. However, the lower oxygen concentration also leads to increased smoke, THC and CO emissions.

2) Increase in charge temperature (in cases where the EGR is not cooled to the same temperature as the charge air). The increase in intake charge temperature reduces its density, resulting in a lower mass of charge inducted for a given intake pressure. This effect is referred to as a thermal throttling effect, and will lead to increased PM emissions. The hot exhaust gas increases the intake charge temperature, which leads to a reduced ignition delay, and hence increased smoke emissions compared with the cooled EGR condition. The hot EGR also increases the NO<sub>x</sub> emissions compared to cooled EGR due to the general high charge temperature during the combustion process. However, the NO<sub>x</sub> emissions are reduced by the thermal throttling effect due to the reduced intake oxygen concentration.

3) The change in composition of the charge (replacement of O<sub>2</sub> with CO<sub>2</sub> and H<sub>2</sub>O) results in an increase in the specific heat capacity of the charge and hence lower temperatures. However, this has been shown to be secondary to the effect of lower O<sub>2</sub> concentrations.

4) The direct (chemical) participation of the CO<sub>2</sub> and H<sub>2</sub>O in the reactions has shown to be minimal. Although both CO<sub>2</sub> and H<sub>2</sub>O will dissociate into their constituent atoms at the temperatures found in the reaction zone, their contribution to the overall combustion event has been shown to be minimal.

All these mechanisms lead to reduced combustion temperature which is the most important factor for the emissions formation processes. The low combustion temperature suppresses thermal NO formation; if sufficient dilution is present, even the PM formation processes can be inhibited (i.e. < ~1600K) (Kuo, 2005). However, the lower temperature does not as significantly reduce the rate of prompt NO formation route, which will become the dominant NO mechanism in LTC mode. The

lower temperature in the reaction zone will also inhibit oxidation process of THC and CO and may lead to earlier bulk and wall quenching of the reactions.

Precise control of the EGR rate and temperature is important to retain the benefits of EGR for clean and high efficiency diesel combustion. Electrically controlled EGR valves have taken the place of vacuum driven EGR systems. These improve the EGR rate control response and accuracy in both steady-state and transient operating conditions (Yokomura *et al.*, 2004). Jointly controlled EGR and VGT systems have been shown to reduce cyclic variations in EGR rate (Shirakawa *et al.*, 2001; Nieuwstadt *et al.*, 2000). The temperature of the EGR is usually managed by a dedicated cooling system controlled by the engine management system; cooling of the EGR helps to maintain a more robust diesel combustion process (Ladommatos *et al.*, 1998b; Tomazic *et al.*, 2002). However, the increased cooling requirements cause increased engine cooling load.

The deviation of EGR gas distribution in different cylinders in multi-cylinder engines also has significant impact on engine emissions since imbalanced EGR distribution leads to non-optimized combustion (Green, 2000; Maiboom *et al.*, 2009). Thus, advanced simulation and experimental technologies have been employed to optimise the EGR system design and control (Page *et al.*, 2002; Siewert *et al.*, 2001). However, when high levels of EGR are being used, the combustion would be expected to be more sensitive to the variations in EGR rate control and distribution.

## **2.4 Low Temperature Diesel Combustion**

A number of low temperature combustion strategies have been developed, such as homogeneous charge compression ignition (HCCI), premixed charge compression ignition (PCCI), partial premixed compression ignition combustion (PPCI), modulated kinetics (MK) and smokeless fuel-rich combustion. In all these systems, the flame temperature is decreased to reduce the NO<sub>x</sub> emissions through the use of high levels of EGR. For PM reduction, either different fuel injection strategies can be used to increase the fuel mixing time and intensity, or the EGR rate is further increased to attain combustion temperatures which are so low that PM formation is suppressed. Kazuhiro Akihama *et al.* (2001) have developed the classic local equivalence ratio – flame temperature ( $\Phi$ -T) map for diesel engine NO<sub>x</sub> and soot formation through combustion kinetics modelling. Needy *et al.* (2005) extended the conceptual model with a more comprehensive understanding of the LTC regimes as shown in Figure 2.1.

The differences between conventional diesel combustion and low temperature combustion are based on the engine emissions. When both the engine-out NO<sub>x</sub> and PM emissions were reduced to ultra low levels (i.e. NO<sub>x</sub> in several ppm, filter smoke number similar to that of the non-EGR combustion conditions) the combustion can be considered to be in the low temperature combustion regime. Control of the local flame temperature and equivalence ratio can have a significant influence on the NO and soot emissions formation. By using flexible fuel injection strategies, air-exchange systems and EGR, the local combustion temperature and fuel-air mixture can be shifted into the zones where NO and soot are unlikely to form.

Among the different combustion strategies, LTC has a wider local equivalence ratio range and a lower combustion temperature range than HCCI and PCCI have. Both HCCI and PCCI feature more extensive pre-mixing than LTC, which leads directly to the lower equivalence ratios; however, they tend to use less EGR, resulting in higher combustion temperatures. These characteristics of LTC help to suppress the NO and soot formation effectively. Furthermore, the wider operational equivalence ratio range allows an easier combustion control in terms of start of combustion phasing and combustion stability. However, there are still significant obstacles for the LTC combustion regimes to overcome before their wider implementation:

- 1) The limitation of their use to the low load and low speed range of the engine operating map;
- 2) High incidence of incomplete combustion;
- 3) Higher THC, CO emissions and fuel consumption compared with conventional diesel combustion;
- 4) Reduced combustion stability; and
- 5) Increased difficulties in engine transient control.



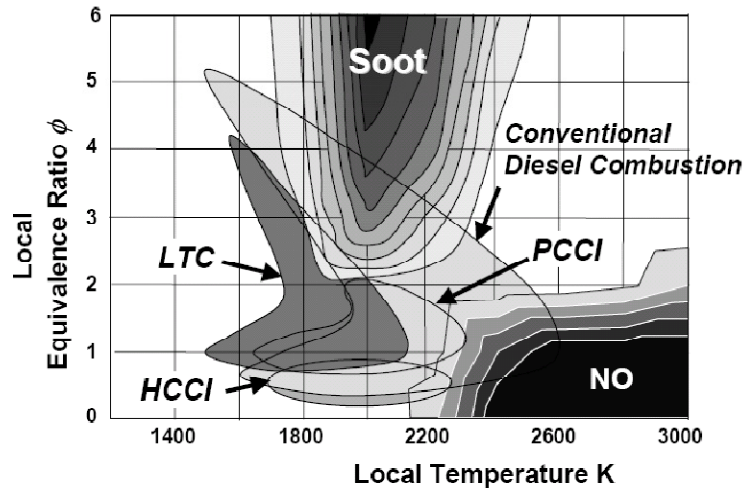


Figure 2.1 Local fuel-air equivalence ratio,  $\Phi$ , versus temperature showing contours of high soot and NO<sub>x</sub> formation regions as well as boundaries of regions within which conventional diesel, PCCI, LTC, and HCCI combustion occur (Akihama *et al.*, 2001; Neely *et al.*, 2005) (Reprinted with permission from SAE Paper No. 2005-01-1091 © 2005 SAE International)

### 2.4.1 Low temperature combustion strategies

For the different LTC strategies outlined in the preceding section, the main principle is to reduce the combustion temperature through the application of EGR, and to prolong the ignition delay and thus to realize a smokeless NO<sub>x</sub>-free combustion. One technique, referred to as partially-premixed compression ignition combustion (PPCI) which used a very early direct injection (or port fuel injection) so that part of the fuel will mix with the air and form a lean premixed charge in the cylinder. A subsequent fuel injection which auto-ignites can be used to control the ignition of all the fuel (Hasegawa *et al.*, 2003; Simescu *et al.*, 2002). If all the fuel is fully premixed before the compression ignited combustion, this combustion strategy is referred to as homogeneous charge compression ignition (HCCI) (Thring, 1989; Zhao *et al.*, 2003). An alternative realisation of low-temperature combustion is Nissan's Modulate Kinetics combustion (MK) (Kimura *et al.*, 2001; Kimura *et al.*, 1999). In this method, a single, late, fuel injection is used along with a reduced compression ratio (of 16:1), where the lower temperature delays ignition until after the injection event has completed. High swirl ratio is used to improve the fuel-air mixing and reduce the heat lost from heat transfer to the cylinder walls. For these combustion strategies, soot formation is suppressed by the improved fuel-air mixing due to the prolonged ignition delay. Smokeless fuel-rich combustion is obtained through increasing the EGR rate to reduce the intake oxygen concentration until the global equivalence ratio is near stoichiometric or even fuel-rich (Ogawa *et al.*, 2007). This type of LTC restricts the

combustion temperature below that for growth of PAH into spherical particles, thus preventing the formation of soot particles even under fuel-rich conditions (Akihama *et al.*, 2001).

For the HCCI, PPCI and the smokeless fuel-rich diesel combustion regimes introduced in the preceding paragraph, a distinctive cool flame reaction phenomenon was exhibited before the main heat release events. A cool flame is the product of a limited exothermic reaction that is associated with a partial conversion of the fuel which takes place at 700K to 900K. The heat released in the reaction can be used for vaporizing the liquid fuel and the amount of heat released is dependent on temperature (Yamada *et al.*, 2006).

These low temperature combustion approaches are now described in more detail:

### **Homogeneous charge compression ignition (HCCI)**

The concept of HCCI is to combine the advantages of spark ignition engines (such as premixed charge and very low soot emissions) and compression ignition engines (high compression ratio, no throttling and high thermal efficiency) and to create a new combustion strategy. This can be used on both gasoline and diesel engines (Thring, 1989; Zhao *et al.*, 2003), aiming at reduced emissions and increased engine efficiency. For diesel HCCI combustion, port fuel injection, early multiple fuel injection strategies (Gray *et al.*, 1997; Risberg *et al.*, 2005; Su *et al.*, 2003) can be used to prepare the premixed charge. The combustion of the lean premixed charge can effectively suppress the soot formation as illustrated in Figure 2.1. The combustion temperatures can also be reduced due to the lean homogeneous charge, reducing NO<sub>x</sub> emissions.

The ignition control of the homogeneous charge and the rapid combustion process after ignition are the main concerns for a diesel HCCI engine. Due to the high ignitability of diesel fuel, the early ignition at HCCI operation may occur, leading to non-HCCI operation of the engine. Misfire may also occur in the lean premixed fuel-air mixture due to the difficulty in forming sustainable ignitable kernels in the combustion chamber (Kawano *et al.*, 2005). The rapid combustion process may cause knock in the combustion (Andreae *et al.*, 2007). Thus, alternative combustion strategies have been studied to overcome these drawbacks.

## **Partial premixed compression ignition diesel combustion (PPCI)**

Concept of PPCI has been introduced to take advantage of low emissions from homogeneous charge combustion while avoiding the difficulties in combustion control. An early direct injection forms a lean premixed charge which experiences low temperature reactions until a later fuel injection occurs to ignite the remainder of the fuel. The subsequent combustion event is then a combination of premixed and non-premixed combustion. The uniform bulky combustion system (UNIBUS) (Hasegawa *et al.*, 2003) is one embodiment of this approach. The timing and mass of the early injection are optimized to avoid high temperature reaction until the second injection occurs. The later fuel is injected into the products of the ongoing low temperature reaction resulting in a short combustion duration and lower combustion temperatures compared to the conventional diesel combustion.

Researchers have investigated the addition of port fuel injection on a direct injection diesel engine (Simescu *et al.*, 2002). Similar to the UNIBUS system, port fuel injection is used to produce the premixed part of the charge in the combustion chamber. There are three stages of the combustion process: a low temperature 'cool-flame' reaction of the inducted fuel; premixed combustion of the inducted fuel; and diffusion combustion of the directly-injected fuel. The PFI fuel-air equivalence ratio, direct fuel injection timing and EGR temperature are key parameters which can influence the fuel consumption and emissions. Like the early direct fuel injection option, it is important to avoid high temperature reactions of the inducted fuel before the direct injection event to preserve the low NO<sub>x</sub> and PM emissions.

The simultaneous reduction in NO<sub>x</sub> and PM emissions is possible in a diesel engine employing a PPCI strategy, as discussed in the examples in the preceding paragraphs. It is attainable with advanced injection timings and high EGR rates. However, PPCI combustion has the following problems:

- 1) The advanced fuel injection timing results in fuel impingement on the cylinder liner, which causes lubrication oil dilution and high THC and CO emissions;
- 2) High fuel consumption derived from lower combustion efficiency; and
- 3) A narrower operating region compared with conventional diesel combustion.

To overcome these drawbacks, different approaches have been investigated by researchers. Narrow spray angle injectors (Lechner *et al.*, 2005; Lee *et al.*, 2006; Walter *et al.*, 2002) and optimized combustion chambers (Walter *et al.*, 2002) were

tested to optimise the fuel distribution and combustion process. However, the narrow spray angle led to unfavoured fuel distribution for the higher load conventional diesel operation with late fuel injection and resulted in compromises in combustion and emissions between the LTC and conventional combustion modes.

For small bore diesel engines, such as passenger vehicle diesel engines, the advanced fuel injection timing causes severe wall fuel impingement on the liner compared to larger bore heavy duty engines (Lechner *et al.*, 2005; Lee *et al.*, 2006; Walter *et al.*, 2002). Thus, for this reason, PPCI combustion is currently considered to be more promising for the larger bore mid- to heavy-duty diesel engines.

### **Modulated Kinetics combustion system (MK)**

The MK system, developed by Nissan employs high EGR rates and retarded fuel injection to achieve premixed low temperature diesel combustion (Kimura *et al.*, 2001; Kimura *et al.*, 1999). It introduces EGR to decrease the intake charge oxygen concentration, which reduces the combustion temperature and suppresses NO<sub>x</sub> formation. To reduce PM formation from the low oxygen combustion, the fuel injection is retarded to increase ignition delay. The very late fuel injection with lower in-cylinder pressure and temperature during the expansion stroke makes the ignition delay longer than the injection duration. The late fuel injection strategy also avoids the fuel impingement that occurs in PPCI combustion as discussed previously. Kimura *et al.* (1999) claimed that the deterioration in engine efficiency and THC emissions is improved by increased swirl ratios (up to 9). High swirl ratios improved the fuel-air mixing and led to lower peak combustion temperatures. This lower temperature gradient between the combustion products and the combustion chamber walls with the high swirl ratios around the walls reduced the cooling losses of the engine.

The three essential conditions for accomplishing MK combustion are the use of high EGR rates, the complete injection of all the fuel prior to ignition and the use of high swirl ratios. The researchers identified two main obstacles to extend the MK combustion system operating range beyond relatively low loads: shortened ignition delay by the higher temperature of EGR and prolonged injection duration by the greater quantity of fuel injection. Cooling of the EGR gas and a reduction in compression ratio can decrease the charge temperature and extend the ignition delay. High pressure fuel injection or larger injector nozzle holes can be used to

increase the fuel injection rate, thus allowing a reduction in the injection duration (Kimura *et al.*, 2001).

The high swirl ratio in the MK system is an obstacle for its wide application since it is difficult for a high swirl ratio system to maintain high engine intake volumetric efficiency. The high swirl ratio configuration for low load engine operation (MK) may sacrifice the high load performance of the engine unless the swirl ratio can be varied as a function of load.

### **Post fuel injection realized low temperature combustion**

Both the PPCI and MK systems reduce the PM formation through prolonged ignition delay and improved fuel-air mixing. Post fuel injection has also been shown to be an effective way to reduce the diesel engine PM emissions without a penalty in NO<sub>x</sub> emissions in conventional diesel combustion (Benajes *et al.*, 2001; Molina *et al.*, 2002). Post injection achieves very favourable emissions in the high EGR diesel combustion regime, since it improves late-cycle mixing and enhances the PM oxidation processes. With a small quantity of fuel injected in the post injection pulse, reduced soot emissions have been achieved (Yun *et al.*, 2007; Yun *et al.*, 2005b). However, the post fuel combustion in the expansion stroke contributes less to the engine torque, and hence leads to reduced engine efficiency.

The dwell time between the main injection and post injection was shown to be very important since the additional mixing at the appropriate time during the late-cycle period played a dominant role in reducing the PM emissions. Simulations suggested that optimal combustion required that the post injection fuel avoid fuel-rich regions formed from the main injection (Yun *et al.*, 2005b). The dwell time had a negligible effect on NO<sub>x</sub> emissions but a significant influence on PM emissions. For example, with a short dwell time, the post injection occurred before the start of main combustion, similar to a PPCI combustion regime. The decrease in PM emissions may have been due to the optimisation of the phasing of combustion rather than from the improvement in the mixing during the late-cycle period or longer dwell times.

The THC emissions increased when the dwell time was prolonged. This indicates that the temperature during the expansion stroke was too low to support a complete combustion of the post-injected fuel. Also, fuel injected in the later combustion phase did not have enough time to burn completely before the exhaust valves opened. With

high EGR operating conditions, the low oxygen concentration would be another restriction for post injection fuel combustion.

### **Smokeless fuel-rich diesel combustion**

Smokeless rich diesel combustion has been shown to achieve a near smokeless and NO<sub>x</sub>-free combustion by using a large amount of cooled EGR under a near stoichiometric and even in a fuel-rich operating condition (Akihama *et al.*, 2001; Ogawa *et al.*, 2007). The mechanism of PM suppression is by the combustion taking place at very low temperature rather than the improvement of fuel-air mixing for PPCI and MK systems. So, even fuel-rich regions are at such that, at low temperatures PM is not formed.

Akihama *et al.* (2001) established an  $\Phi$ -T map as shown in Figure 2.1 by zero dimensional kinetics modelling using a detailed soot formation model. It shows soot formation tendencies as a function of  $\Phi$  and T. They compared conventional (52% EGR) and smokeless fuel-rich combustion (58% EGR) processes at 2000rpm low load operation conditions through 3D-CFD simulation and found that:

- 1) The higher EGR rate shifts the combustion to a lower temperature zone on the  $\Phi$ -T map;
- 2) The combustion temperature plays a dominant role on the soot suppression mechanism, but the fuel-air mixing has insignificant effect on the soot formation when the combustion temperature is low enough.

Ogawa *et al.* (2007) studied the effects of a wide range of EGR levels on combustion of a naturally aspirated 1.0 litre single cylinder direct injection diesel engine. The low temperature combustion regime was realized by ultra high EGR rate (up to 62%, with an oxygen concentration of 9%). As the EGR rate increased, exhaust gas emissions and thermal efficiency varied with the intake oxygen content rather than with the excess air ratio. This agrees with the results found by Alriksson *et al.* (2006), i.e. the higher charge air pressure increased the oxygen availability for the combustion at a constant EGR rate, which extended the smokeless NO<sub>x</sub>-free combustion range. Advancing or retarding the injection timing reduced the smoke emissions, but advancing the injection timing had the advantages of maintaining high thermal efficiency and preventing misfire. The increase in smoke when the EGR rate was lower than needed to achieve LTC could be suppressed by increasing the injection pressure. With decreased compression ratios, the smoke emissions decreased under

high EGR conditions, and the range of smokeless operations was extended to a wider EGR and IMEP range. However, these low compression ratios also reduced the indicated thermal efficiency (Alriksson *et al.*, 2006).

Smokeless fuel rich diesel combustion achieved lower PM emissions than non-EGR combustion. Importantly, the composition of the PM emissions was also changed due to the significant variations in the combustion reactions and the temperatures at which the combustion occurred. The SOF fractions in the PM were increased significantly, as the PM reductions were primarily due to a reduction in soot formation (Ogawa *et al.*, 2007). This suggests that a significant reduction in PM by a DOC could be achieved if one is fitted to the engine (Lehtoranta *et al.*, 2007).

#### **2.4.2 Technologies with LTC**

The principle of LTC is to reduce diesel engine emissions through a reduction in the combustion temperature, since temperature is an essential factor for controlling the emissions formation. Various technologies have been investigated to reduce the temperature through reduction of the oxygen concentration, improvement in fuel-air mixing, and the optimisation of the combustion process, including EGR, fuel injection strategies, swirl ratio, and boost pressure. All these technologies have been introduced in Section 2.3. Of these, EGR is the most important technology to achieve the low temperature combustion regimes as introduced in the preceding section. The reduction in combustion temperature is the key contributor for the reductions in PM and NO<sub>x</sub> emissions and the EGR is the most effective method to reduce the combustion temperature.

### **2.5 Diesel Engine Transient Operation**

For an automotive engine, most of its operation occurs under transient operating conditions where the speed and load vary continuously. As a result, engine transient operation contributes disproportionately to emissions and fuel consumption compared to steady-state engine operations (Black *et al.*, 2007; Burton *et al.*, 2009; Galindo *et al.*, 2001; Hagen *et al.*, 2006). Researchers have studied the diesel engine transient behaviour in different ways to understand what and how engine operation parameters influence emissions and fuel consumption during load and speed transients (Benajes *et al.*, 2002; Payri *et al.*, 2002). The response times of the engine's fuel system, boost systems and EGR systems are the main reasons for deviations between engine transient and steady-state operation. The different inertias

and response behaviour among the engine sub-systems during transient processes result in non-optimized EGR rates, air-fuel-ratios (AFR) and combustion processes. It is a challenge to preserve the combustion characteristics of steady-state operating conditions during transient operation.

The engine's thermal inertia is another source of engine combustion behaviour variations during transient operation. During an engine transient, the thermal conditions of the engine are different from the conditions of the equivalent steady-state conditions. The changing combustion chamber wall temperatures influence the fuel vaporisation and charge temperature, which in turn influence the engine combustion and emissions (Chang *et al.*, 2006; Rakopoulos *et al.*, 2009b).

### **2.5.1 Dynamic behaviour of engine sub-systems during transients**

The delay in response of air exchange systems during engine transient operation leads to deviations in engine combustion processes and emissions from steady-state conditions. The "turbo-lag" is a result of slow turbocharger response to engine acceleration due to a lack of exhaust energy to accelerate the turbine at early stages of the transient event and the inherent gas and mechanical inertias (Serrano *et al.*, 2009a; Serrano *et al.*, 2009b). Due to the insufficient boost pressure during the acceleration transients, the amount of injected fuel has to be limited to avoid excessive smoke levels. This results in a reduced engine transient torque.

The EGR system amplifies the turbo-lag effects (Galindo *et al.*, 2001). The subtraction of exhaust gas flow from the exhaust manifold by EGR reduces the enthalpy in the exhaust gas for driving the turbine and prolongs the low boost period. EGR systems also have an even slower response to transient operation than the turbocharger (Hagena *et al.*, 2006). Delays in EGR valve position change and the existing exhaust gas in the EGR system lead to unpredictable EGR rates for the early part of a transient event. The overshoot effect of the EGR rate controller during transient operation also degrades the engine emissions. Combined with the turbo-lag effect, EGR fluctuations cause smoke 'spikes' in the initial stages of transient accelerations (Galindo *et al.*, 2001; Hagena *et al.*, 2006).

The response of the fuel injection system and hence the mass of fuel injected in any cycle, can be increased much more quickly than the trapped air mass. Even with the engine controller restricting fuel mass on the basis of fuel-air ratio, there are still significant fuel-air ratio deviations between the transient points and steady-state



points. However, after the boost pressure reaches the steady-state value, the boost pressure controller will over-shoot, which causes the boost pressure to be higher than the steady-state map value; this leads to lower fuel-air equivalence ratio and subsequently higher NO<sub>x</sub> emissions (Wijetunge *et al.*, 1999). Unlike injection mass or timing, the fuel injection pressure cannot respond instantaneously to the operation condition changes (Wijetunge *et al.*, 1999), since the fuel system (particularly the fuel rail) acts as a hydraulic accumulator. The insufficient fuel pressure variation rate influences the injection duration and the mixing, and hence, the combustion behaviour. However, it should be predictable and can be accounted for in the engine control algorithm.

### **2.5.2 Effects of engine thermal conditions during a transient**

The combustion chamber wall temperature is an important factor which influences the low temperature combustion process (Chang *et al.*, 2006; Wilhelmsson *et al.*, 2005). It cannot change instantaneously and the slowly changing wall temperature following a load transient will affect the combustion events during the transient. The diesel HCCI combustion phasing has been found to be heavily dependent on wall temperature during a transient operation. Even for a conventional diesel combustion process, the THC emissions were found to significantly increase during engine transient operation due to the temperature differences between the steady-state and transient operation points (Wijetunge *et al.*, 1999).

Low combustion chamber wall temperatures can increase the ignition delay due to less heat transfer to the fuel-air mixture. During an acceleration process of a diesel engine, the lower wall temperature combined with lower boost pressure derived from turbo-lag result in a 'harsher' combustion and increased combustion noise compared with steady-state operations (Dhaenens *et al.*, 2001). The longer ignition delay derived from the 'cold' combustion chamber walls contributes to the increased premixed combustion intensity.

### **2.5.3 Transient combustion behaviour during LTC**

The dynamic characteristics of engine sub-systems have a significant influence on the combustion process and emissions of diesel engines. The transient operation of engines using conventional diesel combustion strategies have been studied widely. However, the transient combustion behaviour of diesel engines using LTC has

received little attention. LTC is expected to be more sensitive to the engine operating parameters compared with conventional diesel combustion since it employs large variations in operating parameters such as very high EGR rates and very advanced or retarded injection timings. Any further fluctuations of these parameters may cause unstable combustion processes. The combustion processes themselves are also much more sensitive to these parameters than in conventional diesel combustion. There are no studies were found by the author that have quantified or even conclusively demonstrated these effects.

#### **2.5.4 Diesel engine combustion characteristics during mode shifts**

As introduced above, new combustion modes such as LTC are being developed to meet the stringent emission regulations implemented for diesel engines. However, these combustion modes have limited operational load and speed ranges. A combination of conventional diesel combustion at higher loads, along with the new combustion techniques at low load, may provide a realistic route to meet the emissions regulations while maintaining engine performance (Hasegawa *et al.*, 2003; Kimura *et al.*, 2001). Managing the transition between these very different combustion modes will be a challenging control task that has not been extensively discussed in the literature to date.

Studies have been conducted on the control of diesel engine combustion during combustion mode shifting (Narayanaswamy *et al.*, 2006; Wang, 2007). These researchers studied the control strategies and algorithms for engine control during combustion mode shifting. However, they did not investigate the combustion behaviour of the diesel engine during these events. A research method of cycle-by-cycle transient combustion analysis has been developed and implemented to study conventional diesel engine transient behaviour (Assanis *et al.*, 2000; Galindo *et al.*, 2001). However, the candidate has not found any published reports of these techniques having been applied to diesel engine transient study during combustion mode shifting.

Several studies have investigated the diesel engine combustion mode shifting at fixed engine operating conditions. Busch *et al.* (2007) studied the process from conventional diesel combustion to low temperature combustion at a fixed engine operating condition. Emissions of NO were found to increase for the initial cycles of the mode shift, primarily due to the transport delay of the EGR system resulting in a low intake CO<sub>2</sub> concentration which led to increases in NO emissions. With higher

fuel injection pressures for both conventional and LTC modes, the first several cycles of a mode shift encountered further NO emission increases. Beatrice *et al.* (2007a) investigated the combustion mode shifts between LTC and PPCI combustion modes with constant fuel injection quantity (i.e. constant desired engine load). The adjustment of the EGR circuit to the new conditions with high EGR rate was slower than in the reverse direction. The fuel injection strategy changed quickly to the desired regime, but the delay of the EGR system caused increased NO<sub>x</sub> emissions. While informative, neither of these studies effectively represents real world transient operation of the engine, where the desired speed and load of the engine are changing at the same time as the engine operating parameters, especially fuel injection quantity, EGR rate and boost pressure.

### **2.5.5 Transient EGR control**

For conventional diesel combustion, during transient operation the EGR valve is conventionally either closed (Wijetunge *et al.*, 1999) or restricted to small openings (Yokomura *et al.*, 2004). These methods are used to reduce the smoke 'spikes' caused by the turbo-lag phenomena. The existence of EGR in the system increases the delay in the air-exchange system and makes the control of the overall equivalence ratio more complicated. The non-optimized fuel-air equivalence ratio or EGR rate for these transient operations causes poor engine performance and emissions; however, the reduction in EGR rate during transient operation contributes to increased NO<sub>x</sub> emissions (Kang *et al.*, 2005; Yokomura *et al.*, 2004). To overcome these difficulties, Yokomura *et al.* (2004) developed a closed loop EGR control system. Compared with the open loop EGR control that has the EGR valve closed during a load ramp, the closed loop controller enabled a reduction of 40% in NO<sub>x</sub> at an equivalent low PM emission level. However, the transient NO<sub>x</sub> level was still higher than the equivalent steady-state operating conditions.

## **2.6 1D Simulation of Diesel Transient Operation**

1D engine simulation is a powerful tool for engine performance simulation, air exchange and turbocharger matching etc. It has the advantage of simulating engine performance and gas dynamics with an acceptable level of accuracy relatively quickly (Albrecht *et al.*, 2005; Gurney, 2001; He, 2005; Narayanaswamy *et al.*, 2006). The engine model is useful for engine development and optimization, subsystems matching and integration.

For simulation of diesel transient operation, the in-cylinder combustion and heat transfer, the gas exchange process and transient thermal inertia of the engine structures need to be considered simultaneously in order to fully understand the engine combustion behaviour (Chang *et al.*, 2006). A predictive ignition model and modified Woschni heat transfer model can be incorporated in many 1D engine simulation codes with empirical correlations for burn rate and combustion efficiency to improve its accuracy. Navratil *et al.* (2004) and Lefebvre *et al.* (2005) studied transient simulation of turbocharged gasoline engines using extrapolated maps of the combustion process and heat transfer as functions of load and speed. This method resulted in improved accuracy in predictions of the engine transient operating parameters. However, accurately modelling the engine combustion and emissions behaviour is impossible for current 1D engine simulation codes.

## **2.7 Identification of Key Knowledge Gaps**

Understanding the sensitivity of the high EGR diesel combustion to engine operating parameters is crucial for the implementation of LTC in automotive diesel engines. From the published literature, it is expected that LTC will be more sensitive to the variations in parameters such as EGR rate, intake temperature and fuel injection strategies since the engine runs at near stoichiometric conditions. However, the relationship between the parameters' variations and the engine combustion performance is not currently clearly understood. Further research into combustion stability, engine emissions and fuel consumption are therefore required to identify the sensitivity of LTC combustion to the engine operating parameters.

Diesel combustion within the LTC modes is expected to be very sensitive to the transient dynamics and interactions of the engine sub-systems such as fuel injection, boost and EGR systems. The engine operating parameters during transients within conventional combustion modes show significant differences compared with those during steady-state operation (e.g. boost pressure and EGR rate). These deviations in the parameters influence engine performance and emissions significantly. Engine parameters, such as EGR rate and fuel injection parameters, need to be varied over wider ranges in LTC compared to conventional diesel combustion mode; as a result, transient response is expected to be slower while the combustion is likely to be more sensitive to the corresponding variability in operating parameters. No studies investigating engine transient behaviour within LTC have been found in the published literature to-date.

The implementation of dual-mode combustion systems (i.e. LTC for low to intermediate load and conventional diesel combustion for high load) on a diesel engine is a promising, cost-effective way for the engine to meet stringent emission legislations while also meeting engine performance demand. The knowledge of diesel combustion behaviour during the combustion mode shifting within driving-cycle tests is important to allow the engines to meet the stringent future emission legislation. However, the details of diesel engine combustion characteristics during mode shifts between LTC and conventional diesel combustion have not been found in the literature to-date.

The distinctive cool flame main combustion heat release phenomenon has been reported for HCCI and PPCI combustion regimes. However, details about the low temperature part of the heat release process are still not clear. An experimental study of the effects of engine operating parameters on the low temperature heat release process could be beneficial for improving the understanding of these early pre-combustion reactions in the LTC combustion regime. The experimental results could also be used to interpret the kinetics of low temperature diesel reactions, which is critical for ignition delay modelling and prediction.

In this chapter, the literature has been surveyed in the area of diesel engine LTC combustion and transient operation. The key knowledge gaps have been identified. The next chapter will introduce the engine experimental system setup and the research apparatus for the study, which were used to contribute to the understanding of LTC and during combustion regime shifting.

## Chapter 3 Research Apparatus and Procedures

### 3.1 Test Engine Specification

An AVL5402 single-cylinder research engine was used for this study. It is a single cylinder version of a four-cylinder automotive high-speed direct injection (HSDI) diesel engine. By avoiding any interactions among the cylinders for a multi-cylinder engine, the single cylinder configuration has increased operational flexibility and enabled the analysis to concentrate on the events in one cylinder; this will be particularly beneficial when working near the combustion limits. With 1<sup>st</sup> order balancers, the single-cylinder engine mechanical dynamics are very similar to those of a multi-cylinder engine in terms of mechanical dynamics. Details of the engine are listed in Table 3.1.

Table 3.1 Engine specifications

Engine	Single cylinder 4-stroke
Fuelling	Direct injection, diesel
Bore/Stroke/Connecting rod length	85/90/148mm
Compression ratio	17.1 : 1
Swept volume	510.7 cm <sup>3</sup>
Chamber geometry	Re-entrant bowl
Fuel injection system	Common rail CP3 (BOSCH)
Injector holes	5 x 0.18 mm x 142° x 0°
Intake ports	Tangential and Swirl Inlet Port
Valves	2 intake, 2 exhaust
Nominal swirl ratio	1.78
Engine management system	AVL-RPEMS™ + ETK7 (BOSCH)
Intake valves open	8 °CA BGTDC
Intake valves close	226 °CA AGTDC
Exhaust valves open	128 °CA ATDC
Exhaust valves close	18 °CA AGTDC

The research engine featured an advanced common rail fuel system and four valves per cylinder. The fuel injection system was capable of injecting the fuel at a range of injection pressures up to 1400 bar, along with up to four injections per combustion event. The specifications of the fuel system are summarized in Table 3.2. The engine control system was a prototype ETAS engine control unit. An open loop fuel injection control strategy designed by AVL was loaded in the ETAS system to allow independent control of fuel injection parameters. The injection parameters for each injection event such as the injection pressure, timing, and quantity could be modified

and logged independently through the INCA software which is used to communicate with the ETAS system.

Table 3.2 Fuel injection equipment system specifications

Injector type	CP3 VCO
Maximum injection pressure	1400 bar
Nozzle type	DSLA 142P
Number of nozzle holes	5
Hole diameter	0.18 mm
Included spray angle	142°
Needle lift	0.20 mm
Steady fuel flow rate @ 0.2 mm lift	375 ml/30 sec
Minimum energize duration	100 $\mu$ s
Minimum dwell between injections	200 $\mu$ s

The combustion chamber was a re-entrant  $\omega$  shape formed by the piston and a flat flame face. It is a typical type of geometry used in passenger car high speed direct injection diesel engines. The combustion bowl geometry is shown in Figure 3.1.

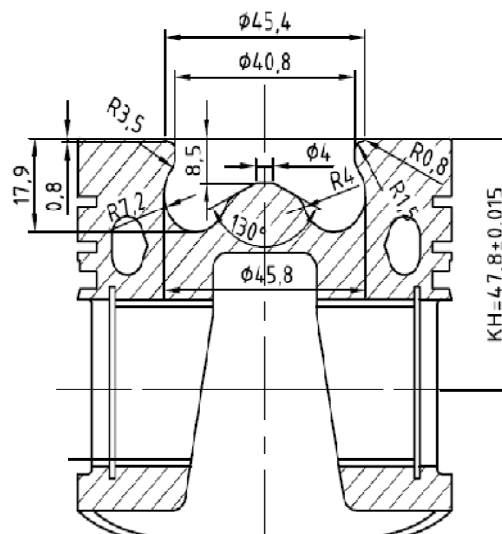


Figure 3.1 Combustion chamber piston bowl geometry

The AVL single cylinder engine compact test bed consisted of an AMK DW motoring dynamometer with rated power of 38 kW, which was a liquid-cooled three-phase asynchronous motor that can both supply and absorb torque. With a stand-alone EMCON 400 system, the engine speed and torque could be controlled independently. The engine speed could be controlled within  $\pm 0.5$  rpm for the desired speed; however, the torque/power readings from the EMCON were unstable especially at low load operating conditions (typically  $< 12$  Nm torque). Due to the high

friction of the single cylinder engine, the torque/break power measurement of the engine dynamometer was not representative of the multi-cylinder engine performance at equivalent operating conditions. Therefore, the work as measured using the in-cylinder pressure was used to represent the engine load in this research.

An AVL-577 cooling water and lubricating oil supply unit was integrated in the compact test bed. The unit established the fluid flow rate and temperature control of the oil and engine coolant, as well as providing pressure control for the oil circuit. The temperature of the coolant and oil were manually pre-set on the unit control panel. The error of control targets were maintained within the range of  $\pm 2$  °C for the desired temperatures. Over-temperature protection was provided for both coolant and oil temperatures. The oil pressure was sensed by a pressure gauge; loss of oil pressure caused the engine to shut down automatically.

### 3.1.1 Research engine systems

To conduct the research, a custom-built boost air-exchange system including EGR was designed and implemented on the test engine. The layout of the experimental air exchange system is shown in Figure 3.2. The air-exchange system was developed specially for the purpose of this study. The flexibility provided by the air-exchange system allowed independent control of air and EGR levels in the engine.

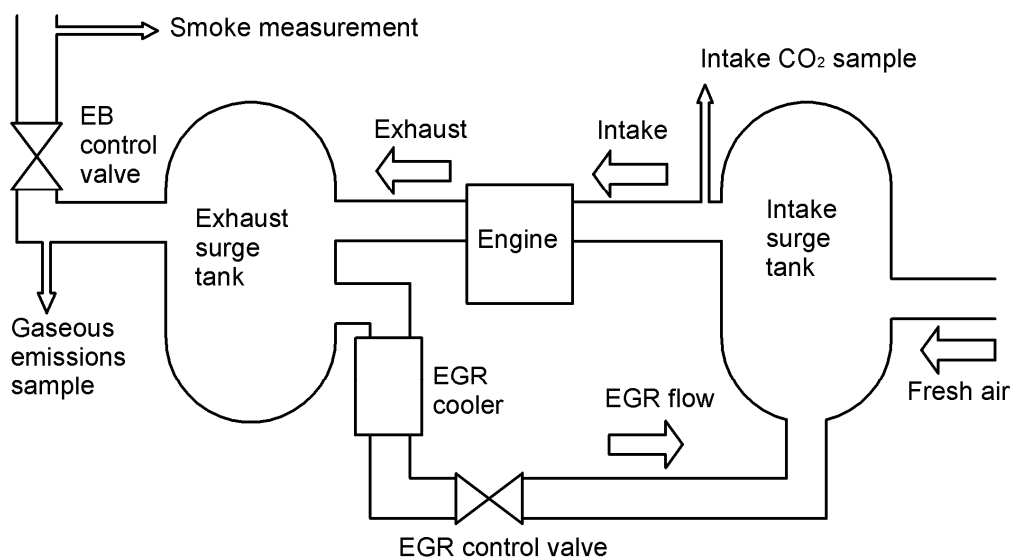


Figure 3.2 Schematic of gas flow in the research engine



## **Air exchange system**

Two 25 litre high-temperature surge tanks were used to reduce the pulsations in the intake and exhaust streams. These tanks, which were manufactured of stainless steel by Echo Engineering, were certificated pressure vessels for pressure up to six bar absolute pressure and temperature up to 650°C. The size of the tanks was defined using a 1-D engine simulation which showed the system to be able to reduce the pulsation in both the intake and exhaust systems to an acceptable level (i.e.  $< \pm 0.01$  bar in the inlet pipe;  $< \pm 0.05$  bar in the exhaust pipe). [Appendix A1](#) shows the effects of different sizes of the surge tanks on the intake and exhaust pressure pulsations with the comparison of simulation results. Since it is a single cylinder engine, a reservoir was desirable to store the exhaust gas from the previous cycles and to supply it to the following cycles. Exhaust samples for emissions analysis were drawn from downstream of the surge tank, as shown in Figure 3.2. Although sampling downstream of the surge tank resulted in some 'ageing' of the exhaust gas species, it avoided sample biasing caused by pressure pulsations and inhomogeneity in the exhaust gas stream if sampled from immediately downstream of the exhaust port. Downstream of the exhaust surge tank (shown in Figure 3.2), an electrically controlled butterfly valve was used to control the pressure in the exhaust system. This was used to exert a specified back-pressure which would normally have been generated by turbocharger and aftertreatment systems within a vehicle exhaust system.

## **EGR system**

The EGR system (shown in Figure 3.2) was developed for providing fully controllable EGR rate and temperature. The EGR gas flow was driven by setting the exhaust back pressure to be a higher level than the intake pressure. The EGR rate was controlled by adjusting the exhaust back pressure valve and the EGR valve positions simultaneously. A proportional valve was installed in the coolant circuit to control the coolant flow rate through the EGR cooler, thereby controlling the EGR temperature. For most of the work reported here, uncompressed ambient air (at test-cell temperature) was used as the fresh-air intake; as a result, the temperature at the intake manifold could be controlled only with the EGR temperature. The actuators for the exhaust back pressure valve, EGR valve and coolant flow valve were fully electrically controlled through a programmable logic controller (PLC) unit coupled with transistor driver modules.

The custom-built PLC system was used to achieve closed loop control of the exhaust back pressure, EGR valve position and EGR temperature. The controller logic was developed using the Moeller EASY-SOFT V6.22 Pro software. The pressure in the exhaust tank was sent to the PLC as a feedback signal or a proportional-integral-derivative (PID) control algorithm; from this, the controller generated an analogue output to command the valve position via a DC motor. The EGR valve had a valve position feedback which was used as the feedback signal for the closed loop control of the EGR valve position. The EGR temperature was controlled based on temperature measurement downstream of the EGR cooler; another PID algorithm was used to generate the valve position command, which was then sent to the proportional valve in the control circuit. The schematic of the closed loop controllers and their application are shown in Figure 3.3.

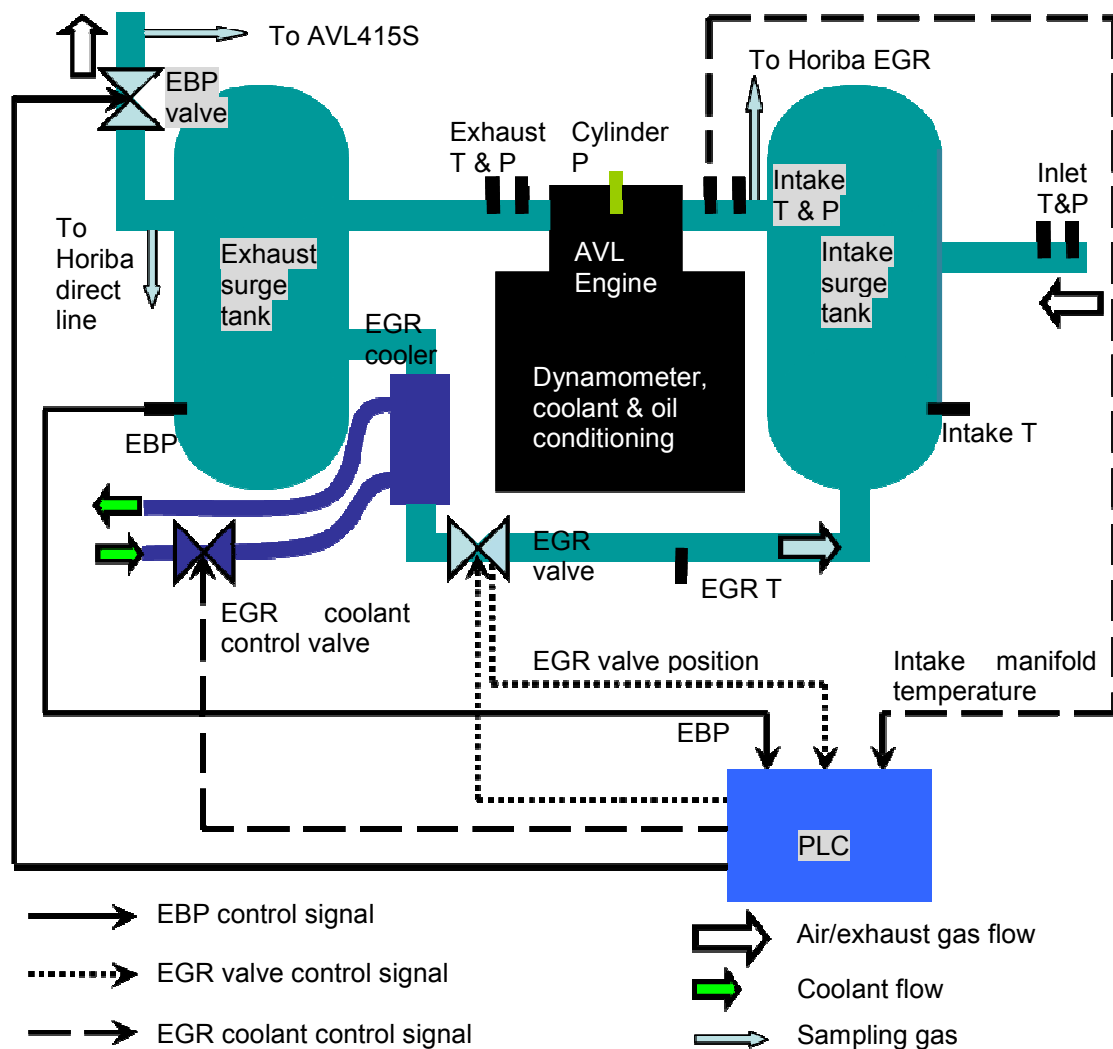


Figure 3.3 Schematic of experimental control system

The maximum EGR rate achieved through adjusting the EGR valve position was about 45%, and then the exhaust back pressure was increased to get higher rates of EGR. With the EGR valve fully open, 3 kPa of increase in exhaust back pressure generated ~70% EGR.

The controllers had been tuned to achieve satisfied control accuracies on exhaust back pressure, EGR rate and intake charge temperature. Through tuning the PID gains and improving the control hardware circuits the following control accuracies were achieved: the back pressure was controlled with an error range of  $\pm 1$  kPa; the EGR rate control accuracy was  $\pm 0.5\%$ , i.e. for a 60% EGR demand, the actual EGR rate was within the range of  $60 \pm 0.5\%$ . The intake charge temperature control was within an error range of  $\pm 3^\circ\text{C}$ .

### **Boost system**

A highly flexible boost system was developed to provide a wide range of intake charge pressures and temperatures. The supercharged air system was designed by another researcher of the research group, Asish Sarangi. A production supercharger driven by an electric motor was used to provide a wide range of boost pressure for the whole engine operation map. An inter-cooler and an electric heater were used to control the intake air temperature to the desired value.

### **3.1.2 Instrumentation and data acquisition**

The research engine facility was fully instrumented with temperature, pressure and flow rate measurement equipment as well as a fuel injector needle lift sensor. A brief description to the most important pieces of instrumentation used in this work is given below; further details on the instruments used, including model number, ranges, and accuracies are provided in [Appendix A2](#).

For the diesel fuel flow-rate measurement, an AVL 733 Dynamic Fuel Meter was used. This instrument determined the fuel consumption by the gravimetric balance method. The mass of fuel in a small reservoir was monitored over time to provide a measure of absolute mass consumption. The fuel meter could not provide a stable measurement at a higher frequency than 0.1 Hz; hence it was only used for steady-state measurement.

Temperatures in the exhaust, EGR, engine cooling and auxiliary systems were measured using standard accuracy Omega K-type thermocouples with diameter of 3

mm. As the intake manifold temperature is a critical parameter for defining engine operation, this temperature was measured more accurately using an Omega RTD (PT100) probe.

Pressures in the intake air stream and in the intake and exhaust surge tanks were measured using Omega PX219-060G10V and PX219-060GI pressure transducers. The exhaust surge tank pressure was used as feedback for the exhaust back pressure control.

Intake and exhaust manifold pressures were measured at high frequency (at a resolution of  $0.5^{\circ}\text{CA}$ ) with Kistler 4045A5, 0-5bar piezo-resistive absolute pressure transducers. The exhaust pressure transducer was fitted with a water coolant adapter and circuit to avoid damage from the hot exhaust gases.

The in-cylinder pressure was also measured every  $0.5^{\circ}\text{CA}$  with a piezoelectric AVL QC34C flush-mounted water-cooled transducer. The charge signal from the sensor was amplified and converted into measurable voltage by an AVL 3076 carrier amplifier which filtered the signal at a frequency of 200 kHz. The in-cylinder pressure data collection process was kept the same for all the test conditions. Cylinder pressure data was collected for over 150 consecutive cycles. The relative pressures recorded from the in-cylinder pressure transducer were referenced to the intake manifold pressure around the end of the intake stroke, just before the start of the compression stroke and approximately  $26^{\circ}\text{CA}$  before the intake valve closed. To reduce the influence of measuring noise, the average pressure over  $20^{\circ}\text{CA}$  (from BDC to  $20^{\circ}\text{CA}$  after BDC - 40 samples) from both the intake manifold and in-cylinder pressure measurements were recorded. The in-cylinder pressure was then adjusted to be the same as the intake manifold pressure over this period ('pegging' of the pressure signal).

The fuel injector needle lift was measured using a customer built needle lift sensor manufactured and supplied by AVL. The needle lift signal was measured every  $0.5^{\circ}\text{CA}$ . There were two fuel injectors used in this project. One injector was instrumented and was not always available during the study. For the standard non-instrumented injector, a customer built injector drive current measurement equipment was used to find the start and duration of a fuel injection event. A comparison between the needle lift signal and the commanded drive current signal showed that there was a  $1^{\circ}\text{CA}$  delay for the actual needle lift compared to the commanded drive current.

The high pressure fuel pipe pressure had been instrumented with a strain gauge SL31D-2000 pressure transducer and the pressure pulsation in the fuel pipe during fuel injection events was measured every 0.5°CA. A DMS amplifier AVL 3009A02 was used to amplify the signals with a 100 kHz filtration.

The crank location was measured using an AVL 364C crankshaft encoder. It generated an index pulse and 360 to 3600 square waves for every crankshaft revolution. In this study, 720 was chosen which equates to a 0.5°CA resolution. The encoder was indexed to the engine's firing TDC. The pulse offset from the real TDC was measured and used as a correction factor in the data acquisition system.

The individual measurements from both the low-frequency and high frequency instruments were collected through a custom-built data acquisition system. The hardware consisted of two pieces of national instruments (NI) hardware: a cDAQ9172 and a USB6125. Both of these were connected to a PC computer through USB cables. The computer ran LabVIEW 8.5, in which all the data acquisition routines were written. Two main routines were used in this research. One collected high frequency (at 0.5°CA resolution) signals including in-cylinder pressure, intake manifold pressure, exhaust manifold pressure and needle lift (injector drive current) as well as the fast-response emissions analyzers (which will be discussed in the next section). The index pulse and the 0.5°CA resolution square pulses were imported to the digital I/O module as trigger and clock for the high-frequency data collection. The other routines collected all the low frequency data: air and fuel flow rates, temperatures and pressures, and conventional (low-speed response) emissions data, all at a frequency of 1 Hz.

The INCA system provided with the test engine management system (EMS) was used to monitoring the engine fuel injection parameters (pressure/timing/duration) processed by the EMS. It was also the interface for changing the engine fuel injection calibrations. Through INCA, the common rail pressure was controlled with an accuracy of  $\pm 1$  bar. There were four independent injection events designed in the EMS. The injection timing and quantity demand for each of the individual injection events were able to be adjusted through the software interface. The resolution of fuel injection timing control was 0.125 °CA. The commanded fuel injection quantity to the EMS was not exactly the actual mass of fuel injected; hence the values were corrected using the AVL fuel meter. In terms of multiple-injection conditions, the actual mass of fuel injected in each of the injection event was unknown. Thus, the

total fuel injection quantity per cycle was the actual mass of fuel injected and the individual quantity of each event was represented by the commanded values.

## **3.2 Emissions Measurement System**

In this study, a HORIBA MEXA 7100HEGR exhaust gas analyser was used to measure the gaseous emissions and an AVL415 smoke meter was used to measure the smoke emissions. Filter smoke number (FSN) was used here to represent the level of particulate matter emissions. The size distribution and total number of particles were measured using a Cambustion DMS500 fast particulate spectrometer. In order to understand the cyclic behaviour for the engine running at specific operating modes/conditions, a Cambustion NDIR500 fast CO/CO<sub>2</sub> analyser was used to measure the cycle resolved CO and CO<sub>2</sub> emissions.

### **3.2.1 Gaseous emissions measurement**

The bulk of the exhaust emissions measurements in this work were conducted using a HORIBA MEXA7100HEGR analyser. This instrument also measured the intake charge CO<sub>2</sub> concentration, which was then used to calculate the volumetric EGR rate (as will be discussed in Section 3.3). The MEXA7100 measured the concentrations of five species in the exhaust: THC (reported in terms of carbon atoms, C1), oxygen (O<sub>2</sub>), CO<sub>2</sub>, CO and NO<sub>x</sub>. The exhaust sample was filtered and conditioned as required for the various analyzers. The measurements of O<sub>2</sub>, CO and CO<sub>2</sub> were sensitive to temperature and water content in the sample and hence the sample was cooled and all the liquid water was removed from the sample before it was passed to these analyzers. A HORIBA MEXA 485L exhaust gas analyser was used for the operating conditions where the CO emissions were above the maximum measurement limit of the MEXA 7100HEGR. It was a portable instrument designed for vehicle tailpipe testing and its accuracy was much lower than the MEXA 7100HEGR bench. However, it did give an indication of CO levels when the main bench level was exceeded. The THC and NO<sub>x</sub> were sampled 'hot' before any water was removed from the sample. The intake CO<sub>2</sub> used a separate sample-handling system drawing a sample from the intake downstream of the surge tank (as shown in Figure 3.2). The operating principles of the various instruments are provided below:

The THC emissions analyser was based on the flame ionisation detection (FID) method. In this method, the gas to be analysed is introduced into a hydrogen flame passing between two electrodes. The burning of the hydrocarbons produces ions.

The ions are then detected using a metal collector which is biased with a high DC voltage. The current across this collector is thus proportional to the rate of ionisation which in turn is proportional to the number of carbon atoms and hence THC could be found. The analyser has a measurement range of 0-50000 ppm.

The oxygen ( $O_2$ ) analyser was based on the magnetopneumatic condenser microphone detection (MPA) method. By applying an uneven magnetic field to a gas by exciting an electromagnet, it draws gases with paramagnetic susceptibility towards the strongest part of the field, thus increasing the pressure at that location. By exciting alternately two electromagnets, the pressure oscillations can be converted to electrical signals via a condenser microphone. This output increases linearly with oxygen concentration. The measurement range of this analyser is 0-25%.

Both the  $CO_2$  and CO emissions analysers were based on the non-dispersive infrared absorptiometry detection (NDIR) method. It is the current industry standard method of measuring the concentration of carbon oxides (CO and  $CO_2$ ). Each constituent gas in a sample will absorb some infrared light at a particular frequency. By directing an infrared light beam through a sample cell (containing CO or  $CO_2$ ), and measuring the amount of infrared light absorbed by the sample at the necessary wavelength, an NDIR detector was able to measure the volumetric concentration of CO or  $CO_2$  in the sample. As  $H_2O$  vapour absorbs infrared light at the same wavelength, the sampling gas has to be dried through a chiller and water separator before crossing the sample cell. Hence the direct concentration measurement results of  $CO_2$  and CO should be converted to the 'wet' basis which accounts for the  $H_2O$  vapour in the exhaust stream. The measurement range for  $CO_2$  is 0-20% and for CO is 0-5000 ppm (0-10% by MEXA 485L).

The NOx emissions analyser was based on the chemiluminescence detection (CLD) method. In this method, a silicon photo-diode adjacent to the reaction chamber senses the chemiluminescent emitting photons. Firstly, the nitrogen dioxide ( $NO_2$ ) fraction of the gas to be analysed is dissociated to form nitric oxide (NO) by high temperatures. Then, the gas is mixed with ozone ( $O_3$ ), leading to light emitting reactions which is proportional to the concentration of NO. The measurement of the chemiluminescent encompasses the concentration of NO and of  $NO_2$  emissions.

A Combustion NDIR500 fast CO and  $CO_2$  analyzer was used to measure the transient  $CO_2$  concentration in the exhaust manifold. It has a response time of < 8 ms

for a 10% to 90% of full scale change and non-linearity is less than  $\pm 2\%$  full scale. The equipment used a carefully selected wavelength and hence it avoids the interference caused by the water vapour in the exhaust. The exhaust gas stream was sampled from the exhaust manifold upstream of the exhaust surge tank to achieve the cycle resolved measurement.

### **3.2.2 Smoke/particulate measurement**

An AVL415 smoke meter was used to measure the steady-state smoke emissions. It has a defined volume (0.5 litre) of exhaust gas flow through the filter paper. The particles in the exhaust are trapped on the filter paper. The darkness of the filter paper caused by the particles is analysed by a reflective photometer, which gives outputs in filter smoke number (FSN).

A Cambustion DMS500 Fast Particulate Spectrometer was used to measure the aerosol size spectrum from 5 nm to 1000 nm. It has the fastest time response available of 10 spectra/second, 200 ms for a 10% to 90% of full scale change (Cambustion, 2010). The exhaust gas was sampled from downstream of the exhaust surge tank to avoid the influence of the pressure pulsations. The exhaust gas was diluted with a dilution ratio of four and a secondary dilution ratio of two by the compressed air supplied in the engine test cell.

The principle of DMS500 is to use electrical mobility measurement to produce particle size/number spectra. The DMS500 uses a corona discharge to place a prescribed charge on each particle proportional to surface area. The charged sample is then introduced into a strong radial electrical field inside a classifier column. This field causes particles to drift through a sheath flow to the electrometer detectors. Particles are detected at different distances down the column, depending upon their electrical mobility. The outputs from the 22 electrometers are then processed in real time to provide spectral data (Cambustion, 2010).

Further details on the instrumentation used, including ranges, accuracy, and serial numbers, are provided in [Appendix A3](#).

### **3.3 Experimental Parameters**

For the specified operating conditions, different experimental parameters were selected to conduct the experiments for the different research objectives. Individual parameters were investigated for all the test sets, and the interactions among them



were studied for the particular research purposes. In this study, EGR rate, fuel injection pressure, timing and quantity, post fuel injection, engine speed, intake manifold temperature, exhaust back pressure and boost pressure were varied. The results will be presented and discussed in subsequent chapters. The main experimental parameters studied in this research are described in this section.

The fuel injection quantity per cycle was calculated based on the AVL733 fuel meter measurement,

$$m_f = \frac{\dot{m}_{\text{fuel}} \left( \frac{1e6}{60} \right)}{\frac{N}{2}} \quad (3-1)$$

where  $m_f$  was the fuel injection quantity in mg/stroke, the  $\dot{m}_{\text{fuel}}$  was the fuel flow meter reading in kg/h,  $N$  is the engine speed (in revolutions per minute).

As discussed previously, in this work the engine load will be represented using the in-cylinder performance. This is represented by the indicated mean effective pressure (IMEP), which only represents the work done on the piston and excluded any frictional losses (either within the engine or in driving auxiliaries). It was defined as

$$\text{IMEP} = \frac{\oint p dV}{V_d} \quad (3-2)$$

where  $p$  was the in-cylinder pressure at given crank angle,  $V$  was the instantaneous cylinder volume at the same crank position,  $V_d$  was the cylinder displacement volume (Heywood, 1988). The definition in (3-2), which is for net IMEP, includes the work done during the charge exchange process. This work does not generally relate strongly to the engine combustion behaviour and performance. As a result, to provide the most representative comparisons when investigating the combustion characteristics, the gross indicated mean effective pressure ( $\text{IMEP}_g$ ) is used instead via the expression

$$\text{IMEP}_g = \frac{\oint_{\text{comp,expansion}} p dV}{V_d} \quad (3-3)$$

This is equivalent to the IMEP (3-2) except for the fact that the integral is conducted over the compression and expansion strokes only. The rate-of-change of the in-cylinder pressure can also be used to evaluate the rate at which chemical energy is being released during the combustion event (commonly referred to as the net heat release rate (Heywood, 1988) -  $HRR_{net}$ ), given by:

$$HRR_{net} = \frac{\gamma}{\gamma - 1} p \frac{dV}{d\theta} + \frac{1}{\gamma - 1} V \frac{dp}{d\theta} \quad (3-4)$$

where the  $\theta$  was the crank angle and  $\gamma$  was the specific heat ratio ( $c_p / c_v = 1.33$ ) assumed constant. The net heat release rate represented the rate of energy release from the combustion processes less wall heat transfer and crevice volume losses. By integrating the heat release rate, the total heat released (THR) by the combustion process was estimated from

$$THR = \int HRR_{net} d\theta \quad (3-5)$$

The integration starts before the start of fuel injection and ends at 50°CA ATDC. Several specific points on the integrated heat release profile were used as the milestones of the combustion process, i.e. the crank angle of 5%, 10%, 50% and 90% of the total heat release. Of these, the crank angle for 5% THR (CA5) was used to define the start of the combustion (SoC) and the crank angle for the midpoint of the THR (CA50) was used to indicate the phase of the combustion. The ignition delay in crank angle was calculated by subtracting the commanded start-of-injection timing from SoC. Since the SoC is not the actual start of ignition timing in the fuel-air mixture, the ignition delay is not exactly the same as the duration between the Sol and the exact igniting. For the low temperature diesel combustion (LTC) cases, the total heat release during the cool flame reaction period was often less than the criterion (5% THR) for the SoC calculation. In these cases, the start of cool flame reaction was defined as being the crank angle at which the HRR crosses the x-axis (i.e. changes from negative to positive). This is discussed in Chapter 5.

Both the IMEP and the HRR are based on 150 cycle averages of the cylinder pressure measurements. Cyclic variability in the in-cylinder pressure, including variations in peak cylinder pressure and its crank angle and in  $IMEP_g$  were found to be useful measures of combustion stability when reported in the form of coefficient of variation (CoV) defined by

$$\text{CoV}(\text{IMEP}_g) = \sigma(\text{IMEP}_g)/\mu(\text{IMEP}_g) \quad (3-6)$$

where  $\sigma$  and  $\mu$  are the standard deviation and the mean values, respectively, over a number of consecutive combustion cycles.

In this study, the intake charge was diluted using exhaust gas recirculation (EGR) and a volumetric based EGR rate was calculated. Both the intake and exhaust  $\text{CO}_2$  volume (or mole) fraction were measured as described in the previous section. Combining these values with the ambient  $\text{CO}_2$  concentration ( $\sim 0.03\%$ ) can be used to define EGR rate as

$$\text{EGR}\% = \frac{[\text{CO}_2]_{\text{int}} - [\text{CO}_2]_{\text{amb}}}{[\text{CO}_2]_{\text{exh}} - [\text{CO}_2]_{\text{amb}}} \cdot 100 \quad (3-7)$$

where suffices int, exh, amb refer to intake, exhaust and ambient respectively. However, EGR rate only represents the volume fraction of exhaust gas recirculated into the intake charge. The variation in the exhaust gas composition for different engine operating conditions made the dilution effects non-comparable between different conditions. For example, the  $\text{O}_2$  concentration in the exhaust gas from a high load operating condition is lower than that from a low load condition due to the different fuel injection quantities. With an identical EGR rate for these two load conditions, the EGR gas replaces the same fraction of the fresh air. However, the overall intake charge  $\text{O}_2$  concentrations will be different for these two load conditions due to the difference in EGR gases  $\text{O}_2$  concentration. Thus, intake oxygen volume/mole fraction was one of the alternatives which can represent the dilution effects uniformly

$$[\text{O}_2]_{\text{int}} = [\text{O}_2]_{\text{air}} \cdot \frac{(100 - \text{EGR}\%)}{100} + [\text{O}_2]_{\text{exh}} \cdot \frac{\text{EGR}\%}{100} \quad (3-8)$$

where  $[\text{O}_2]_{\text{air}}$  represents the mole fraction of oxygen in the fresh air and  $[\text{O}_2]_{\text{exh}}$  represents the mole fraction of oxygen in the exhaust gas.

Oxygen based equivalence ratio  $\Phi$  provided the information on the fuel and oxidant mixture in the combustion chamber, which was defined as

$$\phi = \frac{\left( \frac{m_f}{m_{\text{oxygen}}} \right)_{\text{actual}}}{\left( \frac{m_f}{m_{\text{oxygen}}} \right)_{\text{stoich}}} \quad (3-9)$$

where the  $m_{\text{oxygen}}$  was the total oxygen mass trapped in the combustion chamber, including the oxygen from the fresh air and from the recirculated exhaust gas. This is different from the conventional equivalence ratio calculation which only takes the oxygen in the fresh air into account. In this study, the high-EGR diesel combustion was very sensitive to the intake charge  $O_2$  concentration. Hence, the  $O_2$  in the EGR gases were combined into the equivalence ratio calculation.

By defining the engine speed, fuel injection quantity, IMEP, intake oxygen fraction and combustion phasing (CA50), the operating conditions of the single cylinder engine was fully defined. Gross indicated thermal efficiency  $\eta_{t,\text{gross}}$  was used as the indicator of the engine efficiency, which was given by

$$\eta_{t,\text{gross}} = \frac{\text{IMEP}_g \cdot V_d}{m_f \cdot Q_{\text{LHV}}} \quad (3-10)$$

where  $Q_{\text{LHV}}$  represents the lower heating value of the diesel fuel on a mass basis.

Combustion efficiency  $\eta_{\text{comb}}$  is another important parameter for accessing the quality of low temperature diesel combustion. It was defined by total fuel low energy minus the low heating value of the incomplete combustion products (CO, THC) over the total fuel low energy:

$$\eta_{\text{comb}} = \frac{(m_f \cdot Q_{\text{LHV}}) - (m_{\text{CO}} \cdot Q_{\text{LHV,CO}}) - (m_{\text{HC}} \cdot Q_{\text{LHV,HC}})}{(m_f \cdot Q_{\text{LHV}})} \quad (3-11)$$

In this study, only qualitative combustion efficiency was introduced since the CO measurement was not always available during the experimental work due to the high CO levels encountered in some LTC operating conditions.

### 3.4 1D Engine Simulation

Two separate 1-D engine models were used to support the experimental programme. One related to the research single-cylinder engine described in Section 3.1, while the

other relates to a four-cylinder engine that is generally similar to the single-cylinder engine. Both models used the Ricardo WAVE 1D engine simulation program.

### Single-cylinder engine model

This model was developed to further investigate the performance of the engine and to aid in the design of the air exchange section (for e.g. see Section 3.1.1 regarding the sizing of the surge tanks). As WAVE does not provide a reliable combustion model, experimental heat release rate profiles were used as the input for the combustion processes in the model. A fully mixed scavenging model was selected to simulate the gas exchange during the valve overlap period; this has been considered to be the most suitable scavenging model for four stroke engines (Hiereth *et al.*, 2006). The heat transfer and friction were simulated using the standard models embedded in the software package.

The model, shown in Figure 3.4, is based on the available information about the single cylinder engine's geometry and the custom-built air-exchange system. The performance and accuracy of the model had been validated with experimental data for different combustion modes as shown in [Appendix A4](#).

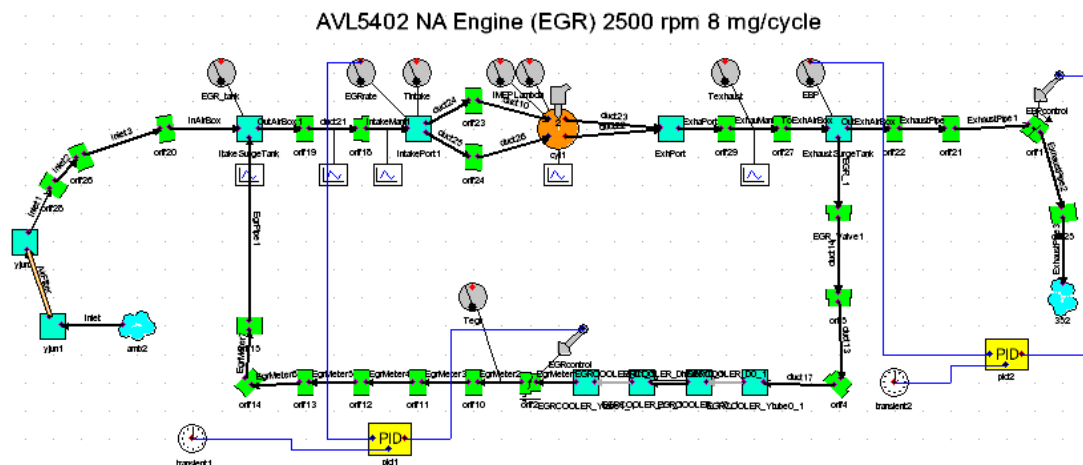


Figure 3.4 1D single-cylinder research engine WAVE model

The main purpose for developing the model shown in Figure 3.4 was to evaluate the charge exchange processes. Particular interest was in the estimation of the trapped residual gas fraction for different operating conditions (see Chapter 6). It was important to account for the residual gas fraction for low temperature diesel combustion conditions because of its potential impact on the dilution of the in-cylinder charge.

### ***Multi-cylinder engine model***

To evaluate the performance of an engine operating in LTC in a real application, a four cylinder Puma diesel engine model was provided by Ford Motor Company. For the purpose of this study, the original Ford model had to be modified to operate under LTC conditions (the original model, while including an EGR loop, only used relatively low EGR levels – on the order of 20%). The original model has the EGR valve controlled by a PID controller requesting the intake airflow rate for different operating conditions. For this study, a specific EGR rate for each operating point is desirable. Thus, an EGR rate controller based on EGR rate sensing in the intake manifold was set up. The new PID controller had its gains tuned to get a fast and accurate EGR rate control. The original VGT controller was based on the boost pressure sensing and controlled the nozzle vane position to achieve the requested boost pressure, and hence was not altered in the model.

One of the objectives of the multi-cylinder engine model was to evaluate the engine operating conditions that would be encountered during an LTC transient. As a result, experimentally-based in-cylinder conditions (i.e., HRR) were not available to use in the combustion model. Instead, WAVE's diesel Wiebe model was used, based on the commanded fuel injection quantity and engine speed. The fuel injection timing was controlled based on the CA50 sensing in the model. The fuel injection pressures were increased in the modified model, as the fuel injection pressures in the original Ford model were about 200 bar lower than those from the AVL single-cylinder engine maps. The higher fuel injection pressures are also desirable for high EGR diesel combustion. However, the fuel injection pressure in the model had insignificant influence on the combustion simulation. The combustion model may not necessarily be precisely correct, however, the main objective of the modelling was to identify the fuel flow, engine speed, and air- and EGR- flow rates. It was not designed to provide predictive combustion modelling results on this work. In-cylinder performance will be evaluated using the research engine operating at test constitutions defined on the basis on the 1-D model results. The model can predict the gases exchange processes such as turbocharger performance and EGR flow which are critical parameters for the transient performance and emissions during high EGR operation.

## **3.5 Design of Experiments**

For some of the aspects of this work, design of experiment (DoE) techniques were used. Throughout the work, tests were conducted with randomization (although this

was sometimes restricted due to the difficulty in exactly replicating EGR levels at all test points). In Chapter 7, more advanced DoE techniques, including half-fractional factorial tests and a Taguchi orthogonal experimental design were used; details of these methods are introduced in that chapter.

### **3.5.1 Operating conditions**

The engine operating conditions for this study were selected based on analysis of the engine behaviour within a standard NEDC driving-cycle. The principle of the selection was to study operating conditions that were representative of the operating points in the driving-cycle. In general, two engine speeds were used: 1500 rpm and 2500 rpm, 8 mg/cycle fuelling and 16 mg/cycle fuelling cases were studied in the research, which cover the low to intermediate speed and load (~3 to 6 bar gross IMEP) conditions of the engine. As reviewed in Chapter 2, the operational range of low temperature diesel combustion regimes is limited to low to intermediate load conditions. Expanding the operational range of the low temperature combustion have been studied by different researchers (Kimura *et al.*, 2001; Ogawa *et al.*, 2007), however, it is out of the scope of this thesis.

### **3.5.2 Analysis of variance (ANOVA)**

ANOVA is a statistical tool to interpret the results from a group of experiments with multiple factors and multiple levels. ANOVA was used in this work (Chapter 7 only) to identify which, main effects and interactions between engine operating parameters were statistically important. An F-test can be used to identify the confidence in the effects of the identified factor. Table 3.3 lists an example of ANOVA for a  $2^3 \times 3^3$  half fractional factorial experimental design. The highlighted contents indicate the factors which show statistically significant influences on the observation. The percentage contribution of these factors to the changes in the experimental result was also highlighted.

Table 3.3 Example of ANOVA routine  
ANOVA table of half fractional factorial test results on CO emissions (1500 rpm 8 mg/cycle)

Factors	f	SS	V	F	P (%)
EGR (A)	1	7.24	7.24	156.75#	51.24
Fuel Q (B)	2	5.25	2.626	56.85*	37.17
Tint (C)	2	0.51	0.257	5.57	3.64
Speed (D)	2	0.05	0.027	0.58	0.38
A X B	2	0.36	0.181	3.92	2.56
A X C	2	0.47	0.233	5.04	3.29
B X C	4	0.15	0.038	0.81	1.06
error	2	0.09	0.046	-	0.54
Total	17	14.13		-	100

+ at least 90% confidence

\* at least 95% confidence

# at least 99% confidence

The f indicates the degree of freedom for the factors and interactions.

$$f_T = N - 1 = 17, N: \text{total test number, } 18;$$

$$f_A = k_A - 1 = 1, k_A: \text{levels of factor A, } 2;$$

$$f_B = k_B - 1 = 2, k_B: \text{levels of factor B, } 3;$$

$$f_{AB} = f_A * f_B = 2;$$

$$f_e = f_A - f_B - f_C - f_{AB} - f_{AC} - f_{BC} = 2 \quad (3-13)$$

SS is the sum of squares, which can be decomposed into different components, and the variation due to factor A is given by

$$SS_A = \frac{A_1^2}{n_{A1}} + \frac{A_2^2}{n_{A2}} - \frac{T^2}{N} \quad (3-14)$$

where  $A_1$  and  $A_2$  are the total variations at each level of factor A,  $n_{A1}$ , and  $n_{A2}$  are the test numbers for each level of factor A, and T is the total variations for the whole test set.

The variation due to factor B is given by

$$SS_B = \frac{B_1^2}{n_{B1}} + \frac{B_2^2}{n_{B2}} + \frac{B_3^2}{n_{B3}} - \frac{T^2}{N} \quad (3-15)$$

where  $B_1$ ,  $B_2$  and  $B_3$  are the total variations at each level of factor B,  $n_{B1}$ ,  $n_{B2}$  and  $n_{B3}$  are the test numbers for each level of factor B.



The variation due to interaction between factors A and B is given by

$$SS_{A \times B} = \frac{(A_1B_1)^2}{n_{A_1B_1}} + \frac{(A_1B_2)^2}{n_{A_1B_2}} + \frac{(A_1B_3)^2}{n_{A_1B_3}} + \frac{(A_2B_1)^2}{n_{A_2B_1}} + \frac{(A_2B_2)^2}{n_{A_2B_2}} + \frac{(A_2B_3)^2}{n_{A_2B_3}} - \frac{T^2}{N} - SS_A - SS_B \quad (3-16)$$

where  $A_iB_j$  indicates the total variations when the factor A at level i and factor B at level j,  $n_{A_iB_j}$  indicates the test number when the factor A at level i and factor B at level j.

The total variation is

$$SS_T = \left[ \sum_{i=1}^N y_i^2 \right] - \frac{T^2}{N} \quad (3-17)$$

The variation due to error factors is given by

$$SS_e = SS_T - SS_A - SS_B - SS_C - SS_D - SS_{A \times B} - SS_{A \times C} - SS_{B \times C} \quad (3-18)$$

The mean square (V) is a result of the sum of square (SS) divided by degree of freedom (f). F is the ratio of a sample/interaction variation to the error variance. The ratio of variances between the factor A and error factor is

$$F_A = \frac{V_A}{V_e} \quad (3-19)$$

The F value is used to do an F-test to identify whether the difference between the main factor/interaction and the error factor is significant.

The percent contribution (P) indicates the relative power of the main factor and/or interactions to the variations. The percent contribution of factor A is given by

$$P_A = \frac{SS_A}{SS_T} \quad (3-20)$$

A pooling technique was used in this study to have better error variance estimation. Some of the main factors and/or interactions show insignificant influences on the experimental results. The minor effects derived from these factors can be combined with the error variance, leading to an increased degree of freedom for the error factor. This can be used to improve the sensitivity of the F-test and help to identify the important factors in the experiment. More detailed information about DoE and ANOVA can be found in the literature (Ross, 1996)

In the next chapter, the effects of different levels of EGR and fuel injection parameters on the research engine performance and emissions are introduced.

## Chapter 4 High EGR Diesel Combustion\*

### 4.1 Introduction

Diesel LTC, as introduced in Chapter 2, offers substantial benefits in terms of reduced NO<sub>x</sub> and smoke emissions. However, THC and CO emissions are increased while efficiency is degraded and instability increases. The purpose of this research, as identified in Chapter 1, is to investigate these effects. Before undertaking a detailed study on the diesel combustion with high EGR, a basic understanding of the engine operation with different levels of EGR was considered essential.

High EGR LTC can be achieved on a diesel engine without requiring significant changes to the combustion system. A LTC system uses a conventional diesel fuel injection system and combustion chamber design. This avoids the sacrifices in combustion optimisation during higher load conventional operation of the engine. With traditional near-TDC fuel injection timing, the combustion process is more controllable compared to HCCI and PCCI combustion regimes.

Emissions of NO<sub>x</sub> can be reduced significantly from conventional diesel combustion by implementation of EGR, but this usually leads to high PM emissions unless very high levels of EGR are used under LTC conditions. As introduced in Chapter 2, the PM emissions are a combined result of PM formation and oxidation. As fuel-rich mixtures are the main source of PM formation, improvement in fuel charge mixing could reduce the PM formation rates (Dec, 1997; Heywood, 1988; Idicheria *et al.*, 2005). An increase in the PM oxidation rate during the late part of the combustion could also reduce the engine-out emissions. The effects of fuel injection pressure, timing and post fuel injection on diesel combustion and emissions were reviewed in Chapter 2. Increases in fuel injection pressure, advances in injection timing and carefully selected post fuel injection events can all reduce the engine-out PM emissions. In this chapter, these operation parameters are also varied under high-EGR realised diesel LTC mode to investigate their influences on the combustion process and emissions.

---

\* Part of the work presented in this chapter was previously presented at the SAE 2010 World Congress, April 2010, Detroit, MI, USA. S. Cong, G. P. McTaggart-Cowan, C. P. Garner, Effects of Fuel Injection Parameters on Low Temperature Diesel Combustion Stability, SAE paper 2010-01-0611.

This chapter aims to elucidate the effects of high rates of EGR on the performance of, and emissions from the research engine over a range of engine speed and fuelling conditions. The objective of this study is to achieve diesel LTC (i.e. nearly smokeless, NO<sub>x</sub>-free) in the test engine. Test results of different levels of EGR on combustion and emissions are introduced. Then, the differences in diesel LTC combustion among the various fuelling and speed are evaluated. The influences of fuel injection timing, pressure and post fuel injection on diesel LTC are also investigated experimentally. From these results, an improved understanding of diesel engine combustion with high rates of EGR has been achieved.

## **4.2 Experimental Methodology**

As the research engine (described in Chapter 3) had not previously been operated with EGR, the first goal of this work was simply to achieve high-EGR LTC. Four operating conditions of 1500 rpm and 2500 rpm with 8 mg/cycle and 16 mg/cycle fuel injection quantities were investigated (as discussed in Section 3.5). The first step in the research was to vary the EGR from low to high levels at each of the four operating conditions. Then, once the general effects of EGR had been established, the effects of specific fuel injection parameters on the combustion and emissions of the LTC operation mode were investigated.

One of the primary objectives of this study was to investigate the effects of different levels of EGR rate on the engine speed and fuelling conditions specified in Chapter 3. The fuel injection pressure was held constant throughout the EGR rate test. With increasing EGR rate, the combustion event was delayed significantly due the increased ignition delay caused by the charge dilution. Hence, the start of fuel injection timing was advanced to avoid a very late combustion process and misfire at high EGR rate conditions. The cylinder pressure rise rates were constrained to below 10 bar/°CA, which is close to the values derived from the engine running without EGR following the engine fuelling maps in the ECU. The EGR (cool-out) temperature was set to 90°C and 120°C with variations less than ±10°C for the 8 mg/cycle and 16 mg/cycle conditions respectively.

The engine operating parameters, such as fuel injection pressure, timing and EGR temperature, may not be optimised in efficiency and emissions for each EGR level. Nor was it the purpose of this work to develop a comprehensive engine calibration. However, the tests reported in this chapter should demonstrate the capability of the research engine to run with a wide range of EGR rates and should provide the

baseline conditions at the selected operating conditions that will be used in the later chapters of this thesis. The operating parameters for the EGR tests are given in Table 4.1.

Table 4.1 Operating conditions for EGR test

Parameter	CASE1	CASE2 <sup>†</sup>	CASE3	CASE4
Speed (rpm)	1500	1500	2500	2500
Fuel Quantity (mg/cycle)	8	16	8	16
Sol (°CA ATDC)*	-33 to -9	-24 to -3	-33 to -9	-24 to -6
Fuel Pressure (bar)	500	650	600	900
EGR Rate (%)	10 - 70	10 - 60	10 - 65	10 - 60
EGR Temperature (°C)	90	120	90	120

\* The Sol was varied alongside the changing EGR rate.

<sup>†</sup> For the 1500 rpm 16 mg/cycle case, a pilot fuel injection was used to control the maximum cylinder pressure rise rate when the EGR rate was lower than 40%.

Fuel injection parameters, such as fuel injection pressure and timing were changed to investigate their effects on LTC combustion behaviour and emissions. The EGR rate and temperature were kept constant while the fuel injection pressure and timing were independently varied. Table 4.2 lists the parameters and their ranges for this study.

Table 4.2 Operating conditions for fuel injection parameters test

Test group	EGR (%)	Sol (°CA ATDC)	Fuel pressure (bar)	Intake temperature (°C)	O <sub>2</sub> Equivalence ratio ( <i>sim</i> *)
1500 rpm 8 mg/cycle, Sol	65	-21 to -15	500	50	0.62
1500 rpm 8 mg/cycle, Pinj	65	-18	450-550	50	0.62
2500 rpm 8 mg/cycle, Sol	65	-33 to -27	650	60	0.60
2500 rpm 8 mg/cycle, Pinj	65	-27	550-650	60	0.60
1500 rpm 16 mg/cycle, Sol	54	-24 to -6	900	70	0.93
1500 rpm 16 mg/cycle, Pinj	50	-18	800-1100	50	0.86
2500 rpm 16 mg/cycle, Sol	50	-24 to -12	900	80	0.82
2500 rpm 16 mg/cycle, Pinj	50	-21	800-1200	80	0.82

\* Oxygen based equivalence ratio derived from 1D engine model results

For the 16 mg/cycle operating conditions, post fuel injection was introduced to evaluate the possibility of reducing PM emissions. Through elevating the post combustion temperature and enhancing late-cycle mixing, previous work (Yun *et al.*, 2007) has suggested that the PM oxidation can be enhanced. With constant EGR rate and temperature, fuel injection pressure and timing, the post fuel injection quantity and timing were varied to investigate their influences on the high EGR diesel

combustion. The total fuel injection quantity was kept constant at 16 mg/cycle for this study. Thus, the main fuel injection quantity varied with the change in the post fuel injection quantity. The operating parameters are listed in Table 4.3.

Table 4.3 Operating conditions for post fuel injection test

Operating conditions	EGR (%)	SoI (°CA ATDC)	Post fuel injection quantity (mg)*	Post fuel injection timing (°CA ATDC)	Fuel rail pressure (bar)	Intake manifold temperature (°C)
1500 rpm 16 mg/cycle	42	-9	1.2 - 2.4	9	800	50
1500 rpm 16 mg/cycle	47	-21	1.2	0 - 12	800	50
2500 rpm 16 mg/cycle	50	-18	3 - 5	6	1200	90
2500 rpm 16 mg/cycle	56	-24	1.2	-3 - 9	900	90

\* Commanded fuel injection quantity

As discussed in Section 3.1, the total fuel injection quantity per cycle could be calculated from the fuel meter as described in Equation (3-1). However, the actual fuel injection quantity for the individual injection events of a multiple-injection condition was not known. The commanded post fuel injection quantity may not be the exact fuel mass injected; however, it provided a reference to the relative quantity of post fuel injection. Thus, the commanded fuel injection quantity for the post fuel injection was used in this study.

As the engine combustion became very sensitive to the variations of EGR rate when it was running under the LTC regime, the tests were not fully randomised. Blocks were used in the experiment design to have a relatively stable EGR rate and make the results more comparable, i.e. the fuel injection parameters were randomised at constant EGR valve position and EBP valve position which realised a stable EGR flow.

Low-frequency emissions measurements were used for this work, as introduced in Section 3.2. Because of the high CO levels encountered with LTC, for some of the operating conditions the CO results are not presented. Where CO was particularly important (for example, in the post injection tests) the Horiba MEXA 485L analyzer was used to estimate CO emissions up to 10% by volume. PM emissions were measured using the AVL smoke meter; further characterization at selected conditions was provided by the DMS500 particle spectrometer.

## 4.3 Results

Diesel combustion processes vary significantly with different EGR rates. The existence of EGR in the combustion chamber influences the oxygen-fuel ratio, ignition delay, combustion duration and heat release rate. In turn, these variations in the combustion process affect the engine performance and emissions. The first set of tests will evaluate engine performance and emissions over a wide range of EGR levels. Subsequent tests will be conducted under the identified LTC conditions to investigate the influences of fuel injection parameters. These effects are expected to be different from under conventional diesel combustion. The details of these influences are investigated over a set of specific LTC operating points selected from the tests.

### 4.3.1 EGR rate test

For each of the four operating conditions identified in Section 3.5, tests were conducted where the EGR level was increased from zero to the highest EGR level for which stable combustion could be maintained.

### Emissions

The research engine's NO<sub>x</sub> and smoke emissions over the range of EGR and operating conditions considered are shown in Figures 4.1 and 4.2. They illustrate the classic LTC emissions profile as shown in the literature, i.e. (Ogawa *et al.*, 2007). When the EGR rate was increased above a certain limit for each of the operating conditions (illustrated by the vertical lines in the figures), the NO<sub>x</sub> emissions approached zero (< 10 ppm) and the smoke numbers started to drop quickly. However, the THC and CO emissions increased significantly, indicating reduced combustion efficiency. This demonstrates another trade-off between the smoke emissions and the THC and CO emissions for diesel engines running with high levels of EGR. The sources of THC and CO here are expected to have included the flame quenching due to the low combustion temperature, a lack of oxygen due to the high rate of dilution from EGR and over-mixing of the fuel due to the significantly increased ignition delay.

The smoke emissions at the 8 mg/cycle cases (Figure 4.1) showed different behaviour between the 1500 rpm and 2500 rpm operating conditions. The smoke numbers were generally lower for 1500 rpm cases which may be due to a longer cycle time available to oxidise the particulates formed in the combustion process.

However, when shifted into the LTC regime, the smoke number dropped more rapidly with the increases in EGR rate (reduction in intake oxygen concentration) for the 2500 rpm than for the 1500 rpm operating conditions.

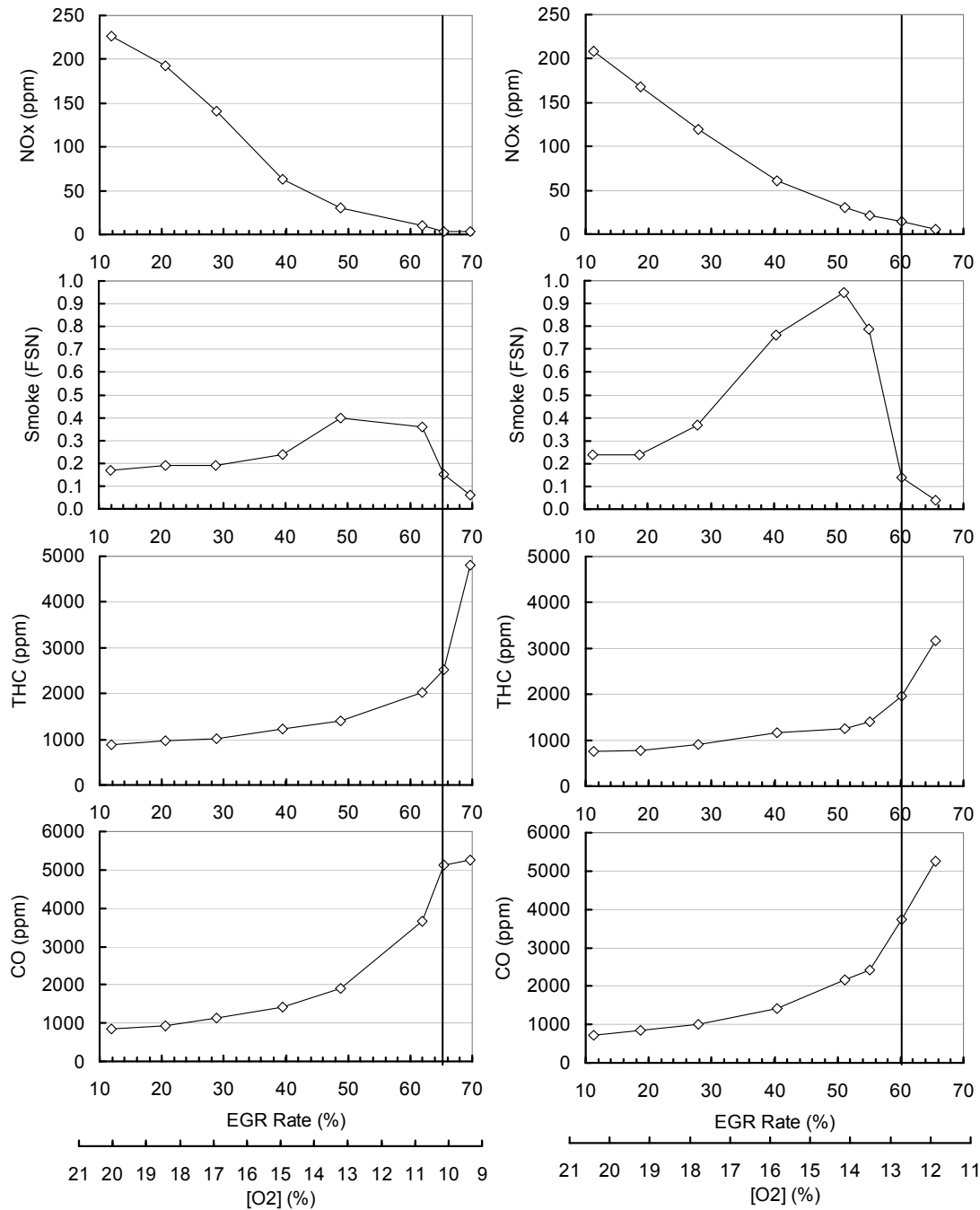


Figure 4.1 Effects of EGR rate on diesel engine emissions at 8 mg/cycle fuelling conditions (Left column: 1500 rpm; Right column: 2500 rpm)

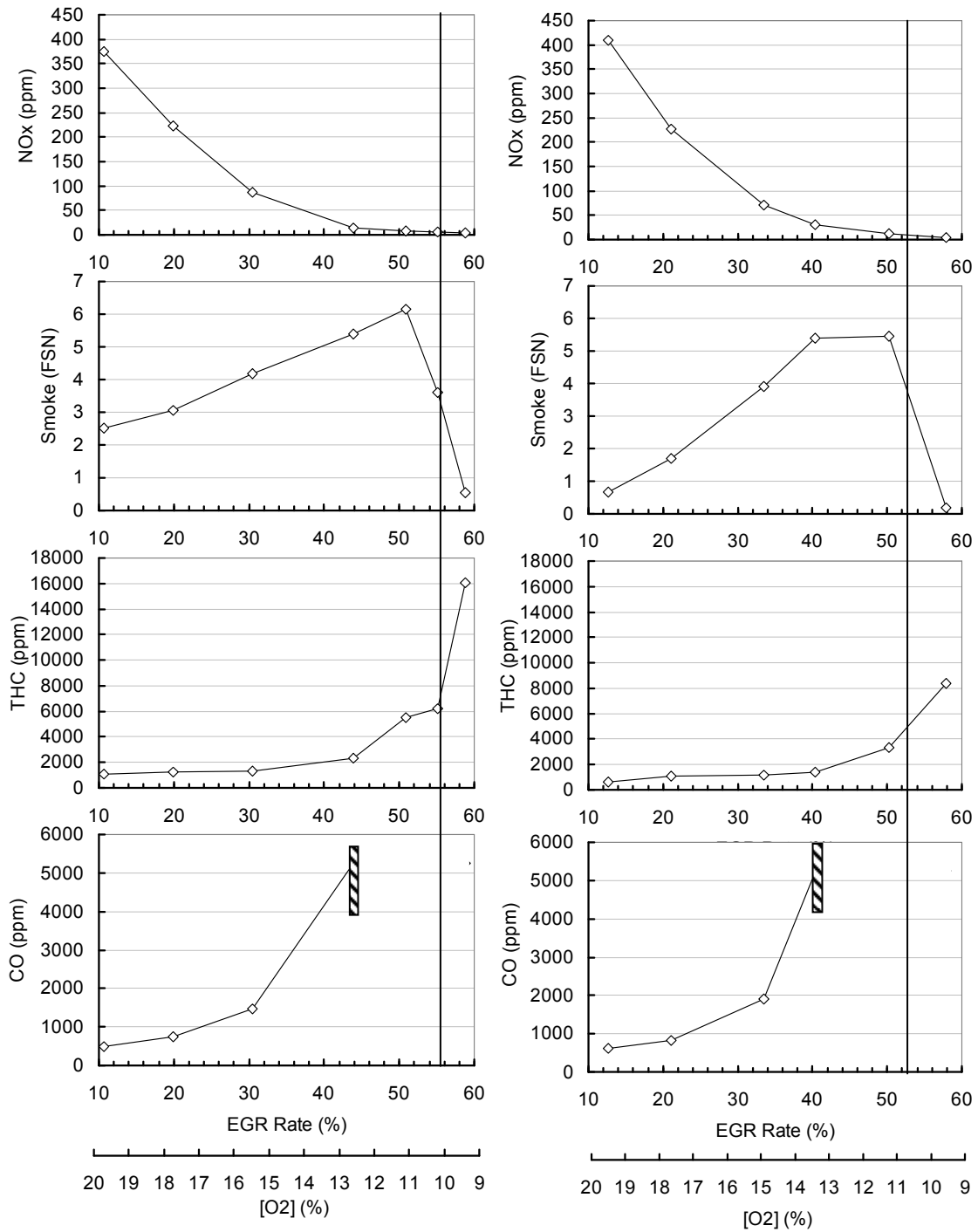


Figure 4.2 Effects of EGR rate on diesel engine emissions at 16 mg/cycle fuelling conditions (Left column: 1500 rpm; Right column: 2500 rpm)

At high EGR, the stronger air motion in the combustion chamber generated by the higher piston velocity at 2500 rpm may have improved the mixing and contributed to a more homogeneous combustion process, and hence more significantly reduced smoke emissions. This also indicates that, with high levels of EGR, the engine-out PM emissions may be more dominated by the particulate formation rate as the oxidation rate of particulate under this condition might be limited. Approaches that



can improve the mixing are thought to be beneficial for low smoke diesel combustion because the increased homogeneity in the charge is expected to reduce the particulate formation rates. This suggests that fuel injection parameters may have a significant impact on LTC; as a result, these are going to be evaluated in this chapter.

For the 16 mg/cycle cases, shown in Figure 4.2, there was less of an effect of speed than for the 8 mg/cycle cases. The smoke numbers were slightly lower for the 2500 rpm conditions in the low temperature combustion regime. The improvement in mixture homogeneity through enhancing charge motion may have marginal effects for the smoke emissions from the overall fuel-rich LTC regime.

The effects of fuel injection quantity on LTC are more significant than the effects of engine speed. For the 8 mg/cycle fuelling conditions, intake oxygen concentrations of less than 12% were the threshold for the engine to operate under the nearly smokeless, NO<sub>x</sub>-free LTC combustion mode; this was achieved without any penalty in efficiency by advancing the injection timing. Higher engine speeds improved the mixture formation and extended the LTC operating range to relatively higher oxygen concentration conditions. For the 16 mg/cycle conditions, at 12% intake oxygen, the smoke FSN reached its peak. The intake oxygen concentration required to achieve LTC combustion was reduced to 9~10%. This resulted in less oxygen being available to the combustion processes, leading to significantly reduced combustion efficiency, and THC and CO emissions substantially above those seen at lower load.

### **Combustion process**

An increase in EGR rate led to a longer ignition delay (as defined in Chapter 3, the duration between start of fuel injection and 5% total heat release). The reduction in oxygen concentration is the main contributor to these changes. As shown in Figures 4.3 and 4.4, the ignition delay increased more significantly at the highest EGR rates. The charge temperature was increased by the high level of EGR, which tended to reduce the ignition delay, while the dilution effects of the EGR increased it due to the reduction in oxygen concentration.

The combustion phasing indicated by CA<sub>50</sub> was able to be advanced for the high EGR rate conditions. Due to the lower heat release rate caused by the intake charge dilution, the peak cylinder pressure rise rate could be retained below the limit of the 10 bar/°CA for more advanced injection timings. The higher EGR rate also avoided the increase in NO<sub>x</sub> emissions normally caused by advancing the combustion

phasing. For the highest EGR rate tested for each of the cases, the CA50 was retarded significantly no matter how much the fuel injection timing was advanced. This indicates that, once the oxygen concentration became too low for the combustion process to be sustained, the effects of advancing fuel injection timing on combustion phasing becomes small.

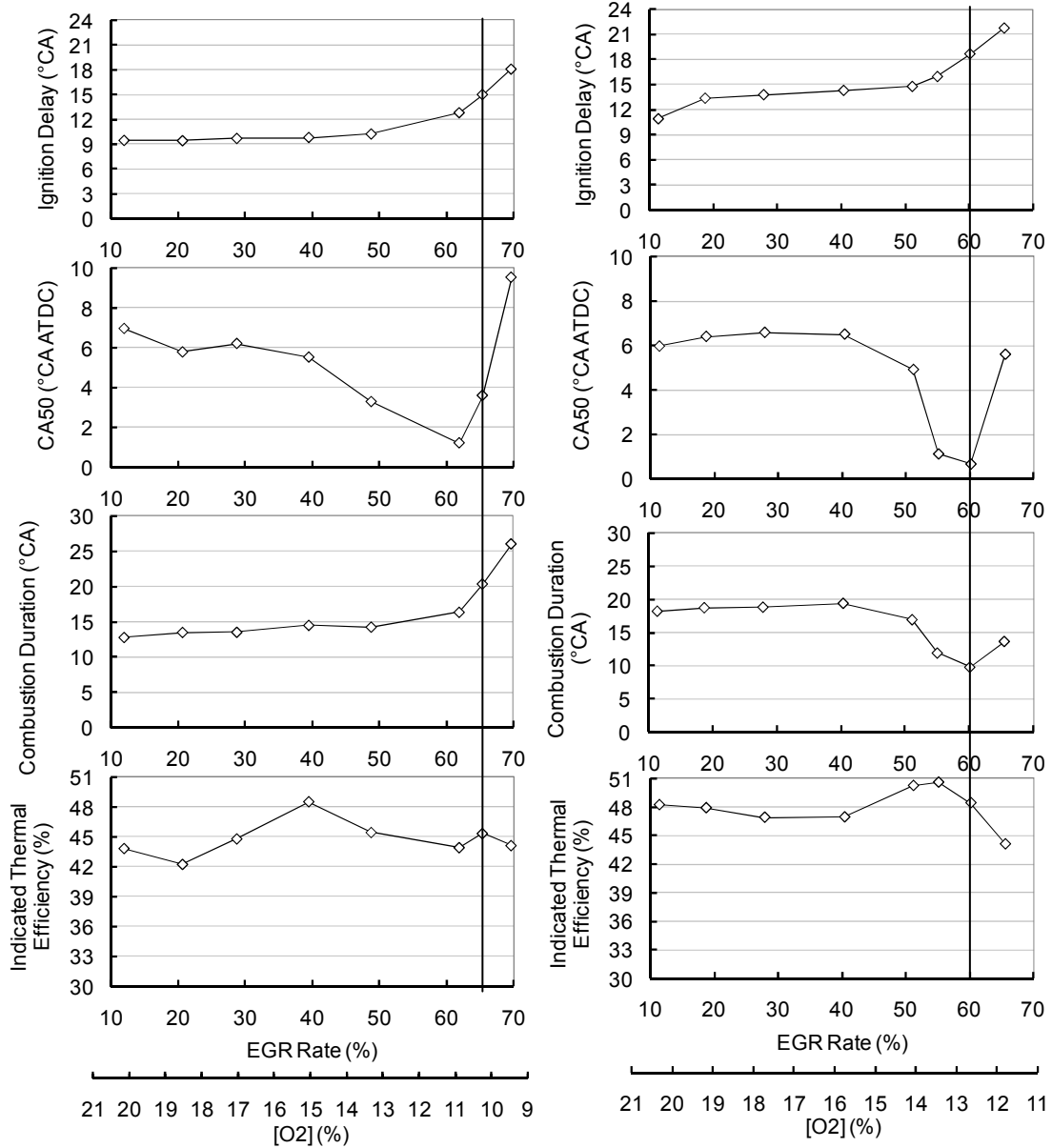


Figure 4.3 Effects of EGR rate on diesel engine combustion process at 8 mg/cycle fuelling conditions (Left: 1500 rpm; Right: 2500 rpm)

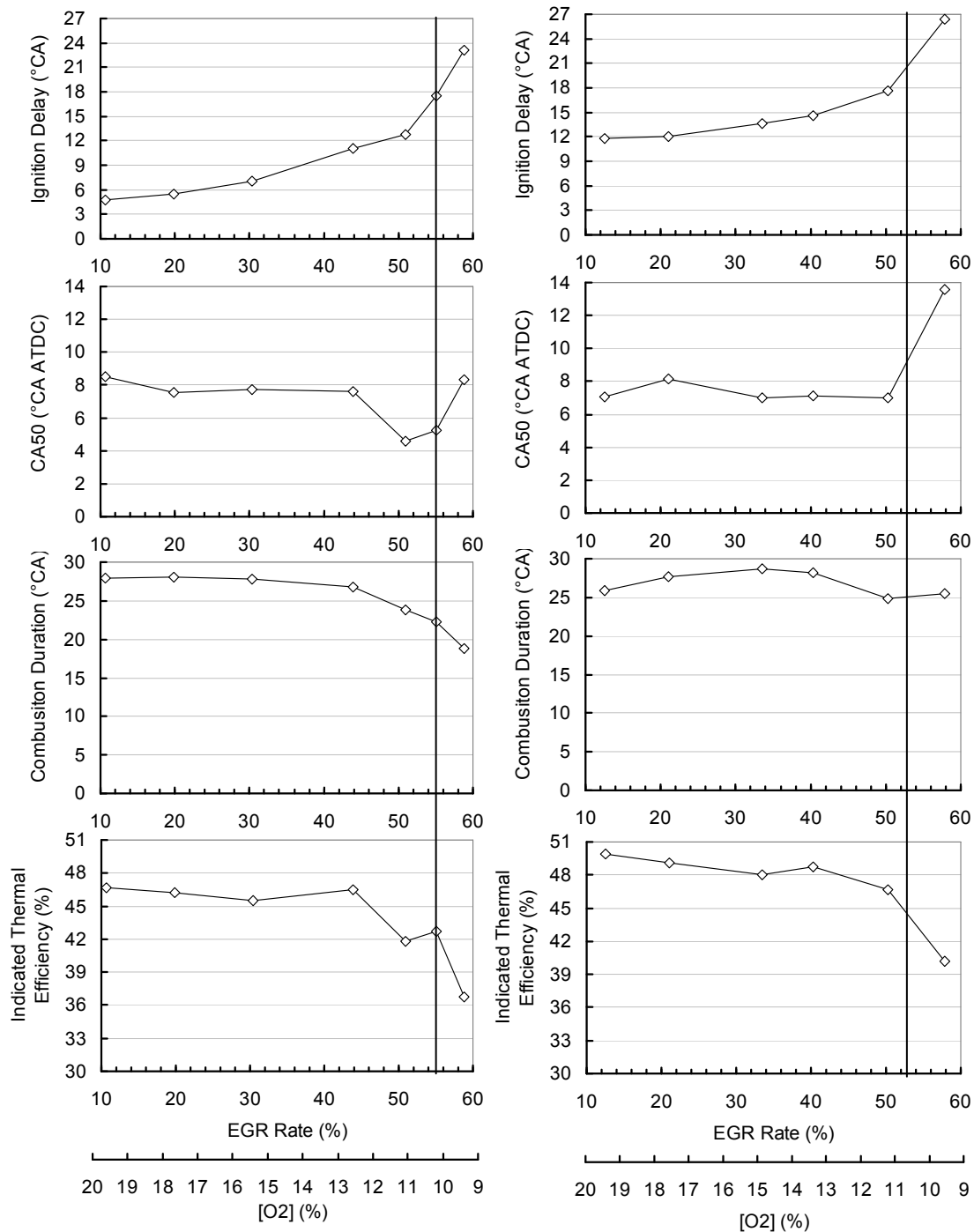


Figure 4.4 Effects of EGR rate on diesel engine combustion process at 16 mg/cycle fuelling conditions (Left column: 1500 rpm; Right column: 2500 rpm)

The combustion duration (as defined by the CA5-CA90 duration) was increased with higher EGR rates for the 1500 rpm 8 mg/cycle case. The reduction in oxygen concentration restricted the rate at which the fuel was being oxidized and the combustion temperature. The longer ignition delay could also lead to over-mixing of the fuel, which makes the combustion events become longer and emit higher THC and CO emissions. The lower combustion temperature would also make it less likely

for these emissions to be oxidized later in the combustion event. For the 2500 rpm condition, the higher piston velocity generated turbulence in the combustion chamber which might have led to a shorter combustion duration than 1500 rpm condition. For the 16 mg/cycle operating conditions, the combustion duration was reduced for the highest EGR rate conditions. Here, the combustion terminated before the fuel had been fully consumed (as shown by the high partial-combustion by-products shown in Figure 4.2), as there was not enough oxygen to oxidise all the fuel injected and the low temperature combustion could not propagate into the over-mixed zones either.

For the 8 mg/cycle operating conditions, the indicated thermal efficiency showed a generally increased trend with the higher EGR rates even with increased THC and CO emissions (which suggest reduced combustion efficiency). The improvement in efficiency can be attributed to the significantly advanced combustion phasing, which at certain points is more than the energy lost in the THC and CO emissions. However, for the 16 mg/cycle conditions, an increase in EGR rate led to much higher THC and CO emissions than were observed for the low fuelling cases. For the low to intermediate level EGR tests, the 16 mg/cycle condition's combustion phasing could not be advanced as much as for the 8 mg/cycle cases due to the significantly increased cylinder pressure rise rate. For the high EGR rate conditions, the combustion phasing was retarded, as the advanced injection timing led to misfire. This misfire might be due to the fuel impingement that could have occurred when the fuel injection timing was advanced. Thus, the increase in EGR rate led to a reduced thermal efficiency for the 16 mg/cycle conditions.

The overall combustion performance (as shown in Figures 4.3 and 4.4) is clearly sensitive to the EGR rate. These differences can be more completely assessed from the heat-release profile, as shown in Figures 4.5 and 4.6. Higher EGR rates led to smoother combustion processes. The oscillatory combustion pressure indicated by the 'ringing' on the cylinder pressure trace and heat release rate for the low to intermediate EGR rate conditions disappeared in the higher EGR rate cases. For traditional premixed compression ignition combustion, the heat release process tends to have a rapid pressure rise, which in these cases was causing oscillation in the cylinder pressure. However, with higher EGR rates, although the mixture was more premixed (because of the very long ignition delay), the combustion was controlled mainly by the availability of oxygen in the mixture which led to a lower rate of pressure rise and hence less acoustic waves within the combustion chamber.

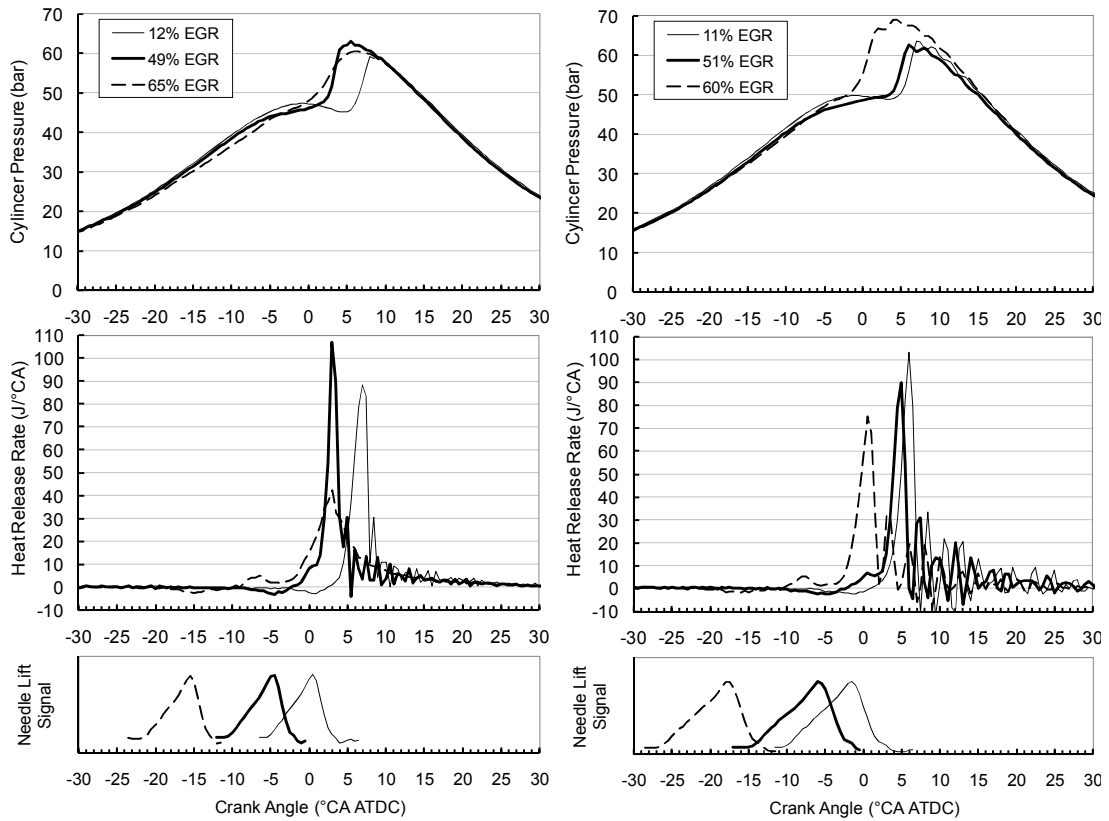


Figure 4.5 Effects of EGR rate on diesel engine combustion at 8 mg/cycle fuelling conditions (Left column: 1500 rpm; Right column: 2500 rpm)

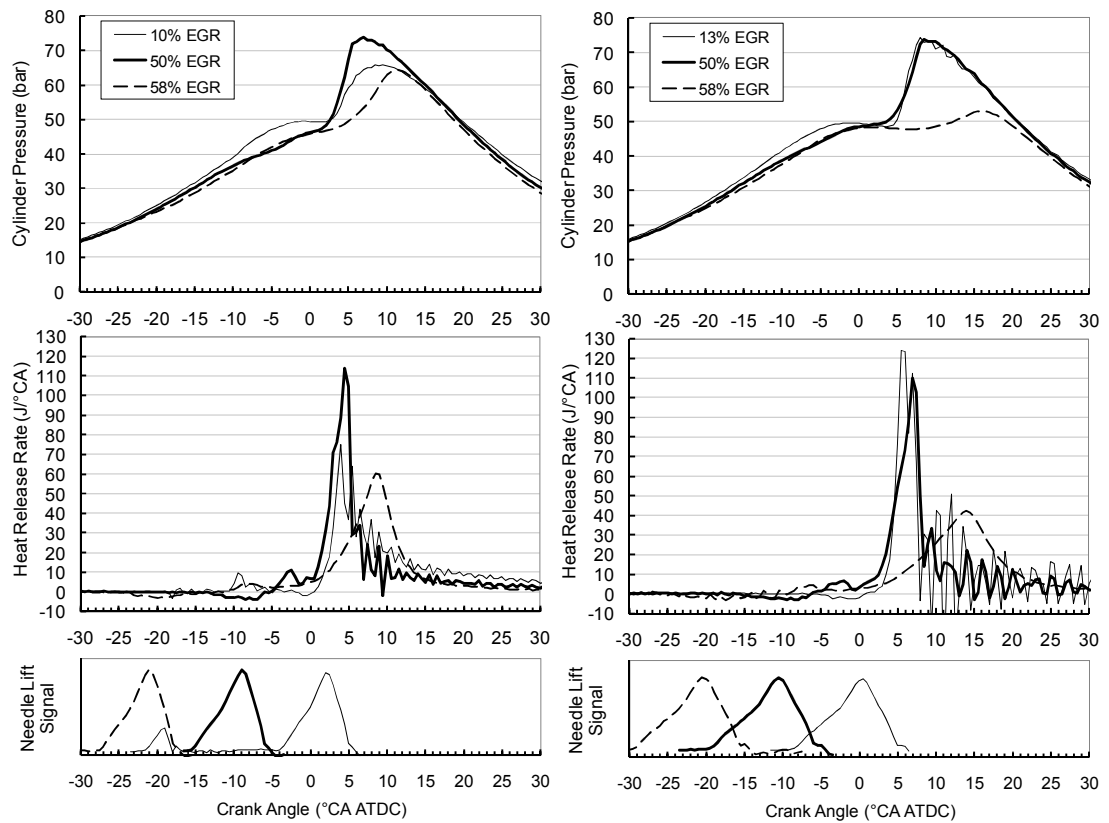


Figure 4.6 Effects of EGR rate on diesel engine combustion at 16 mg/cycle fuelling conditions (Left column: 1500 rpm; Right column: 2500 rpm)

The peak of heat release rate was reduced and the duration of the heat release was extended for the high-EGR operating conditions. For the 8 mg/cycle conditions (Figure 4.5), with increased EGR rate, the combustion event was able to be advanced by the advanced fuel injection timing. For the 16 mg/cycle conditions (Figure 4.6), the combustion was retarded significantly even though the fuel injection timing was advanced.

There was a clearly two stage heat release pattern for the high-EGR diesel combustion conditions. The main heat release profile followed a distinctive cool flame reaction and a period with a very low heat release rate. The phenomenon was discussed in Chapter 2 and the details of this low temperature reaction phenomenon and its influence on LTC combustion and emissions will be investigated in Chapter 5.

The effects of high levels of EGR on the combustion stability and completeness, as indicated by the CoV(IMEP) and the THC emissions are shown in Figure 4.7. Both the CoV(IMEP) and the THC emissions increased with higher EGR rates for all the engine operating conditions evaluated. The increase in EGR rate caused a greater increase in the THC emissions for the 16 mg/cycle fuelling conditions than for the 8 mg/cycle conditions, while the changes in CoV(IMEP) did not show a significant difference between the different fuelling conditions. The combustion stability (as represented by CoV(IMEP)) appeared to vary with EGR independent of engine speed or load. THC emissions, however, increased more substantially at higher loads. This is most likely a result of the lower oxygen content in the charge at the high-load condition. This results in more fuel-rich pockets that lead to higher emissions of unburned or partially oxidized fuel.

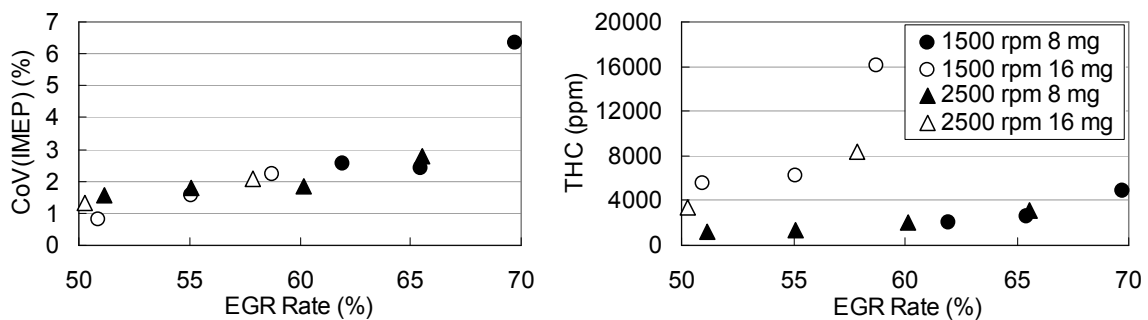


Figure 4.7 Effects of EGR rate on CoV(IMEP) and THC emissions

The EGR sweep tests showed that the test engine is capable of operating over wide ranges of EGR, and that a low-smoke, low-NO<sub>x</sub> LTC regime had been established with high levels of EGR at all four engine speed and load conditions tested. However, the LTC combustion regime exhibited high levels of THC and CO emissions and

reduced combustion stability, especially at the intermediate load cases. The engine efficiencies for these conditions were also significantly reduced for the LTC combustion regime. These results were developed based on a single injection event, the timing of which was advanced to maximize efficiency. The effects of varying the injection strategy (timing, pressure, and post-injection) will be discussed later in this chapter.

### **4.3.2 Particle number and size distribution**

Limits on the number of particles emitted from engines have been introduced as part of the Euro VI regulation. Conventional mass-based PM limits do not take the number and size of the particulates into account. Because of the complexity of the PM formation processes (see Section 2.1), changes in PM mass (or smoke number) are not necessarily representative of changes in particle number (PN). Part of establishing the baseline for LTC operation on the research engine was to evaluate the effects of LTC on PN and particle size distribution using a Cambustion DMS500 fast particulate spectrometer.

An Increase in EGR rate from zero to LTC levels had a significant impact on the particle size distribution, as shown in Figures 4.8 – 4.10. The figures show the particle size spectral densities in number and volume for the EGR sweep at the 1500 rpm 8 mg/cycle, 1500 rpm 16 mg/cycle and 2500 rpm 16 mg/cycle operating conditions. Increasing the EGR first shifted the particle size distribution towards larger diameters and then, at even higher EGR rates, caused the particle size distribution to shift towards smaller diameters. For all cases, the particles with mobility diameter larger than 1000 nm were not measured. This was most likely only significant at 1500 rpm 16 mg/cycle, where the large particles take a significant fraction in the particulate volume even though they have a small number, as shown in the Figure 4.9. The pilot fuel injection used to control the cylinder pressure rise rate may have caused the emission of large diameter particles. As the pilot fuel injection could have increased the soot formation in the combustion process as discussed in Chapter 2.

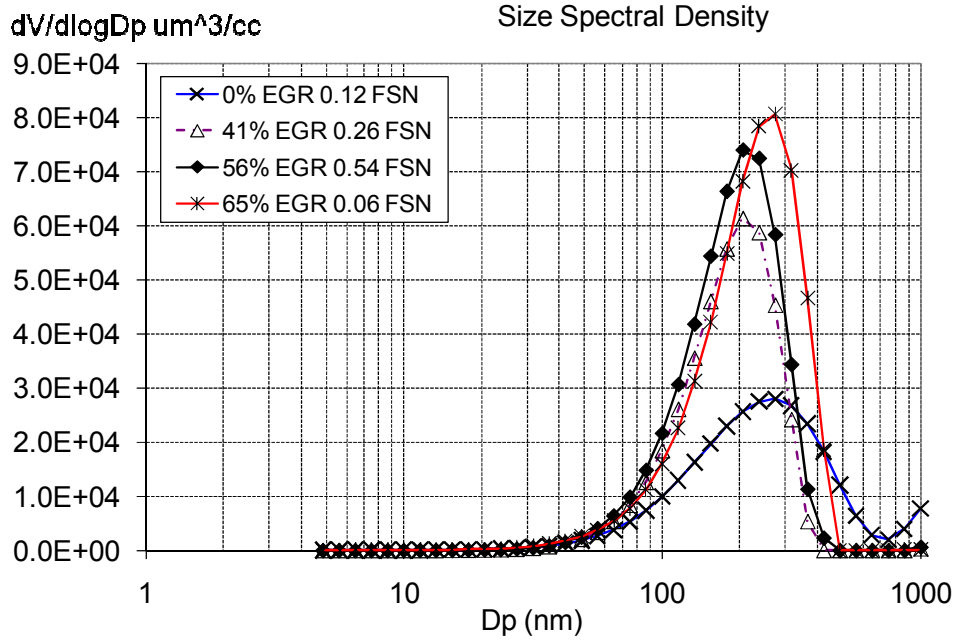
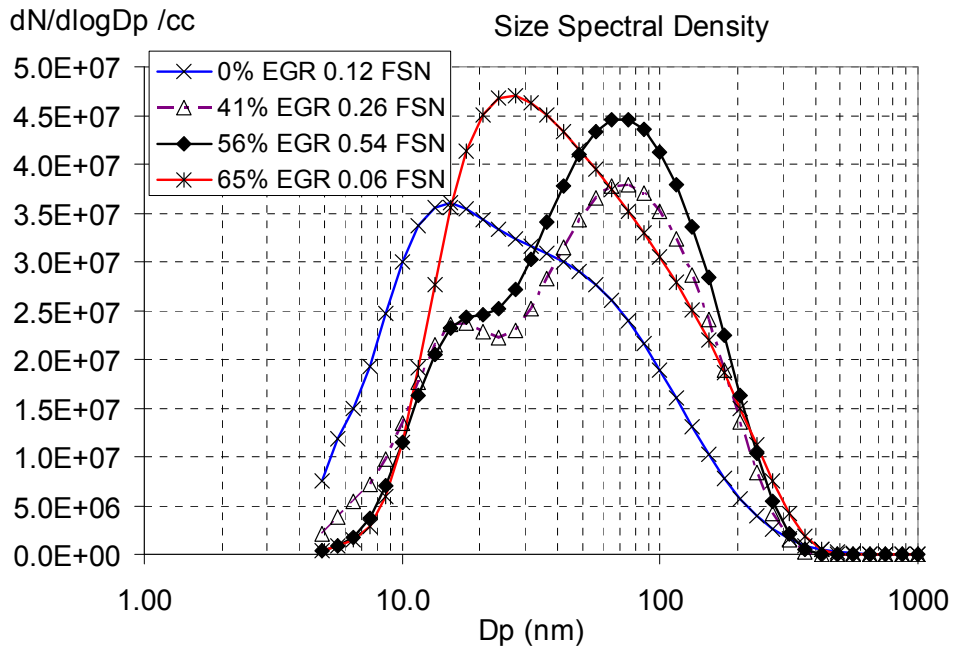


Figure 4.8 1500 rpm 8 mg/cycle particle size distribution with EGR sweep



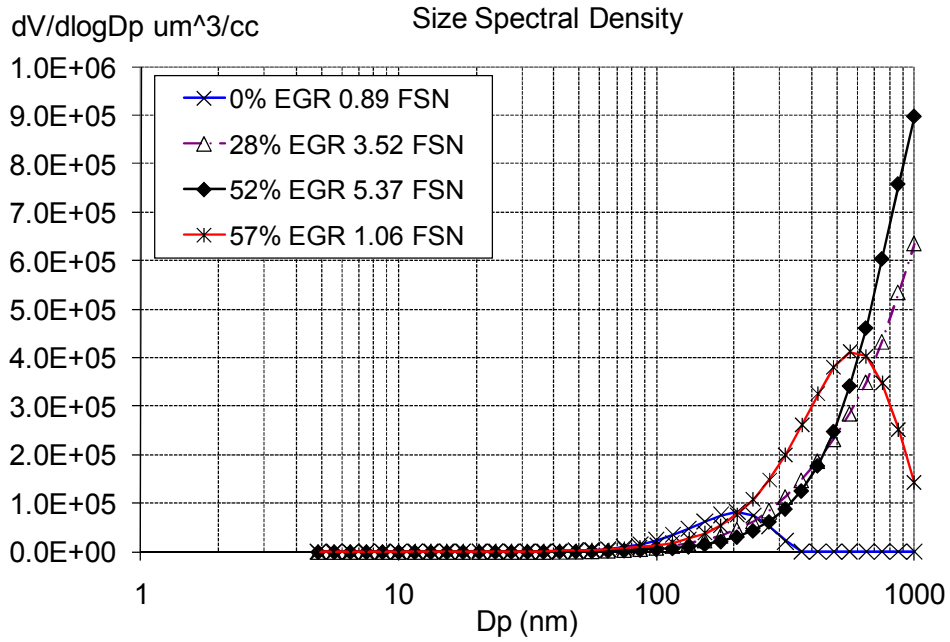
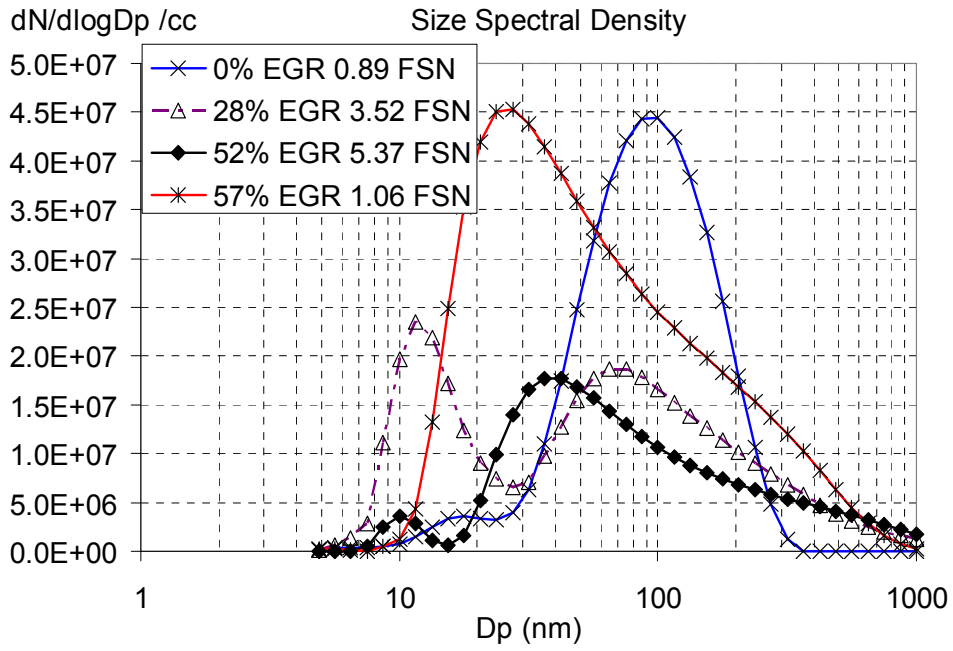


Figure 4.9 1500 rpm 16 mg/cycle particle size distribution with EGR sweep

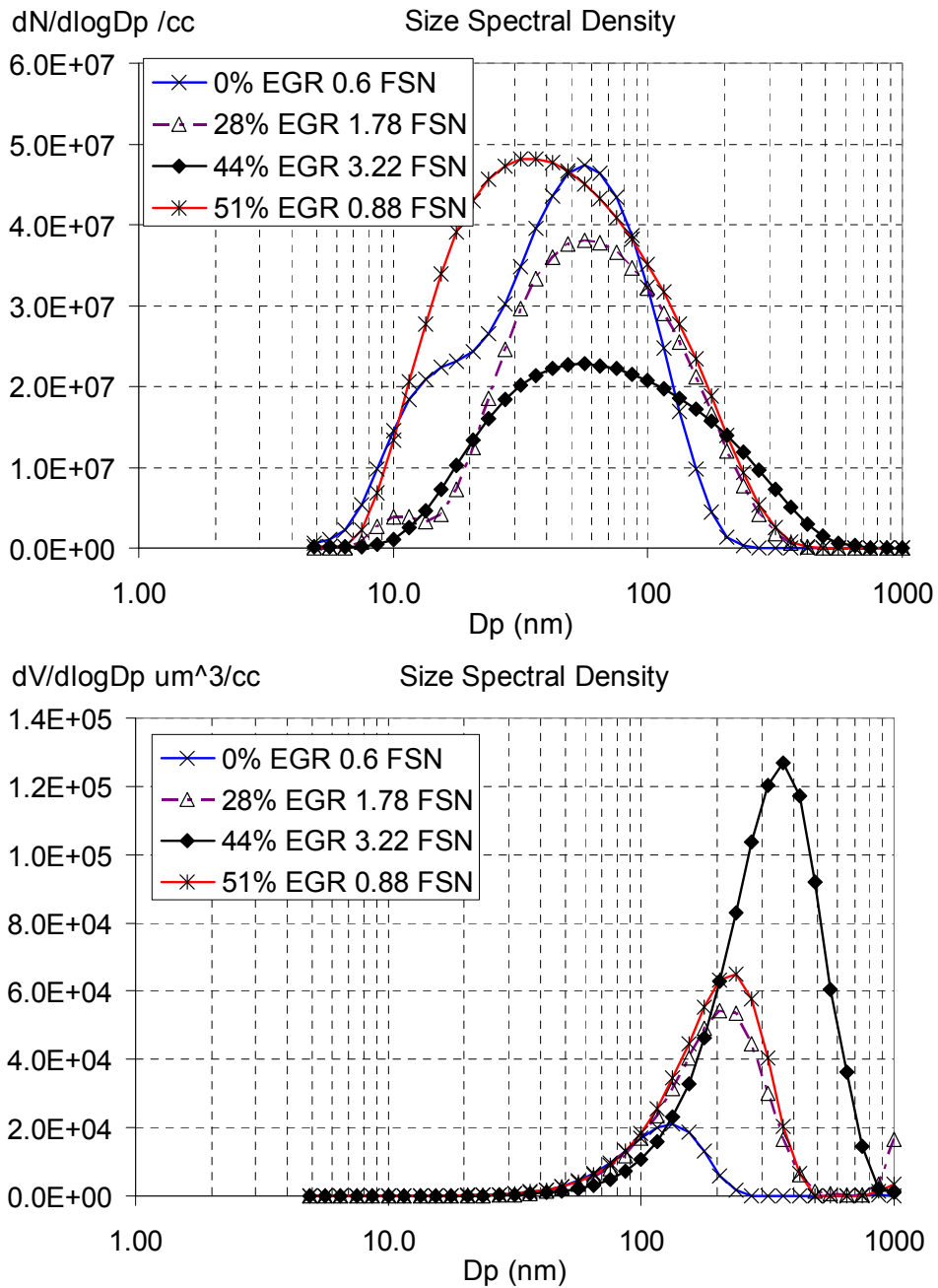


Figure 4.10 2500 rpm 16 mg/cycle particle size distribution with EGR sweep

The total particle number concentration (integral of  $dN/d\ln D_p$  between 1 and 1000 nm) first decreases with increasing EGR rate and then increases again as the LTC regime is approached for all the different engine operating conditions. This is opposite to the trend in smoke number measurement, shown in Figures 4.1 and 4.2; this comparison is emphasised in Figure 4.11. This suggests that a higher concentration of particles was emitted within LTC mode even though the smoke number measurement was low.

The total particulate volume shows a nearly linear correlation with the smoke number measurement for the 2500 rpm 16 mg/cycle operating condition. Since the smoke number measurement is based on reflectance of a light beam from the filter paper, the total PM volume may have a direct influence on the blackness of the filter paper, and hence on the FSN measurement. The reduction in total PM volume in the LTC mode is less significant than the reduction in smoke number as shown in Figure 4.11. The change in PM composition from black carbon dominated to the SOF dominated mode as suggested by (Ogawa *et al.*, 2007) could be the reason for the higher PM volume at the LTC cases with low smoke numbers. For the 8 mg/cycle condition, the smoke number is at a very low level throughout the test and the correlation is not clear. For the 1500 rpm 16 mg/cycle case, the larger diameter (> 1000 nm) particulates were excluded from the measurement as indicated in Figure 4.9. The total PM volume measurement here is hence lower than the real engine-out emissions level due to the missing large particulates. This may explain why the PM volume does not closely follow the variation in smoke number as a function of EGR level.

The overall particle number from each combustion cycle was reduced for the LTC combustion cases. The particle numbers were normalized to the non-EGR operating conditions considering the reduced exhaust flow rate and were shown in Figure 4.12. With increased EGR rate, the number of particles emitted from each combustion cycle reduced first, then, for the LTC cases, the particle numbers increased and were higher than that of the intermediate EGR conditions. For the 16 mg/cycle conditions, the LTC particle numbers increased more significantly than the low fuelling condition. However, they were still lower than those from the non-EGR conditions.

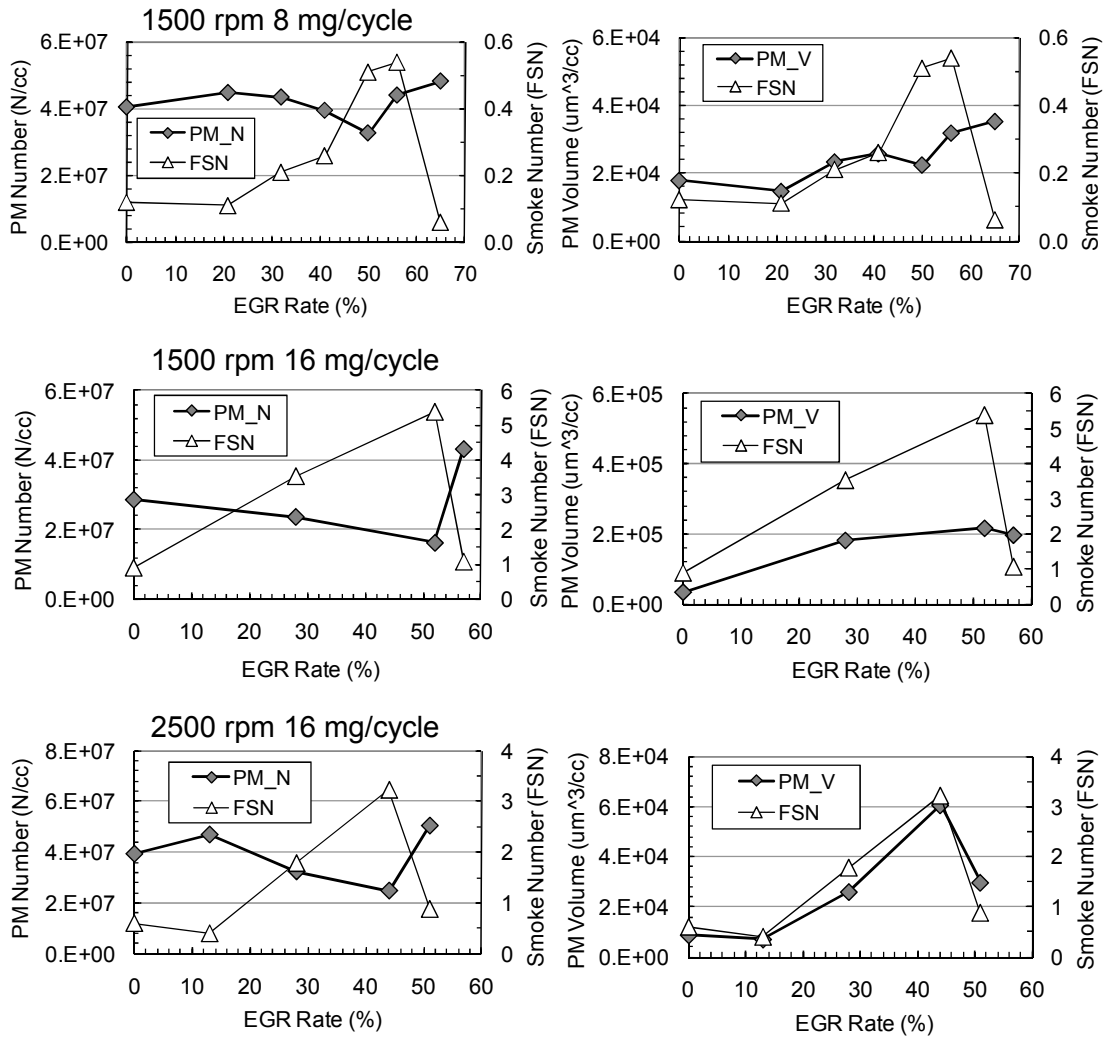


Figure 4.11 Total particle number and volume vs. filter smoke number

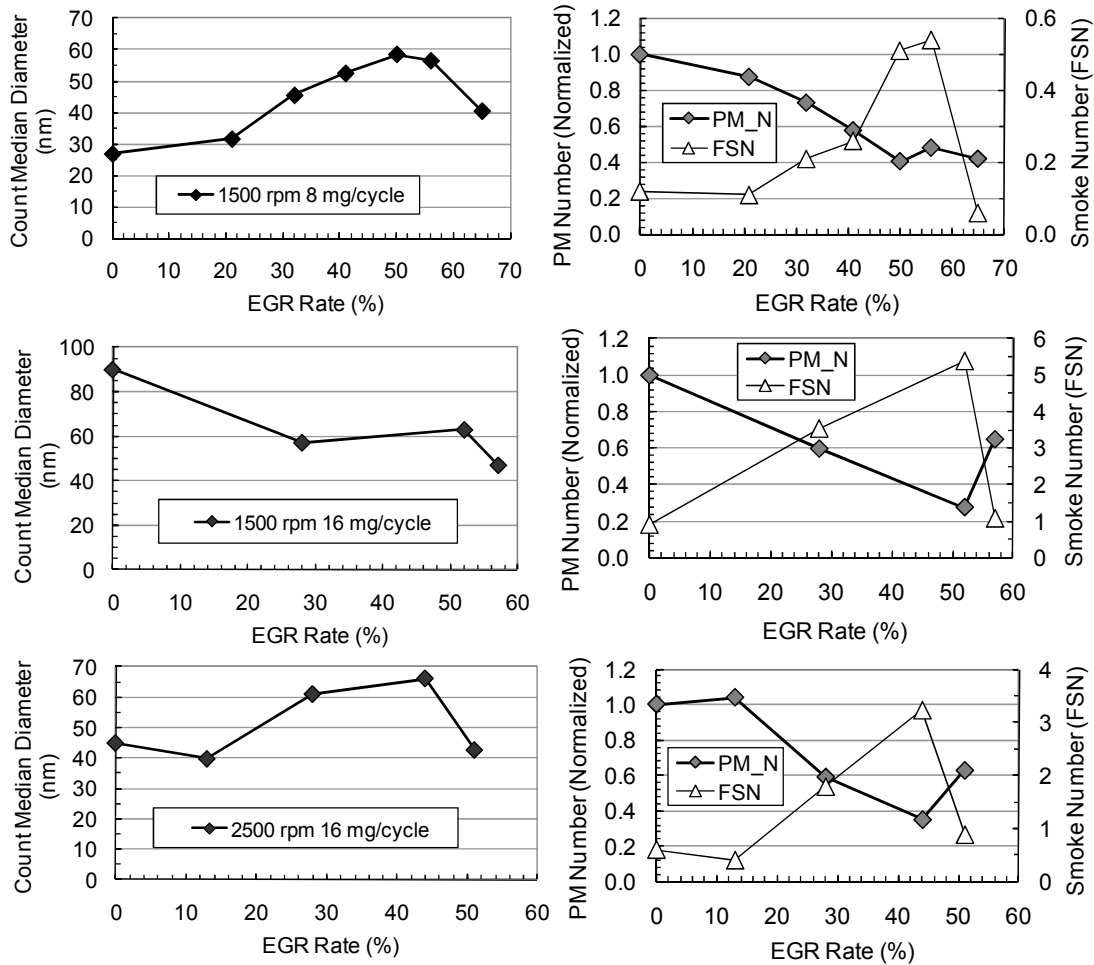


Figure 4.12 Particulate CMD and normalized number vs. EGR rate for the three operating conditions

The particle count median diameter (CMD) is approximately 40 nm for all the different operating conditions in LTC mode. The CMD shows a general trend of first increasing and then decreasing with increased EGR rate, as shown in Figure 4.12 for the 1500 rpm 8 mg/cycle and 2500 rpm 16 mg/cycle cases. The same effect was not seen at the 1500 rpm 16 mg/cycle condition, where the particle size distribution measurement excluded a significant number of particles with diameters greater than 1000 nm. This shifted the CMD to lower values for the intermediate EGR cases. Another reason for the largest CMD encountered under non-EGR condition is that there was a pilot fuel injection used to control the cylinder pressure rise rate. As discussed in Chapter 2, the pilot fuel injection could have led to increased smoke emissions. The pilot fuel injection may have contributed to the increase in mean particle diameters. However, the results have shown that transition to LTC does result in a significant change in the particle size distribution, which needs to be considered in light of upcoming emissions regulations.

### 4.3.3 Effects of fuel injection parameters on LTC

The fuel injection parameters, specifically the timing and pressure, are important parameters used in conventional diesel engine combustion and emissions control. They also offer significant potential to optimise LTC combustion, as was demonstrated in Section 4.3.1, where thermal efficiency could be improved with increasing EGR by advancing the combustion timing. The effects of fuel injection timing and pressure were investigated on the same set of engine speed and fuelling conditions as in the previous section. As the NO<sub>x</sub> and smoke emissions for these test conditions were all at very low levels, and the changes caused by the variations in the fuel injection parameters were not resolvable using the emissions measurement equipment available. Emissions of CO, as mentioned in the previous section, exceeded the maximum level measurable by the available equipment, and are hence not presented in this section. As a result, the results here focus on THC emissions, the combustion stability and thermal efficiency, and are subdivided on the basis of load.

#### 8 mg/cycle Conditions

Injection timing has a consistent influence on combustion phasing. This is shown in Figure 4.13, where advancing the injection by 3°CA achieves a similar advance in both the low-temperature and main combustion events. With advanced timings, both the cool flame and the main combustion reactions occurred earlier in the cycle. For the 1500 rpm cases, the peak of the main heat release rate also increased with advanced injection timing. This indicates that an earlier combustion event may lead to higher combustion temperatures which are associated with the higher peak HRR and the faster combustion progress. However, for the 2500 rpm cases, the peak of the main HRR was reduced for the earliest timing case while the peak HRR was advanced. This may be due to fuel impingement or to fuel penetrating into the squish region, as either effect tends to reduce the amount of fuel which is at a combustible stoichiometry prior to the start of the main combustion event (Boot *et al.*, 2010; Han *et al.*, 2009).

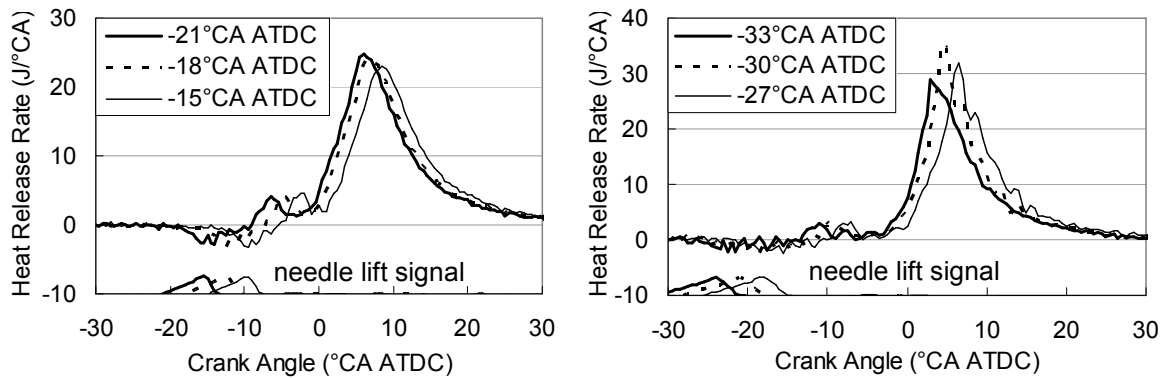


Figure 4.13 Effects of Sol on 8 mg/cycle LTC heat release rate, needle lift (not to scale) also shown (Left: 1500 rpm 8 mg/cycle, fuel injection pressure 500 bar, EGR rate 65%; Right: 2500 rpm 8 mg/cycle, fuel injection pressure 650 bar, EGR rate 65%)

Increased fuel injection pressures (Figure 4.14) showed no clear effect on the cool flame reactions but a significant effect on the main combustion events. The cool flame reaction rate is governed mainly by the time after the start of injection and the temperature in the combustion chamber; therefore, it is reasonable to expect that injection pressure would not significantly affect this stage of the combustion. More details about these early-stage, low-temperature reactions within LTC are presented in Chapter 5. The main combustion event (or at least the rate of progression of its early stage) is sensitive to how well mixed the fuel and charge are, as well as to the temperature in the combustion chamber. For the 1500 rpm cases, increased fuel injection pressure appears to have improved fuel-charge mixing which led to advanced and faster main combustion. For the 2500 rpm cases, the increased fuel injection pressure reduced and delayed the peak HRR for the main combustion event. This may be explained by the fact that higher engine speed introduces stronger charge motion, while higher fuel injection pressure increases liquid fuel penetration and generally improves spray atomization (Wahlin *et al.*, 2004). These factors may lead to over-mixing of the fuel. At high speed and low load LTC conditions, a stable combustion kernel may not survive in these over-mixed zones due to the very low temperatures in the cylinder and the relatively high local turbulence intensities.

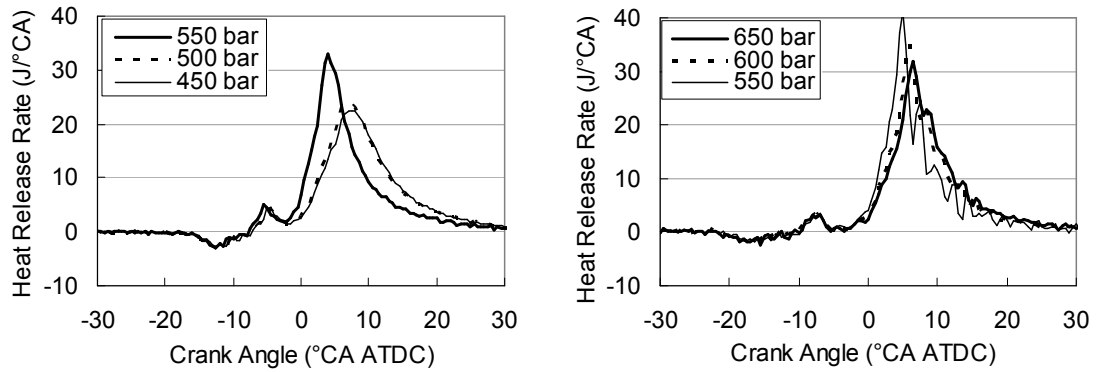


Figure 4.14 Effects of fuel injection pressure on low load LTC heat release rate (Left column: 1500 rpm 8 mg/cycle, Sol -18°CA ATDC, EGR rate 65%; Right column: 2500 rpm 8 mg/cycle, Sol -27°CA ATDC, EGR rate 65%)

High fuel injection pressure tended to reduce CoV(IMEP) and THC emissions at a given timing. The effects of fuel injection pressure and start of fuel injection timing on CoV(IMEP) and THC emissions for the 1500 rpm 8 mg/cycle operating conditions are shown in Figure 4.15. Increasing the fuel injection pressure reduced the CoV(IMEP) and THC emissions. This is consistent with the higher peak heat release rate shown in Figure 4.14. The improvement in fuel atomization by the higher injection pressure may have led to a more even local fuel distribution in the combustion chamber. This may give the fuel more chance to react with the limited oxygen and hence improve the combustion stability. The fuel injection timing was found to have a greater influence on THC emissions than it did on CoV(IMEP). Later fuel injection timing reduces the time available for the charge to mix and burn; this may cause deterioration in combustion, leading to increases in THC emissions. The earliest fuel injection led to increased CoV(IMEP). The possible over-mixing may have caused unstable engine power output.

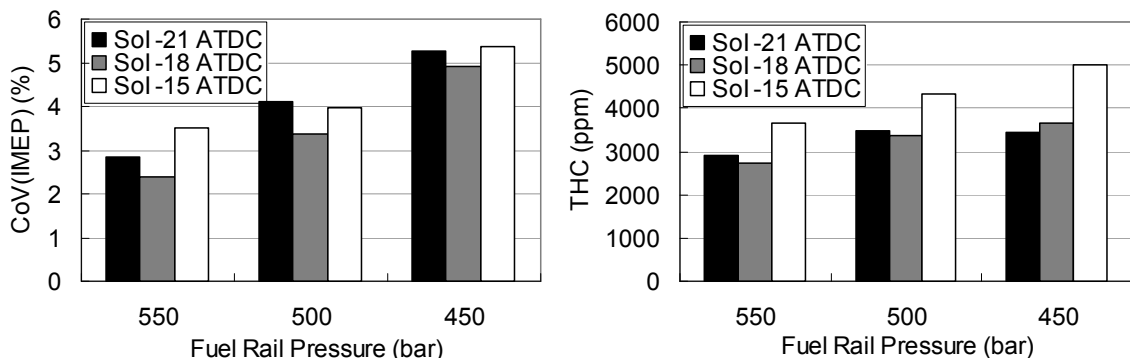


Figure 4.15 Effects of fuel injection pressure and Sol on CoV(IMEP) and THC emissions (1500 rpm 8 mg/cycle, EGR rate 65%)



As the heat release rates indicated (Figure 4.14) the effects of fuel injection pressure at 2500 rpm were different from those shown at 1500 rpm (Figure 4.15). Increased fuel injection pressure and advanced fuel injection timing both caused increases in CoV(IMEP) and THC emissions at 2500 rpm, as shown in Figure 4.16. For the earliest fuel injection timing cases, fuel impingement on the walls may be a reason for the observed deterioration in CoV(IMEP) and THC emissions. As discussed in Section 2.3, with increased fuel injection pressure, the fuel penetrates further and more fuel may impinge on either the piston or the cylinder liner. For the later fuel injection cases, the fuel injection pressure showed less significant effects on the combustion stability. This finding agrees with the impingement hypothesis, where later injection timings would be less likely to result in fuel impingement. Other possible causes of the higher THC emissions are more fuel over-mixing prior to ignition or fuel reaching the squish region and not participating in the main reactions. The relatively small changes in fuel injection parameters used in this work are unlikely to lead to significantly large changes in fuel spray mixing and distribution; as a result, impingement appears to be the most likely cause of the observed increases in THC and combustion instability. However, conclusive validation of this hypothesis requires optical assessment of the injection process; this is an area of our group's ongoing research.

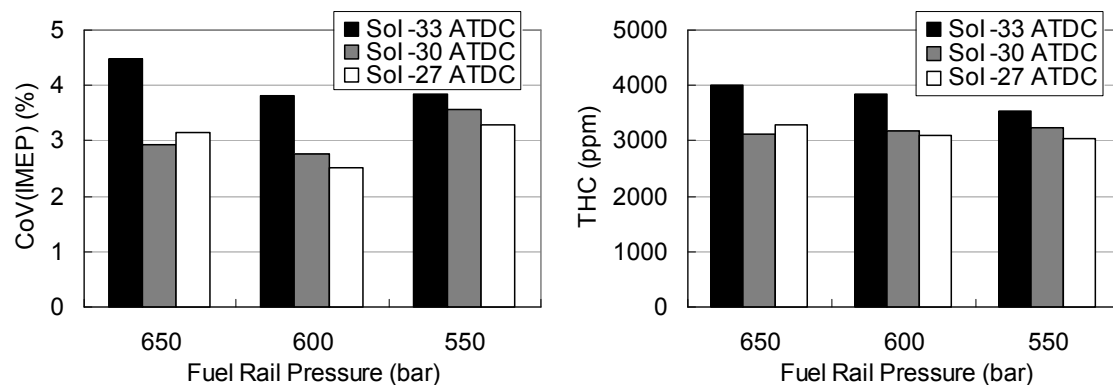


Figure 4.16 Effects of fuel injection pressure and Sol on CoV(IMEP) and THC emissions (2500 rpm 8 mg/cycle, EGR rate 65%)

Changes in the injection process ultimately affect the phasing of the combustion, which can also influence the stability of the combustion event and emissions. These implications are shown in Figure 4.17 for the low-load cases. The CoV(IMEP) is only slightly affected by the combustion phasing, with a tendency towards lower variability with more advanced combustion phasing. The wide variability in these results, however, indicates that other engine operating parameters have a more significant influence on the combustion variability. Advanced combustion processes tend to

have lower THC emissions as the combustion temperature is higher and there is a longer time for fuel oxidation to occur before the exhaust valves open. Both advanced fuel injection timing and increased fuel injection pressure tend to advance the combustion phasing and in general showed lower LTC emissions. However, the cases with possible fuel impingement (the earliest injection timing as at 2500 rpm, circled in Figure 4.17) show an increase in THC emissions even with advanced combustion phasing. This agrees with the impingement hypothesis, where the earlier injections would result in larger penetration distances before combustion starts to occur, leading to more likelihood of interaction between the spray and piston.

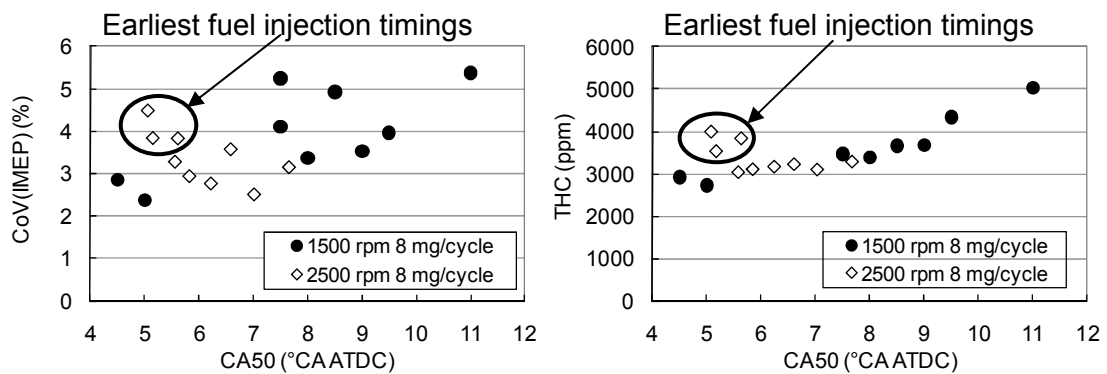


Figure 4.17 Effects of combustion phasing (CA50) on CoV(IMEP) and THC emissions for 8 mg/cycle LTC conditions (EGR rate 65%)

Advanced combustion phasing tends to increase the indicated thermal efficiency. However, the high THC emissions derived from the possible fuel impingement indicates reduced combustion efficiency which in turn leads to reduced engine thermal efficiency. The relationship between the thermal efficiency and combustion phasing is shown in Figure 4.18. At 1500 rpm, the high thermal efficiency points are from the early fuel injection timing and high fuel injection pressure cases. The THC emissions from these points are the lowest as shown in Figure 4.17. For the 2500 rpm condition, the thermal efficiency reached its peak for cases where the CA50 was around 6°CA ATDC cases. Further advancing of the combustion phasing led to reduced thermal efficiency, which correlates with the increase in THC emissions for these points shown in Figure 4.17. It is likely that the reduced combustion efficiency for these cases cancelled out the benefit in increased thermal efficiency provided by the advanced combustion phasing.

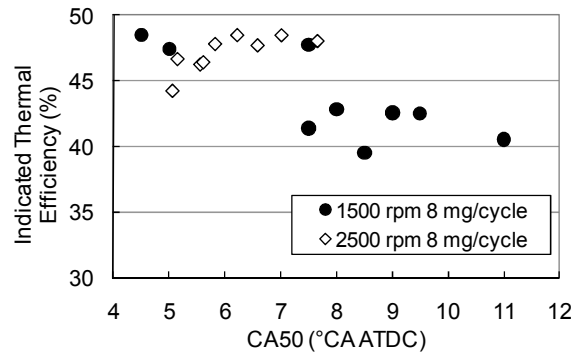


Figure 4.18 Effects of combustion phasing (CA50) on indicated thermal efficiency for 8 mg/cycle LTC conditions (EGR rate 65%)

The earlier fuel injection timing and higher fuel injection pressure cases (550 bar, -21°CA ATDC; 550 bar, -18°CA ATDC; 500 bar, -21°CA ATDC) lead to the three high thermal efficiency points in Figure 4.18 for the 1500 rpm 8 mg/cycle condition. For the 450 bar -21°CA ATDC timing case, even though the CA50 is the same as that of the 500 bar -21°CA ATDC case (i.e. ~7.5°CA ATDC), the thermal efficiency is significantly reduced. For the low fuel injection pressure conditions, the peak heat release rates were significantly reduced, as shown in Figure 4.14 (not particular the -21 °CA ATDC timing cases). The significantly reduced combustion temperature and prolonged combustion duration may have contributed to the reduced thermal efficiency. As the indicated thermal efficiency is also influenced by the combustion efficiency, the reduced combustion stability (as shown in Figure 4.15) due to the degraded fuel-charge mixing for the low fuel injection pressure case may have caused low combustion efficiency and led to the reduced thermal efficiency. However, because the CO emissions were over the maximum measurement limit of the equipment used for this part of study, the variations in combustion efficiency are not known. A further study in the LTC combustion efficiency for different fuel injection parameters is recommended in the future work.

For the low load LTC operating conditions, in general, increased fuel injection pressures and advanced injection timings potentially improved the homogeneity of the charge and led to more complete combustion. This led to more stable combustion, as demonstrated by the lower CoV(IMEP) and THC emissions. The cool flame reaction rates were affected by the fuel injection pressure and fuel impingement; these will be discussed in the next chapter in more detail. The heat release rates of the main combustion events were more sensitive to the fuel injection pressure and timing. Combustion phasing was advanced by early fuel injection timing and higher injection pressures, and this earlier combustion is expected to have led to

higher combustion temperatures. The engine thermal efficiency was increased by advanced combustion phasing, except for the cases with possible fuel impingement or over-mixing which led to higher THC emissions and reduced combustion efficiency. The previous results, however, only apply to the low-load case; as shown in Section 4.3.1, the effects at high load can differ significantly from those at low load.

### **16 mg/cycle Conditions**

For the intermediate load (16 mg/cycle) conditions, the high level of dilution required to keep the combustion in the LTC regime resulted in a significant increase in oxygen-fuel equivalence ratio approaching unity under certain conditions. Thus, the THC emissions were higher than the 8 mg/cycle cases because of a lack of oxygen in the charge. Despite the high THC emissions, it is still important to make the best use of the limited oxygen in the charge to improve the combustion stability and fuel conversion efficiency. In this section, the effects of fuel injection timing and pressure on combustion stability for this higher load LTC operating condition are described.

The fuel injection timing showed a consistent influence on the peak heat release rate and phasing for the intermediate load LTC combustion processes, as shown in Figure 4.19. The heat release rates during the cool flame reactions (as detailed in Figure 4.20) demonstrate that these reactions started earlier with advanced injection timings. In general, the cool flame phasing varied by a smaller magnitude than did the injection timing. However, for the latest injection timings, the cool-flame reactions were delayed more than the timing of the fuel injection. The magnitudes of these early heat-release rates were similar, independent of injection timing. The phasing of the main combustion events were more delayed by later fuel injection timings compared to the effects on the cool flame reactions. As a result, more of the combustion occurred later in the expansion stroke, where the cylinder pressure and temperature were decreasing more rapidly. The main combustion duration was also increased significantly for the later fuel injection cases due to the lower combustion chamber temperatures as indicated by the significantly reduced peak HRR in the combustion process.

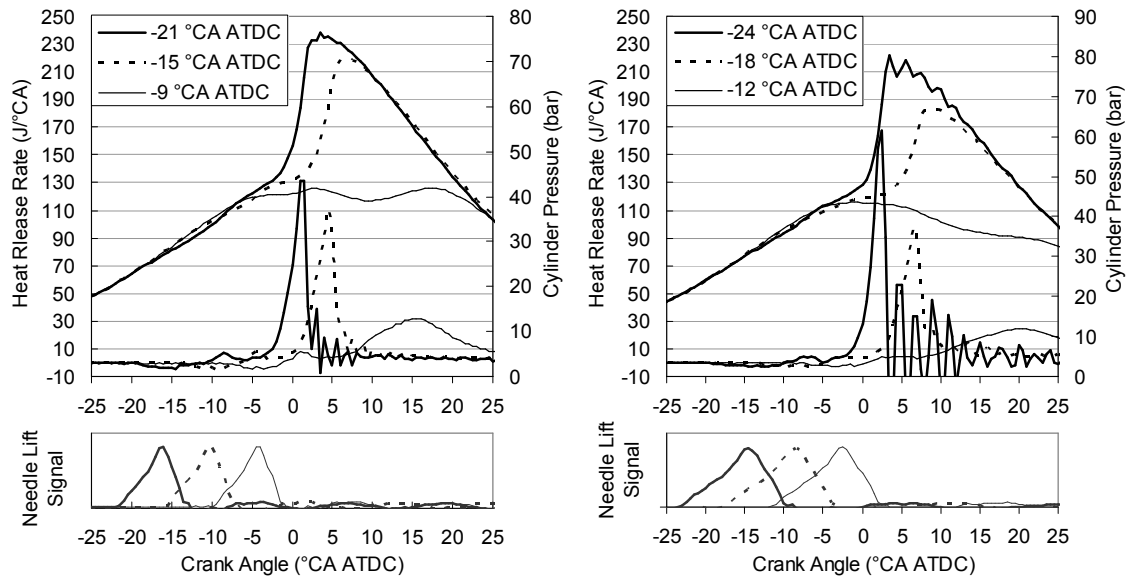


Figure 4.19 Effects of Sol on intermediate load (16 mg/cycle) LTC heat release rate and cylinder pressure (Left: 1500 rpm 16 mg/cycle, fuel injection pressure 900 bar, EGR rate 54%; Right: 2500 rpm 16 mg/cycle, fuel injection pressure 900 bar, EGR rate 50%)

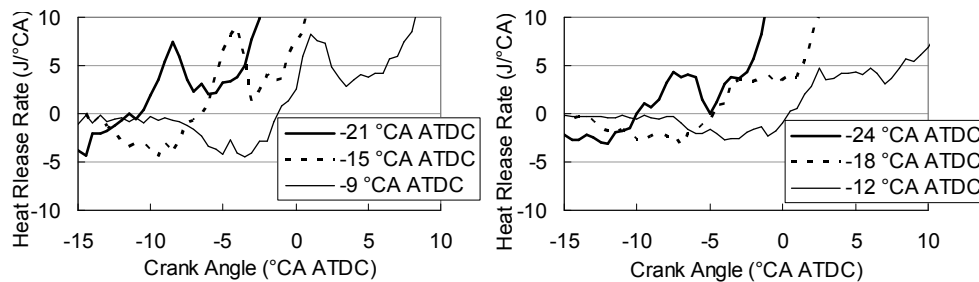


Figure 4.20 Details of cool flame reaction heat release of Figure 4.19. Left: 1500 rpm 16 mg/cycle. Right: 2500 rpm 16 mg/cycle

The effects of fuel injection timing on the combustion stability at the intermediate load LTC conditions, shown in Figure 4.21, differed from those of the light load case discussed previously. For the 16 mg/cycle operating conditions, the start of combustion (CA5) and the subsequent combustion event tended to be more repeatable than for the lower load conditions. This stability in the combustion, demonstrated by low CoV(IMEP), was high for those injection timings where the start of high temperature heat release occurred before TDC. Very retarded timings led to increased CoV(IMEP) and THC emissions, most likely because of bulk quenching in the expansion stroke before all the fuel had been consumed. However, for the 1500 rpm condition, when the fuel was injected too early, the THC emissions increased even though the CoV(IMEP) stayed low. Fuel impingement may have been the reason for this phenomenon.

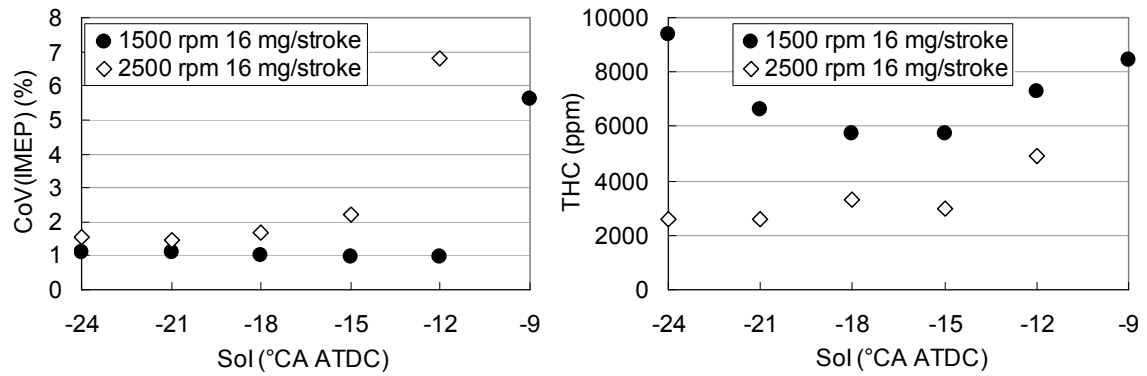


Figure 4.21 Effects of Sol on CoV(IMEP) and THC emissions for intermediate load LTC conditions

Fuel injection pressure shows only small effects on the intermediate load LTC combustion process, as shown in Figure 4.22. The increase in injection pressure led to a shorter injection duration as shown by the needle lift signal. This shorter injection duration, and the increased kinetic energy in the fuel spray from the higher injection pressure, slightly advanced and increased the magnitude of the cool flame reaction as shown in Figure 4.23. However, the main combustion was not significantly influenced as it is mainly controlled by the availability of oxygen and temperature in the combustion chamber for these operating conditions.

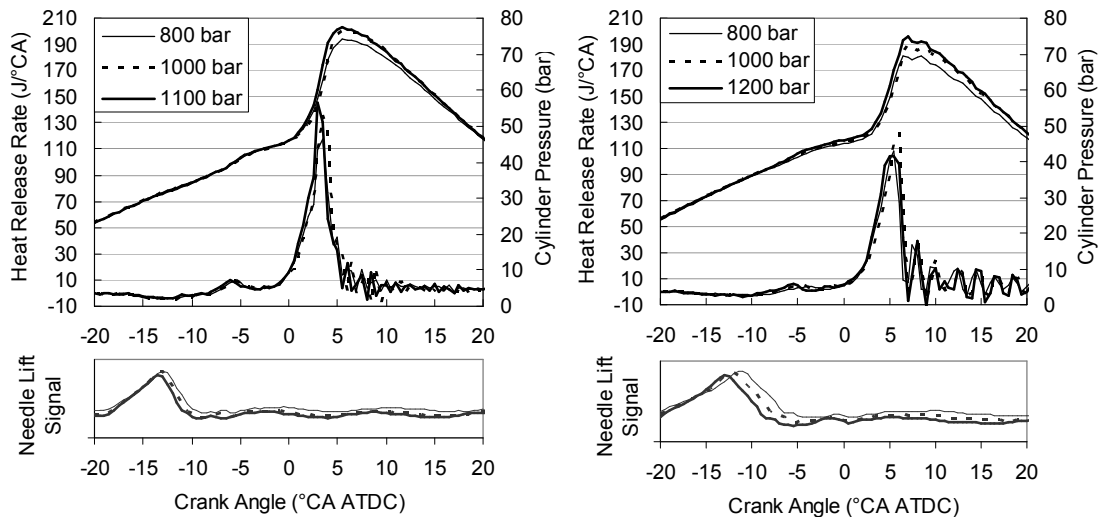


Figure 4.22 Effects of fuel injection pressure on intermediate load (16 mg/cycle) LTC heat release rate and cylinder pressure (Left: 1500 rpm 16 mg/cycle, Sol -18°CA ATDC, EGR rate 50%; Right: 2500 rpm 16 mg/cycle, Sol -21°CA ATDC, EGR rate 50%)

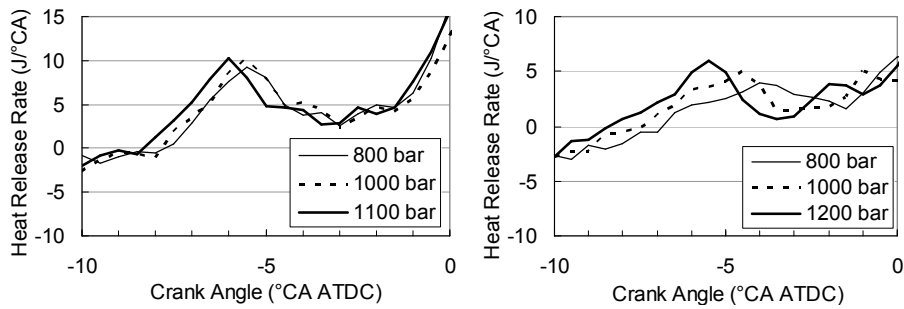


Figure 4.23 Details of cool flame reaction heat release rate of Figure 4.22 (Left: 1500 rpm 16 mg/cycle; Right: 2500 rpm 16 mg/cycle)

The combustion instability, represented by CoV(IMEP) for the intermediate load LTC conditions was at a relatively low level. The fuel injection pressure had an inconsistent influence on CoV(IMEP) and THC emissions, as shown in Figure 4.24. The increase in fuel injection pressure led to an increase in CoV(IMEP) for the 2500 rpm condition, but it showed an opposite trend for the lower speed condition. The THC emissions did not show a consistent trend at 2500 rpm, but appeared to reach a peak value at 1000 bar for the 1500 rpm case. The higher fuel injection pressure should increase spray atomization, improve the fuel-charge mixing and thereby potentially stabilise the combustion. The hydrocarbon emissions are not necessarily a direct result of unstable combustion, especially when the equivalence ratio is close to unity. The fact that these effects do not produce a consistent trend with speed indicates that there is an interaction between the increased fuel spray kinetic energy and the potential increase in charge motion or shorter reaction times at higher engine speeds. However, further work is required to clarify these competing influences.

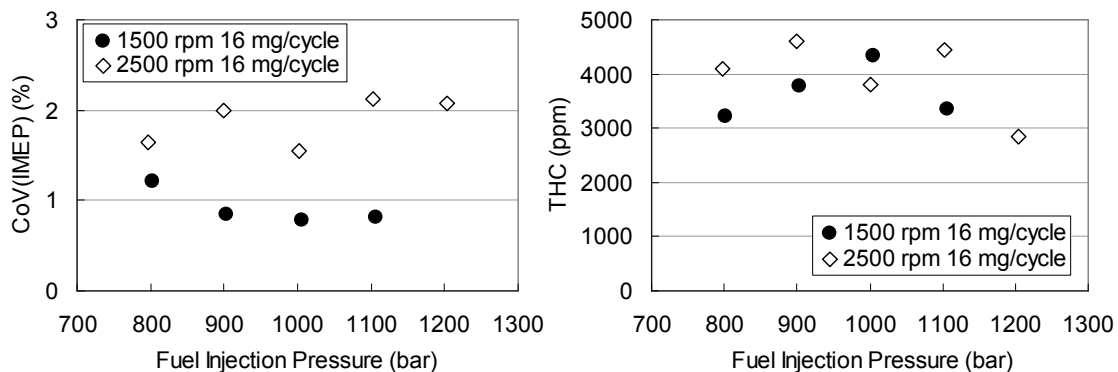


Figure 4.24 Effects of fuel injection pressure on CoV(IMEP) and THC emissions for 16 mg/cycle load LTC

Fuel injection timing had a more significant influence on combustion phasing than injection pressure. Advanced combustion processes tended to have lower CoV(IMEP) and THC emissions as the combustion temperature was higher and there

was a longer time for fuel oxidation to occur before the exhaust valves opened. As suggested in Figure 4.22, changes to fuel injection pressure for this load condition showed only small influences on the combustion phasing. This is supported in Figure 4.25, where the injection pressure variations (at constant Sol) show no significant correlation between combustion stability and phasing.

As introduced earlier, changes in fuel injection timing led to significant variations in combustion phasing. Earlier injections advanced the CA50 and led to decreased CoV(IMEP) and reduced THC emissions for the 2500 rpm case, as shown in Figure 4.25. For the 1500 rpm case, earlier injections with more advanced combustion phasing also reduced the CoV(IMEP), but led to increased THC emissions. This effect may be due to early Sol causing fuel impingement or over-mixing of the fuel. The combustion of the fuel that impinges on the piston crown or reaches areas such as the squish zone is complicated by the lower oxygen content in the charge and relatively low combustion temperatures under LTC conditions (Han *et al.*, 2009).

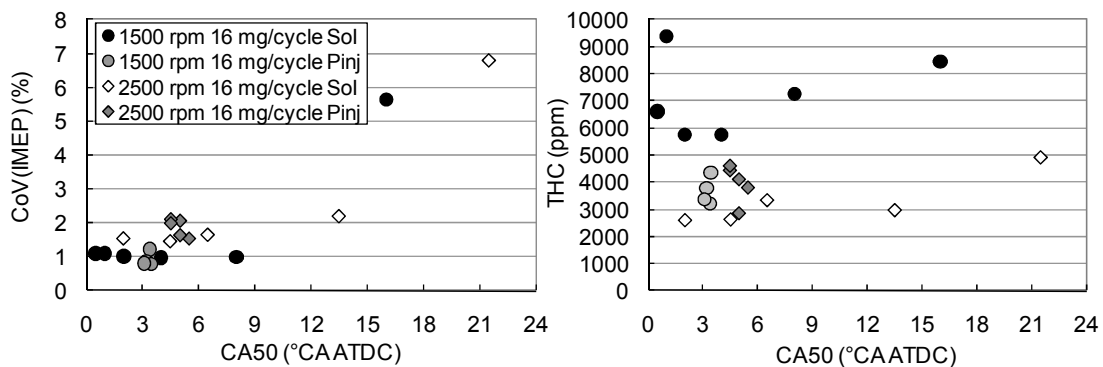


Figure 4.25 Effects of combustion phasing (CA50) on CoV(IMEP) and THC emissions for 16 mg/cycle LTC conditions (Pinj: test conditions where injection pressure was varied; Sol: test conditions where fuel injection timing was varied)

For the intermediate load conditions, advanced combustion timing tended to lead to increased engine thermal efficiency as shown in Figure 4.26. This effect is similar to the low load conditions shown in Figure 4.18. The peak thermal efficiency was achieved with the points where the CA50 was around 3-6°CA ATDC. For the 1500 rpm conditions, the earliest fuel injection cases had increased THC emissions, which suggest reduced combustion efficiency and consequently low thermal efficiency. However, with slightly advanced CA50, the increased fuel injection pressure led to slightly increased thermal efficiency.



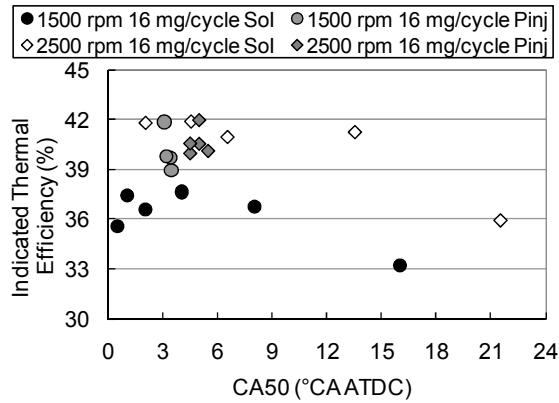


Figure 4.26 Effects of combustion phasing (CA50) on indicated thermal efficiency for 16 mg/cycle LTC conditions (Pinj: test conditions where injection pressure was varied; Sol: test conditions where fuel injection timing was varied)

For the intermediate load conditions, to realize LTC, the engine had to run at nearly stoichiometric conditions as listed in Table 4.2. The shortage of oxygen available to support the fuel combustion was the dominant source of THC emissions at this condition. Due to the large quantity of fuel injected and the fact that for most cases the injection process had terminated prior to ignition, the ignition and heat release of the fuel were less significantly affected by the fuel injection parameters, i.e. the combustion was more robust. Thus, the fuel injection parameters had a smaller effect on the CoV(IMEP) for the intermediate load conditions than for the low load LTC conditions. From an engine performance point of view, the engine-out torque was stable for this condition. However, the THC emissions showed significant sensitivity to the fuel injection parameters. Too early fuel injection timings led to increased THC emissions, which in turn reduced the engine thermal efficiency.

#### 4.3.4 Effects of post fuel injection

For the 16 mg/cycle operating conditions, to reduce the smoke emissions by simply increasing the EGR rate caused deterioration in the combustion efficiency and increased THC and CO emissions. As introduced in Section 2.4, post fuel injection has been suggested as a method to introduce extra turbulence and energy into the later combustion stage and thereby enhance the soot oxidation reactions (Yun *et al.*, 2005a).

The influence of post fuel injection quantity and timing on combustion and emissions under LTC conditions were investigated experimentally. The post fuel injection quantity tests were conducted with the post fuel injection around CA50, as is recommended in previous work (Yun *et al.*, 2005a). For the 1500 rpm 16 mg/cycle

case, the smoke emissions were increased by the introduction of post fuel injection as shown in Figure 4.27. The solid symbols represent the single main fuel injection cases. The introduction of post fuel injection led to increased smoke, THC and CO emissions. As the total fuel injection quantity per cycle was kept constant, the increase of post fuel injection quantity meant more fuel was injected later in the combustion cycle into the high temperature combustion products. Due to the lack of oxygen and increased cylinder temperatures, the combustion of the post fuel likely formed extra soot and caused increases in THC and CO emissions. For the 2500 rpm 16 mg/cycle case shown in Figure 4.28, the smoke emissions were not significantly influenced by the post fuel injection. The combustion of the post injected fuel increased the THC emissions and reduced the CO emissions, indicating that the fuel injected after the main fuel combustion did not get oxidized completely. The post fuel injection quantity showed insignificant influence on the engine thermal efficiency as shown in Figure 4.29. It is interesting that the poor combustion of the post-injected fuel did not affect the cycle efficiency significantly. This may be a result of the fact that the combustion of the main fuel injection occurred at a higher oxygen-fuel-ratio (because of the reduction in the main fuel injection quantity) which could have increased the thermal efficiency of the main combustion event under these high EGR operating conditions.

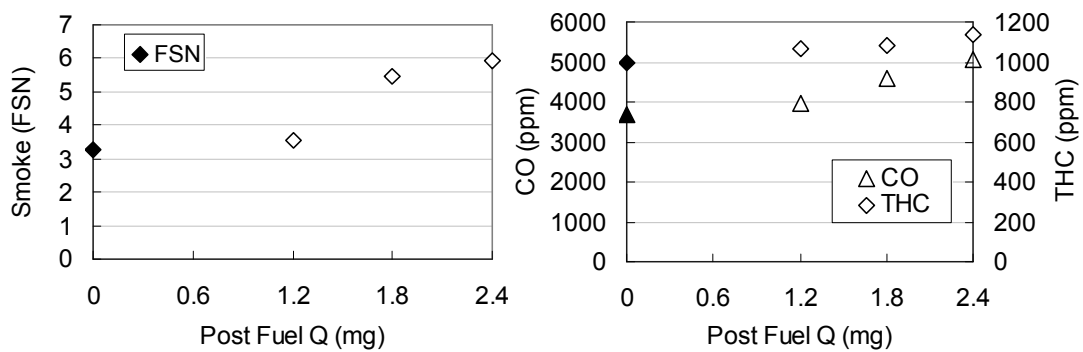


Figure 4.27 Effects of post fuel injection quantity on emissions (1500 rpm 16 mg/cycle; main Sol: -9°CA ATDC; post timing: 9°CA ATDC; injection pressure: 800 bar; EGR: 42%) (Solid symbols: single main injections)

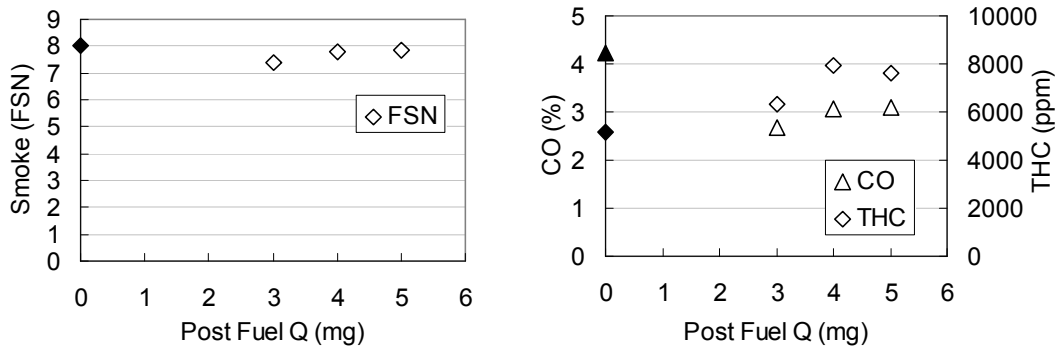


Figure 4.28 Effects of post fuel injection quantity on emissions (2500 rpm 16 mg/cycle; main Sol: -18°CA ATDC; post timing: 6°CA ATDC; injection pressure: 1200 bar; EGR: 50%) (Solid symbols: single main injections)

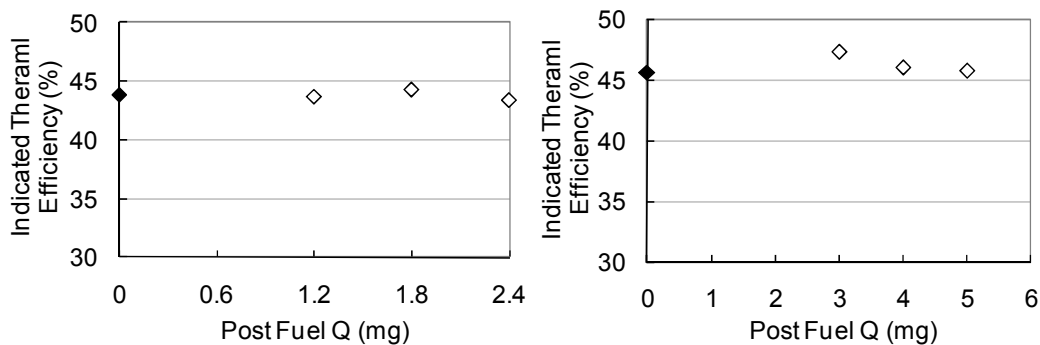


Figure 4.29 Effects of post fuel injection quantity engine on thermal efficiency (Left: 1500 rpm; Right: 2500 rpm) (Solid symbols: single main injections)

The heat release shown in Figure 4.30 indicated that the post fuel combustion heat release rate was negligible. The main fuel combustion was advanced for the higher post fuel injection quantity cases. The lower equivalence ratio due to the smaller quantity of fuel injected in the main fuel injection event led to faster and higher temperature combustion.

Due to the high EGR rate and near-stoichiometric fuel-oxidizer ratio at this load condition, there was only limited oxygen left in the combustion products after most of the main fuel was burned. The post injected fuel had to be burned within a high temperature low oxygen concentration environment in a relatively short time. As a result, the minimum amount of fuel appeared to be the most promising option. Thus, the minimum fuel injection quantities achievable by the injector were selected to investigate the effects of post fuel injection timing on combustion and emissions at intermediate load conditions.

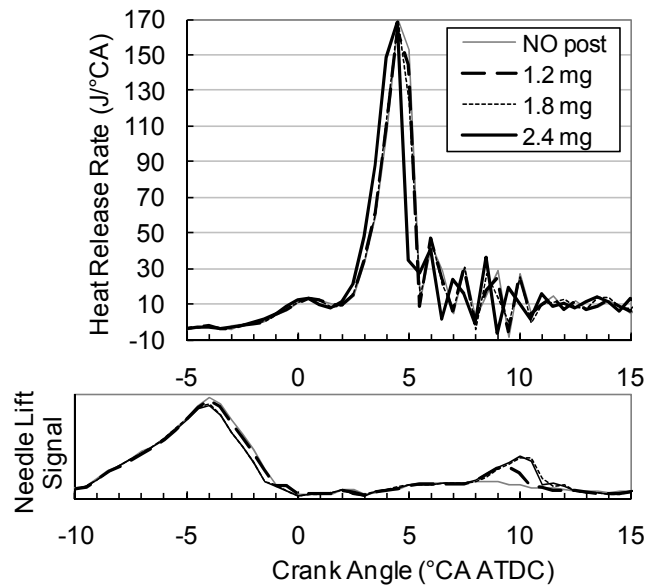


Figure 4.30 Effects of post fuel injection quantity on heat release rate (1500 rpm 16 mg/cycle, 42% EGR, post timing 9°CA ATDC)

For the 1500 rpm and 2500 rpm operating conditions, different EGR rates were selected in the study to evaluate the potential of a small post-injection to reduce PM at both LTC and high-smoke conditions. The smoke emissions from these conditions fell on the left and right hand sides of the smoke number peak as previously shown in Figure 4.2. The effects of post fuel injection timing on emissions are shown in Figure 4.31. The black symbols represent the baseline single fuel injection results. The lowest smoke emissions achieved were from the 3°CA ATDC start of post fuel injection cases for all the operating conditions. However, the reduction in soot emissions was quite small. The 1.2 mg fuel injected at this timing took part in the combustion event while the charge temperature was still high and had some oxygen to support the post fuel to burn. The turbulence and heat generated by the post fuel combustion may have improved the oxidation of the soot formed during the main fuel combustion.

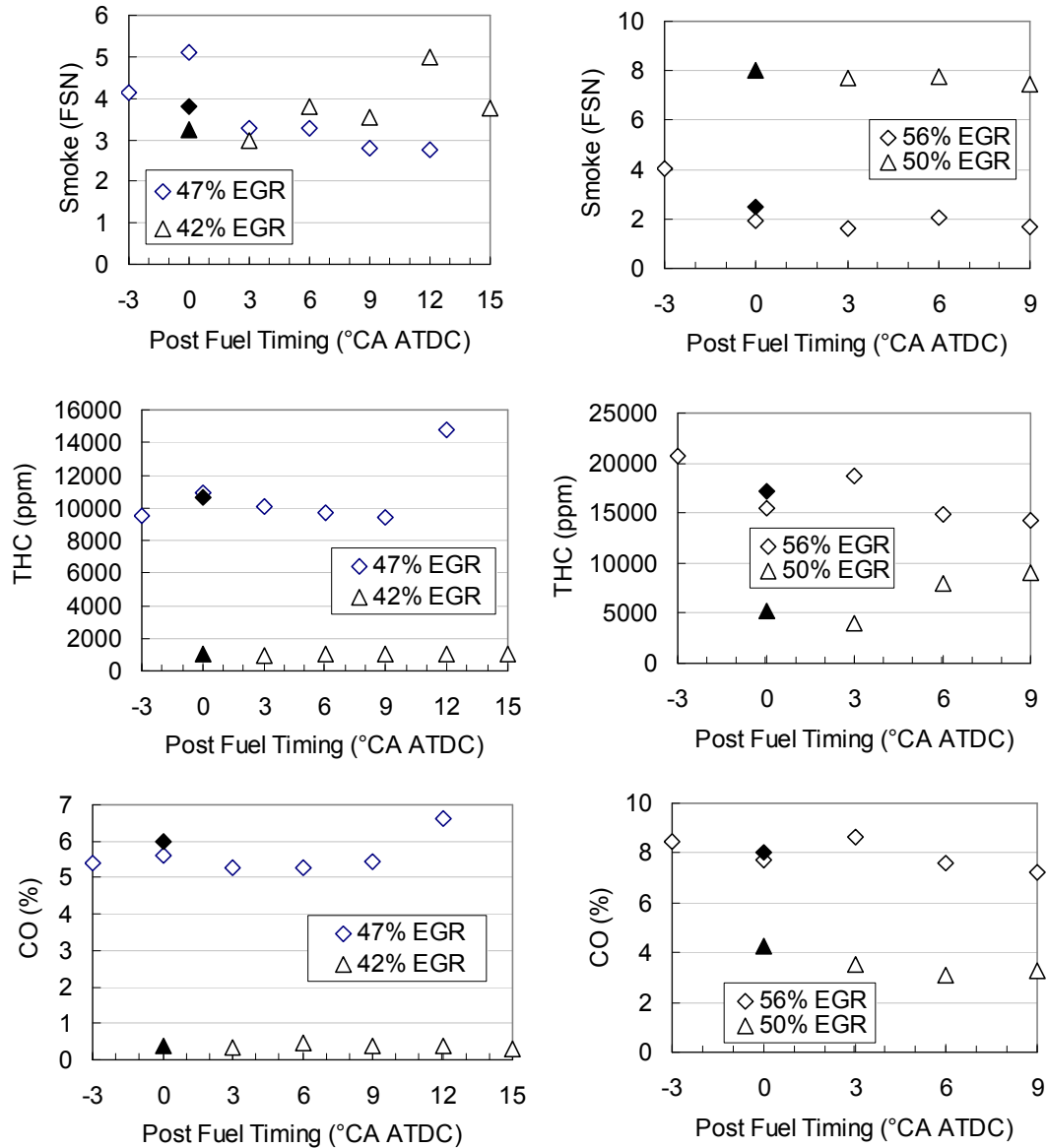


Figure 4.31 Effects of post fuel injection timing on emissions (Left column: 1500 rpm 16 mg/cycle; Right column: 2500 rpm 16 mg/cycle; post fuel injection quantity: 1.2 mg) (Solid symbols: single main injections without post injection)

For those cases where the post fuel injection occurred before the main heat release had the smoke emissions increased. Enhanced pyrolysis of the liquid fuel at high temperatures under low oxygen conditions is encountered when the fuel was injected into the burned gas cloud. For the 1500 rpm conditions, later post fuel injection caused increased smoke emissions especially for the low EGR rate case. The late post fuel injection most likely did not burn completely and contributed to the increase in soot emissions. For the 2500 rpm conditions, the EGR rates were high and the smoke emissions fell on the right side of the peak of the smoke emissions profile (i.e.

decreasing with higher EGR) in Figure 4.2. The delay in post fuel injection timing did not affect the engine-out smoke emissions significantly.

Post fuel injection timing had no significant influence on the heat release rate, as shown in Figure 4.32. For the case where the post fuel injection occurred before the main combustion event, the post-injected fuel led to a faster and higher temperature combustion event.

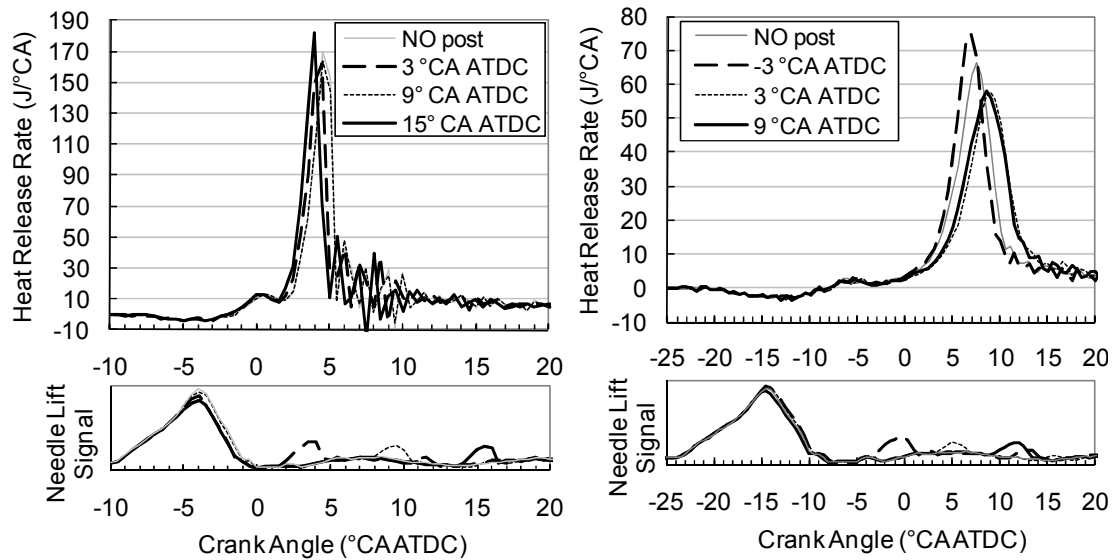


Figure 4.32 Effects of post fuel injection timing on heat release rate (Left: 1500 rpm 16 mg/cycle, 42% EGR, post timing -9°CA ATDC ; Right: 2500 rpm 16 mg/cycle, 56% EGR, post fuel injection quantity 1.2 mg)

The timing of the post fuel injection did influence the main fuel injection behaviour, as shown by the needle lift signals. The post fuel injection may have generated pressure perturbations in the high pressure fuel pipe, these pressure waves could have influenced the main fuel injection event in the following cycle (Michailidis *et al.*, 2010; Zhong *et al.*, 2003). The effective fuel injection pressure for the main fuel injection events may be different for the different post fuel injection timings. This could be another factor that influenced the combustion process.

#### 4.4 Discussion

Figure 4.33 shows a modified  $\Phi$ -T map based on the work of Akihama *et al.* (2001) that illustrates the conceptual effects of engine operating parameters on soot and NOx emissions. The effects of engine operating parameter variations in LTC mode on local  $\Phi$ , T and smoke emissions are illustrated by the arrows. The trends shown are only used as a conceptual illustration based on qualitative analysis of the

parameters to aid the discussion here. The starting points of the arrows in the figure were chosen arbitrarily to represent the local combustion zones which are presumed during different load high EGR diesel combustion conditions. For low load (Figure 4.33a), the combustion generally occurs within the relatively low equivalence ratio and low temperature zones where the soot formation is low. The variations shown in the operating parameters all lead to a reduction in soot formation. For the intermediate load (Figure 4.33b) the combustion tends to occur within relatively higher equivalence ratio and temperature zones where the soot formation rates tend to be higher. Variations in engine operating parameters in this case can have a more significant influence on soot emissions than for the low load condition.

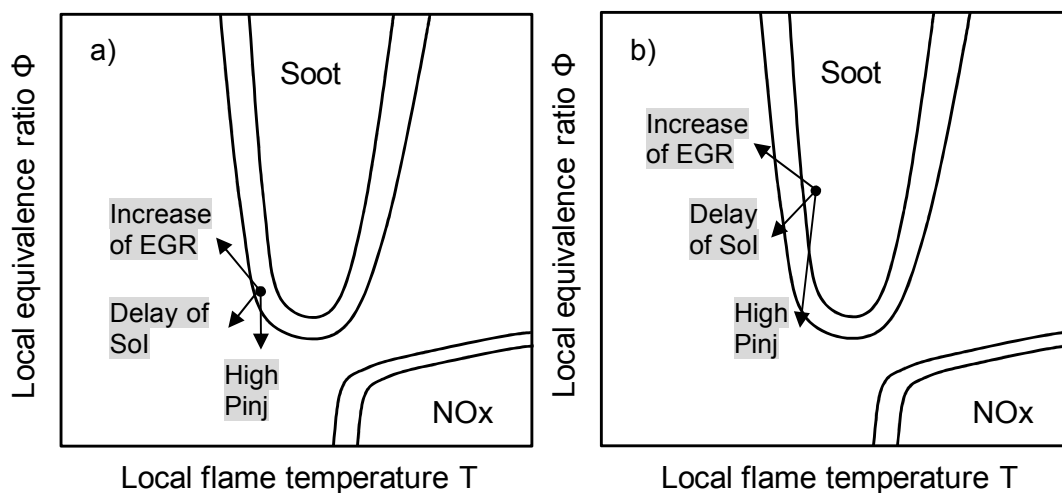


Figure 4.33 Conceptual effects of the variations in EGR rate, fuel injection timing (Sol) and injection pressure (Pinj) on  $\Phi$ , T and soot emissions (starting point, magnitudes and directions for illustration only) (a): low load condition; b): intermediate load condition)

Both an increase in EGR rate and a delay in fuel injection timing can reduce the local equivalence ratio and flame temperature, which shifts the combustion into the LTC zone (bottom left hand) in the  $\Phi$ -T map. An increase in fuel injection pressure can improve the fuel-air mixing and lead to reduced local equivalence ratios. Combustion temperature is influenced by the fuel injection pressure in a more complicated way. The improved mixing can enhance the combustion process and subsequently lead to higher combustion temperatures. However, the homogeneous charge could also lead to reduced flame temperatures. Thus, the effect of fuel injection pressure on soot emissions is a result of the combination of these two trends.

For the operating modes investigated here, the LTC diesel engine generated very high levels of THC and CO emissions due to the characteristics of LTC diesel combustion, especially for the intermediate load conditions. Reduction in THC and

CO emissions by enhancing the combustion may not be enough to ensure that an LTC engine meets the regulated CO and THC emissions levels. However, the high levels of THC and CO could be used as reactants for the regeneration of diesel exhaust aftertreatment devices (DPF or LNT) which are likely to be needed for emissions control at the higher load conditions which cannot be achieved by LTC.

Emissions of PM are mainly formed by soot (black carbon) and soluble organic fractions (SOF). Other studies have shown that the composition of PM is significantly influenced by the engine operating conditions. Within conventional diesel combustion modes, black carbon (soot) dominates the PM on a weight basis. When the EGR rate is increased to levels required to achieve LTC, other researchers have found that the SOF becomes the dominant component in the particles (Ogawa *et al.*, 2007). A diesel oxidation catalyst could be an effective device to remove any remaining particles under LTC conditions as well as the high levels of gaseous THC and CO. However, the lower exhaust temperature and (at intermediate load) near-stoichiometric oxygen concentration would need to be accounted for during the implementation of this technology (Han *et al.*, 2008; Jacobs *et al.*, 2008).

A larger number of small particulates were generated from LTC combustion than the conventional intermediate level EGR conditions. The total particulate volume for the LTC mode was also higher, while the smoke number measurement was lower for the LTC conditions. Changes in particulate composition with EGR rate may be used to explain the phenomenon observed in the LTC mode that a low FSN accompanied with a high total particle volume. For the intermediate load conditions, total particulate volume correlated with FSN for the different EGR levels, except for the LTC conditions, where the total volume was slightly higher.

The interactions between the injection events for the multiple fuel injection strategy cannot be neglected. The fuel pipe pressure fluctuations generated by the injection events could be significant and they will affect the subsequent injection event and may lead to unexpected fuel injection behaviour. These changes in the effective injection pressure and the consequent changes in injector behaviour and duration derived from the multiple fuel injection events cannot be ignored, as diesel combustion is very sensitive to these parameters.

To improve the intermediate load conditions thermal efficiency under LTC, an increase in the oxygen concentration through intake boosting may be effective. Increasing the oxygen content in the charge could help to expand the LTC region of



the engine operating map. However, this could also influence the NO<sub>x</sub>/PM trade-off. More work is required to clarify its effects, which will be introduced briefly in Chapter 8 but is primarily the focus of ongoing work subsequent to that reported here (Sarangi *et al.*, 2010).

## 4.5 Conclusions

For the results presented in this chapter it can be concluded that:

- 1) When the intake oxygen concentration is reduced to 12-14%, the formation of NO<sub>x</sub> is suppressed and the smoke number reaches a peak. Further dilution to 9-11% oxygen concentration reduces the smoke number significantly, while the NO<sub>x</sub> remained at near-zero levels, thereby achieving a 'smokeless, NO<sub>x</sub>-free' LTC. The THC and CO emissions increase significantly within the LTC mode.
- 2) LTC showed an increase in the total particle number and volume compared to the intermediate EGR cases. For the high-smoke intermediate level EGR combustion, the total particle number was lower, but the particle size distribution had a larger count median diameter. The count median diameter in the LTC mode is reduced compared to the conventional high EGR diesel combustion for the intermediate load conditions.
- 3) Both the combustion rate and the maximum pressure rise rate were significantly reduced with LTC. This removes the need to delay the combustion phasing, as the peak pressure rise rate and NO<sub>x</sub> were both reduced. This allowed greater freedom in optimising the injection timing for thermal efficiency.
- 4) For the 8 mg/cycle fuelling cases, the overall combustion is still lean in the LTC mode. By taking advantage of more advanced combustion phasing, the thermal efficiency of LTC could be made higher than conventional diesel combustion. However, for the 16 mg/cycle cases, the engine had to be run at such high levels of EGR to effectively suppress smoke emissions that the global mixture was nearly-stoichiometric. Thus, despite the more advanced combustion phasing, the high emissions of partial-combustion by-products reduced the combustion efficiency.
- 5) The smokeless NO<sub>x</sub>-free combustion was achieved with a lower EGR rate at 2500 rpm operating conditions compared to 1500 rpm. A sharper drop in smoke emissions was shown for the 2500 rpm conditions when the dilution ratio was increased.

6) Generally, advanced injection timing advanced the combustion phasing and resulted in improved thermal efficiency and more stable combustion in the LTC regime. However, too early fuel injection or too high an injection pressure can lead to fuel impingement which results in higher THC emissions and needs to be avoided. The corresponding deterioration in combustion efficiency wastes more energy than that achieved from the advanced combustion phasing for the high load conditions.

7) An increase in fuel injection pressure enhances the mixing process, increases the combustion rate and reduces the hydrocarbon emissions. However, at very early timings and high speeds, the fuel is thought to impinge on the walls, leading to significant increases in THC emissions.

8) Post fuel injection had an insignificant effect on LTC combustion and emissions, as the oxygen was almost consumed by the main fuel injection and hence relatively few oxidation reactions occurred after the end of the main combustion event. As a result, the combustion of post fuel injection contributes little to the engine-out soot reduction.

The results presented in this chapter indicated that the injection event and combustion process were related, and that in particular the 'cool flame' reactions were sensitive to the injection and had a significant impact on the subsequent main combustion event. In the next chapter, the details of the low temperature reaction and its influence on LTC combustion and emissions will be discussed. The EGR rate, intake manifold temperature, fuel injection pressure and timing are varied to study their influence on low temperature heat release, negative temperature coefficient and the main combustion process.

## **Chapter 5 Low Temperature Diesel Combustion**

### **5.1 Introduction**

In Chapter 4, the characteristics of the research engine running with different levels of EGR to achieve low temperature diesel combustion were introduced. Despite the benefits of ultra low NO<sub>x</sub> and smoke emissions when operating in LTC mode, the engine suffered from increased THC and CO emissions and degraded combustion stability. A deeper understanding of LTC diesel combustion and emissions behaviour is needed to help improve the LTC combustion in efficiency and emissions.

LTC diesel combustion shows a two-stage combustion process, with distinct low temperature heat release (LTHR) and main combustion regimes, which is different from the conventional premixed-diffusion based diesel combustion process. The low temperature reaction regime is a combination of the cool flame and the negative temperature coefficient region (NTC) (Naidja *et al.*, 2003; Olivier *et al.*, 2005). Cool flame is the product of a limited exothermic reaction that is associated with a partial conversion of the fuel. It is governed by a complex low-temperature oxidation (LTO) process (Hiroyuki *et al.*, 2008). The NTC is a unique phenomenon in hydrocarbons oxidation, in which the overall reaction rate decreases with increasing temperature and it behaves as a barrier to the occurrence of auto-ignition (Hiroyuki *et al.*, 2008). The low temperature regime produces energy and intermediate radicals for the rapid fuel vaporization and the following high temperature ignition event (Jansons *et al.*, 2008; Musculus, 2006).

In this chapter, a detailed step-by-step combustion progress study is conducted with the LTC mechanism aiding to the interpretation of the combustion characteristics and emissions. The relations among different stages of the combustion and their effects on emissions are evaluated. With theoretical support from the published literature on the low temperature oxidation processes, a deeper understanding of how the LTC operating parameters influence the combustion and emissions can be developed from the experimental results.

### **5.2 Low Temperature Oxidation of Hydrocarbons**

The low temperature hydrocarbon oxidation contains five main processes (Pilling, 1997) and are introduced as follows.

1) Primary initiation (Generates radicals from parent molecules, such as fuel decomposition):



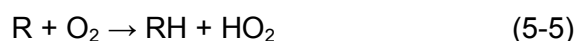
Here, the RH is the parent alkane, R is an alkyl radical. This is an extremely endothermic process that includes oxygen attack and disassociation of hydrocarbon molecules. Increases in charge temperature and concentration of reactants can increase these reaction rates.

2) Propagation of the chain (no change in the number of radicals):



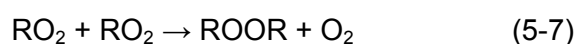
Here, the X can be OH, H, CH<sub>3</sub>, CH<sub>3</sub>O<sub>2</sub> and HO<sub>2</sub>. They are influential in removing RH or in determining reaction rates, ignition limits, flame speeds or ignition time delays. These reactions are mainly exothermic and contribute to the cool flame heat release.

3) Termination of the radical chain (reduce the number of radicals):



The termination steps produce inert radicals, HO<sub>2</sub> and small alkyl radicals R<sub>small</sub>. These reactions compete with the branching reactions for the remaining radicals R.

4) Branching (multiplication of the number of radicals);



The thermal decomposition of ROOR to two radicals is the branching step in the mechanism. It provides the multiplication in the number of radicals needed for the phenomenon of auto-ignition.

5) Secondary initiation (or degenerate branching), where new radicals are formed from a "stable" intermediate product. Here, the M is the third body in the reaction.



This is often used as an indicator of the start of high temperature combustion in engines; specifically, OH is frequently used to indicate ignition within LTC combustion regime (Costa *et al.*, 2005; Westbrook, 2000).

At successively higher temperature, the reaction:



has its equilibrium shifted to the left hand, and the termination reactions (5, 6) through R become more dominant than the branching reactions through  $RO_2$  (7, 8). Thus, the low temperature reaction gets slower. This is the cause of the negative temperature coefficient (NTC). Hence, the NTC is a temperature dependent phenomenon. When the temperature is below the NTC region, increasing the temperature enhances the low temperature reactions of the hydrocarbon mixture (through reactions 7 and 8). Once the temperature is within the NTC range, an increase in mixture temperature leads to reduced reaction rates (because of reactions 5 and 6). When the temperature is higher and exceeds the NTC region (i.e. ~900 - 1100 K) (Warnatz *et al.*, 1999; Westbrook, 2000), the combustion is in high temperature mode and a further increase in temperature will lead to an increase in reaction rates as expected for most hydrocarbon oxidation reactions.

Low temperature oxidation of fuel exhibits a strong influence on the ignition timing of high temperature combustion (Warnatz *et al.*, 1999; Westbrook, 2000). The heat release in the cool flame strongly affects the point at which the in-cylinder temperature reaches a level to initiate the main combustion event. Researchers have detected cool flame reactions at temperature as low as 393 K under engine-like conditions. The radicals generated from the cool flame reactions were consumed in the temperature interval from 623 to 673 K followed by disappearance of the cool flame (Naidja *et al.*, 2003). The ignition for the main combustion event occurs at the temperature where the core mixture reaches the  $H_2O_2$  decomposition temperature of about 900 - 1100 K (Westbrook, 2000).

### 5.3 Research Methodology

The main objectives of the work described in this chapter were to investigate in detail the preliminary, low-temperature reactions in an LTC combustion event. The research engine was run under LTC operating conditions based on the experimental results from Chapter 4. In this chapter only one of the engine operating parameters was changed for each set of tests, with the other parameters kept constant to identify the effects of individual parameters on LTC combustion. Table 5.1 lists the details of the experimental conditions. Initially, the effects of EGR rate were investigated for the 1500 rpm 8 mg/cycle, and 16 mg/cycle and 2500 rpm 16 mg/cycle conditions; then, the intake manifold temperature was varied at 1500 rpm at both 8 and 16 mg/cycle

fuelling conditions; the fuel injection pressure and timing were also changed for the two fuelling conditions at 1500 rpm.

To evaluate the LTC combustion process in detail, it was divided into five stages by different combustion phasing parameters as introduced in Chapter 3 and as shown in Figure 5.1. The first stage of the combustion is the ignition delay of the low temperature heat release (IDL), defined as the duration from start of fuel injection (Sol) to the start of low temperature heat release (SoCL – start of combustion, low temperature). SoCL has been defined as the crank angle where the heat release rate is first positive (i.e. crosses the x-axis from negative to positive value). At this point, the integrated heat release is at its minimum value and starts to increase. The 5% heat release crank angle (CA5) has been used to define the start of high temperature combustion (SoCH). From this point, the heat release rate was much higher compared to the HRR during the LTHR period. The duration between SoCL and CA5 is named as duration of the low-temperature reactions (DurL), which covers both the cool flame regime and the NTC region. The 50% heat release crank angle (CA50) has been used to separate the main/high temperature heat release into two parts: from SoCH to CA50 is the stage of rapid high temperature combustion process; while from CA50 to CA90 (90% heat release crank angle) is the post high temperature combustion. The duration of these two parts are named as DurF and DurP, respectively.

Table 5.1 Engine operating conditions

Test set	EGR (%)	Sol (°CA ATDC)	Pinj (bar)	T intake (°C)	O <sub>2</sub> Equivalence ratio (sim*)
1500 rpm 8 mg EGR	62 - 68	-21	1000	70	0.66 – 0.79
1500 rpm 16 mg EGR	52 - 56	-12	1000	70	0.98 – 1.07
2500 rpm 16 mg EGR	47 - 52	-15	900	80	0.89 - 0.98
1500 rpm 8 mg Tint	65	-21	1000	50 - 90	0.69 - 0.76
1500 rpm 16 mg Tint	54	-12	1000	50 - 90	0.97 -1.07
1500 rpm 8 mg Pinj	65	-21	800 - 1200	70	0.72
1500 rpm 16 mg Pinj	54	-12	800 - 1200	80	1.03
1500 rpm 8 mg Sol	65	-24 - -18	1000	70	0.72
1500 rpm 16 mg Sol	54	-15 - -9	1000	70	1.02

\* Oxygen based equivalence ratio derived from 1D engine model results

The coefficients of variation of the IMEP and the peak heat release rate were used to indicate combustion stability. The standard deviations of the combustion phasing parameters were used to indicate the variations in the combustion process. Gaseous emissions and smoke number were measured throughout the experiments. For the gaseous emissions, ppm was used to indicate the emissions levels. As the variations in the engine operating parameters only caused a maximum 3% change in the intake air flow rate, therefore using of volumetric concentrations (ppm) was acceptable since the main component of the normalizing value (air flow rate) was not changing significantly. The use of ppm values increases the precision of the results, since the air flow measurements were not accurate to within  $\pm 3\%$ . Smoke number measurements for the 8 mg/cycle fuelling conditions were nearly zero for all the tests conducted in this work and hence are not presented.

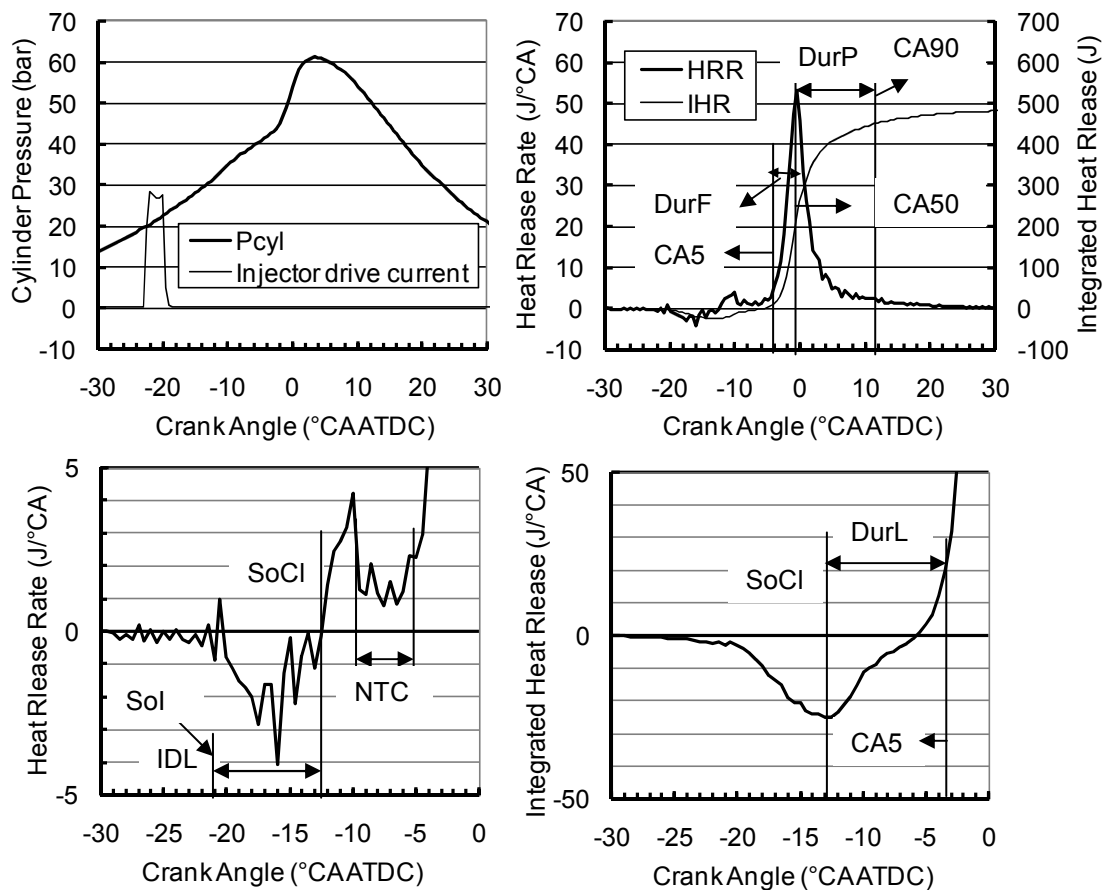


Figure 5.1 Typical low temperature diesel combustion cylinder pressure and heat release curves, details of low temperature reactions shown in the right hand side (1500 rpm, 8 mg/cycle, fuel injection pressure 800 bar, Sol -21°CA ATDC, intake temperature 70°C, EGR rate 65%)

## 5.4 Results

In this section, the effects of EGR rate, intake manifold temperature and fuel injection pressure, timing, and quantity on the LTC combustion process and emissions are presented for the different load and speed conditions.

### 5.4.1 Effects of EGR rate

An increase in EGR rate by several percentage points showed a significant influence on LTC heat release rate, for both the low temperature heat release and the main combustion events, as shown in Figure 5.2. It retarded the main combustion event and reduced the peak heat release rate significantly. The peak of the low temperature heat release rate was about 10% that of the main combustion event. However, the influence of the EGR rate on the heat release rate during the LTHR was still detectable. An assessment of the heat release rate curves for the LTHR period, shown in the right hand column of Figure 5.2, showed that higher EGR rates led to a later cool flame and a lower LTHR reaction rate at constant start of injection timing. As the intake manifold temperature was kept constant for the different EGR levels, the LTHR processes appeared to be sensitive to the charge composition. For the higher EGR rates, the reduction in oxygen concentration and increase in heat capacity due to the increased concentration of CO<sub>2</sub> and H<sub>2</sub>O in the charge should lead to slower fuel reaction rates and lower charge temperatures during the LTHR period. This lower temperature and lower O<sub>2</sub> concentration may have reduced the formation and propagation rates of the initial radicals, and the concentration of the intermediate compounds during the LTHR period.



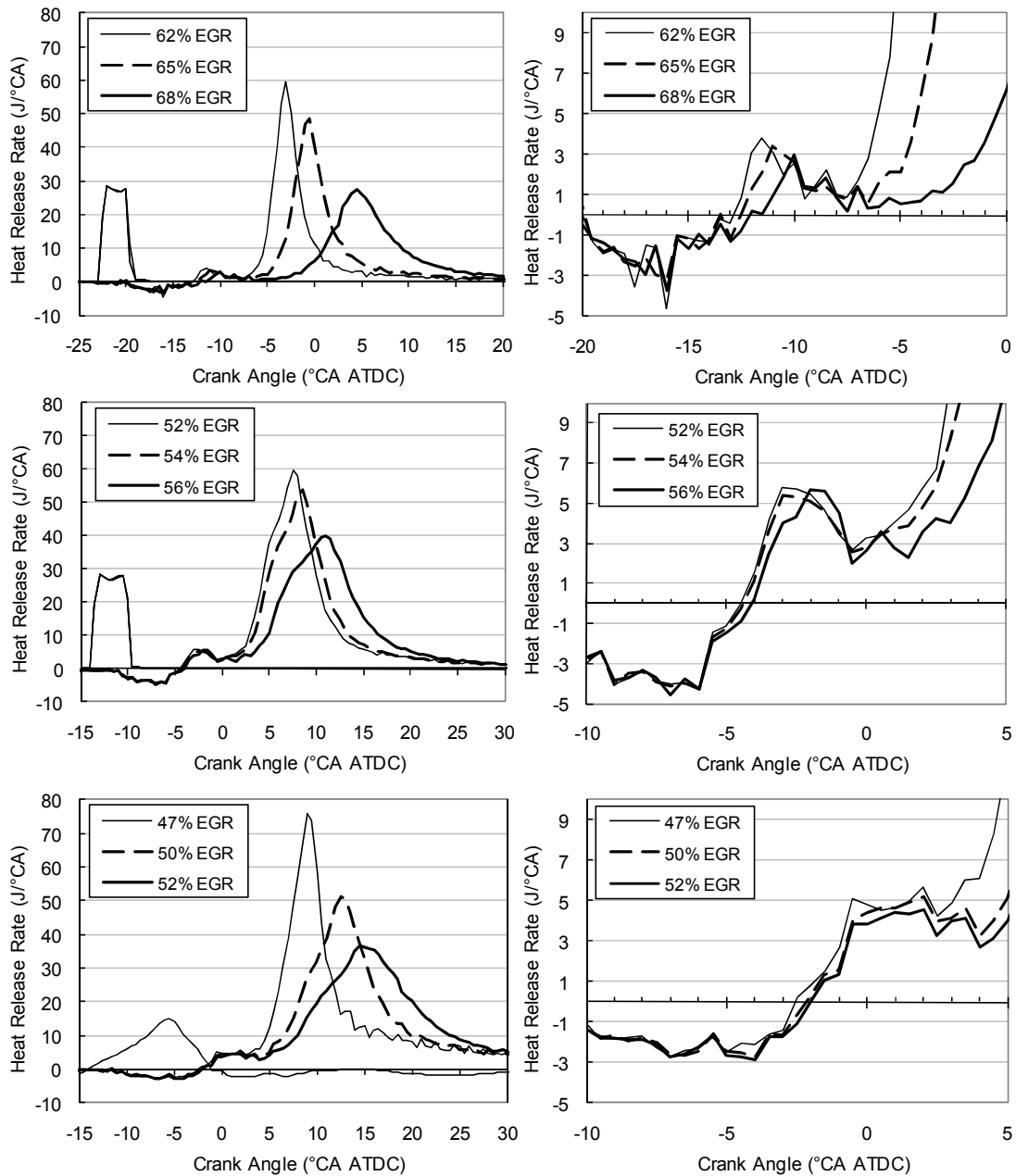


Figure 5.2 Effects of EGR rate on LTC heat release (Top: 1500 rpm, 8 mg/cycle, fuel injection pressure 800 bar, Sol -21°CA ATDC, intake temperature 70°C; Middle: 1500 rpm, 16 mg/cycle, fuel injection pressure 1000 bar, Sol -12°CA ATDC, intake temperature 70°C; Bottom: 2500 rpm, 16 mg/cycle, fuel injection pressure 900 bar, Sol -15°CA ATDC, intake temperature 80°C)

A higher EGR rate led to a retarded combustion phasing and an increased combustion duration, as shown in Figure 5.2 and summarised in Figure 5.3. The change in intake charge composition had a more significant influence on the phasing of the main combustion than it had on the LTHR. This indicated that the two combustion stages were governed by different mechanisms. The LTHR rate was controlled by the intake charge composition with the constant temperature cases in

this set of tests. The in-cylinder temperature would take a longer time to reach the temperature threshold where the NTC region terminates (i.e. when the high temperature reactions start), and hence the duration of the LTHR (DurL) was increased. In terms of the main combustion event, the different charge composition caused by the EGR and the LTHR processes led to a more significant influence on the combustion phasing parameters. The retarding of the start of the main combustion phase and of the CA50 by an increase in the EGR rate was longer than the delay in the start of the LTHR. The duration of the first half of the main combustion events, DurF, was increased by the increase in EGR rate, indicating a slower heat release process for the premixed combustion event. The duration of the second half of the main combustion (DurP) was increased by the higher EGR rates for the 8mg/cycle fuelling case while it was reduced for the 16mg/cycle fuelling cases. A lack of oxygen in the charge, a reduction in the concentrations of intermediate radicals and an increase in the ignition delay were all expected to contribute to the retarded and slower main combustion event.

For the 16 mg/cycle cases, the change in LTHR by the EGR rate is less significant than for the 8 mg/cycle cases. The higher fuel concentration could reduce the LTHR sensitivity to the intake charge dilution ratio. The doubled fuel injection quantity led to a higher equivalence ratio for these conditions, which will have increased the fuel concentration and lead to increased primary radicals formation and propagation processes even with reduced oxidant concentrations. Thus, the in-cylinder temperature increased more rapidly for this load condition and entered the NTC region sooner after the start of the cool flame reactions than for the low load case. The rapid increase in temperature for the 16 mg/cycle fuelling condition also led to a shorter NTC region than for the 8 mg/cycle fuelling condition. For the 16mg/cycle conditions, the change in duration of the LTHR (which incorporated both the cool flame reactions and the NTC region) was only about a half of that from the low fuelling conditions.

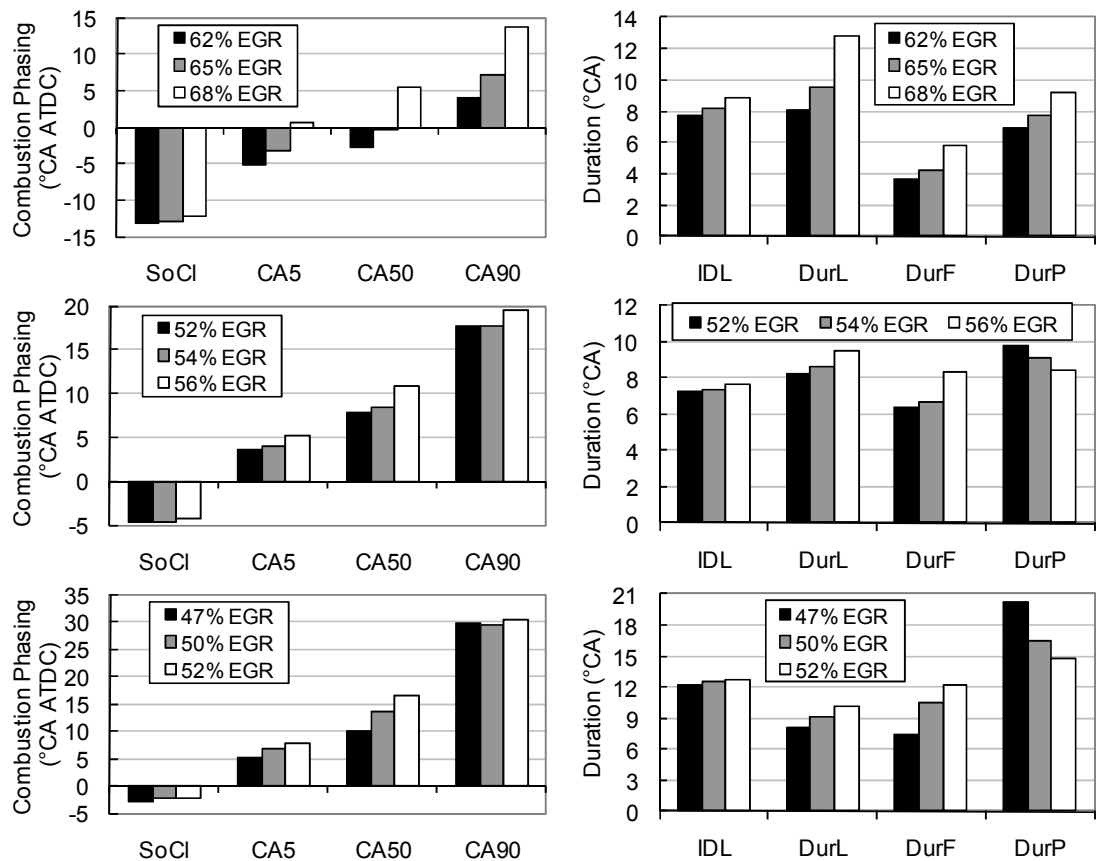


Figure 5.3 Effects of EGR rate on LTC combustion phasing (IDL: ignition delay of LTHR; DurL: SoCl-CA5; DurF: CA5-CA50; DurP: CA50-CA90) (Top: 1500 rpm, 8 mg/cycle, fuel injection pressure 800 bar, Sol -21°CA ATDC, intake temperature 70°C; Middle: 1500 rpm, 16 mg/cycle, fuel injection pressure 1000 bar, Sol -12°CA ATDC, intake temperature 70°C; Bottom: 2500 rpm, 16 mg/cycle, fuel injection pressure 900 bar, Sol -15°CA ATDC, intake temperature 80°C)

The EGR level significantly influences combustion stability and emissions, as discussed in detail in Chapter 4; the emissions and combustion stability for the specific points of interest in this chapter are shown in Figure 5.4. The combustion stability represented by CoV(IMEP) and CoV(MaxHRR) was degraded with higher EGR rates. The standard deviations of SoCL, CA5 and CA50 were also increased, indicating a more variable timing of the start of LTHR and main combustion by the increased intake charge dilution. The NO<sub>x</sub> and smoke emissions were both reduced with the increased EGR rate, while the THC and CO emissions were increased due to the reduction in the intake charge oxygen concentration, as shown in Figure 5.4. All these results are consistent with the previous chapter's view of the effect of EGR rate on LTC emissions. The longer NTC region increased the time available for mixture formation, which led to more homogeneous combustion and reduced NO<sub>x</sub> and soot formation. The increases in THC and CO emissions were the results of a

combined effect from reduced oxygen concentration, possible over-mixing and bulk quenching due to the longer ignition delay and reduced peak bulk temperature.

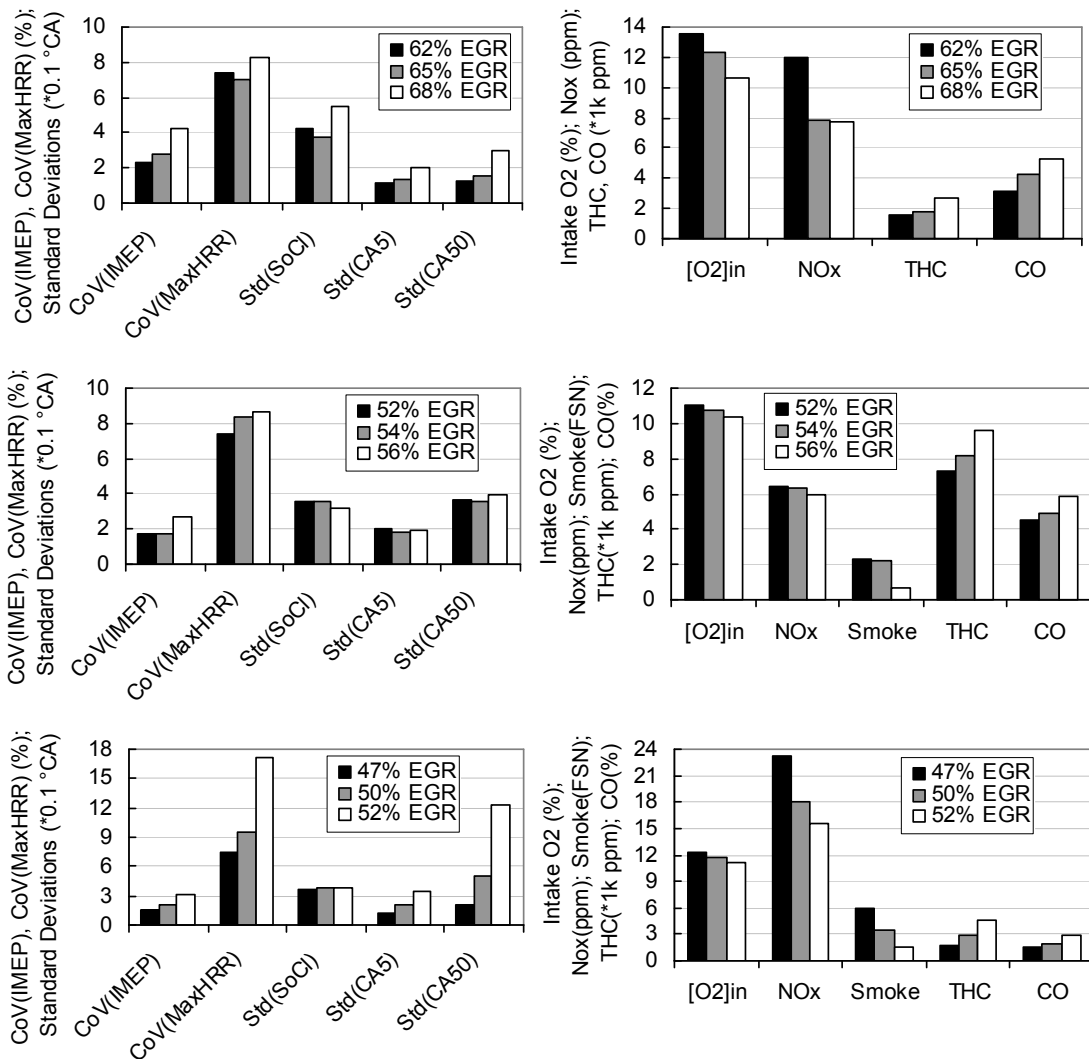


Figure 5.4 Effects of EGR rate on LTC stability and emissions (Top: 1500 rpm, 8 mg/cycle, fuel injection pressure 800 bar, Sol -21°CA ATDC, intake temperature 70°C; Middle: 1500 rpm, 16 mg/cycle, fuel injection pressure 1000 bar, Sol -12°CA ATDC, intake temperature 70°C; Bottom: 2500 rpm, 16 mg/cycle, fuel injection pressure 900 bar, Sol -15°CA ATDC, intake temperature 80°C)

The higher EGR rates led to lower LTHR rates and longer LTHR durations. This suggests that the LTHR was influenced by the charge composition, and the NTC region was mainly influenced by the in-cylinder temperature. For the low rate of LTHR caused by the higher dilution ratio, there was a longer period for the reaction to release enough chemical energy to push the charge temperature into the NTC region.

At higher load, the increase in fuel injection quantity led to increased fuel concentration taking part in the low temperature oxidation processes, resulting in higher reaction rates. The enhanced cool flame reaction for the higher fuelling conditions led to a more rapid increase in the charge temperature. This higher temperature resulted in an earlier occurrence of the NTC regime, which terminated the cool flame reactions.

For the same fuel injection quantity, engine speed showed an insignificant influence on the LTC mechanism. The duration of the cool flame reaction and ignition delay on time basis (in ms) were almost the same for the 1500 rpm and 2500 rpm conditions with 16 mg/cycle fuelling. This indicates that the chemical kinetics dominated the low temperature oxidation processes. Thus, the effects of intake charge temperature, fuel injection pressure and timings were studied for 1500 rpm cases only. The effects of engine speed were evaluated further and the results are presented in Chapter 7.

#### **5.4.2 Intake charge temperature**

Higher intake manifold temperature led to advanced and rapid heat release processes, as shown in Figure 5.5. The peak heat release rate for the main combustion event was increased with the higher intake temperature. However, the peak of the cool flame heat release rate was reduced for the higher intake temperature cases. The increase in intake manifold temperature by 20°C led to an increase in in-cylinder temperature by about 50°C at the end of the compression stroke\*. The higher charge temperature enhanced the radicals' primary initiation and propagation processes in the LTHR. It also enhanced the evaporation of the fuel and increased the homogeneity of premixed fuel-air mixture to support the early stage of the main combustion, leading to a higher peak HRR. However, due to the higher charge temperature, the cylinder temperature may have reached the NTC region earlier during the LTHR process. Hence, the NTC terminated the low temperature oxidation processes and led to reduced LTHR rates for these cases.

---

\* The calculated end of compression temperature was based on assuming adiabatic, polytropic compression, with polytropic exponent of 1.35, from IVC (-134°C ATDC) to Sol (-21°C ATDC).

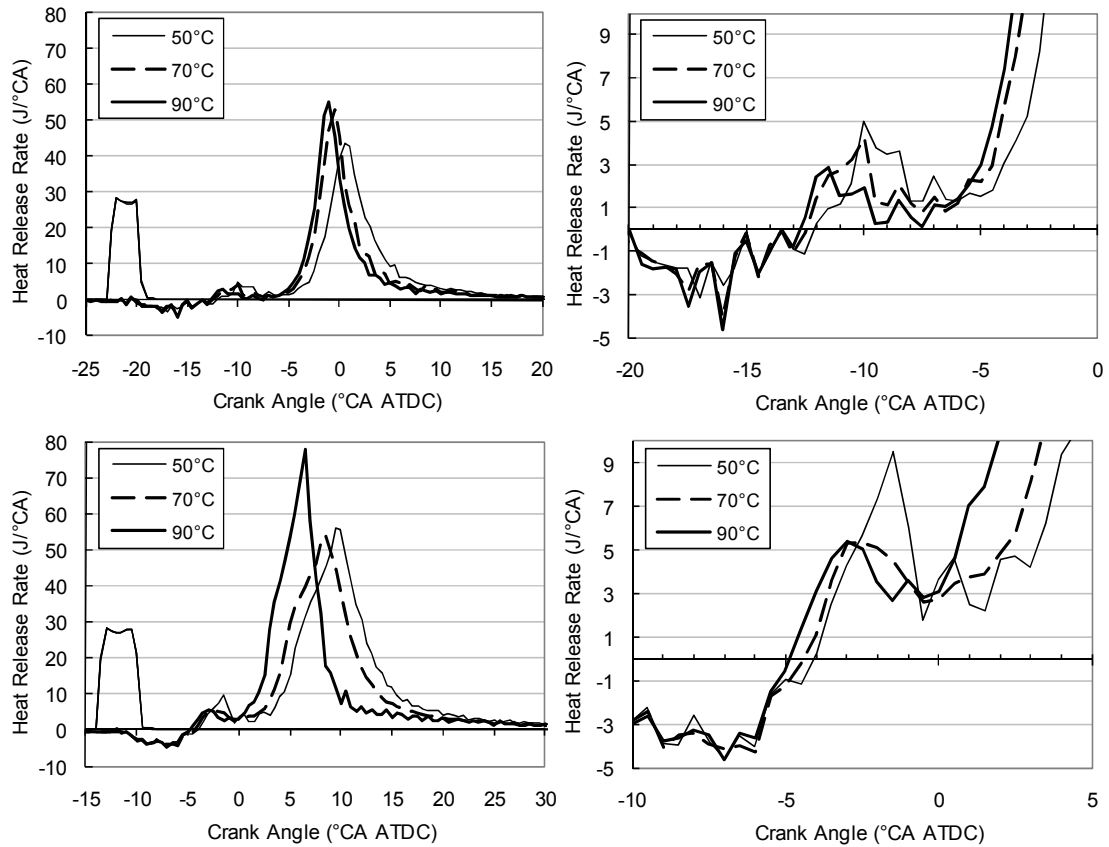


Figure 5.5 Effects of intake manifold temperature on LTC heat release (Top: 1500 rpm, 8 mg/cycle, fuel injection pressure 800 bar, Sol -21°CA ATDC, EGR rate 65%; Bottom: 1500 rpm, 16 mg/cycle, fuel injection pressure 1000 bar, Sol -12°CA ATDC, EGR rate 54%)

For the 50°C intake temperature cases, the LTHR rates were significantly higher than that for the higher temperature cases. As the temperature is the decisive factor for the occurrence of the NTC region, the terminating effects of the NTC on the low temperature oxidation processes would be less significant for the lower mixture temperature cases. The wide temperature difference between the start of reaction (decided by the intake charge temperature) and the temperature for NTC to occur (at constant temperature) enabled a higher intensity of LTHR rate.

Increased intake charge temperature led to advanced combustion events for the whole combustion process. The combustion phasing and duration shown in Figure 5.6 suggest that the higher intake temperature reduced the ignition delay for the LTHR (IDL). The higher charge temperature led to an earlier occurrence of primary radical initiation and propagation. While the NTC region is a function of the temperature, the cylinder temperature reached the NTC region and terminated the radical formation chains sooner for the higher intake temperature cases. With less heat released from the cool flame reaction process, the cylinder temperature

increased slowly for the high intake temperature cases. However, the in-cylinder temperature is a combined result of the intake charge temperature and LTHR. Hence, even with lower LTHR, the higher intake temperature cases may still have had a higher charge temperature and passed through the NTC region more rapidly. This led to shorter ignition delay for the main combustion event.

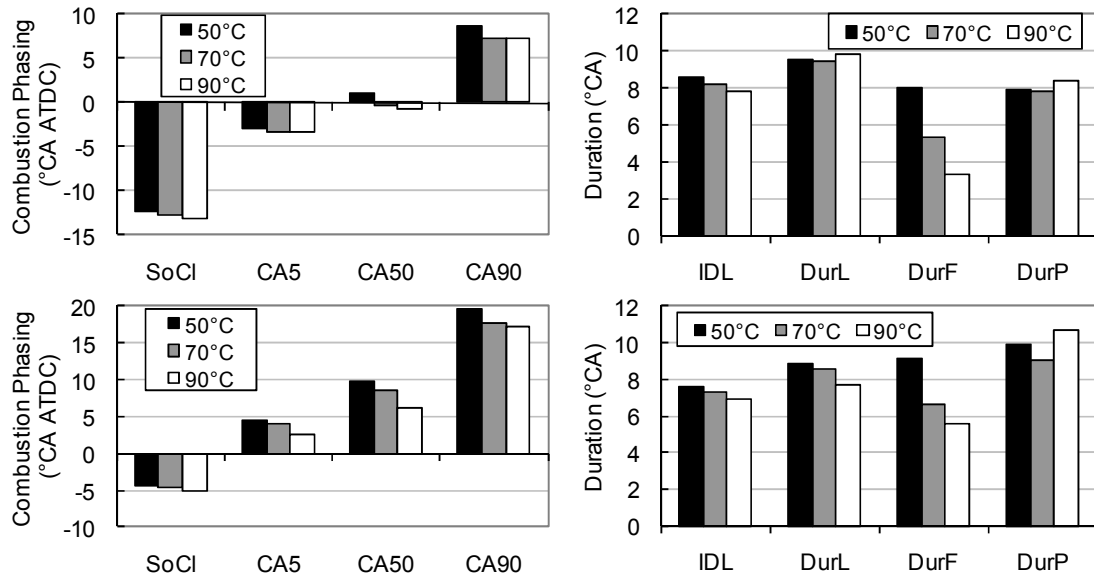


Figure 5.6 Effects of intake manifold temperature on LTC combustion phasing (IDL: ignition delay of LTHR; DurL: SoCI-CA5; DurF: CA5-CA50; DurP: CA50-CA90) (Top: 1500 rpm, 8 mg/cycle, fuel injection pressure 800 bar, Sol -21°CA ATDC, EGR rate 65%; Bottom: 1500 rpm, 16 mg/cycle, fuel injection pressure 1000 bar, Sol -12°CA ATDC, EGR rate 54%)

The duration of the first half of the main combustion was reduced significantly by the higher intake temperature, while the duration of the second half was not significantly affected. The rapid first half heat release of the main combustion event associated with the higher charge temperature which could lead to enhanced fuel oxidation. The reduction in low temperature oxidation rates during the early stage of the cycle by increased intake temperature could be another reason for the increases in the main combustion heat release rates. The reduction in the LTHR for the fuel may have led to a different charge composition for the main combustion event. The later part of the main combustion event, however, was mainly governed by the availability of oxygen in the mixture and would therefore be less sensitive to the intake temperature, as the results shown in Figure 5.6 demonstrate.

The combustion stability was improved by the higher intake temperatures, with the earlier and higher temperature combustion generally leading to reduced combustion variability as represented by variability in both heat release rate and combustion

phasing, as shown in Figure 5.7. However, the standard deviation of SoCL was increased for the low load condition, which is consistent with a lower intensity of LTHR caused by the higher intake charge temperature.

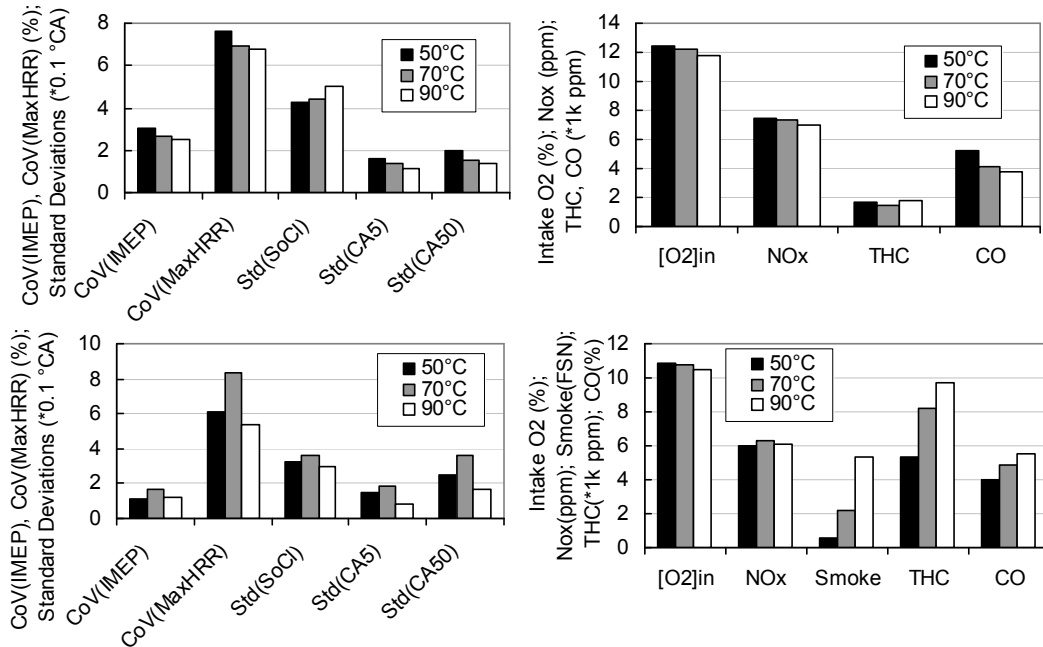


Figure 5.7 Effects of intake manifold temperature on LTC combustion stability and emissions (Top: 1500 rpm, 8 mg/cycle, fuel injection pressure 800 bar, Sol -21°CA ATDC, EGR rate 65%; Bottom: 1500 rpm, 16 mg/cycle, fuel injection pressure 1000 bar, Sol -12°CA ATDC, EGR rate 54%)

The smoke emissions for the intermediate load condition were increased significantly with higher intake temperature despite a reduction in the intake oxygen content. The reduction in ignition delay due to the higher charge temperature and shorter NTC region in the LTC regime led to increased combustion temperature and subsequently increased soot emissions. This is reasonable, as for the LTC operating condition, the soot formation is suppressed by the low combustion temperature, and an increase in combustion temperature could lead to increased soot formation rates. However, the soot oxidation rates were not significantly increased under this mode due to low intake oxygen concentration, which is supported by the relatively small change in later-phase combustion duration as shown in Figure 5.6.

The THC and CO emissions showed different trends for the two fuelling cases with increased intake charge temperature, as shown in Figure 5.7. For the 8 mg/cycle condition, the THC was hardly affected by the higher intake charge temperature, and the CO was reduced by it. For the 16 mg/cycle condition, the increase in charge temperature led to increased THC and CO. More advanced main combustion events



normally tend to emit lower THC and CO emissions due to the higher combustion temperature and longer oxidation time before exhaust valve opening. However, the thermal ‘throttling’ effect of the higher intake charge temperature reduced the intake oxygen content; for hot EGR this has been shown to increase THC and CO emissions (Ogawa *et al.*, 2007). The competitive effect of a higher combustion temperature and a reduction in oxygen content resulted in unchanged THC and reduced CO emissions for the low load operating condition, indicating that the higher temperature was the more dominant effect. However, at the 16 mg/cycle condition, the equivalence ratio was substantially higher and hence the reduction in oxygen content was a more dominant factor in increasing the THC and CO emissions. This resulted in a net increase in THC and CO emissions under this condition.

Higher intake charge temperature enhanced the LTC combustion process with improved combustion stability and advanced combustion phasing. It increased the peak of the main heat release rate but reduced the LTHR heat release rate. The NTC contributed to the reduced LTHR rate due to its earlier occurrence with higher intake charge temperatures. The first half of the main combustion event exhibited a higher heat release rate when the intake charge temperature was high. The reduced LTHR rate may have left more reactive reactants to burn during this stage. The smoke number was increased presumably due to the higher local combustion temperature derived from the faster main combustion event resulting from higher intake temperatures.

Other engine parameters are also able to encourage more rapid main combustion; for example higher fuel injection pressures, which promote more rapid mixing, have been shown in Chapter 4 to enhance LTC reaction rates.

### **5.4.3 Fuel injection pressure**

As previous studies have shown, fuel injection pressure significantly influences both conventional and low temperature diesel combustion (see Sections 2.3 and 4.4). An increase in the fuel injection pressure led to advanced cool flame reactions with higher LTHR rates; this is shown in detail in Figure 5.8. The higher fuel injection pressure led to improved fuel-charge mixing (Fang *et al.*, 2010). During the cool flame reaction period, the more evenly distributed fuel in the charge had increased an opportunity to meet and react with oxygen molecules, leading to more rapid cool flame heat release. The LTHR heat release rate started to drop earlier for the high injection pressure cases. This suggests that the LTHR could have started to

terminate when the total heat released from the cool flame reaction reached a threshold where the mixture temperature was in the NTC region.

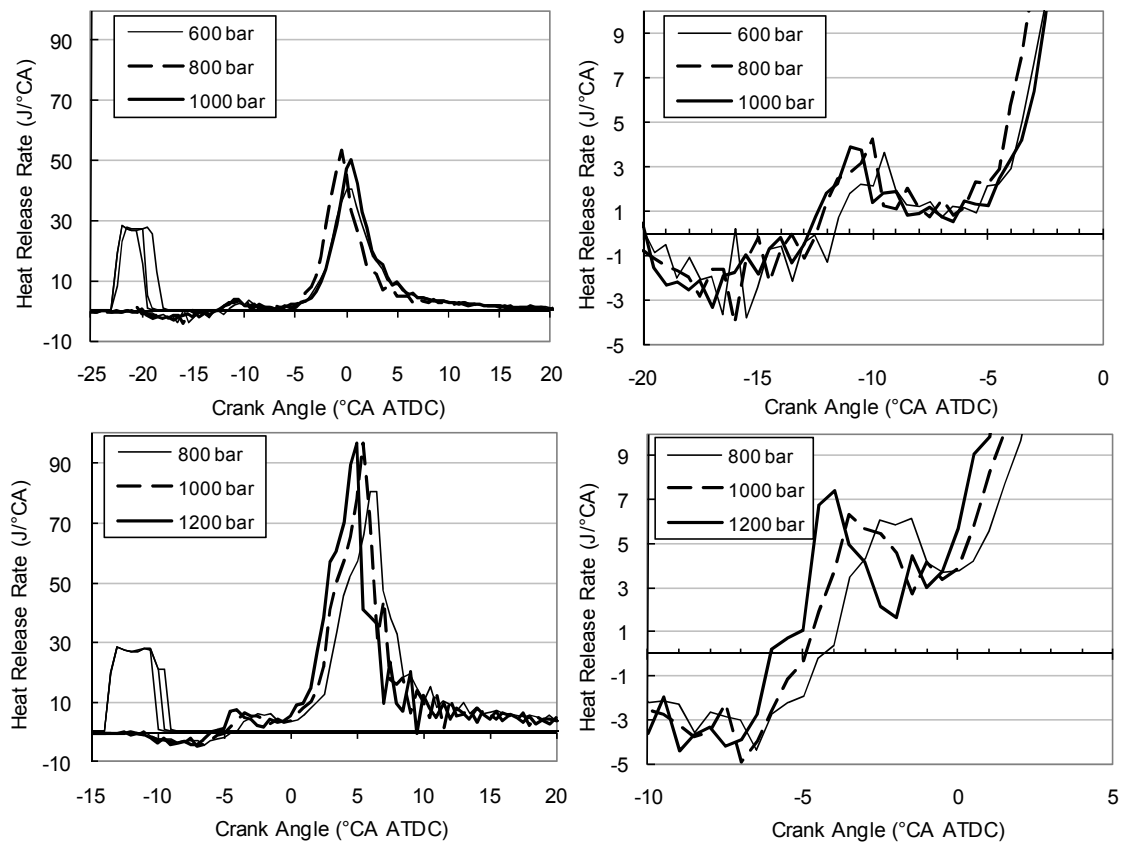


Figure 5.8 Effects of fuel injection pressure on LTC heat release (Top: 1500 rpm, 8 mg/cycle, Sol -21°CA ATDC, EGR rate 65%, intake temperature 70°C; Bottom: 1500 rpm, 16 mg/cycle, Sol -12°CA ATDC, EGR rate 54%, intake temperature 80°C)

The main combustion was affected by the increase in fuel injection pressure with different trends for the two fuelling conditions. For the 8 mg/cycle condition, the main combustion heat release rate was increased and advanced when the fuel injection pressure was increased from 600 bar to 800 bar. A further increase in the fuel pressure led to retarded high temperature heat release and lower peak heat release rates. Conversely, the higher injection pressure led to advanced main combustion events with higher peak values for the higher fuelling conditions. The improved mixing could have led to over-mixing of the fuel, which delayed the combustion event for the low load LTC high fuel injection pressure (1000 bar) case. However, for the higher fuelling conditions, the air-fuel-ratio is lower; the increased mixing intensity led to earlier and more intense combustion process with higher peak heat release rates.

The combustion phasing parameters such as start of LTHR, CA5, CA50 and CA90 were generally advanced with increased fuel injection pressure for the 16 mg/cycle

fuelling condition, as shown in Figure 5.9. This is most likely a result of improved mixing enhancing the fuel burn rate, leading to a shorter duration of the first half of the main combustion event. For the low load condition, however, only the start of LTHR was advanced by the higher fuel injection pressure, and the phasing parameters of the main combustion showed no consistent trend. The possible over-mixing at the highest fuel injection pressure case made it more difficult for the ignition to occur. The duration of the LTHR was increased due to the later start of the main combustion (CA5) for this case. The duration of the first half of the main combustion was increased due to the slow combustion caused by the possible over-mixing.

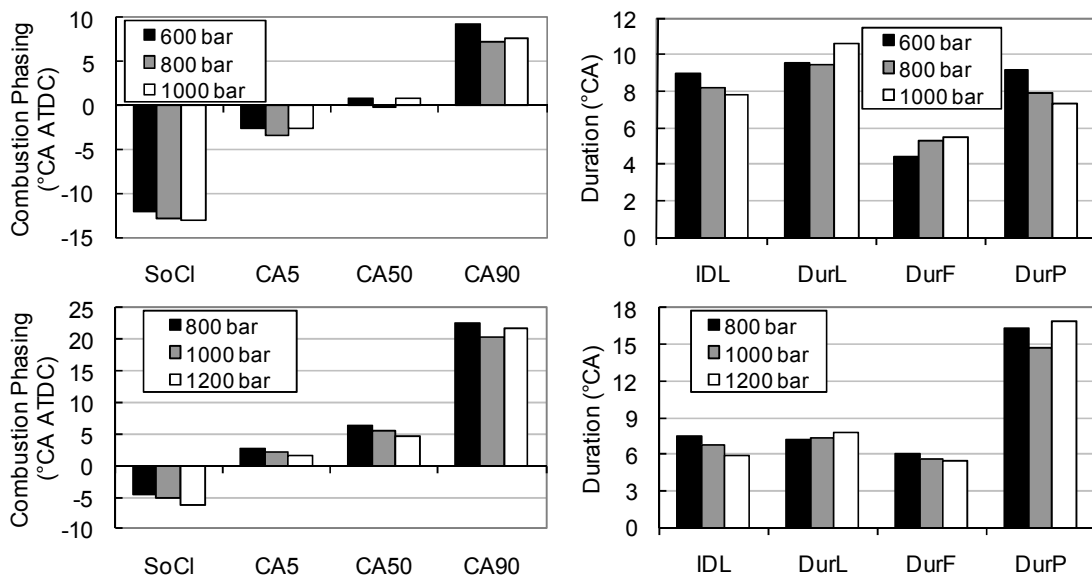


Figure 5.9 Effects of fuel injection pressure on LTC combustion phasing (IDL: ignition delay of LTHR; DurL: SoCI-CA5; DurF: CA5-CA50; DurP: CA50-CA90) (Top: 1500 rpm, 8 mg/cycle, Sol -21°CA ATDC, EGR rate 65%, intake temperature 70°C; Bottom: 1500 rpm, 16 mg/cycle, Sol -12°CA ATDC, EGR rate 54%, intake temperature 80°C)

The combustion variability was unchanged or reduced by the increasing fuel injection pressure for the 16 mg/cycle condition, but variability was increased for the low fuelling conditions, as shown in Figure 5.10. At the higher fuelling condition, improved mixing due to the high fuel injection pressure may have improved the utilisation of the limited quantity of oxygen in the charge, leading to a more stable LTC combustion. This may explain why, with increased injection pressure, the mid-load LTC combustion stability was improved. However, at the lower load where there was more excess oxygen, high fuel injection pressure may have led to over-mixing of fuel which in turn caused weak flame propagation and bulk quenching. This hypothesis is supported by the higher THC and CO emissions for the low load high fuel injection pressure case shown in Figure 5.10. For the low load LTC, the significant increase in

the variability of the peak heat release rate and IMEP suggests the occurrence of over-mixing.

Results presented in Chapter 4 showed that fuel injection pressure can strongly influence the LTC emissions. The smoke, THC and CO emissions were reduced with increased fuel injection pressure for the 16 mg/cycle conditions, as shown in Figure 5.10. The improved homogeneity of the mixture led to low formation rates of soot even with increased combustion temperature. The higher combustion temperature and the increased turbulence resulting from the high injection pressure reduced the THC and CO emissions. However, for the low fuelling condition, the lowest THC and CO were for the intermediate 800 bar fuel injection pressure case. Increasing or reducing the fuel injection pressure from this point increased the THC and CO emissions. For the low fuel injection case, the poor mixing due to less kinetic energy in the injection event could lead to under-mixing of the fuel; partial oxidation of under-mixed fuel is a possible source of combustion by-products like CO and THC. On the other hand, the high injection pressure may have resulted in over-mixing and increased the possibility of quenching, which is a source of THC and CO emissions.

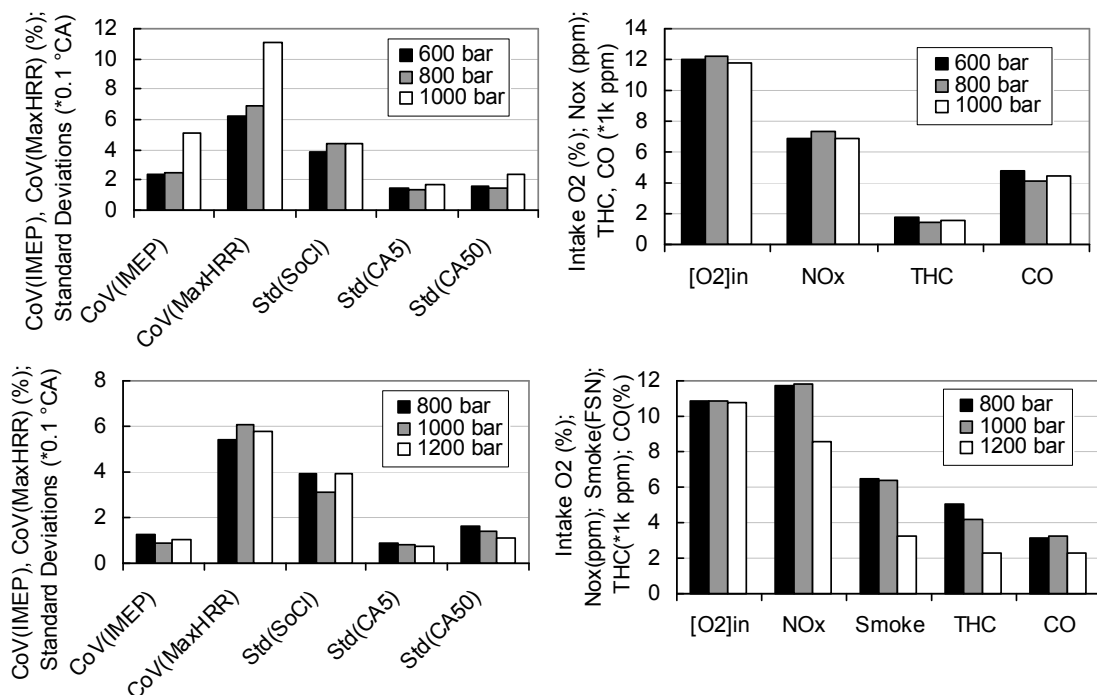


Figure 5.10 Effects of fuel injection pressure on LTC combustion stability and emissions (Top: 1500 rpm, 8 mg/cycle, Sol -21°C ATDC, EGR rate 65%, intake temperature 70°C; Bottom: 1500 rpm, 16 mg/cycle, Sol -12°C ATDC, EGR rate 54%, intake temperature 80°C)

## 5.4.4 Fuel injection timing

The timing of the injection event, like the fuel rail pressure discussed in the previous section, can have a significant influence on the diesel engine combustion and emissions. The effects of injection timing on the combustion event under LTC are shown in Figure 5.11. Early fuel injection led to an early occurrence of the cool flame heat release and the main combustion events. The phasing of the LTHR event was shifted with the timing of the injection event, but its magnitude was relatively insensitive to its timing. The peak heat release rate was increased with advanced timing except for the earliest timing low load (8mg/cycle) case. With the combustion phasing advanced, the charge temperature around TDC was higher, which led to increased peak heat release rate. For the earliest injection case under low load conditions, the mid-point of the combustion occurred before TDC; this could be the reason for the lower peak heat release rate.

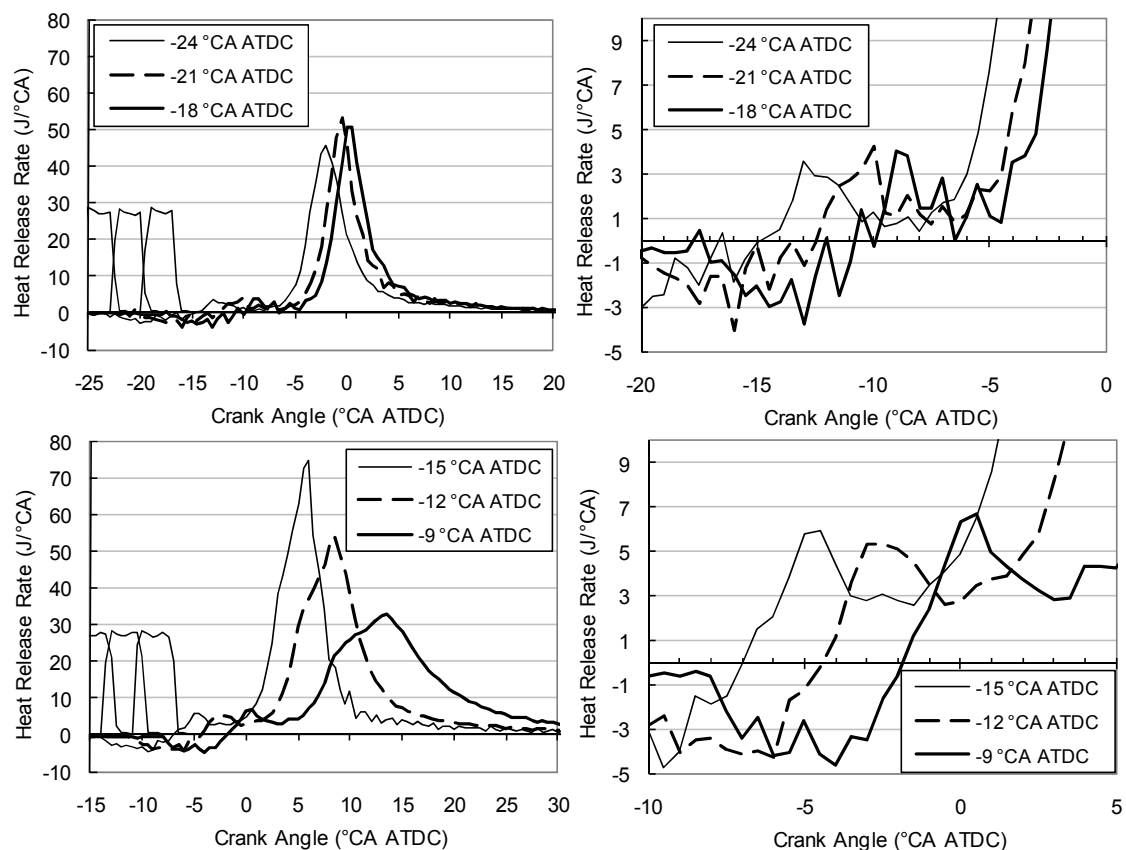


Figure 5.11 Effects of Sol on LTC heat release (Top: 1500 rpm, 8 mg/cycle, fuel injection pressure 800 bar, EGR rate 65%, intake temperature 70°C; Bottom: 1500 rpm, 16 mg/cycle, fuel injection pressure 1000 bar, EGR rate 54%, intake temperature 70°C)

Changes in fuel injection timing shifted the combustion phases in the same direction as shown in Figure 5.12. However, the delay of the start of the LTHR with retarded

timing was smaller than the change in the fuel injection timing. The ignition delay of the cool flame reaction was increased with advanced fuel injection timing. Fuel injection earlier in the compression stroke led to the fuel being injected into a lower pressure and temperature environment. Under these circumstances, the start of the formation of the primary radicals would tend to be delayed and the reaction rates could also be low. This hypothesis is supported by the fact that the duration of the LTHR was increased with advanced timing except for the 16 mg/cycle case with the latest fuel injection. The charge pressure and temperature were lower during the LTHR process in the early compression stroke and caused lower LTHR rate. However, for the 16 mg/cycle case with the latest timing, part of the LTHR occurred after TDC, where the cylinder expansion started to reduce the charge pressure and temperature. As a result, it took a longer time for the cylinder temperature to pass the NTC boundary temperatures and to realise the start of main combustion for this case.

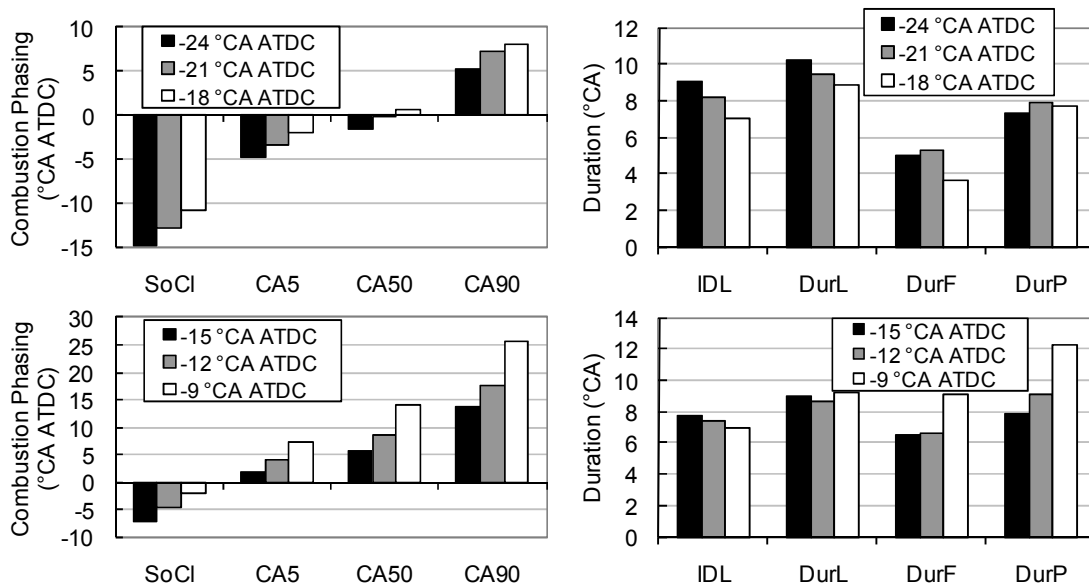


Figure 5.12 Effects of Sol on LTC combustion phasing (IDL: ignition delay of LTHR; DurL: SoCI-CA5; DurF: CA5-CA50; DurP: CA50-CA90) (Top: 1500 rpm, 8 mg/cycle, fuel injection pressure 800 bar, EGR rate 65%, intake temperature 70°C; Bottom: 1500 rpm, 16 mg/cycle, fuel injection pressure 1000 bar, EGR rate 54%, intake temperature 70°C)

The combustion phasing had a significant influence on the intermediate load LTC main combustion durations, as shown in Figure 5.12. When the CA50 was close to TDC, the durations of the two parts of the main combustion, DurF (CA5-CA50) and DurP (CA50-CA90) were insignificantly affected by the change of fuel injection timing. However, for the late fuel injection case, the main combustion occurred mainly in the expansion stroke. This delay led to the observed significant increase in combustion duration for the latest fuel injection timing.

The combustion stability, as shown in Figure 5.13 by CoV of IMEP, CoV of peak HRR, and standard deviations of CA5 and CA50 was degraded with advanced fuel injection timing for the 8 mg/cycle condition. The extended ignition delay led to improved mixing and a more homogeneous charge for the main combustion. The start of main combustion (CA5) showed higher standard deviation as the start of LTHR process may have suffered significant cyclic variations from the early fuel injection. This phenomenon suggests that the over-mixing could have occurred for the early injection low load LTC condition. The possible over-mixing could have made the ignition more difficult, leading to an instable start of combustion.

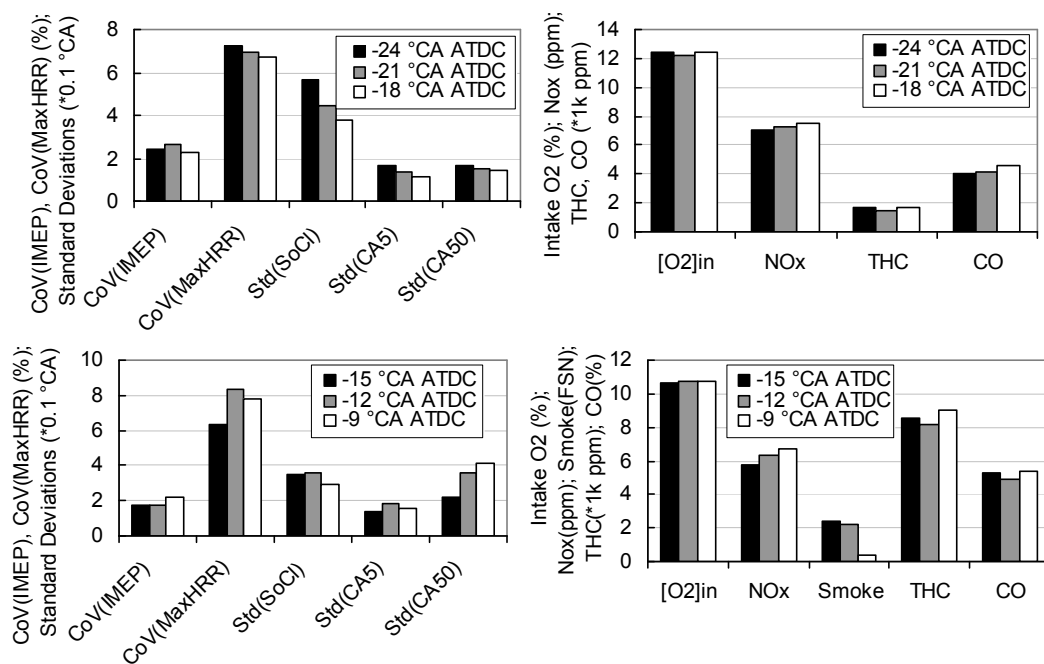


Figure 5.13 Effects of Sol on LTC combustion stability and emissions (Top: 1500 rpm, 8 mg/cycle, fuel injection pressure 800 bar, EGR rate 65%, intake temperature 70°C; Bottom: 1500 rpm, 16 mg/cycle, fuel injection pressure 1000 bar, EGR rate 54%, intake temperature 70°C)

An early fuel injection led to reduced CoV of IMEP and peak HRR, and standard deviations of CA5 and CA50 for the higher fuelling condition. As shown in Figure 5.12, the early injection for this case resulted in CA50 being close to TDC. Hence, the charge temperature was higher and led to more stabilised combustion. However, the start of LTHR occurred in the compression stroke. The lower charge temperature during the early fuel injection case led to higher standard deviation of the start of the LTHR (SoCI).

The smoke emissions (only shown for the 16 mg/cycle case) were reduced with delayed fuel injection timing. For this case, the main combustion occurred during the

expansion stroke and had a significantly reduced peak heat release rate. As a result, the combustion temperature should have been lower, leading to a reduced soot formation rate. This also suggests that the soot under these conditions is primarily a result of formation, and oxidation is not as significant, as oxidation would expect to be impeded by later combustion.

Emissions of THC and CO were reduced with advanced fuel injection timing except for the earliest fuel injection cases. Advanced timing led to the occurrence of the combustion close to TDC with higher combustion temperature. The early combustion enabled a longer time for the oxidation of THC and CO formed during the combustion. The high combustion temperature could also reduce the unburned emissions by enhancing their oxidation. However, it is likely that too early fuel injection may have caused over-mixing or wall impingement of fuel and have led to higher THC and CO emissions.

## 5.5 Discussion

Diesel combustion is a complex process. Detailed chemical kinetic analysis of the reaction paths under LTC conditions is beyond the scope of this thesis. However, with basic knowledge from the literature (Hiroyuki *et al.*, 2008; Pilling, 1997; Westbrook, 2000), the results presented in this chapter can be interpreted to provide more detailed understanding of the characteristics of the two-stage low temperature diesel combustion progress.

Low temperature reactions in LTC diesel combustion are temperature and charge composition dependent processes. Higher charge temperature, higher concentration of reactants and improved mixing led to early start of cool flame reaction, as shown with lower EGR rate, higher intake charge temperature, and earlier timing and higher injection pressures, shown in Figures 5.2, 5.5, 5.8 and 5.11, respectively. The higher charge temperature improved the primary initiation reactions (Reactions 5-1 and 5-2 in Section 5.2), while the reduction of the EGR rate with higher oxygen concentrations increased the reaction rates of primary initiation, propagation (Reactions 5-3 – 5-4) and branching (Reactions 5-7 - 5-8). For the higher fuelling conditions, the LTHR rates were higher than in the low fuelling conditions. This is due to the higher concentration of fuel in the charge that led to an increased LTHR rate.

The NTC is a temperature dependent phenomenon. The intake charge temperature and the heat release rate during LTHR are the main factors that control the NTC.



With higher intake temperature, the LTHR duration (cool flame plus NTC) was reduced even with a lower heat release rate from the cool flame. The higher charge temperature may have reduced the LTHR during the cool flame period. The higher cool flame heat release rate from the higher fuelling condition led to a higher charge temperature rise rate and resulted in a shorter duration of NTC.

Increased intake charge temperature and higher fuel injection pressure both led to advanced combustion processes, for both the cool flame reactions and the main combustion event. However, these two approaches resulted in very different effects on smoke, THC and CO emissions. Increased intake charge temperature led to increases in these emissions while higher fuel injection pressure reduced them. The difference in the LTHR regime for these two approaches was the intensity of the cool flame reaction rate and the concentration of intermediate radicals. The higher fuel injection pressure cases could have generated more heat and intermediate radicals than the higher intake temperature cases due to the increased fuel injection pressure leads to improved mixing and a higher intensity of low temperature reactions. The increased heat and radicals may have influenced the composition and concentration of particulate matter, THC and CO before they were emitted from the cylinder.

The heat released and the reactive products generated from the cool flame reactions affected the main combustion event and emissions. However, the importance of these factors compared to the direct influence of the varied parameters on the main combustion could not be identified in this study. More comprehensive understanding of the LTHR process will be desirable for a better understanding of the advanced diesel combustion technologies. Further work is required to understand how it can be influenced by, for example, different fuels and intake charge species, and how to use it to control the high temperature combustion process and emissions formation.

The THC and CO emissions are not likely to be avoidable through the in-cylinder combustion control. Although the cool flame reaction products may have the potential to reduce the concentration of these species. The engine-out emissions are sufficiently large that it is likely that they will still be unacceptably high for any high-EGR LTC engine.

## **5.6 Conclusions**

The LTC diesel combustion showed a cool flame – NTC – high temperature thermal reaction process. The difference in the in-cylinder conditions, such as the

temperature, pressure, and charge composition, had a noticeable influence on these different combustion stages. With the engine operating parameters changed individually, the influences of these parameters on LTC combustion and emissions were isolated. The key conclusions are:

1) An increase in EGR rate reduced oxygen concentration in the charge which delayed the low temperature heat release process. The lower oxygen concentration also limited the LTHR rates. The main combustion event was more sensitive to the EGR rate than the LTHR. The peak heat release was reduced while its phasing was delayed significantly with increased EGR rate.

2) An increase in intake temperature led to an early occurrence of LTHR and reduced the duration of the initial low-temperature ('cool flame') reactions. Once the in-cylinder temperature reached the NTC region, the cool flame reactions were terminated regardless of the engine operating parameters. Thus, for the high intake temperature condition, the time left for the cool flame reaction was shorter due to the narrower temperature band between the end-of-compression temperature and the NTC temperature.

3) An increase in intake temperature reduced the THC and CO emissions for low load operating conditions and increased them for intermediate load conditions. The increased charge temperature is likely to have increased the combustion temperature, which should have reduced the THC and CO emissions. The thermal throttling effect, where the higher charge temperature results in a lower mass of fresh air being inducted, led to an increased equivalence ratio. These two factors have competitive effects on the THC and CO emissions. For the low load conditions, the temperature was more dominant than the thermal throttling effect on the unburned emissions formation. For the mid-load conditions, the reduction in oxygen concentration by ~0.5% due to the thermal throttling led to an increase in the THC and CO emissions greater than any reduction attributed to the increased combustion temperature.

4) Under most conditions, a higher fuel injection pressure led to earlier, more intense cool-flame heat release events. It also resulted in generally earlier and more intense main combustion events. These effects are thought to be a result of improved fuel-oxidizer mixing with higher injection pressures generating a more homogeneous charge prior to the start of combustion.

5) The timing of the start of fuel injection can be used to control the combustion phasing effectively. Advanced fuel injection timing led to earlier low temperature and main (high temperature) reactions. However, to achieve a specified change in the combustion phasing, a larger change in injection timing than the desired phasing change was needed.

6) The results suggest that over-mixing and bulk quenching were both sources of partial combustion by-products. Both early and late injections and high and low injection pressures could, under certain conditions, lead to increased THC and CO emissions.

7) Smoke emissions depended on combustion temperature and mixture formation under mid-load conditions (smoke emissions were very low for all the low load conditions). An increase in EGR rate led to reduced smoke numbers with reduced combustion temperature and more homogeneous mixtures derived from the increased ignition delay. An increase in charge temperature at constant EGR rate reduced the ignition delay, leading to an increase in smoke number. Both the increased charge temperature and reduced ignition delay contributed to increased smoke emissions. Higher fuel injection pressure improved the mixing and reduced the smoke emissions even though the peak heat release rate was increased, which suggested that the combustion temperature was higher. Later fuel injection timing led to longer ignition delays and reduced the peak heat release rate; both these factors resulted in reduced smoke emissions.

8) An increase in the injected fuel quantity led to higher concentrations of fuel in the charge. This increased the cool flame reaction rates and advanced the combustion phasing. The high fuelling conditions had shorter LTHR durations due to the higher rates of cool flame reaction that led to a more rapid temperature rise of the charge and triggered the NTC region to occur sooner.

The results in this chapter have demonstrated the sensitivity of both the low-temperature and main phases of diesel LTC to in-cylinder conditions, including temperature and fuel-air mixing. Another parameter that could significantly influence the LTC event is the residual gas fraction, which is sensitive to the exhaust back pressure. In the following chapter, the effects of exhaust back pressure on

conventional diesel and LTC combustion are evaluated on the basis of the combustion process and emissions.

# Chapter 6 Effects of Exhaust Back Pressure on Conventional and Low Temperature Diesel Combustion\*

## 6.1 Introduction

In diesel engines, exhaust back pressure (EBP) is normally kept low to limit pumping losses; an increase in EBP at constant intake manifold pressure linearly increases pumping work. While turbocharging increases EBP, it also increases intake manifold pressure; as a result, it has relatively little influence on the pumping work. Other advanced engine technologies often cause, or even require, increased EBP. For example, EGR in diesel engines is frequently driven by elevating EBP or by throttling the intake (Millo *et al.*, 2009; Vitek *et al.*, 2008). In either case, the net effect is the same – a large differential pressure between intake and exhaust streams. Using high EGR rates to achieve LTC, as shown in Chapters 4 and 5, requires EGR rates as high as 70%; to achieve this requires an increase in the EBP. Elevated EBP is also generated by most exhaust gas aftertreatment systems, (Masoudi *et al.*, 2000; Wirojsakunchai *et al.*, 2007), the fouling of which can change the EBP during the engine operation; some exhaust energy-recovery systems also significantly influence EBP (Hountalas *et al.*, 2007).

Aside from pumping work, the greatest influence of EBP is on the quantity of post-combustion gases which are retained in the cylinder from one cycle to the next. This cylinder residual gas fraction (RGF) is affected by engine design and operating conditions (Heywood, 1988; Hiereth *et al.*, 2006; Wang, 2006), but it is especially sensitive to the difference between the EBP and the intake manifold pressure. In [Appendix A4](#), a technique for the measurement and estimation of RGF using experimental and numerical techniques has been described; validated 1D engine simulation code has been demonstrated as an effective tool for estimating the RGF. Higher EBPs led to higher RGFs, the main effects of which were the replacement of fresh charge with burned gases and an increase of the charge temperature at the

---

\* A modified version of this chapter was presented at the IMechE Internal Combustion Engines: Performance, Fuel Economy and Emissions Conference, London, December 2009. S. Cong, G. P. McTaggart-Cowan, C. P. Garner. The Effects of Exhaust Back Pressure on Conventional and Low Temperature Diesel Combustion.

\* Part of Section 6.2 Research Methodology was presented at the SAE Powertrains, Fuels and Lubricants Meeting, June 2009, Florence, ITALY. S. Cong, G. P. McTaggart-Cowan and C. P. Garner. Measurement of Residual Gas Fraction in a Single Cylinder HSDI Diesel Engine through Skip-firing. SAE paper 2009-01-1961.

start of the compression stroke. The dilution effect reduces the charge oxygen concentration and hence the global oxygen-fuel ratio. The higher temperature of the RGF increases the temperature at the end of compression, which reduces the ignition delay as well as reducing charge density. Effectively, the increase in RGF behaves in a fashion generally similar to adding 'hot' (i.e., uncooled) EGR into the charge.

The work reported in this chapter investigated the effects of EBP on diesel engine combustion behaviour and emissions under both conventional diesel combustion and LTC modes. To help to explain the experimental results, an engine model developed using Ricardo WAVE was used to predict RGF at different EBPs. This work provides an analysis of the impacts of EBP and RGF on the important questions of combustion progression, combustion stability and pollutant emissions under LTC conditions.

## **6.2 Research Methodology**

In this section, a residual gas fraction measurement method is introduced. With the aids of 1D engine modelling, RGFs for different operating conditions with EGR can be estimated. The concept of effective EGR, which takes the RGF into account, will be presented. This concept will then be used to help interpret experimental results investigating the effects of changes in exhaust back pressure during both conventional and LTC diesel operation.

### **6.2.1 Measurement of RGF**

The concept of the RGF measurement through exhaust manifold gas sampling with skip-firing is illustrated in Figure 6.1. The CO<sub>2</sub> concentration measured (using the fast response Cambustion NDIR500, introduced in Section 3.2) near the exhaust port gives the concentration of CO<sub>2</sub> formed in the previous combustion cycle. If the fuel injection is stopped, there will be no fuel injection or combustion in the subsequent cycle, and the exhaust gas from this skip-fired cycle is therefore the mixture of the trapped residual gases and fresh intake air. This is defined in Equation (6-1), with [CO<sub>2</sub>]<sub>f</sub> representing the firing cycle CO<sub>2</sub> concentration, [CO<sub>2</sub>]<sub>rg</sub> representing the first motoring cycle CO<sub>2</sub> concentration and [CO<sub>2</sub>]<sub>amb</sub> representing the ambient CO<sub>2</sub> concentration as measured after 5 non-firing cycles (value ~0.03%).

$$\text{RGF}(\%) = \frac{([\text{CO}_2]_{\text{rg}} - [\text{CO}_2]_{\text{amb}})}{([\text{CO}_2]_{\text{f}} - [\text{CO}_2]_{\text{amb}})} \cdot 100\% \quad (6-1)$$

An example of exhaust gas CO<sub>2</sub> concentration measurements during successive skip firing cycles is shown in Figure 6.2. There is a delay between exhaust valves opening (EVO) and detection of the CO<sub>2</sub> concentration at the sensor. The initial part of the CO<sub>2</sub> reading during the early part of the cycle is discarded due to large pressure oscillations in the exhaust manifold which cause the measured CO<sub>2</sub> values to be inaccurate. The CO<sub>2</sub> emitted from the first motoring cycle during the skip fire event originates from the trapped combustion products from the previous firing cycle. These two effective CO<sub>2</sub> measurements are averaged separately and used to determine the residual gas fraction, as defined above.

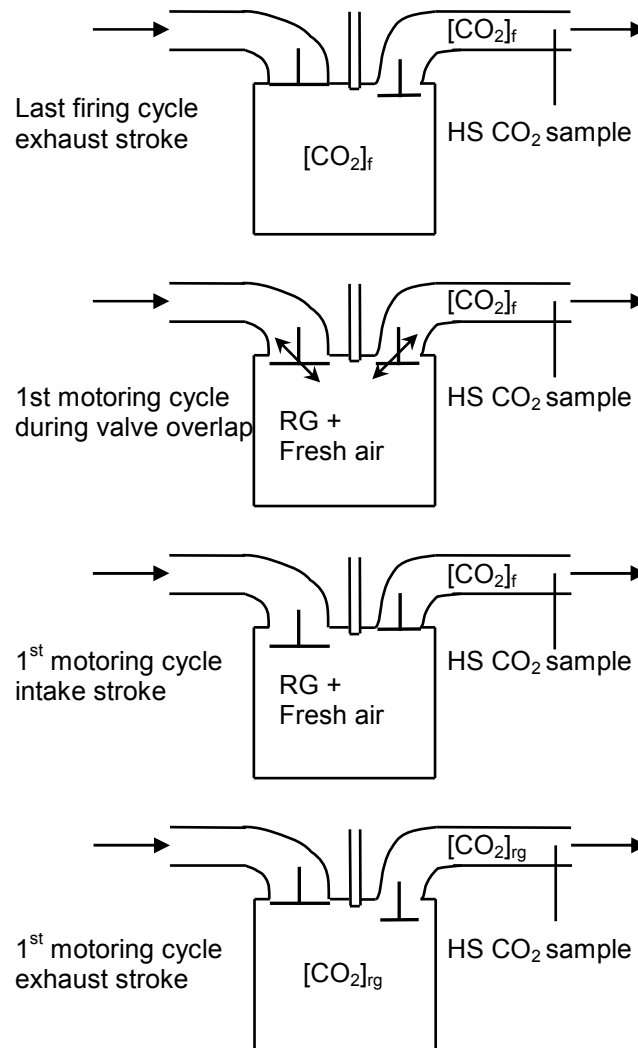


Figure 6.1 Concept of the RGF measurement

The single cylinder WAVE model described in Section 3.4 was used to simulate the research engine running under different exhaust back pressures. The model predicted the residual gas fractions which were closely matched with the measurement results at different engine operating conditions. More details about this RGF measurement and model validation are given in [Appendix A4](#).

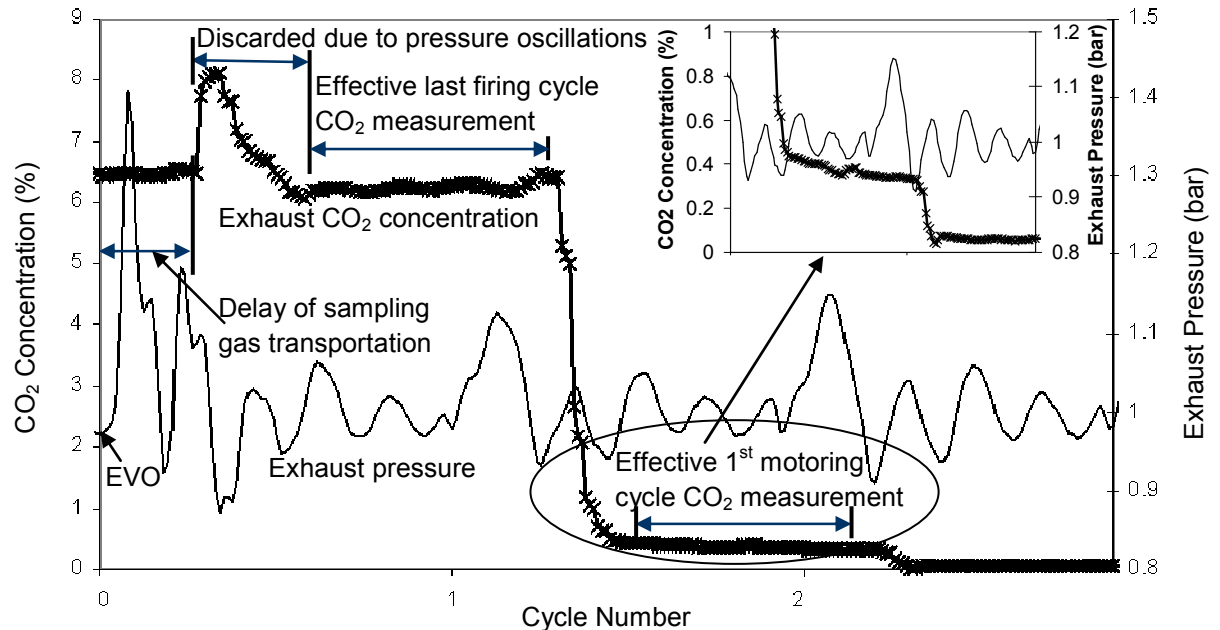


Figure 6.2 CO<sub>2</sub> concentration and absolute exhaust manifold pressure measurement during a skip-firing event

To take the residual gas into account, an 'effective' EGR rate ( $EGR_{eff}$ ) was calculated based on the EGR rate determined using Equation (6-2) and the RGF predicted by the 1-D model, using:

$$EGR_{eff} = EGR_{hebp} + k * (EBP_h - EBP_l) \quad (6-2)$$

where  $EGR_{hebp}$  refers to the EGR rate in percent for the high exhaust back pressure case and  $EBP_h$  and  $EBP_l$  refer to the exhaust pressures in the high and low back pressure cases, respectively. The variable  $k$  represents the proportional change in the RGF that resulted from a one bar increase in the EBP. This parameter will be used in interpreting the experimental results from an investigation of the effects of EBP on conventional combustion and LTC in a diesel engine.

## 6.2.2 Engine operating conditions

The engine operating conditions for the conventional diesel and LTC mode are given in Tables 6.1 and 6.2, respectively. The four selected test points represent low-to-



intermediate speed and load conditions for the engine. To simplify the test programme, only a single fuel injection even was used for most of the tests. For the 1500 rpm 16 mg/cycle conventional diesel case, however, a pilot fuel injection (1.2 mg/cycle) was used to prevent excessive rates of cylinder pressure rise during the early combustion phase. This pilot injection was not included in the LTC combustion as the pressure-rise rates were substantially lower. The injection timing was set at the low EBP case for each operating condition and the timing selected was as advanced as possible while maintaining stable combustion and a maximum cylinder pressure rise rate lower than the 10 bar/°CA limit. Once set for a given operating condition, the injection timing, pressure and quantity were fixed and did not vary over the range of EBPs investigated.

Table 6.1 Engine Operating Conditions (conventional diesel\*)

Engine speed (rpm)	1500	1500	2500	2500
Fuelling (mg/cycle)	8	16	8	16
Sol (°CA ATDC)	-3.5	(-20 <sup>†</sup> , -2.5)	-6	-9
Fuel injection pressure (bar)	500	650	600	850
Exhaust back pressure (bar)	1.1 - 1.5	1.1 - 1.5	1.1 - 1.5	1.1 - 1.5
Equivalence ratio <sup>#</sup>	0.202 - 0.208	0.404 - 0.418	0.193 - 0.198	0.386 - 0.399

\* EGR rate = 0%

<sup>†</sup> Pilot fuel injection timing

<sup>#</sup> Oxygen based equivalence ratio derived from 1D engine model results

Table 6.2 Engine Operating Conditions (LTC)

Engine speed (rpm)	1500	1500	2500	2500
Fuel (mg/cycle)	8	16	8	16
EGR rate at low EBP (%)	64.6	60.1	65.4	55.1
EGR rate at high EBP (%)	64.8	60.5	65.6	55.4
Sol (°CA ATDC)	-18	-24	-30	-30
Fuel injection pressure (bar)	500	650	600	850
Low EBP (bar)	1.07	1.06	1.07	1.07
High EBP (bar)	1.47	1.32	1.39	1.24
Equivalence ratio low EBP <sup>#</sup>	0.354	0.937	0.339	0.818
Equivalence ratio high EBP <sup>#</sup>	0.357	0.982	0.347	0.859

<sup>#</sup> Oxygen based equivalence ratio derived from 1D engine model results

For all the cases, the intake manifold pressure and temperature were kept constant throughout the test. The intake manifold pressure was dictated by the test cell pressure, as the engine was running under naturally aspirated mode. Pressure losses in the intake system were less than 1 kPa; variations in the measured intake pressure over the entire test programme were less than 1 kPa. Without EGR, the intake temperature was the ambient temperature in the test cell (15°C); with EGR, the EGR temperature was adjusted to maintain the intake charge at 50°C. While every effort was made to ensure that the EGR level was fixed, it was not possible to

avoid small variations (as shown in Table 6.2). The effects of these fluctuations on the results are accounted for in the results using the 'effective EGR' concept introduced in the previous section.

### **6.2.3 Engine modelling**

To support the experimental programme, an engine model was developed using the Ricardo WAVE 1D engine simulation program as described in Section 3.4. This model has been shown to predict RGF for conventional diesel combustion. The RGF depends on fixed engine parameters (primarily engine compression ratio, valve timing and lift profiles) that are independent of charge composition. Furthermore, the engine model was validated using measured values (e.g. manifold pressures and temperatures during the intake and exhaust strokes) that are not sensitive to charge composition. As a result, it was expected that the RGF prediction should be acceptable for LTC operation, even though it was not specifically validated under LTC conditions.

## **6.3 Results**

The results presented here focus on the experimental measurements of combustion and emissions, while the model results help to interpret the experimental findings by predicting the RGF. The predicted RGFs have been used to estimate the charge composition at the end of the compression stroke for the different combustion regimes. By estimating the trapped residual gas fraction, the links between EBP and engine combustion performance and emissions can be investigated. Finally, the effects of RGF can then be compared on the basis of effective EGR.

### **6.3.1 Simulated RGF results**

The WAVE model introduced above was used to predict RGF, as shown in Figure 6.3, for conventional and LTC diesel combustion. The EBP, fuel injection quantity and pressure, and EGR rate were set to be identical with each of the corresponding experimental engine operating conditions (listed in Tables 6.1 and 6.2). The predicted RGF for both the combustion regimes showed a similar trend, increasing by approximately four percent for a one bar increase in EBP ( $k = 4 \text{ \%}/\text{bar}$  in Equation 6-2).

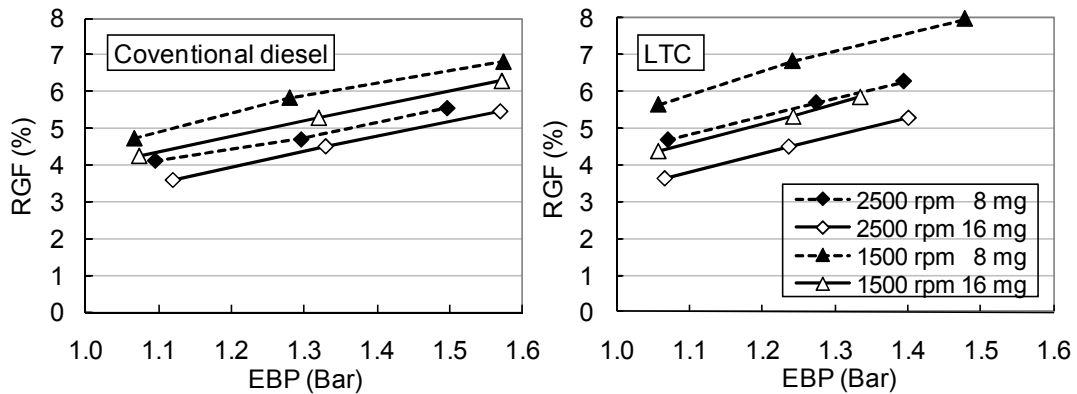


Figure 6.3 Simulation results of RGF vs. EBP for conventional and LTC diesel combustion

Residual gas dilutes the fresh charge trapped in the cylinder and increases the fuel-oxidizer equivalence ratio. The effects of residual gas fraction on equivalence ratio, as predicted by the WAVE model, are shown in Figure 6.4. At the intermediate load conditions, the effect of increased RGF on equivalence ratio was significant due to both the lower concentration of  $O_2$  in the exhaust gas and the higher exhaust gas temperature. The simulation results further show that the charge temperature at intake valve closure was increased by 2-5°C with increased RGF; this leads to increases in end of compression temperature between 5 and 12°C. These variations in charge temperature and equivalence ratio have the potential to influence the combustion event and emissions under both conventional diesel and LTC conditions.

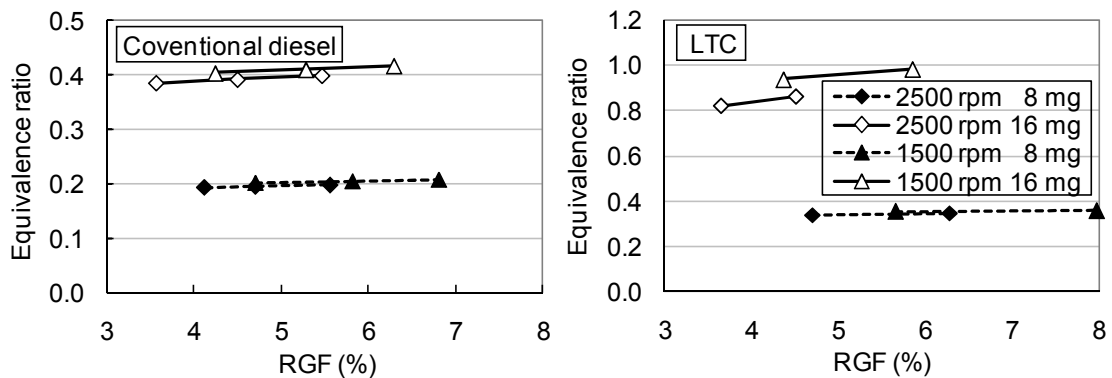


Figure 6.4 Simulation results of oxygen based equivalence ratio over RGF for conventional and LTC diesel combustion

### 6.3.2 Conventional diesel combustion

For conventional diesel combustion, the experimental results demonstrated little sensitivity to the investigated range of EBPs. The small increases in charge dilution (the volumetric oxygen content was reduced from 21% to 20.5% when the EBP was increased from 1.1 to 1.5 bar) and charge temperature (2 to 4°C based on the

simulation results) with increased RGF showed small effects on the combustion processes. The increased charge temperature was expected to reduce ignition delay while the dilution effect should have increased it. The comparison of heat release rates for the 1.1 bar and 1.5 bar EBP cases is shown in Figure 6.5. Increased EBP advanced the CA50 slightly (less than 0.5°CA), for all but the 1500 rpm 16 mg/cycle case. These results suggest that the effects of temperature (thermal effect, which would tend to reduce the ignition delay) were more significant than the influence of the higher RGF (dilution effect, which would tend to increase the ignition delay).

For the high load / low speed case (Figure 6.5c), increasing the EBP did not have a discernable influence on the combustion event. This may have been a result of this operating condition including a pilot injection. The initial HRR induced by the pilot was small, so that slight influences of the increased RGF on the ignition delay were not discernable. However, by the start of the main combustion, the RGF had no significant effect on the main combustion process, as the cylinder temperature and composition had already been influenced by the pilot combustion; as a result the influence of the change in RGF was not detectable.

The effects of EBP on the gaseous emissions from conventional diesel combustion were generally insignificant, as shown in Figure 6.6. For low load (8 mg/cycle) conditions, an increase in the EBP had a negligible effect on smoke emissions. However, at intermediate load (16 mg/cycle), the smoke was reduced slightly at 2500 rpm but increased at 1500 rpm with higher EBP. The fact that higher EBP led to a more advanced combustion process for the 2500 rpm 16 mg/cycle case, as shown in Figure 5d, may have contributed to the observed reduction in smoke emissions. The higher combustion temperature improves the soot oxidation reaction rates (Pickett *et al.*, 2004; Tree *et al.*, 2007) due to the more rapid combustion process even though there is a relatively small increase in RGF (from 3.5% to 5.3%). The different effect at 1500 rpm, where smoke increased with EBP, may have been a result of the hot residual gases influencing the pilot fuel combustion, which could in turn influence PM formation in either the pilot or main combustion event.

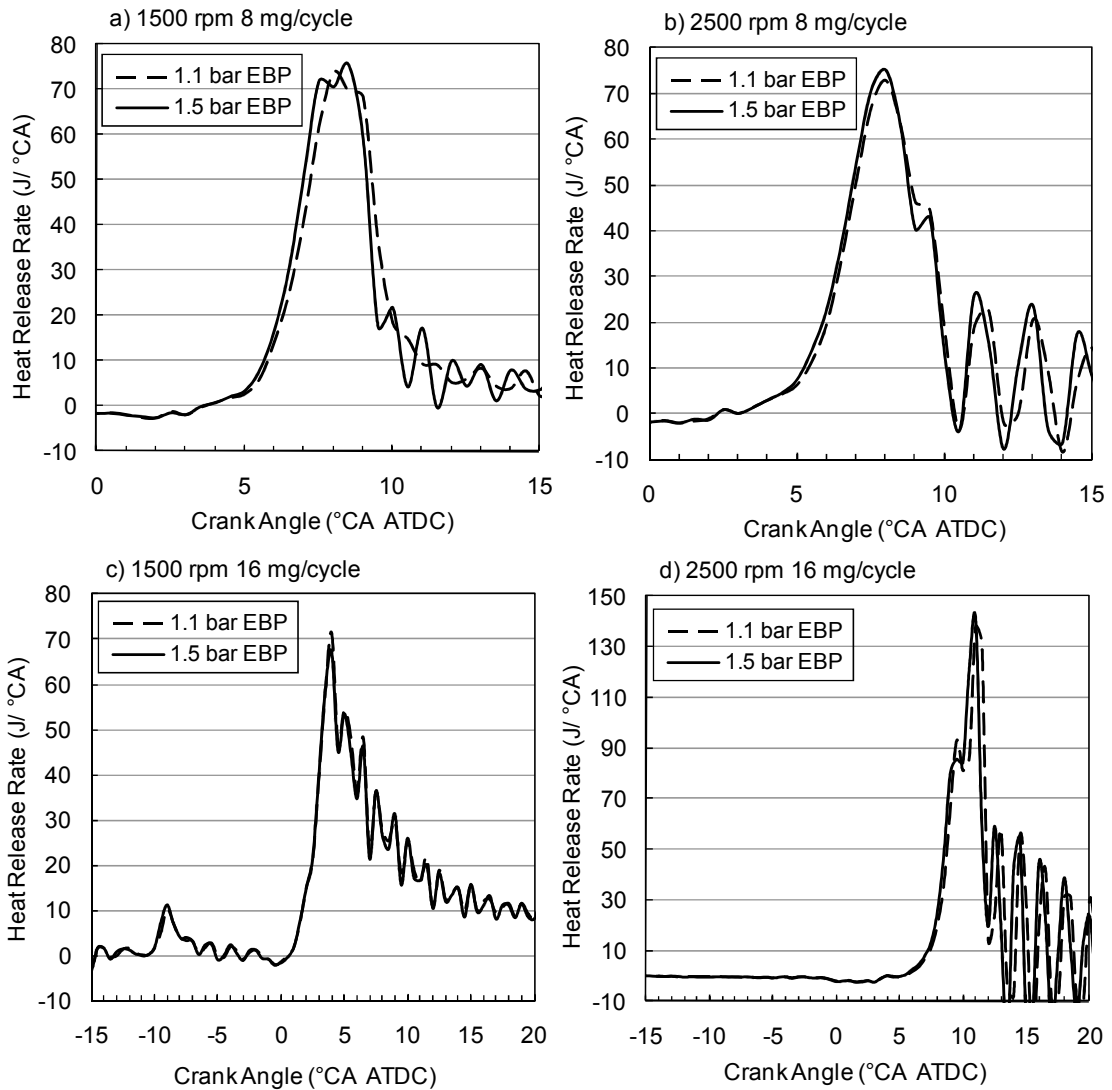


Figure 6.5 Effects of EBP on conventional diesel combustion heat release rate (a) 1500 rpm 8 mg/cycle, Sol -3.5°CA ATDC; b) 2500 rpm 8 mg/cycle, Sol(main) -6°CA ATDC; c) 1500 rpm 16 mg/cycle, Sol -20°CA ATDC for pilot, -2.5°CA ATDC for main; d) 2500 rpm 16 mg/cycle, Sol -9°CA ATDC.)

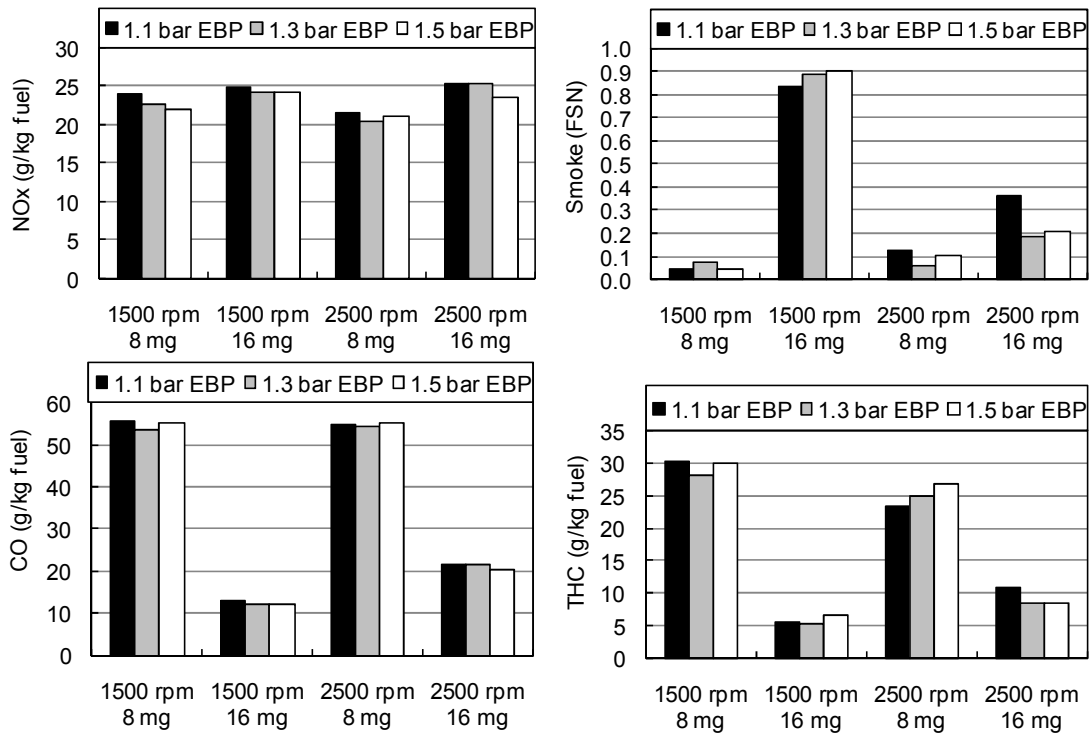


Figure 6.6 Effects of EBP on conventional diesel combustion emissions

### 6.3.3 Low temperature diesel combustion

In LTC, the general effect of RGF reducing the charge oxygen concentration and increasing its temperature was similar to that of conventional diesel combustion. Reducing the oxygen content increased the effective EGR level and had the potential to reduce both the NO<sub>x</sub> and PM emissions in LTC, as described in previous chapters. Conversely, the increase in charge temperature resulting from the larger quantity of hot residuals could have increased the rates of the pollutant-forming chemical reactions, leading to increases in NO<sub>x</sub> and PM emissions.

The effects of EBP on the heat release rate and cylinder pressure for LTC at the four investigated engine operating conditions are shown in Figure 6.7. The high EBP increased the amount of residual gas trapped in the combustion chamber as shown in Figure 6.3. This resulted in increased dilution ratio of the charge and a corresponding increase in the overall fuel-oxidizer equivalence ratio as shown in Figure 6.4.

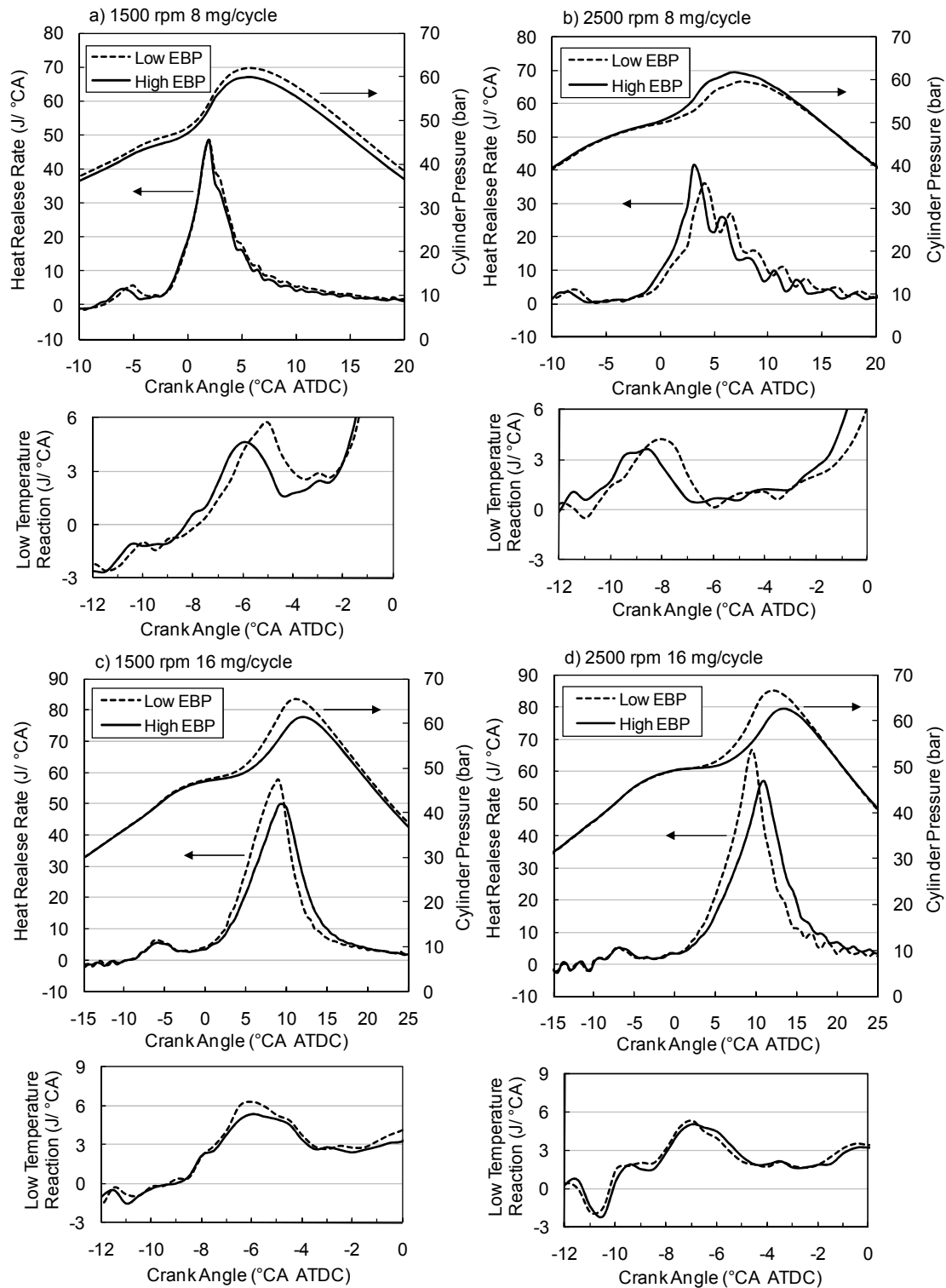


Figure 6.7 Effects of EBP on LTC heat release rate (a) 1500 rpm 8 mg/cycle, Sol  $-18^{\circ}\text{CA}$  ATDC; b) 2500 rpm 8 mg/cycle, Sol  $-30^{\circ}\text{CA}$  ATDC; c) 1500 rpm 16 mg/cycle, Sol  $-24^{\circ}\text{CA}$  ATDC; d) 2500 rpm 16 mg/cycle, Sol  $-30^{\circ}\text{CA}$  ATDC.)

For the 8 mg/cycle fuelling cases (Figures 6.7a and 6.7b), the increase of EBP led to a slightly earlier ( $< 1^{\circ}\text{CA}$ ) start of both the low temperature reaction and the main combustion event. This indicates that the thermal effect of the hot residual gas had a

greater influence on the combustion process than the dilution effect. This is logical, since in these cases the equivalence ratios were relatively low, and hence there was more available oxygen. As a result, the combustion was more sensitive to changes in charge temperature.

For the 16 mg/cycle fuelling cases (Figures 6.7c and 6.7d), the increased dilution ratio retarded the main combustion while the preliminary 'cool flame' reactions occurred at the same crank angle regardless of the EBP. This meant that the dilution effect of the residual gases had a similar effect to increasing the EGR rate in LTC operation. In LTC, the start of combustion is mainly controlled by the fuel injection timing as described in Chapter 4, but the combustion rate is mainly controlled by the availability of oxygen (Beatrice *et al.*, 2007a). The reduction in oxygen due to the higher RGF, as shown by the fuel-oxygen equivalence ratio (Figure 6.3) significantly reduced the main combustion rate.

The low temperature reaction heat release rate was influenced by the trapped charge composition and temperature as introduced in Chapter 5. The increased dilution by the residual gas for the high EBP led to a delay in the low temperature reactions and a lower reaction rate, consistent with the effects of increased EGR. Conversely, the hot residual gas affected the cool flame reactions by causing an early occurrence of low temperature reaction, an increased heat release rate and an early occurrence of NTC, as shown in Chapter 5 with the increases in charge temperature. The combination of these two features resulted in a reduction in low temperature reaction heat release rates for all the operating conditions, and showed different influences on the phasing of the low temperature heat release process for low load and intermediate load conditions. For the low load conditions, the high temperature of residual gas advanced the low temperature reaction and increased the reaction rates more than the dilution effect retarded and decreased the low temperature reaction rates. With increased fuel injection quantity shifting the equivalence ratio to near unity, the low temperature reaction phasing of the intermediate load conditions showed insignificant sensitivity to the EBP. The dilution effect of residual gas here may have been significant enough to balance the influences of the thermal effect.

The main combustion peak heat release rates were increased for the low load conditions and decreased for the intermediate load conditions with higher EBP. At the high EBP cases, the RGF in the engine increased, resulting in higher charge temperatures; these higher temperatures led to shorter ignition delays for the 8 mg/cycle cases. For the 16 mg/cycle cases, the reduction of the oxygen in the



combustion chamber, which led to equivalence ratios in excess of unity (see Figure 6.4), resulted in reductions in the peak heat release rates for the main combustion.

The in-cylinder pressure and heat-release rate results shown in Figure 6.7 indicate that the main influence of the EBP is on the combustion phasing. To provide a more complete comparison between operating conditions, the combustion phasing parameters for high and low EBP are shown in Figure 6.8. The figure shows the start of low temperature reaction (SoCL), start of main combustion (SoCH, equals to CA5), and the CA50. As discussed in detail earlier, at the low load conditions, the increased EBP tended to advance the combustion phasing for the whole combustion process. For the intermediate load conditions, the start of the cool flame reactions (SoCL) were insignificantly affected by EBP, while the early part of the main combustion events were delayed with increased EBP.

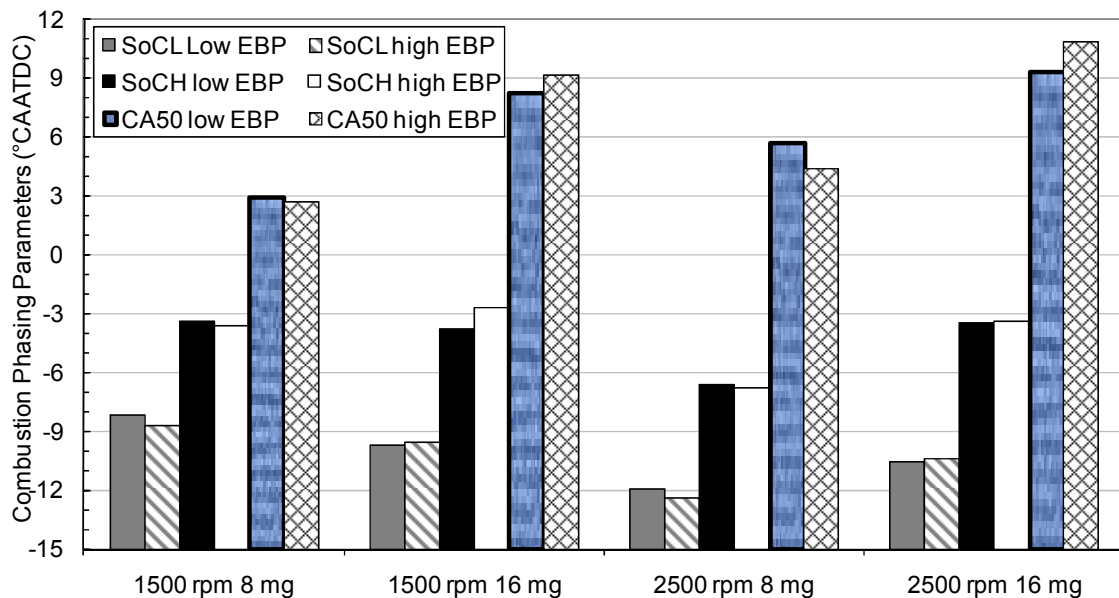


Figure 6.8 Effect of EBP on LTC combustion phasing (SoCL: start of low temperature reactions; SoCH: start of high temperature reactions, CA5)

The influence of EBP on the combustion stability in the LTC regime varied for the different fuelling conditions. CoV(IMEP), which represents the combustion stability, is shown in Figure 6.9. For the 8 mg/cycle operating conditions, higher EBP increased the combustion stability, while for the 16 mg/cycle cases higher EBP reduced the combustion stability, regardless of engine speed. These trends are similar to those followed by the combustion phasing (CA50), as shown in Figure 6.8. It is possible that for the low load conditions, the higher charge temperatures with higher EBPs (thermal effect), helped to maintain a more stable combustion process while the lack

of oxygen at the intermediate load cases resulted in increased instability (due to dilution effect).

For all the cases, the engine emitted near zero NO<sub>x</sub> emissions (< 10 ppm) and very low smoke emissions. The effects of EBP on emissions under LTC operation are shown in Figure 6.10. For these conditions, the CO emissions were beyond of the measurement range of the analyser (> 5000 ppm), and hence are not presented here. The very low levels of NO<sub>x</sub> meant that small changes in emissions were not detectable and hence the results are not presented here either. For the 16 mg/cycle cases, the smoke emissions were reduced significantly by the increased EBP. This agrees with the characteristics of LTC, with higher EGR levels leading to reduced smoke emissions. For the 8 mg/cycle conditions, however, the smoke emissions were unchanged with higher EBP.

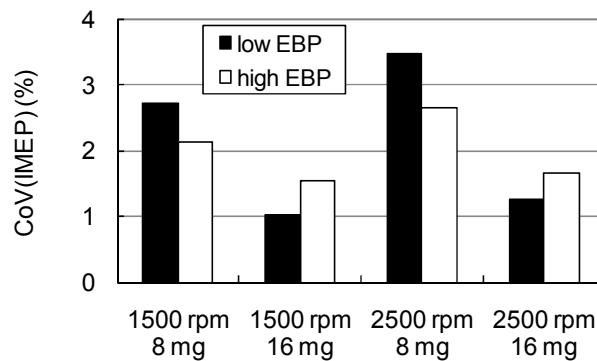


Figure 6.9 Effects of EBP on combustion stability represented by CoV of IMEP

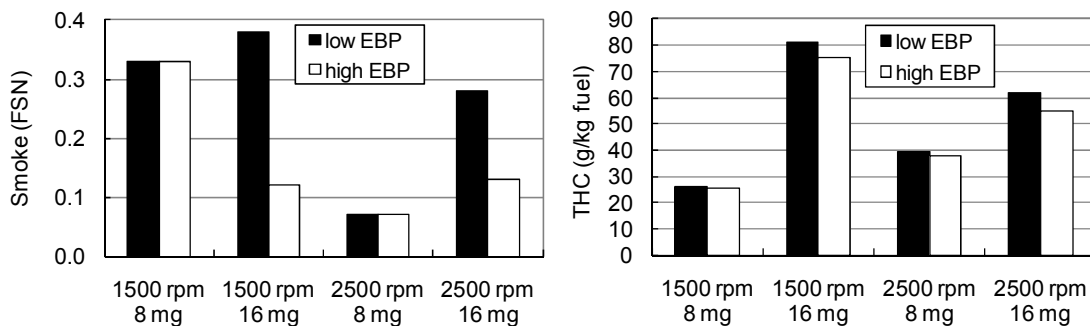


Figure 6.10 Effects of EBP on LTC smoke and THC emissions

The THC emissions behaved similarly to the smoke emissions; at intermediate load, emissions were reduced with higher EBPs, although the magnitude of reduction was much smaller than that for the smoke emissions. At the low load condition, there was no significant effect of EBP on HC emissions. This reduction (or no change) in THC differs from the expected increase in RGF with LTC, i.e., that an increase in charge dilution ('effective' EGR rate) would be expected to increase THC emissions. Since

the principal difference between residual gases and external EGR was temperature, the reduced THC emissions from the high EBP are believed to be a result of the higher in-cylinder charge temperature. This higher charge temperature may have improved the oxidation of hydrocarbons and encouraged their conversion to CO, even with a reduction in available oxygen in the charge.

#### **6.3.4 Effective EGR**

The previous section showed that the increase in RGF that resulted from higher EBP had similar effects on the combustion and emissions as did high levels of external EGR; however, these results were not consistent across all emissions species or operating conditions. The main physical difference between increased RGF and higher external (cooled) EGR was the resulting higher in-cylinder temperature. The RGF also contained unaged particles and reactive radicals that were unlikely to survive long enough in the EGR loop to be reingested. By combining the measured EGR level with the simulated RGF at each operating condition, it is possible to define an 'effective' EGR, as previously given in Equation (6-2). As described in section 6.3.1, the value of 'k' was determined using 1-D modelling to be a value of approximately 4%/bar.

The effects of effective EGR vs. external EGR on smoke and THC emissions for the 2500 rpm 16 mg/cycle and 1500 rpm 8 mg/cycle fuelling conditions in LTC are shown in Figure 6.11. The baseline emissions (shown with the black diamonds) are from tests of LTC over a wider range of EGR levels than required for this study on the effects of EBP. These results demonstrate the reduced smoke and increased HC emissions commonly associated with increasing EGR under LTC conditions (Alriksson *et al.*, 2006; Beatrice *et al.*, 2007b; Ogawa *et al.*, 2007). For the 16 mg/cycle case (Figure 6.11a) the increased EBP reduced the smoke number more than an equivalent amount of external EGR would have done. This is thought to be a result of the effective EGRs' higher temperature, which reduced the engine's volumetric efficiency and the quantity of trapped oxygen. These effects resulted in both a lower combustion rate (as shown in Figures 6.7c and 6.7d) and lower smoke emissions (Figure 6.10). For the 8 mg/cycle case (Figure 6.11b), the increased RGF with higher EBP did not influence the smoke emissions. In this case, the dilution effect of the increased RGF less significantly influenced the equivalence ratio, compared with the higher load cases (as shown in Figure 6.4). The thermal effect of increased RGF should have increased the combustion temperature, which under LTC conditions would have been expected to increase PM emissions. For the THC

emissions, the effective EGR for all the cases demonstrated that while the increase in RGF did not increase the THC emissions (and for the intermediate load case it actually decreased them), while an equivalent increase in external EGR would have been expected to increase the THC substantially. This difference is expected to be a result of the higher trapped charge temperature resulting in better THC oxidation which offset the increased THC formation due to higher charge dilution.

In general, the 'effective' EGR results provide further support to the separation between the effects of increased dilution and increased charge temperature due to higher RGFs which are a result of increased EBP. The dilution effect of the increased RGF tended to reduce the smoke emissions, while the thermal effect tended to increase the combustion temperature and PM formation in LTC. Since the equivalence ratios for the 16 mg/cycle operating cases were high, the dilution effect had more significant influence on the combustion and emissions than the thermal effect did under these conditions. At low load, however, equivalence ratios were lower; the dilution effect was correspondingly smaller and the thermal effect appears to have been dominant.

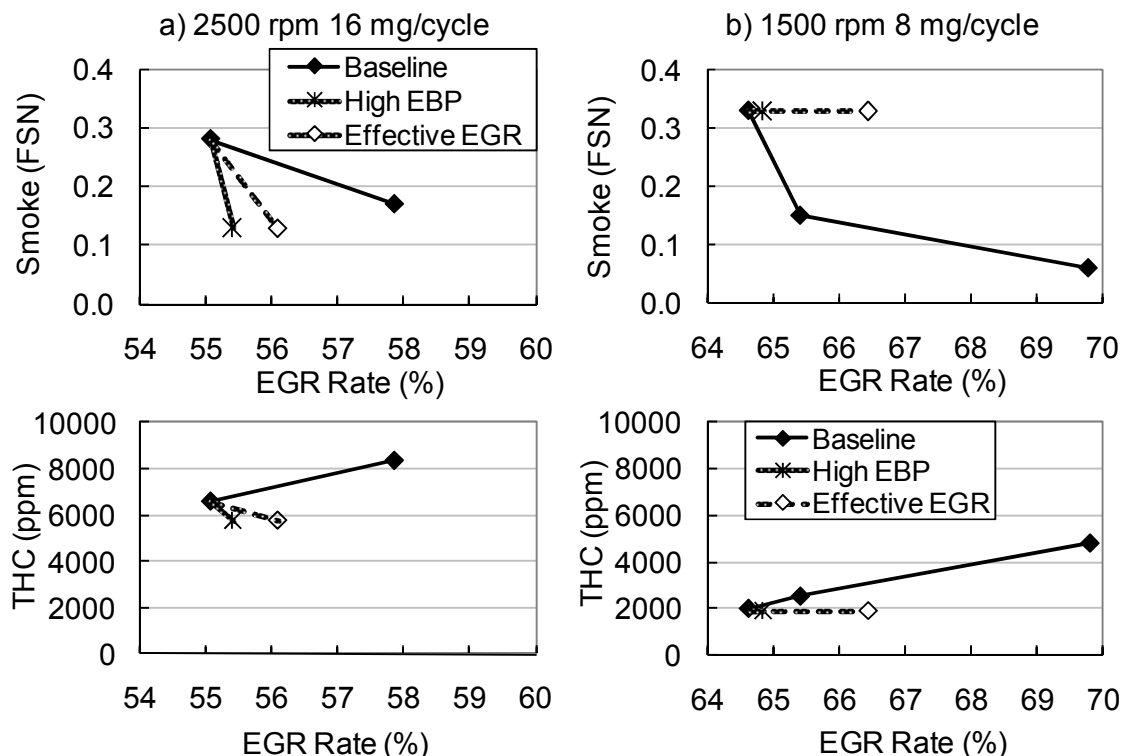


Figure 6.11 Effective EGR vs. external EGR on LTC emissions (a) 2500 rpm, 16 mg/stroke, Sol -30°C/CA ATDC; b) 1500 rpm, 8 mg/stroke, Sol -18°C/CA ATDC.) 'Baseline' points are low EBP conditions over a range of EGR levels; 'high EBP' are the high back pressure cases plotted against their external EGR rate; 'Effective' EGR are these same points (from the high EBP cases) plotted against the calculated effective EGR level (including RGF).

## 6.4 Conclusions

Increasing the exhaust back pressure (EBP), and the corresponding increase in residual gas fraction (RGF), was found to affect the combustion and emissions of a diesel engine under conventional diesel and low temperature diesel combustion (LTC) modes in the following ways:

1) An increase in EBP showed noticeable influence on conventional diesel combustion progression or emissions.

2) In high EGR LTC, increasing the EBP by one bar increased the RGF by approximately 4%. The higher RGF increased the charge temperature and reduced the oxygen content, influencing the combustion event and pollutant formation.

3) For the intermediate load LTC conditions, the increase in RGF retarded and slowed the main heat release reactions, but did not influence the start of the 'cool flame' reactions. This suggests that the intermediate load cases were more sensitive to the dilution effect. Because of the high equivalence ratio under these conditions, the combustion was more sensitive to oxygen concentration.

4) For the low load LTC conditions, the higher RGF resulting from increased EBP advanced both the cool flame reactions and the main heat release events. Compared to the intermediate load case, the low load cases' lower charge equivalence ratios meant that the combustion was not as limited by oxygen availability and hence was more sensitive to temperature.

5) The influence of EBP on low temperature combustion stability followed the same trends as its influence on the phasing of the main combustion event. At intermediate loads, the higher EBP delayed the CA50 and increased the CoV(IMEP). Conversely, at low load, the higher EBP advanced the CA50 and reduced the CoV(IMEP).

6) For the intermediate load LTC conditions, the higher RGF with increased EBP reduced smoke emissions more significantly than an equivalent amount of external cooled EGR would have done. At low load, the smoke emissions were not reduced with higher EBP, even though the 'effective' EGR suggested that they should have been. This is most likely a result of the higher charge temperature having offset the effects of increased dilution. The higher temperature of the residual gases, compared to EGR, meant that for the same 'effective' EGR level, the higher EBP case resulted in lower THC emissions.

This chapter has demonstrated how LTC diesel operation is more sensitive to one specific operating parameter (EBP) than is conventional diesel combustion. The sensitivity of LTC to small variations in other engine operating parameters, in particular EGR level, speed, fuel quantity and intake temperature, will be introduced in the next chapter. Small variations ('micro-transients') that the engine could encounter during daily operation are studied to identify the critical control parameters for stable LTC operation.

# Chapter 7 Sensitivity of LTC to Engine Operating Parameters

## 7.1 Introduction

Engine operating parameters are constantly changing due to the variations in the operating environment. These changes come from the driver demands, the road conditions and the engine's dynamic characteristics, leading to continuously transient engine operation. These 'small-scale transients' take place within a very short time and may influence the combustion processes and emissions. Production inconsistencies and long-term degradation of engine parts are also sources of variations in engine operation. Thus, the engine combustion and emissions control should need to take both short-term and long-term variations in engine operating conditions into account. When investigating advanced combustion strategies, the combustion sensitivity to these variations should be identified.

For conventional diesel combustion, precise control of fuel delivery, boost pressure and EGR rate have been adopted to increase the consistency of the combustion and emissions throughout the engine operating maps (Nakayama *et al.*, 2008; Yokomura *et al.*, 2004). These controls reduced the cyclic and cylinder-to-cylinder control variations, achieving improved engine performance and reduced emissions. In-cycle fuel and intake charge control techniques are also being developed to enhance the robustness of engine operation (Liebig *et al.*, 2008; Nieuwstadt *et al.*, 2000; Zheng *et al.*, 2009).

Implementation of LTC on diesel engines could potentially lead to either removal or reduction in size of NO<sub>x</sub> and PM aftertreatment systems, because of the low engine-out NO<sub>x</sub> and PM emissions from this combustion mode. However, impaired engine combustion stability (in addition to limited load) in the LTC regime could be one of the barriers to its wider application. Other emissions species of LTC, such as the THC and CO, are often at very high levels, and are sensitive to small changes in engine operating parameters. Also, it would be easy to see PM increase dramatically with a small change in operating parameters. Thus, understanding the sensitivity of LTC to the engine operating parameters will be a critical feature to a successful application of this combustion strategy.

To achieve LTC, engine operating parameters need to be controlled within narrow ranges as discussed in the previous chapters. The optimised value of a specific

parameter for LTC operation may be sensitive to a change in the level of another parameter. The effects of these individual parameters, and their interactions, will likely have significant influences on the robustness of LTC operation, and the associated engine performance and emissions during both steady-state and transient operation.

In this chapter, the sensitivity of LTC to small changes in key engine operating parameters EGR rate (EGR), fuel injection quantity (Fuel Q), engine speed (Speed) and intake charge temperature (Tint) have been investigated. The influences of the individual parameters and their interactions were analysed using design of experiment (DoE) and ANOVA tools. With this knowledge, the critical control parameters for achieving a robust LTC operation can be identified.

## **7.2 Design of Experiments and ANOVA**

Design of Experiments (DoE) is an effective tool for studying engine performance and emissions where these results are sensitive to the changes of many engine operating parameters. With a procedure of factors selection, observation and analysis, the influence of individual parameters on the engine performance and emissions can be identified. With proper use of DoE, the interactions among the variables can also be investigated.

### **7.2.1 Selection of the factors**

During daily operation, an engine's load and speed are subject to changes in driver demands and road conditions. Even in 'cruise' at near-constant speed, the engine's load and speed will vary slightly due to atmospheric conditions, road gradient, traffic, and driver behaviour. The control of individual parameters is also sensitive to specific variations. EGR rate control accuracy suffers from cylinder-to-cylinder inconsistency and cyclical variability. Intake charge temperature is sensitive to the engine thermal situation and the environmental conditions. The changes of these parameters cover most of the small variations in an engine's daily operation. Longer-term variability due to vehicle system degradation can also influence engine performance and long-term alignment with emissions regulation. However, degradation of the fuel system is important, and will be investigated on the basis of changes in fuel injection quantity; the change in EGR rate is relevant for variations in the EGR system such as fouling of the EGR valve, and changes in intake charge temperature could be a result of EGR fouling or intercooler performance degradation. The effects of factors such as



engine wear, fuel property change and other changes in atmospheric conditions (i.e., humidity) on LTC are not specifically evaluated here.

The intervals of the parameters were estimated through analysing the engine behaviour within driving-cycle test data and extended to the engine real world operation. The variations in engine speed and fuel injection quantity during non-transient operating modes showed less a than  $\pm 5\%$  change. However, in the real world usage, the road condition could be different from the driving-cycle test, and  $\pm 5\%$  of the speed and fuel injection quantity range was assumed to be able to cover the 'small-scale transients' of the engine operation. Larger than  $\pm 5\%$  variations can be considered as normal transients operation of the engine and are going to be investigated in Chapter 8. Accurate EGR rate control is always a challenging task. The cylinder-by-cylinder and cyclic variations are expected to be controlled within  $\pm 5\%$  to meet the emissions regulations for a modern diesel engine (Page *et al.*, 2002). Thus, the variation in EGR rate was set to a total variation of  $\pm 5\%$  (e.g.  $60\% \pm 3\%$ ). Intake manifold temperature is sensitive to the engine thermal situation and the environmental conditions. It is influenced by the ambient temperature, exhaust temperature, the compressor-out temperature and the cooling system performance. Intake charge temperature control has a relatively slow response and an accuracy of  $\pm 10^\circ\text{C}$  during the 'small-scale transient' conditions was considered to be reasonable. As a result, for this study, an estimated short term  $\pm 10^\circ\text{C}$  control error was selected to represent the temperature variations. This may also be considered to be representative of a change in ambient temperature. These values are expected to represent most of the 'small-scale transients' of an engine within a real world operating environment. The parameters and their levels in this study are listed in Table 7.1. The fuel injection timing and pressure are kept constant for each group of the tests and are also listed in the table.

Table 7.1 Factors investigated and the other engine operating parameters

Factor	Name	1500 rpm 8 mg/cycle	1500 rpm 16 mg/cycle	2500 rpm 8 mg/cycle	2500 rpm 16 mg/cycle
A	EGR	$65\% \pm 3\%$	$56\% \pm 2\%$	$65\% \pm 3\%$	$53\% \pm 3\%$
B	Fuel Q	$8 \pm 0.4$ mg	$16 \pm 0.8$ mg	$8 \pm 0.4$ mg	$16 \pm 0.8$ mg
C	Tint	$65 \pm 10^\circ\text{C}$	$80 \pm 10^\circ\text{C}$	$70 \pm 10^\circ\text{C}$	$80 \pm 10^\circ\text{C}$
D	Speed	$1500 \pm 75$ rpm	$1500 \pm 75$ rpm	$2500 \pm 125$ rpm	$2500 \pm 125$ rpm
-	Sol	$-18^\circ\text{CA ATDC}$	$-12^\circ\text{CA ATDC}$	$-27^\circ\text{CA ATDC}$	$-27^\circ\text{CA ATDC}$
-	Fuel P	600 bar	1000 bar	800 bar	1000 bar

## 7.2.2 Observations/responses

Engine performance and emissions parameters were measured during the test procedure. Gaseous emissions and smoke number, gross IMEP, CA50 and CoV of IMEP, as described in Chapter 3, were compared and analysed statistically using the ANOVA tool (Ross, 1996). In LTC modes, the NO<sub>x</sub> emissions were at very low levels (< 10 ppm). Although changes in the engine operating parameters may have influenced the NO<sub>x</sub> emissions slightly, any changes were smaller than the resolution of the NO<sub>x</sub> analyser. Hence, the NO<sub>x</sub> is not presented in the results of the observations.

## 7.2.3 DoE methods

Design of experiments can effectively reduce the required number of tests in an experimental programme without significantly compromising the quantity and quality of the information derived from the experiment. For this study, each of the factors (EGR, Fuel Q, Tint and Speed) was evaluated over three levels. A full factorial experimental design (where every combination would be tested once) would lead to  $3^4 = 81$  test points for each of the speed-load operating conditions. The numbers of tests, when replications are included, for the complete set of four operating conditions would be too demanding given the limited time and resources allocated. To reduce the number of test points, both a half fractional factorial experiments and the Taguchi method were adopted to investigate the sensitivity of LTC to the specified engine operating parameters under the 'small-scale transients' operating conditions.

A half fractional factorial experimental design can reduce the test number from 81 to 27. The cost of this reduction in the number of tests is the omission of high order interactions and the aliasing of the main effects by them (Montgomery, 2009). For the  $3^4$  half fractional factorial test, the fourth order interaction of the four parameters is not investigated, the third order interactions were aliasing with the individual main effects and the second order interactions were aliasing with each other as listed in Table 7.2. The high order interactions normally have an insignificant influence on the results and are frequently neglected. In this study, the variations in the parameters were designed within very narrow ranges. Hence, the third and fourth order interactions were not expected to have statistically significant influences on the observed results. Two EGR rates were used in the experimental design to reduce the half fractional factorial test number further to 18 without sacrificing the interactions in

the test. As the effects of EGR rate on LTC is already quite clear, as introduced in the previous chapters, a two-level EGR rate design can still help to investigate the interactions and can be used to justify the Taguchi method which does not take the interactions into account. The  $2 \times 3 \times 3 \times 3$  half fractional factorial test plan is listed in Table 7.3. Only the 1500 rpm 8 mg/cycle operating condition was tested with this experimental design.

Table 7.2 Aliasing in half fractional factorial design

Main	A	B	C	D	AB	AC	BC
Aliasing	BCD	ACD	ABD	ABC	CD	BD	AD

Table 7.3 Half fractional factorial design ( $2 \times 3 \times 3 \times 3$ )

Number	A (EGR rate)	B (Fuel Q)	C (Tint)	D (Speed)
1	1	1	1	1
2	1	1	2	2
3	1	1	3	3
4	1	2	1	2
5	1	2	2	3
6	1	2	3	1
7	1	3	1	3
8	1	3	2	1
9	1	3	3	2
10	2	1	1	2
11	2	1	2	3
12	2	1	3	1
13	2	2	1	3
14	2	2	2	1
15	2	2	3	2
16	2	3	1	1
17	2	3	2	2
18	2	3	3	3

Levels 1, 2 and 3 represent baseline -, baseline and baseline +

Despite the significant reduction in the number of required tests achieved by the fractional factorial work, an even greater reduction was desired to cover all four operating conditions. To achieve this, a Taguchi L9 experimental design was implemented for all the operating conditions listed in Table 7.1. Because the Taguchi method further restricts the experiment, the half-fractional factorial test was conducted first to justify the Taguchi method.

The Taguchi L9 design (Ross, 1996) was derived from a  $3^4$  orthogonal array, as listed in Table 7.4. With 9 tests, the basic influence of the individual factors on LTC can be identified. However, the interactive effects of the factors could not be studied directly in this case. Hence, a pooling technique was used to combine the smallest column effects to estimate the error variance. This method eliminates the insignificant factors from the table and brings the opportunity of investigating the interaction effects among the significant factors.

Table 7.4 Taguchi  $3^4$  L9 design

Number	A (EGR rate)	B (Fuel Q)	C (Tint)	D (Speed)
1	1	1	1	1
2	1	2	2	2
3	1	3	3	3
4	2	1	2	3
5	2	2	3	1
6	2	3	1	2
7	3	1	3	2
8	3	2	1	3
9	3	3	2	1

Levels 1, 2 and 3 represent baseline -, baseline and baseline +

## 7.2.4 ANOVA

Analysis of variance (ANOVA) is a statistically based tool used to interpret the results from a group of experiments. It can detect the differences in average performance of sets of tests. Sum of squares (SS), degrees of freedom (f), mean squares (V), ratio of sample variance to the error variance (F) and percent contribution (P) can be calculated in the process. The percent contribution indicates the relative power of a factor and/or interaction to the change in observations, and should not be confused with the more widely recognised P (probability) value used in the statistical tests. If the factor and/or interaction levels are controlled precisely, then the total variation can be reduced by the amount indicated by the percent contribution (Ross, 1996). F-tests were carried out to check if the variance caused by a factor and/or interaction is significantly different to the variance caused by the error factors in the experiment. F values with the 90%, 95% and 99% confidence levels (can be 90% certain, 95% certain and 99% certain) were used to identify the statistically significant influences from the factors and interactions. This analysis was conducted in MS Excel™ using the available statistical packages combined with custom-written analysis routines that were validated using known results.

## 7.3 Results

A half fractional factorial test was conducted on the 1500 rpm 8 mg/cycle operating condition to evaluate the sensitivity of the engine in an LTC mode to variations in the engine operating parameters and their interactions. The results from the test set were also used to evaluate the feasibility of the Taguchi method for this application. Then, a L9 test was tried on the same operating condition, and the ANOVA tables of these two sets of tests were compared. The LTC sensitivity for the other speed and load conditions were also studied using the validated Taguchi method.

### 7.3.1 Fractional factorial test

The half fractional factorial test evaluated the LTC sensitivity to two levels of EGR and, three levels of fuel injection quantity, intake charge temperature and engine speed. Gaseous emissions (except NO<sub>x</sub>), smoke measurements, and engine performance parameters such as gross IMEP, CA50 and CoV(IMEP) were used as the responses to the experiment. All other engine operating parameters were held constant as defined either in Table 7.1 or at their standard conditions. The results of the 18 tests are listed in Table 7.5.

Table 7.5 Half fractional factorial test results (1500 rpm 8 mg/cycle)

No.	Factors				Results							
	EGR (%)	Fuel Q (mg)	Tint (°C)	Speed (rpm)	NO <sub>x</sub> (ppm)	FSN	THC (ppm)	CO (%)	O <sub>2</sub> (%)	IMEP (bar)	CA50 (°CA ATDC)	CoV (IMEP) (%)
1	62	7.6	55	1425	7.4	0.13	2021	1.09	12.11	2.86	2.5	2.78
2	62	7.6	65	1500	6.9	0.08	2522	1.38	11.44	2.80	5.6	3.22
3	62	7.6	75	1575	6.5	0.14	2504	1.41	11.48	3.04	5.6	3.08
4	62	8.0	55	1500	6.1	0.05	3452	1.65	11.46	2.89	7.9	3.76
5	62	8.0	65	1575	6.1	0.04	3960	1.95	10.93	2.83	9.3	4.02
6	62	8.0	75	1425	6.0	0.05	3780	1.99	10.45	2.81	7.8	3.62
7	62	8.4	55	1575	4.6	0.06	5282	2.36	10.99	2.82	11.2	5.47
8	62	8.4	65	1425	6.2	0.02	4538	2.31	10.53	2.86	9.0	4.47
9	62	8.4	75	1500	5.8	0.13	4239	2.14	10.46	3.09	9.3	2.99
10	65	7.6	55	1500	5.4	0.04	5535	2.22	10.77	2.37	11.0	6.31
11	65	7.6	65	1575	5.5	0.07	4589	2.02	11.08	2.51	10.9	5.66
12	65	7.6	75	1425	6.1	0.04	4772	2.43	10.16	2.43	10.8	6.15
13	65	8.0	55	1575	4.9	0.07	7888	2.88	10.58	2.39	14.5	10.10
14	65	8.0	65	1425	5.5	0.09	5310	2.63	10.30	2.62	12.1	6.35
15	65	8.0	75	1500	5.3	0.06	8007	3.82	9.82	2.16	14.1	11.93
16	65	8.4	55	1425	4.9	0.05	8186	3.75	10.03	2.47	14.3	10.75
17	65	8.4	65	1500	4.6	0.07	7745	3.63	10.11	2.49	14.9	9.87
18	65	8.4	75	1575	6.0	0.06	8979	4.30	9.88	2.36	14.5	9.37

As an example, the ANOVA table of THC emissions for the test is shown in Table 7.6. The table shows that EGR rate and fuel injection quantity have a significant influence on this emission with > 99% and > 95% confidence levels respectively. The variation in EGR rate explains 59% of the variations in the THC emissions, while the fuel injection quantity contributes another 32% of it. The intake temperature, engine speed and all the interactions show insignificant influence on the THC emissions.

Table 7.6 ANOVA table of fractional factorial test results on THC (1500 rpm 8 mg/cycle)

Factor	F	SS	V	F	P (%)
EGR (A)	1	45798576	45798576	159.34#	58.73
Fuel Q (B)	2	24576347	12288173	42.75*	31.52
Tint (C)	2	1487532	743765.9	2.59	1.91
Speed (D)	2	1799753	899876.7	3.13	2.31
A X B	2	799341.8	399670.9	1.39	1.03
A X C	2	2183692	1091846	3.80	2.80
B X C	4	756126.2	189031.6	0.66	0.97
error	2	574839.9	287420	-	0.74
Total	17	77976207	-	-	100

+ at least 90% confidence

\* at least 95% confidence

# at least 99% confidence

The P values of all the observations are used to indicate the power of influence for each factor/interaction on their variations (Ross, 1996). As explained in the research methodology section, the F test was used to identify the significance of the difference between a factor/interaction and the error factor. In Table 7.7, the factors/interactions with 90%, 95% and 99% confidence levels were identified with different symbols. The engine speed and all the interaction factors show negligible influence on the outcome measures, except for the interaction factor of EGR rate and fuel injection quantity, which shows a 35.7% contribution to the variation in smoke number with 90% confidence. However, EGR rate and fuel injection quantity individually show insignificant influence on smoke number. As shown in Table 7.5, the smoke number measurements from these tests were at very low levels and the effects of small changes to the engine operating parameters may not be distinguished from the measurement error.

Table 7.7 Summary of the ANOVA for the half fractional factorial test results on the observations (1500 rpm 8 mg/cycle case)

Factor	f	THC		CO		FSN		O <sub>2</sub>		CA50		CoV(IMEP)	
		F	P (%)	F	P (%)	F	P (%)	F	P (%)	F	P (%)	F	P (%)
EGR (A)	1	159.3 <sup>#</sup>	58.7	156.8 <sup>#</sup>	51.2	3.5	6.7	363.6 <sup>#</sup>	41.0	298.7 <sup>#</sup>	62.4	60.6 <sup>*</sup>	67.0
Fuel Q (B)	2	42.8 <sup>*</sup>	31.5	56.9 <sup>*</sup>	37.1	2.4	9.1	144.2 <sup>#</sup>	32.5	71.7 <sup>*</sup>	30.0	6.8	15.0
Tint (C)	2	2.6	1.9	5.6	3.6	1.6	6.2	73.6 <sup>*</sup>	16.6	0.06	0.02	0.8	1.7
Speed (D)	2	3.1	2.3	0.6	0.4	0.4	1.5	10.3	2.3	8.8	3.7	0.5	1.0
A X B	2	1.4	1.0	3.9	2.6	9.2 <sup>+</sup>	35.7	6.9	1.6	2.1	0.9	2.1	4.6
A X C	2	3.8	2.8	5.0	3.3	6.8	26.2	7.3	3.9	1.7	0.7	1.5	3.2
B X C	4	0.7	1.0	0.8	1.1	1.4	10.7	5.4	2.5	2.3	1.9	1.2	5.3
error	2	-	0.7	-	0.7	-	3.9	-	0.2	-	0.4	-	2.2
Total	17	-	100	-	100	-	100	-	100	-	100	-	100

+ at least 90% confidence

\* at least 95% confidence

# at least 99% confidence

The experimental data from the fractional factorial test can be plotted to show the effects of individual factors and the interactive influences. As shown in Figure 7.1, increases in EGR rate and fuel injection quantity lead to significant increases in the THC and CO emissions. Changes (of magnitude investigated) in intake charge temperature and engine speed were found to have insignificant effect on the emissions. The EGR rate shows insignificant influence on the other parameters. For the combustion phasing (CA50) and combustion stability CoV(IMEP), as shown in Figure 7.2, these only show clear trends with EGR rate and fuel injection quantity. The fact that there are no significant interactive effects can be attributed to the relatively small changes of the parameters (factors).

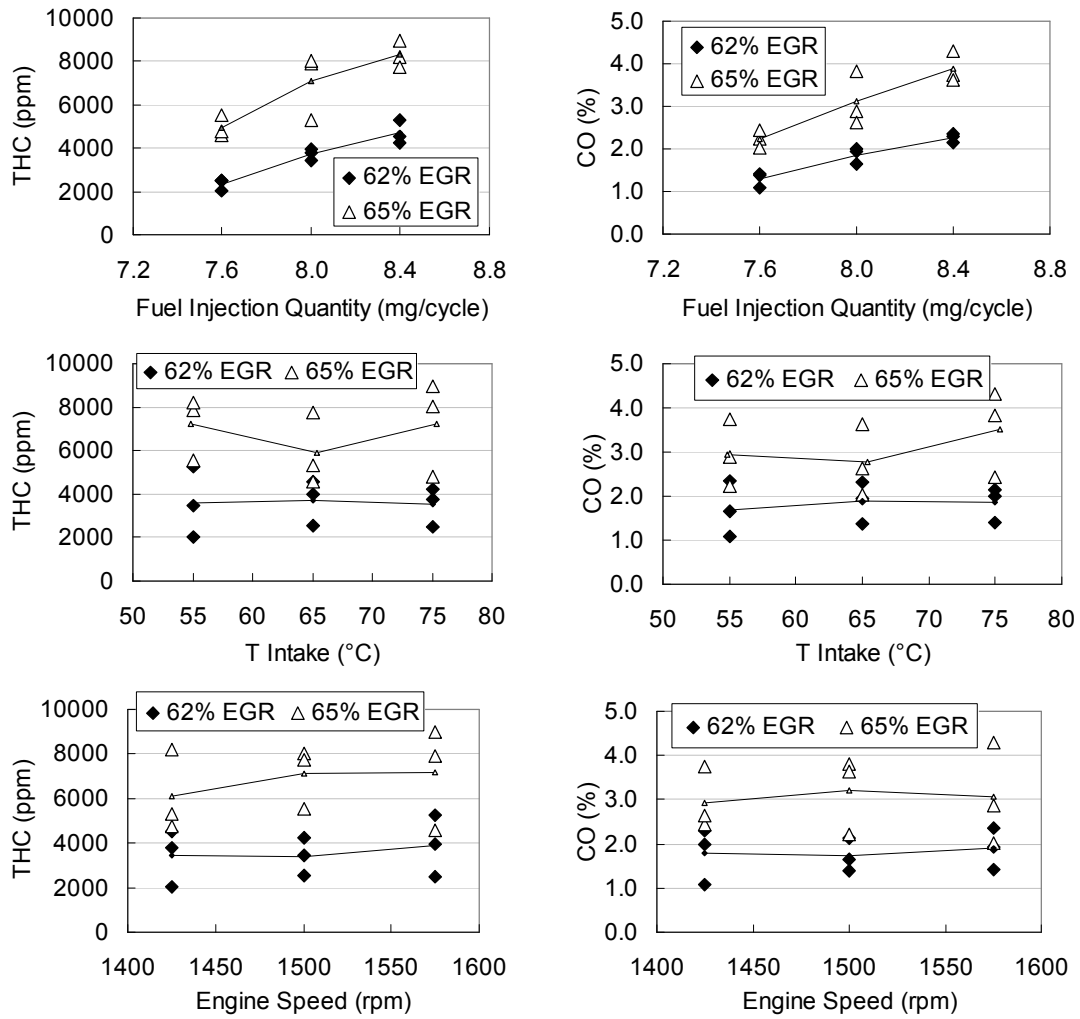


Figure 7.1 Plots of the THC and CO emissions over the main factors and the interactive influence of EGR rate with other parameters. The symbols represent the individual emissions data for the whole set of tests; the lines are the average values for the specific factors and levels. (1500 rpm 8 mg/cycle, half fractional factorial test)



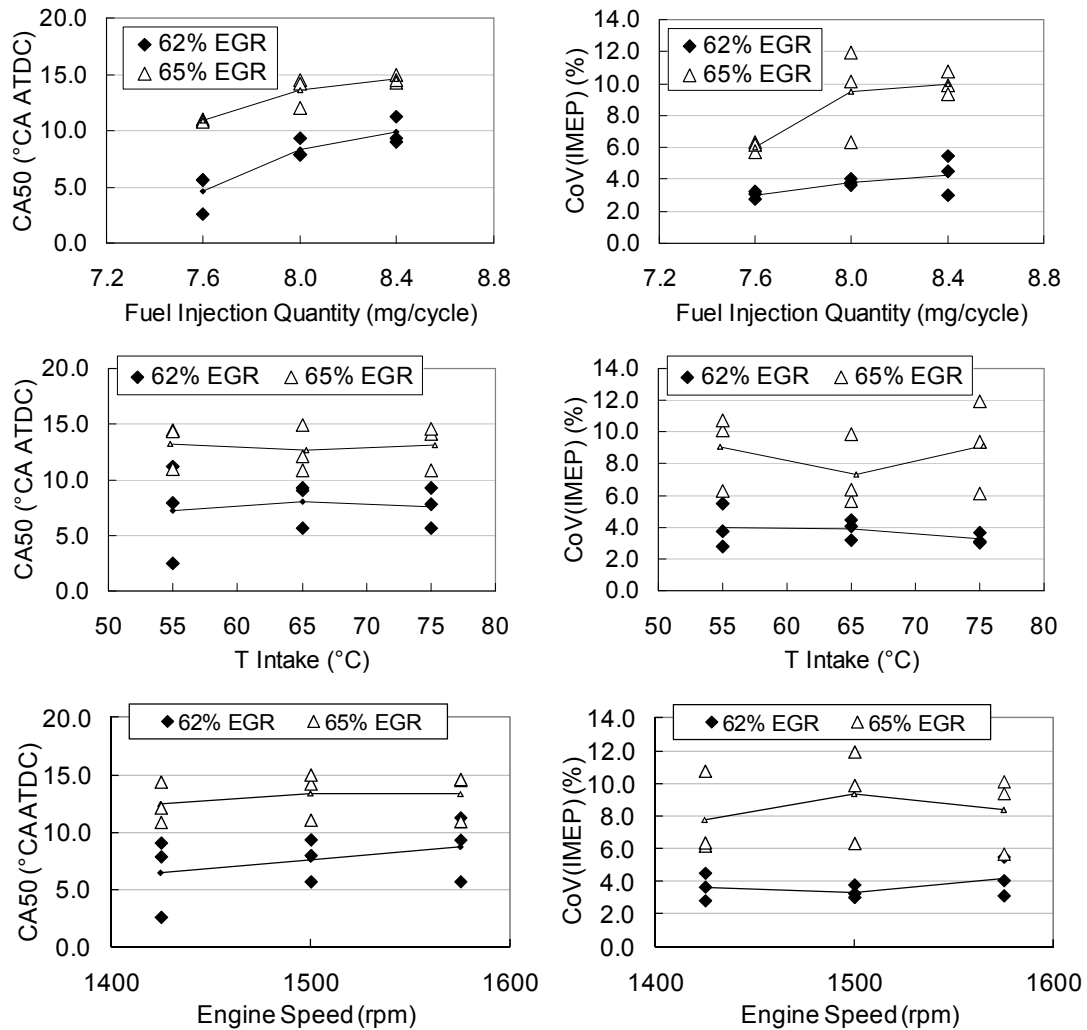


Figure 7.2 Plots of CA50 and CoV(IMEP) over the main factors and the interactive influence of EGR rate with other parameters. The symbols represent the individual emissions data for the whole set of tests; the lines are the average values for the specific factors and levels. (1500 rpm 8 mg/cycle, half fractional factorial test)

A Taguchi L9 orthogonal array for the 4-factor 3-level experimental design ignores the interactions among the factors. The results derived from the half fractional factorial test suggest that the interactions have insignificant influence on LTC combustion for the range of variations investigated in this work. However, the smoke emissions for the intermediate load conditions would be more detectable and the interactive effects of EGR rate and fuel injection quantity may not be insignificant. As a result, the study of LTC sensitivity to the specified engine operating parameters should be achievable using the Taguchi design with this limitation.

### 7.3.2 Taguchi L9 test result

A Taguchi L9 experimental design was implemented on the 1500 rpm 8 mg/cycle operating condition to evaluate the difference between the two DoE methods. The nine test results are listed in Table 7.8. The ANOVA table of THC is shown in Table 7.9. In the table, the degree of freedom of error factor ( $f_e$ ) is zero. Hence there is not error variance estimation available for the confidence check (F test). Percent contribution (P) of engine speed is very low and the fractional factorial test suggested that the changes of engine speed have insignificant influences on LTC performance and emissions. Thus, a pooling technique (Ross, 1996) was used here and the column for speed factor was treated as the error variance. The pooled ANOVA table is shown in Table 7.10.

The EGR rate shows significant influence on LTC THC emissions ( $P = 77.46$ ) with 90% confidence. The contribution of the fuel injection quantity is insignificant in this set of tests, although it is the second significant factor on THC emissions in the fractional factorial test. The reason for the different results between the two DoE tests is that the fuel rate measurement equipment used in this study had  $< \pm 5\%$  accuracy, which is close to the designed variations for the fuel injection quantity. For the small test number (9) in the Taguchi method, the fuel metering error cannot be removed through averaging and this could lead to increased error variance. The intake charge temperature and engine speed show very little influence on the THC in this set of tests as was found in the fractional factorial experiments.

Table 7.8 Taguchi L9 test results (1500 rpm 8 mg/cycle)

No.	Factors				Results							
	EGR (%)	Fuel Q	Tint (°C)	Speed (rpm)	NOx (ppm)	FSN	THC (ppm)	CO (%)	O <sub>2</sub> (%)	IMEP (bar)	CA50 (°CA ATDC)	CoV (IMEP) (%)
1	62	7.6	55	1425	12.7	0.03	2283	0.61	12.84	2.62	1.5	2.22
2	62	8.0	65	1500	12.3	0.36	2990	0.77	11.60	2.82	4.0	2.04
3	62	8.4	75	1575	12.1	0.58	3582	1.10	10.91	3.09	5.8	3.48
4	65	7.6	75	1500	12.0	0.13	3229	0.95	11.04	2.52	5.2	2.63
5	65	8.0	55	1575	11.8	0.46	3886	1.23	11.11	2.77	9.3	3.48
6	65	8.4	65	1425	12.4	0.00	4492	1.52	10.21	2.91	9.5	3.33
7	68	7.6	65	1575	11.5	0.02	6998	1.86	10.42	2.25	12.4	6.26
8	68	8.0	55	1425	11.7	0.16	4997	1.52	10.54	2.58	11.0	4.88
9	68	8.4	75	1500	12.0	0.06	7214	2.81	9.51	2.57	13.4	6.36

Table 7.9 ANOVA table for Taguchi L9 test results on THC (1500 rpm 8 mg/cycle, non-pooled)

Factor	f	SS	V	F	P (%)
EGR (A)	2	19178776	9589388	-	77.46
Fuel Q (B)	2	2198118	1099059	-	8.88
Tint (C)	2	2151896	1075948	-	8.69
Speed (D)	2	1230471	615235	-	4.97
error	0	-	-	-	-
Total	8	77976207	-	-	100

Table 7.10 ANOVA table for Taguchi L9 test results on THC (1500 rpm 8 mg/cycle, pooled)

Factor	f	SS	V	F	P (%)
EGR (A)	2	19178776	9589388	15.59+	77.46
Fuel Q (B)	2	2198118	1099059	1.786	8.88
Tint (C)	2	2151896	1075948	1.749	8.69
Speed (D) <sup>^</sup>	(2)	-	-	-	-
error	2	1230471	615235	-	4.97
Total	8	77976207	-	-	100

+ at least 90% confidence

\* at least 95% confidence

# at least 99% confidence

<sup>^</sup> indicates the factor that was used to generate the pooled error estimation

A comparison between the summary of the ANOVA for Taguchi L9 test (Table 7.11) and fractional factorial test (Table 7.7) shows that the reduction in test number for the Taguchi method led to reduced confidence (F) in the significance of the main factors. This is mainly a result of the smaller number of degrees of freedom (f) in the more restricted test design. It is reassuring that the same group of factors showed significant influence on the engine performance and emissions for both the sets of tests. As a result, the use of the Taguchi method to reduce the number of required test conditions is considered to be an acceptable approach for the remainder of the operating conditions investigated in this chapter. However, the severe limitations of this method imposes on the assessment of higher-order effects is acknowledged.

Table 7.11 Summary of the ANOVA for the Taguchi L9 test results on the observations (1500 rpm 8 mg/cycle)

Factor	f	THC		CO		FSN		O <sub>2</sub>		CA50		CoV(IMEP)	
		F	P (%)	F	P (%)	F	P (%)	F	P (%)	F	P (%)	F	P (%)
EGR (A)	2	15.6 <sup>+</sup>	77.5	17.9 <sup>+</sup>	63.7	0.7	25.2	10.5 <sup>+</sup>	47.7	17.6 <sup>+</sup>	81.4	12.7 <sup>+</sup>	84.2
Fuel Q (B)	2	1.8	8.9	6.4	22.7	0.9	30.7	6.2	28.2	2.5	11.8	1.0	6.4
Tint (C)	2	1.7	8.7	2.8	10.1	0.2	8.0	4.3	19.6	0.5	2.2	0.4	2.8
Speed (D) <sup>^</sup>	(2)	-	-	-	-	-	-	-	-	-	-	-	-
error	2	-	5.0	-	3.6	-	36.2	-	4.6	-	4.6	-	6.7
Total	8	-	100	-	100	-	100	-	100	-	100	-	100

+ at least 90% confidence

\* at least 95% confidence

# at least 99% confidence

<sup>^</sup> indicates the factor that was used to generate the pooled error estimation

### 7.3.3 Taguchi method for different load and speed conditions

For different speed and load conditions, LTC shows different response to the small changes in the engine operating parameters investigated. The other three operating conditions listed in Table 7.1 were studied using the Taguchi L9 method as was discussed above for the 1500 rpm 8 mg/cycle condition.

#### 2500 rpm 8 mg/cycle

For the 2500 rpm 8 mg/cycle condition, the ANOVA table (Table 7.12) shows similar F and P values as for the 1500 rpm 8 mg/cycle condition. The parameters show similar percent contributions to the variations in the observed values with similar levels of significance. For these low load LTC operating conditions, the variations of EGR rate contributed most of the variations in THC and CO emissions. There were no dominant factors on the smoke emissions, most likely due to the very low smoke levels, which were below the smoke meters ability to accurately resolve differences. In terms of combustion phasing and stability, EGR rate was still the controlling parameter. The engine speed was an independent parameter for LTC within the range of speed variations for these two cases. This suggests, that the low load LTC combustion shows similar combustion patterns (same EGR rate and fuel injection quantity) and that the LTC sensitivities to the engine operating parameters are similar regardless of engine speed not only within the small variations but also in the 1500 rpm to 2500 rpm change.

Table 7.12 Summary of the ANOVA for the Taguchi L9 test results on the observations (2500 rpm 8 mg/cycle)

Factor	f	THC		CO		FSN		O <sub>2</sub>		CA50		CoV(IMEP)	
		F	P (%)	F	P (%)	F	P (%)	F	P (%)	F	P (%)	F	P (%)
EGR (A)	2	23.5*	87.2	55.2*	93.8	0.9	24.1	12.0*	66.6	26.0*	88.1	3.6	70.0
Fuel Q (B)	2	1.3	4.6	1.2	2.0	0.6	15.6	2.0	10.9	1.3	4.5	0.2	4.6
Tint (C)	2	1.2	4.5	1.5	2.5	1.1	32.2	3.0	16.9	1.2	4.0	0.3	5.7
Speed (D)^	(2)	-	-	-	-	-	-	-	-	-	-	-	-
error	2	-	3.7	-	1.7	-	28.1	-	5.6	-	3.4	-	19.7
Total	8	-	100	-	100	-	100	-	100	-	100	-	100

+ at least 90% confidence

\* at least 95% confidence

# at least 99% confidence

^ indicates the factor that was used to generate the pooled error estimation

### 1500 rpm 16 mg/cycle and 2500 rpm 16 mg/cycle conditions

For the intermediate load conditions, the percent contributions of EGR rate, fuel injection quantity and intake charge temperature to the observed variations in THC and CO emissions were distributed more evenly than for the low load cases, as shown in Tables 7.13 and 7.14. The EGR rate was still the most significant source of the variance of the LTC emissions and combustion parameters. However, the importance of fuel injection quantity and intake temperature was increased for these cases. These two parameters contribute more to the changes in THC and CO emissions for the intermediate load LTC conditions than for the low load LTC conditions (Tables 7.11, 7.12).

Table 7.13 Summary of the ANOVA for the Taguchi L9 test results on the observations (1500 rpm 16 mg/cycle)

Factor	f	THC		CO		FSN		O <sub>2</sub>		CA50		CoV(IMEP)	
		F	P (%)	F	P (%)	F	P (%)	F	P (%)	F	P (%)	F	P (%)
EGR (A)	2	15.0 <sup>+</sup>	56.4	89.6 <sup>+</sup>	67.2	21.9 <sup>+</sup>	85.8	205.6 <sup>#</sup>	89.3	5.3	75.2	0.9	35.8
Fuel Q (B)	2	6.9	26.0	31.5 <sup>+</sup>	23.7	0.6	2.5	18.8 <sup>+</sup>	8.2	0.4	5.1	0.3	14.1
Tint (C)	2	3.7	13.9	11.1 <sup>+</sup>	8.4	2.0	7.8	5.0	2.2	0.4	5.4	0.2	9.1
Speed (D) <sup>^</sup>	(2)	-	-	-	-	-	-	-	-	-	-	-	-
error	2	-	3.7	-	0.7	-	3.9	-	0.3	-	14.3	-	41.0
Total	8	-	100	-	100	-	100	-	100	-	100	-	100

+ at least 90% confidence

\* at least 95% confidence

# at least 99% confidence

<sup>^</sup> indicates the factor that was used to generate the pooled error estimation

Table 7.14 Summary of the ANOVA for the Taguchi L9 test results on the observations (2500 rpm 16 mg/cycle)

Factor	f	THC		CO		FSN		O <sub>2</sub>		CA50		CoV(IMEP)	
		F	P (%)	F	P (%)	F	P (%)	F	P (%)	F	P (%)	F	P (%)
EGR (A)	2	7.2	61.2	14.9 <sup>+</sup>	63.7	42.2 <sup>+</sup>	84.3	121.8 <sup>#</sup>	92.0	11.6 <sup>+</sup>	84.9	1.0	27.3
Fuel Q (B)	2	1.6	13.6	3.5	14.7	3.1	6.1	4.4	3.3	0.5	3.6	0.8	2.0
Tint (C)	2	2.0	16.8	4.1	17.4	3.8	7.6	5.2	3.9	0.6	4.1	0.7	20.2
Speed (D) <sup>^</sup>	(2)	-	-	-	-	-	-	-	-	-	-	-	-
error	2	-	8.4	-	4.2	-	2.0	-	0.8	-	7.3	-	28.6
Total	8	-	100	-	100	-	100	-	100	-	100	-	100

+ at least 90% confidence

\* at least 95% confidence

# at least 99% confidence

<sup>^</sup> indicates the factor that was used to generate the pooled error estimation

The smoke numbers showed high sensitivity to the EGR rate with 95% confidence for both speeds at the intermediate load conditions. The smoke number falls rapidly with EGR rate when the combustion approaches LTC mode (as shown in Chapter 4, Figure 4.2). Thus, a small change in EGR rate may cause a large increase in smoke number. Furthermore, the intermediate load LTC showed higher smoke numbers, so that variations could be more easily resolved with the available equipment. Thus, it is reasonable to expect that the intermediate load LTC smoke emissions were more sensitive to the EGR rate variations than under the low load conditions.

For CA50 and CoV(IMEP), the significance of variances was much smaller, and the unexplained error (which included the effect of speed) was larger, than for the low load cases. This agrees with the results presented in Chapter 4, in that for the intermediate load conditions, the IMEP based combustion stability is not significantly influenced by the engine operating parameters. This is a result of the combustion being nearly fuel-rich (global equivalence ratio approaching unity). Also the engine-output power is more repeatable under these circumstances. The combustion phasing is sensitive to EGR rate, fuel injection quantity and intake manifold temperature as introduced in Chapters 4, 5 and 6. However, for the variations studied in this chapter, there may not be a dominant parameter which has statistically significant influence on the change in CA50.

## **7.4 Discussion**

The application of the Taguchi method to experiment design faces the compromise between reduced test number and loss of information. However, the most significant factors can still be identified from a significantly reduced test array.

The interactive factors were expected to be relatively insignificant as this study focused on 'small-scale transients' conditions. The individual factors were varied within very narrow ranges and showed nearly linear influences on the engine combustion and emissions where any effect was seen. Therefore, it was reasonable to expect that the interactions among the factors with small changes would be negligible. This was supported by the results from the half-factorial experiment conducted at the 1500 rpm 8 mg/cycle test condition.

For different load conditions, the engine showed different combustion and emissions behaviour. Thus, the sensitivity of LTC to the engine operating parameters showed different patterns (interactions) as a function of engine load. For the low load conditions, the LTC combustion stability was sensitive to the EGR rate and fuel injection quantity, while for the intermediate load conditions, the combustion stability was generally not sensitive to any of the parameters, primarily due to the nearly fuel-rich combustion. However, larger steps in EGR rate changes (larger than the values adopted in this chapter) significantly influenced the combustion stability for the intermediate load conditions, as shown in Chapter 4. Smoke emissions from LTC mode were especially sensitive to the EGR rate for the intermediate load cases, due to the fact that the smoke emissions fall very steeply with EGR rate for these cases.

This will have a significant implication on engine-out emissions during steady-state and transient operation.

A change of 5% in EGR rate value for LTC diesel combustion significantly influenced the THC and CO emissions. The control target of EGR rate in modern diesel engines is normally within 5% of the set point values, which includes cycle-to-cycle and cylinder-to-cylinder variations. This study suggests that the EGR rate control accuracy of 5% will not be sufficient and will need to be improved for both steady-state and transient operating conditions within LTC modes.

Small changes in fuel injection quantity showed significant influences on the LTC THC and CO emissions. Increasing the fuel injection quantity increased the fuel oxygen ratio with constant EGR rate and led to higher rates of partially oxidized fuel. These sorts of changes could also be due to injector-to-injector variations or degradation of injectors. As a result, consistency of injector design and ability for the engine control to account for long-term reduction in injector performance will be required to achieve the required level of control over LTC combustion and emissions.

Intake charge oxygen concentration is the direct influencing factor for the LTC combustion and emissions, as shown in Figure 7.3 and as introduced in Chapters 2, 3 and 4. The EGR rate controls the combustion by influencing the quantity of intake oxygen as found by Ladommatos *et al.* (2000); these findings also apply at the high EGR levels used in this study. Measurement or estimation of the intake charge oxygen concentration and use of it in engine control may be an effective method to control the engine combustion and emissions, especially for highly-sensitive LTC diesel combustion.



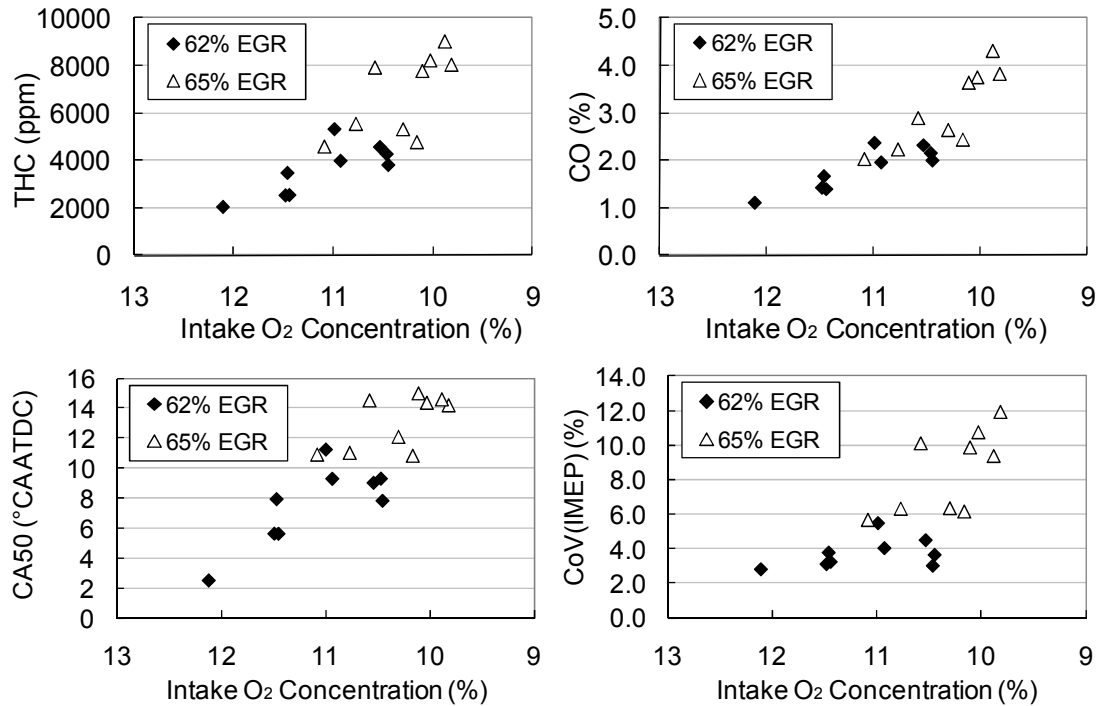


Figure 7.3 Effects of intake oxygen concentration on LTC THC and CO emissions, and CA50 and CoV(IMEP) (1500 rpm 8 mg/cycle, half fractional factorial test)

Engine intake charge oxygen concentration is dictated by EGR rate and fuel injection quantity. Under LTC mode, a small increase of oxygen concentration led to a higher combustion temperature and an increased soot formation rate. In particular, for the intermediate load conditions, the combustion temperature and equivalence ratio may be close to the boundaries where the soot forms in the  $\Phi$ - $T$  map as discussed in Section 2.4 (Akihama *et al.*, 2001). A small reduction in oxygen concentration led to significantly increased THC and CO emissions, since both the reductions in combustion temperature and air-fuel ratio led to increased flame quenching effects.

## 7.5 Conclusions

From the results presented in this chapter, the following conclusions can be made:

- 1) Emissions of THC and CO from LTC combustion and the combustion stability showed significant sensitivity to EGR rate variations at all operating conditions. An increase of 5% (i.e. 60% to 63%) in EGR rate doubled THC and CO emissions and impaired combustion stability. To realise a stable and robust LTC operation, accurate EGR rate control is essential.
- 2) LTC is less sensitive to the fuel injection quantity than to the EGR rate. The most substantial influence of this parameter was that an increase of injection quantity led

to increased THC and CO emissions due to reduced air-fuel ratio at most of the speed-load conditions tested.

3) Intake charge temperature and engine speed showed a negligible influence on the LTC combustion processes and emissions.

4) Smoke emissions showed significant sensitivity to the changes in EGR rate for the intermediate load LTC conditions. The higher combustion temperature and air-fuel ratio under this condition are likely to be close to the soot formation threshold in the  $\Phi - T$  map (Akihama *et al.*, 2001). Thus, the mid-load LTC requires more precise EGR rate control to keep the smoke emissions low.

5) Oxygen concentration in the intake charge was the decisive parameter for the LTC combustion and emissions. It is primarily controlled by EGR rate and secondarily controlled by fuel injection quantity.

6) In this study, the half fractional factorial results demonstrated that the engine operating parameters were independent of each other. The interactions among these parameters were negligible within the test arrays investigated. As a result, the Taguchi L9 method could be used as an efficient DoE tool for studying 'small-scale transients' that could have been encountered by a diesel engine operating in an LTC mode.

The results presented in this chapter demonstrate that even small variations in engine operating condition can have a significant effect on an LTC engine's performance and emissions. The sensitivity of this combustion mode to the larger variations that would be encountered during driving-cycle transients needs to be investigated. The following chapter introduces a method of conducting steady-state tests on a single-cylinder engine to represent the conditions that would be encountered by an LTC engine undergoing transient operation. These pseudo-transient operating points identified through engine transient simulation are then investigated experimentally to evaluate their impact on the combustion processes and emissions.

# Chapter 8 Pseudo-Transient Operation of an LTC Diesel Engine

## 8.1 Introduction

The characteristics of low temperature diesel combustion (LTC) at steady-state operating conditions have been evaluated in the previous chapters. However, one of the main concerns with its use in automotive applications is its ability to handle in-service transients, both between modes within the LTC regime and from LTC to conventional diesel combustion. The sensitivity of LTC to small changes in engine operating parameters was investigated in Chapter 7. However, these small changes do not represent the large scale transients which an in-service engine will encounter during driving-cycle tests. The sensitivity of LTC to these transients is the focus of this chapter.

Engine performance during transients is particularly sensitive to the performance of the air exchange system. The slow response of the engine subsystems to transient demands and the control variations from the close-coupled air-path controllers imposes severe difficulty on engine combustion and emissions control (Black *et al.*, 2007; Hagen *et al.*, 2006; Rakopoulos *et al.*, 2009a). As introduced in Section 2.3, turbo-lag is an inherent phenomenon in a turbocharged engine during transient operation. It results in a delay in the increase of boost pressure during engine transients with increasing load, which leads to reduced air-fuel-ratio and increased smoke emissions (Hagen *et al.*, 2006). The turbocharger response also influences the EGR rate, which is a function of EGR valve position and pressure gradient between exhaust and intake manifolds. Turbo-lag also leads to reduced control accuracy during the transient process due to the continuous change of turbocharger performance alongside the engine transient. In the exhaust, the existence of EGR induces more perturbations in the turbocharger control as the EGR by-passes a significant fraction of the exhaust gases from the turbocharger and reduces the exhaust temperature. Thus, it amplifies the turbo-lag effect since the turbocharger suffers from significantly reduced efficiency under this condition (Otoibe *et al.*, 2010).

In this chapter, the values of critical engine operating parameters during engine transients have been identified through engine transient modelling. These values were used to identify steady-state engine conditions that were representative of the conditions encountered during the transient. These 'pseudo-transient' operating

points allowed steady-state engine tests to be conducted to interpret the engine transient performance and emissions under conditions similar to those encountered during a transient. Transients both within LTC and between LTC and conventional diesel combustion (mode shifting) were investigated by conducting experiments on the single-cylinder research engine introduced in Chapter 3. The effects of boost pressure, fuel injection pressure and timing were evaluated for this pseudo-transient operation on the basis of improved combustion and emissions control.

## 8.2 Research Methodology

A set of new European driving-cycle (NEDC) test data, which is from a Ford Transit vehicle equipped with a four cylinder two litre Puma diesel engine, was used to analyse the behaviour of a real engine during a driving-cycle test. The NEDC driving-cycle is composed of four stages of the urban driving-cycle (ECE) followed by one stage of the extra-urban driving-cycle (EUDC). The vehicle speed during the driving-cycle is shown in Figure 8.1.

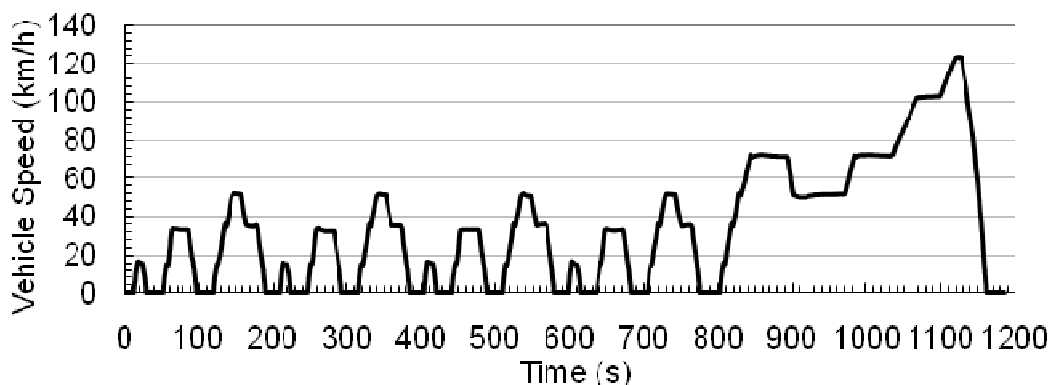


Figure 8.1 NEDC driving-cycle vehicle speed profile (DieselNet, 2010)

The previous chapters demonstrated the relation of LTC up to fuel injection quantities of 16 mg/cycle and engine speeds of 1500 rpm to 2500 rpm. These were achieved using naturally aspirated operation, as described in Section 3.1; highly flexible boost system was added to the research facility towards the end of the research programme. With the introduction of this boost system, 20 mg/cycle LTC operation was expected to be achieved. This fuelling condition generated a gross IMEP of approximately eight bar on the research engine. This arbitrarily selected 20 mg/cycle will be used as the upper limit of achievable LTC operation of the work reported here.

Parts of the NEDC driving-cycle data provided by Ford are shown in Figure 8.2. For the urban component of the driving-cycle test, the engine speed and fuelling were within the LTC region of the engine operating map (< 20 mg/cycle). The figure only

shows the final replication of the ECE component of the driving-cycle (the speed-torque profile will be the same for the other three replications of the ECE). For the extra-urban component, only about one third of the duration (< 110 seconds) of the test cycle was at fuelling conditions above the boundary for the LTC region as defined here (> 20 mg/cycle).

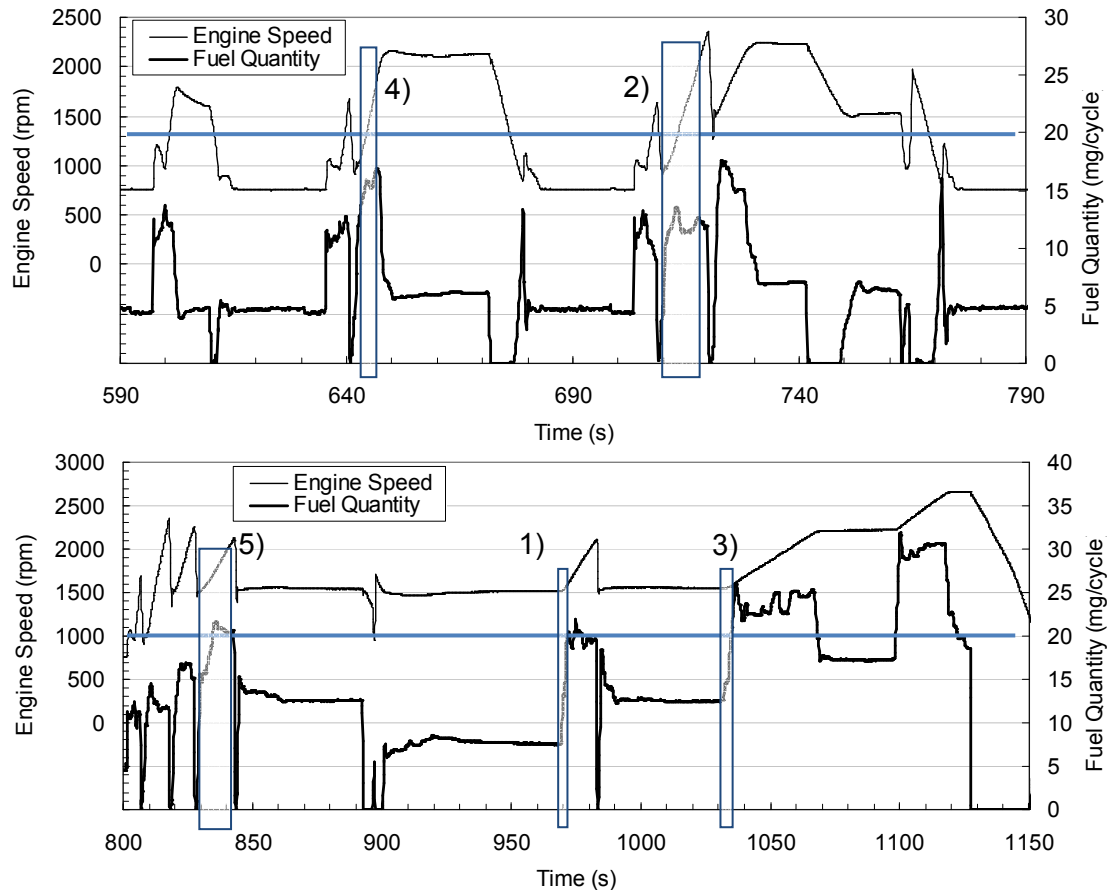


Figure 8.2 Engine fuel injection quantity and speed profile during a NEDC urban and extra urban driving-cycle test (provided by Ford). (Upper plot: the fourth replication of the ECE cycle; Lower plot: EUDC)

Critical load and speed transients were identified from the NEDC driving-cycle test data as shown in Figure 8.2. Five types of transients were identified in driving-cycle data, as labelled on the figure: 1) load transient within LTC; 2) speed transient within LTC; 3) load transient crossing combustion modes; 4) speed and load transient within LTC and 5) speed and load during a combustion mode shift. The largest speed and/or load ramps for the five types of transients are listed in Table 8.1. These represent the engine transient behaviour within the NEDC driving-cycle test. All these transients are expected to suffer from the turbo-lag effect and the slow response of

the EGR flow and mixing due to the inherent time delays within the air-exchange system.

Table 8.1 Representative transient routes

Transient Route	Engine Speed (rpm)	Fuel Q (mg/cycle)	EGR (%)	Boost Pressure (bar)	Duration (s)
1) Load transient within LTC	1500	8	60	1.03	2.1
	1500	20	48	1.10	
2) Speed transient within LTC	1000	12	52	1.03	8.9
	2300	12	52	1.24	
3) Load transient crossing combustion modes	1500	13	60	1.07	3.5
	1500	22	20	1.18	
4) Speed and load transient within LTC	1300	14	54	1.03	3.8
	2000	17	50	1.28	
5) Speed and load transient crossing combustion modes	1500	16	51	1.07	13.6
	2200	21	25	1.35	

While the five types of transients identified above are all important, some are more likely to impose greater difficulties on the engine systems. Rapid engine load transients are the main concern in diesel engine transient control; engine speed acceleration generally experiences smaller magnitudes of turbo-lag and hence is easier to control (Ford, 2010; Rakopoulos *et al.*, 2009a). Changes of engine speed also take longer than the same percent of change in load as demonstrated in Table 8.1. This slower rate of change in speed allows the turbocharger and the EGR system to follow smoother paths and leads to less significant deviations in engine operating condition than an equivalence load change. Within LTC mode, the change of EGR rate during a speed transient is also relatively smaller than that required during a load transient. The sensitivity study described in Chapter 7 also showed that changes in engine speed had relatively little influence on LTC combustion and emissions. Thus, in this study, only load transients<sup>†</sup> (number 1 and 3 in Figure 8.2 and Table 8.1) were evaluated as the speed transients showed less significant influence than the load transients on the engine operating parameters identified from engine simulation.

---

<sup>†</sup> Ford agreed with this conclusion and supported the decision to focus on load-transients. Ford Dunton Technical Centre, 17th March 2010. (Ford, 2010)

## 8.2.1 Engine modelling

A WAVE engine model\* of the Ford Puma engine used by the Transit vehicle shown in Figure 8.2 was modified to run under LTC mode for low to intermediate load conditions ( $< 20$  mg/cycle). Details of the engine model modification were described in Chapter 3. For the higher load ( $> 20$  mg/cycle) part of the engine operating map, two separate EGR strategies were used: one was operation derived from the Ford baseline model (on the order of 20% EGR) and the other was based on current high-load EGR values (on the order of 40% EGR) reported in the literature (Osada *et al.*, 2010; Shetty *et al.*, 2009). Thus, the selected transient routes with these different EGR strategies were simulated. The operating conditions identified from the transient simulation results were experimentally investigated on the single-cylinder research engine.

The modified Puma engine model was used to simulate engine operating conditions over the transient steps listed in Table 8.1. The EGR rates were adjusted to high levels for the low to intermediate load ( $< 20$  mg/cycle) part of the engine operating map. Because experimental combustion-progression data was not available, WAVE's embedded diesel Wiebe model was used to simulate the combustion process. Since the engine model is mainly used to identify the charge exchange information from the engine, the accuracy of the combustion simulation was not a critical concern. The EGR valve position and VGT position were controlled by PID controllers to get the required EGR rates and intake manifold pressures.

The test data of engine speed and load demand from the driving-cycle was fed into the model for the transient simulation. The operating conditions at the steady-state start and end points for the simulation were based on data from the Ford model combined with the optimum LTC operating strategies identified in Chapter 4 of this thesis. (The EGR rate and intake temperature were of particular importance; the injection process was of less relevance given the crudeness of the combustion model.) The initial steady state condition (starting point) for each transient was run for 250 cycles to ensure that the model had converged before the start of the transient simulation. At the end of the transient simulation, the model continued running until the final transient point reached the steady-state condition. The start and end points of EGR valve position were fixed in advance for the transient. The boost pressure was controlled using a PID controller by adjusting the VGT vane position, with

---

\* This baseline model was provided by Ford Motor Company.

predefined start- and end-point conditions. The profiles of EGR valve position and boost pressure demand followed the commanded engine speed and fuel injection quantity, as these parameters dictate EGR and boost in typical engine control systems. However, due to the delays in the response of the turbocharger and EGR valve during the transient process, the EGR rate and boost pressure at the end of the physical transient (i.e. when the engine speed and load reached the final conditions) were different from those of the steady state engine operating maps.

For the transients selected from the driving-cycle test data, the engine model was employed to simulate the engine operation throughout the processes. The model predicted the EGR rate and the boost pressure on a cycle-by-cycle basis during the transient, to accompany the known parameters including the commanded fuel injection quantity and engine speed. From this information, the engine operating condition can be fully described for each engine cycle during the transient process.

### 8.2.2 Pseudo-transient operating points

The engine conditions at any point during the transient could be defined on the basis of the engine speed, injected fuel quantity, boost air pressure and EGR level. This information was all derived either from the driving-cycle data or from the transient model results. From this information, individual points were identified that could be replicated (under steady-state conditions) on the single-cylinder research engine. These points are referred to in this work as 'pseudo-transient' points because they represent engine combustion conditions encountered during the transient but will in fact be used as inputs to steady-state tests. The selection of which points during the transient were to be investigated further as these 'pseudo-transient' points was based on those conditions which were most representative of the conditions encountered during the transient. For the purpose of the research reported here, four independent 'pseudo-transient' test points were identified for each of the transients being investigated. These points are described in Tables 8.2 and 8.3. The rationale for the selection of these points is provided below.

Table 8.2 Selected pseudo-transient points from load transient within LTC [1]

Pseudo-transient point No.	1	2	3	4
Fuel Q (mg/cycle)	8.7	13	15	20.2
EGR (%)	62	56	54	49
Fuel injection pressure (bar)	600	800	850	1100
Intake manifold temperature (°C)	40	40	50	50



Table 8.3 Selected pseudo-transient points from load transient crossing combustion modes [3]

Pseudo-transient point No.	1	2	3	4
Fuel Q (mg/cycle)	13	14.5	15.3	21
EGR (%)	59	42	35	29
Fuel injection pressure (bar)	800	900	900	1000
Intake manifold temperature (°C)	40	40	40	40

From observation of each transient profile, it was apparent that the first cycles of both the load transients suffered from severe turbo-lag with high levels of EGR. One pseudo-transient point was selected from the starting part of each transient.

Secondly, by the end of both the transients being investigated (i.e., when the fuel quantity reached the final demanded quantity), the turbocharger had started to pick up speed and the boost pressure was starting to rise. However, the boost pressure at this point was still significantly lower than the demanded value. Because this point could result in poor combustion and high emissions, the simulation results were used to define a pseudo-transient point at this final point. After the fuel injection quantity reached its target, the engine model was allowed to continue at fixed fuel quantity and speed until it reached steady state. Under these conditions, the model experienced a continuous rise or overshoot in boost pressure due to the feedback controller configuration, as would be encountered in a real engine. However, the discrepancies in boost pressure and EGR rate during this period were relatively small and were less significant than that of the selected end-of-transient pseudo-transient point.

Finally, some of the middle points of transients with high equivalence ratios were also selected to evaluate the in-transient performance and emissions of the engine.

To evaluate the potential impacts of engine operating parameters on the transients, the transient event and the corresponding pseudo-transient points were repeated using selected variations in operating parameters. For the load transient within LTC, the tests were repeated with higher boost pressures while the other operating parameters were unchanged; this aimed to evaluate the potential benefits of improved turbocharger performance on the performance of an LTC engine during transient operation.

For the transient during a combustion mode shift from LTC to conventional diesel combustion, the EGR rate of the end transient point in the conventional diesel

combustion mode may vary for different emissions control strategies. Different EGR rates of the end of transient point also influence both the performance and the control route taken for the turbocharger and EGR systems, and hence can significantly impact the engine combustion and emissions throughout the transient processes. The EGR rate for the 22 mg/cycle conventional diesel operating point (point 4 in transient (3)) in the Ford model was about 20%, which was used for the transient evaluation. An increase in conventional diesel EGR rate to 40% and a reduction in LTC EGR rate meant a smaller step change for the EGR rate during the transient process. The high EGR rate for the conventional diesel could also be used to control the NO<sub>x</sub> emissions effectively (Osada *et al.*, 2010; Shetty *et al.*, 2009). As the load was still not very high (on the order of 8 bar gross IMEP), a high EGR rate is not unreasonable for this condition. Three pseudo-transient points were selected from this process and are listed in Table 8.4. The 14.5 mg/cycle case listed in Table 8.3 was not included in this set of tests since the 15.3 mg/cycle case had quite similar operating parameters, especially when the EGR rate was always high. For all these test conditions, the fuel injection quantity was used as an indicator of load. However, in the various transient points, the high (or at least sub-optimal) EGR rate may lead to substantially reduced engine efficiency and hence lower engine brake power. In a real vehicle, this would result in an inability to follow the driving-cycle. While this limitation is acknowledged, for the purposes of this research, it was felt to be more important to hold the oxygen-fuel ratio constant (as done in previous chapters). In the future, this work could be extended to the higher fuelling conditions that would be needed to follow the vehicle driving-cycle transient.

Table 8.4 Selected pseudo-transient points from load transient crossing combustion modes [3] with high EGR rate for conventional diesel combustion

Pseudo-transient point No.	1	2	3
Fuel Q (mg/cycle)	13	15.3	21
EGR (%)	53	49	46
Fuel injection pressure (bar)	800	900	1200
Intake manifold temperature (°C)	40	40	40

### 8.2.3 Engine experiments

The pseudo-transient points identified from the transient simulation were implemented on the single-cylinder research engine to reveal the engine combustion and emissions during the transient processes. Once these baseline points were established, the boost pressure was varied to investigate whether it could be used to

improve the combustion event at the pseudo-transient operating points. Fuel injection timing and pressure were also varied along with the boost pressure at selected pseudo-transient points to evaluate potential strategies for minimizing pollutant emissions and maximizing combustion stability. The experimental parameters and the ranges investigated in this study are listed in Table 8.5. The range of timings, pressures, and boost pressures investigated were based on the driving-cycle test data provided by Ford and the engine operating parameters specified in the previous chapters.

Table 8.5 Effects of fuel injection parameters over individual pseudo-transient operating point

Fuel Quantity (mg/cycle)	EGR rate (%)	Fuel injection pressure (bar)	Fuel injection timing (°CA ATDC)	Boost pressure (bar)
20.3	46	800 to 1200	-15 to -6	1.08 to 1.18
21.5	32	800 to 1200	-3 to 3	1.18

## 8.3 Results

In this section the overall transient performance and emissions of the engine for the selected transient processes are introduced first. The effects of boost pressure on these transient processes are then evaluated. Finally, more detailed combustion and emissions studies are conducted at the individual pseudo-transient points, incorporating variations in boost pressure, fuel injection timing and pressure.

### 8.3.1 Transient within LTC

The simulation results for the engine operating parameters during a transient within LTC mode are shown in Figure 8.3. As determined in Chapter 4, the EGR rate was reduced with an increase in fuel injection quantity; however, it stayed at a relatively high level (> 50%) to realise LTC operation throughout the transient process. The response of the turbocharger was slow as the high rate of EGR bypassed more than half of the exhaust gas flow and there was not enough enthalpy in the exhaust gases to rapidly accelerate the turbine, which was operating in a lower-efficiency zone of its operating map (low flow rate, low pressure ratio). In Figure 8.3, the lines represent the simulation results while the diamonds represent the actual pseudo-transient test points studied (presented in Table 8.2). Of particular note in the figure is how the oxygen based equivalence ratio increased with the increase in fuel injection quantity; this is one of the features of LTC combustion that was shown in Chapter 4. Figure 8.3 also shows the alternative 'high boost' configuration on the right hand column.

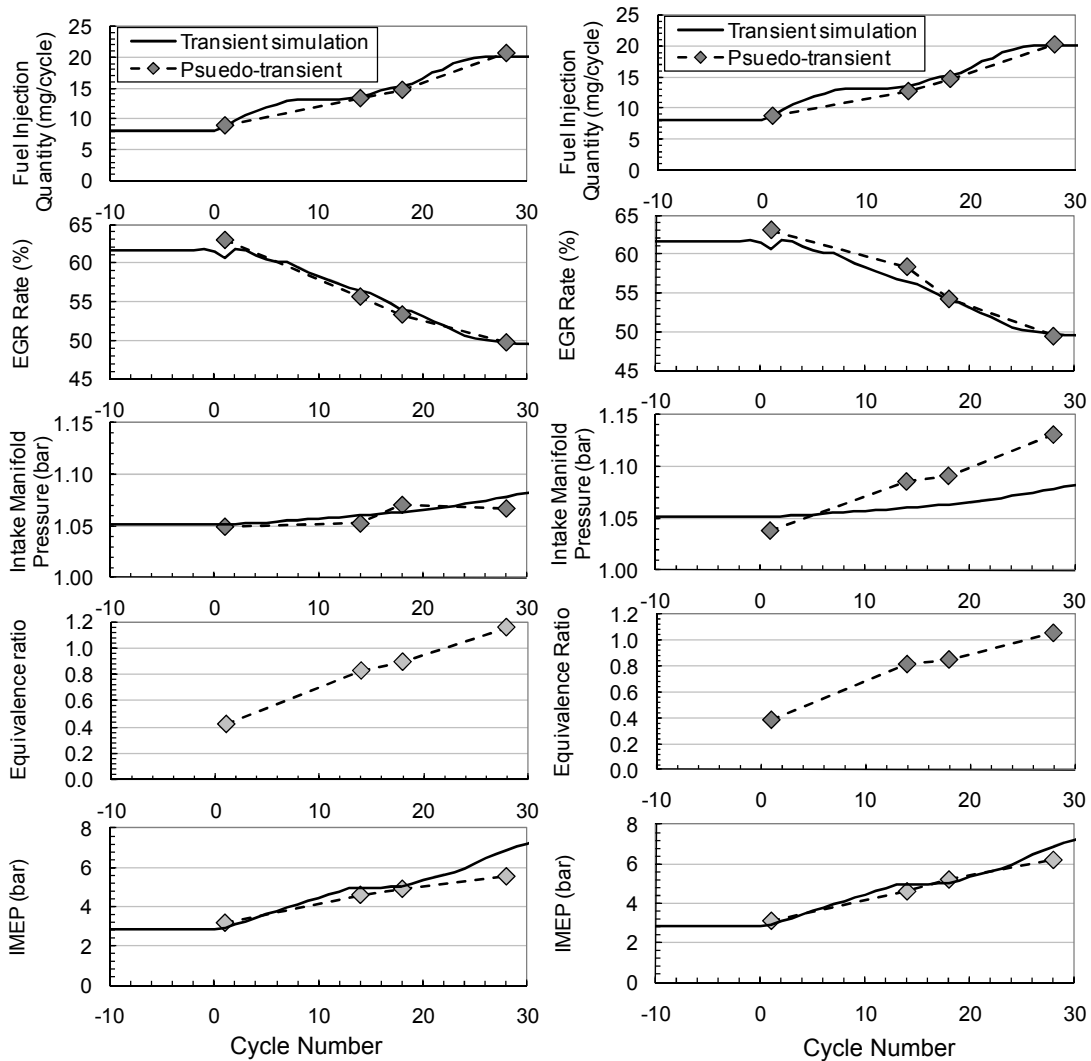


Figure 8.3 Engine operating command parameters (first three pairs) and performance for the pseudo-transient operating points during a load transient within LTC mode (right hand column with increased boost pressure)

The experimental results of the four pseudo-transient operating points of the LTC load transient (Table 8.2) are shown in the left-hand plots in Figures 8.3 and 8.4. The increase in fuel injection quantity led to higher gross IMEP and a corresponding trend in brake power, as required to follow the driving-cycle. The emissions showed similar trends as introduced in Chapter 4, with high THC and CO emissions at all points in the process. The NO<sub>x</sub> was constantly at a very low level (< 10 ppm) for all four points tested. The smoke emissions were also kept at a low level except for the 20.2 mg/cycle fuelling case. This high fuel injection quantity led to an increased overall combustion temperature which likely increased the soot formation rate. The combustion phasing was kept close to TDC by adjusting the fuel injection timing to keep the engine efficiency high and to avoid combustion instability at later

combustion phasing. The thermal efficiency of the high fuelling case was lower than those of the lower fuelling cases, which is in part attributable to the reduced combustion efficiency that is also indicated in the very high THC and CO emissions.

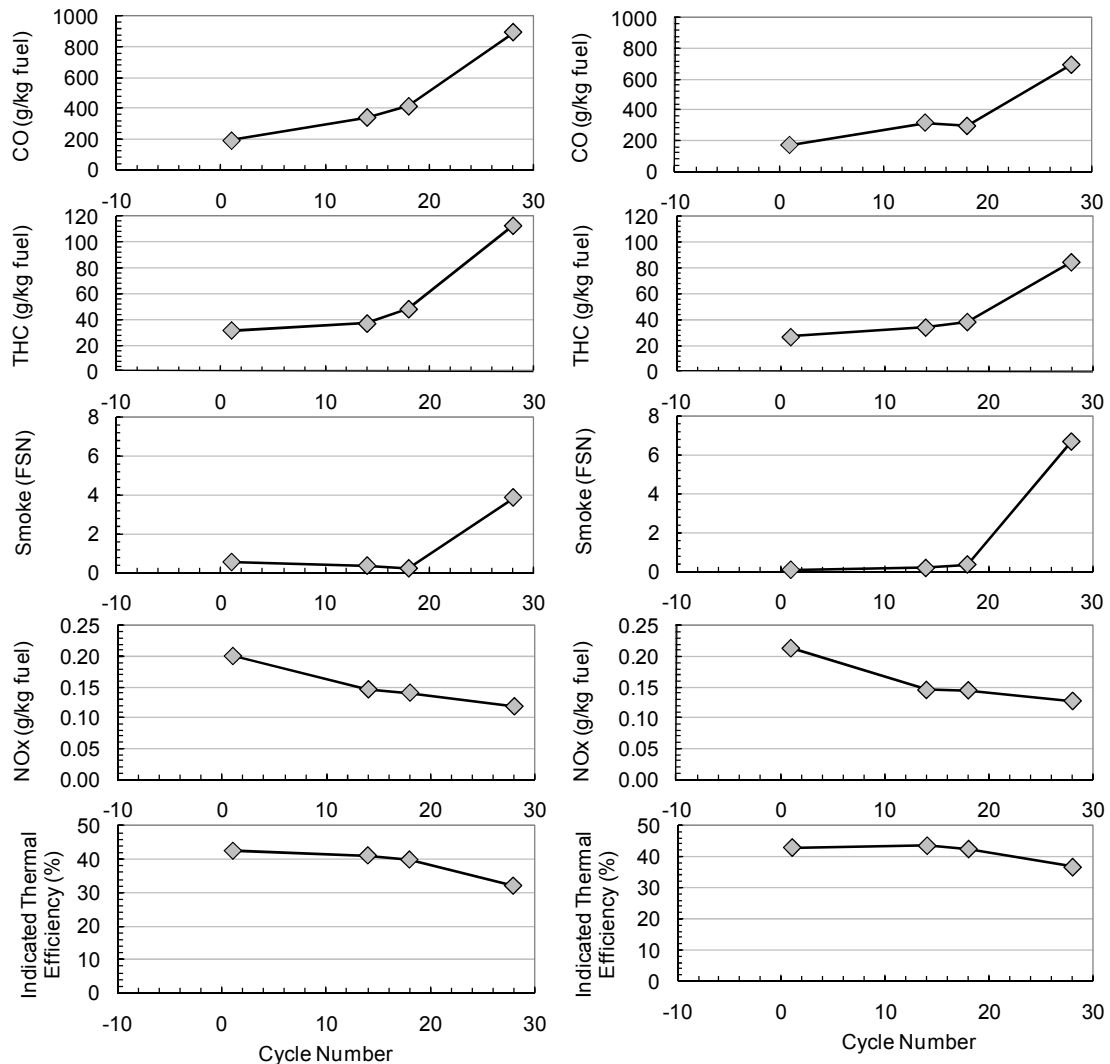


Figure 8.4 Emissions and efficiency of the pseudo-transient operating points during a load transient within LTC mode (right hand column with increased boost pressure)

## Boost pressure

Higher boost pressure for the pseudo-transient operating points was evaluated in the anticipation that advanced boost technology, such as a two-stage turbocharger, may be introduced in the future to compensate the slow response of the stock turbocharger used in the simulation. Predicting the performance of such a system, and its implications on a transient within LTC, was beyond the scope of the current work. However, to evaluate the potential that such a system could provide, the boost pressures were increased by 3-7 kPa over the baseline transient simulation results,

as shown in the right hand column in Figure 8.3. This high boost pressure resulted in a higher IMEP and reduced unburned emissions as shown in the right-hand column in Figure 8.4. This was a direct result of improved fuel conversion efficiency due to the lower oxygen equivalence ratio (leaner global mixture). Thus, both the combustion and thermal efficiency had been increased by the high boost pressure. The engine also better follows the driving-cycle engine power requirements under the high boost pressure condition.

Higher boost pressure had an insignificant influence on the smoke emissions for the first three operating points as shown in Figure 8.4, where the fuel injection quantities were less than 16 mg/cycle. For the fourth point, the high boost pressure case had a significantly higher smoke number compared to the lower boost pressure case. The increase in boost pressure reduced both the ignition delay and the peak heat release rate of the combustion, as shown in Figure 8.5. The lower peak heat release rates for the high boost pressure cases suggest that the shorter ignition delay led to a lower fraction of premixed combustion. For the lower-load case, the reduced ignition delay did not significantly increase soot emissions, as shown in Figure 8.4. For the high fuelling case, however, the combustion is expected to be occurring closer to the temperatures where the soot formation starts to increase in the  $\Phi$ -T map (Akihama *et al.*, 2001). The increased boost pressure, with its resulting smaller premixed and hence greater non-premixed, combustion event, will shift the combustion to the higher soot formation zone. This will then lead to increased smoke emissions, as observed in this case.

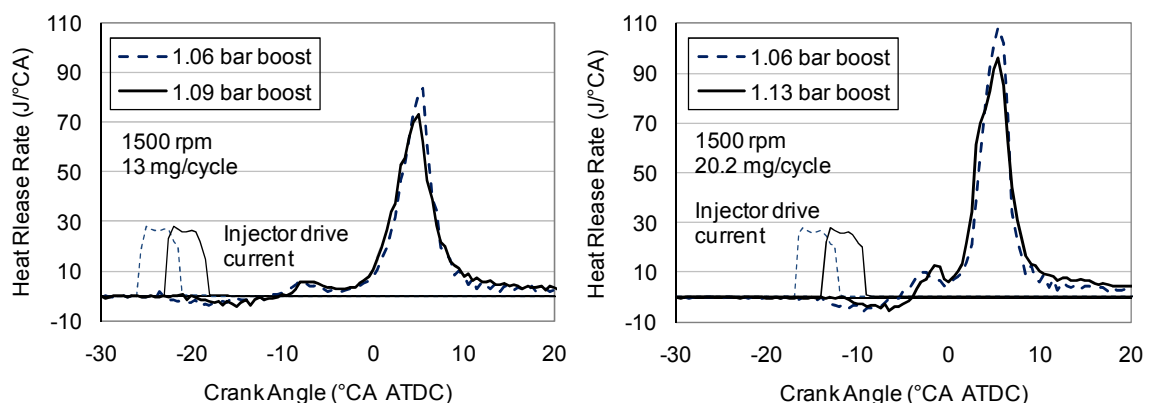


Figure 8.5 Effect of boost pressure on heat release rate for the pseudo-transient operating points (Left hand: 13 mg/cycle, 56% EGR; Right hand: 20.2 mg/cycle, 49% EGR) of LTC transient

The intermediate load LTC points showed high sensitivity to the transient process, specifically with high smoke emissions. For this condition, the overall combustion

temperature may be around the soot formation boundary, and a small variation in EGR rate or boost pressure can influence the engine-out soot emissions significantly. For the lower load LTC ( $< 16$  mg/cycle), in general the transient performance and emissions were not affected by the slow response of the turbocharger and EGR system, with emissions remaining relatively constant through these first three points in the transient event. Even in these cases, an increase in boost pressure was beneficial, as it led to improved engine thermal efficiency without elevating the smoke emissions.

The 'within LTC' transient described in this section demonstrates the difficulty encountered as the engine operating mode approaches the limits of LTC operation. To reach higher loads, the engine operating mode will have to shift from LTC to conventional diesel. During combustion mode shifting, the engine will experience even larger changes in boost pressure and EGR rate. A detailed investigation of the transient from LTC to conventional diesel combustion modes will be introduced in the following section.

### **8.3.2 Transient during combustion mode shifting**

For the transients during combustion mode shifting, two types of conventional diesel combustion configurations were used as the end-point in the simulation as introduced in Section 8.2. Both conditions had a fuelling rate of 22 mg/cycle; the variation was in EGR rate, with one test being conducted with a relatively low EGR rate (around 25%, derived from the baseline Puma engine model) and the other having a higher EGR rate of 40%. For the low-EGR point, NO<sub>x</sub> emissions were lower than non-EGR operation but were not as low as the nearly zero level in LTC mode, while the smoke emissions were relatively high. At the higher EGR conditions, the NO<sub>x</sub> emissions were reduced to nearly zero but the smoke emissions were increased further.

For the low EGR conventional diesel combustion route, the step reduction of EGR rate led to an increase in boost pressure and a lower equivalence ratio during the transient process, as shown in the left hand column of Figure 8.6. Because the transient involved a rapid change in fuelling, the EGR system response was to quickly close the EGR valve. This in turn resulted in a rapid reduction in the EGR rate to attempt to provide sufficient fresh air to burn the extra fuel being added. The rapid drop in EGR resulted in the combustion mode transitioning into a conventional diesel regime at the second point of the test, where the fuel injection quantity was 14.5 mg/cycle. This fuelling would normally still fall in the region of LTC operation mode

under steady-state operation of the engine. The emissions, shown in Figure 8.7, behaved as would be expected; the NO<sub>x</sub> and smoke emissions increased significantly, while the CO and THC were substantially reduced. These results are fully consistent with moderate-EGR (non-LTC) operations at similar conditions as shown in Section 4.3.

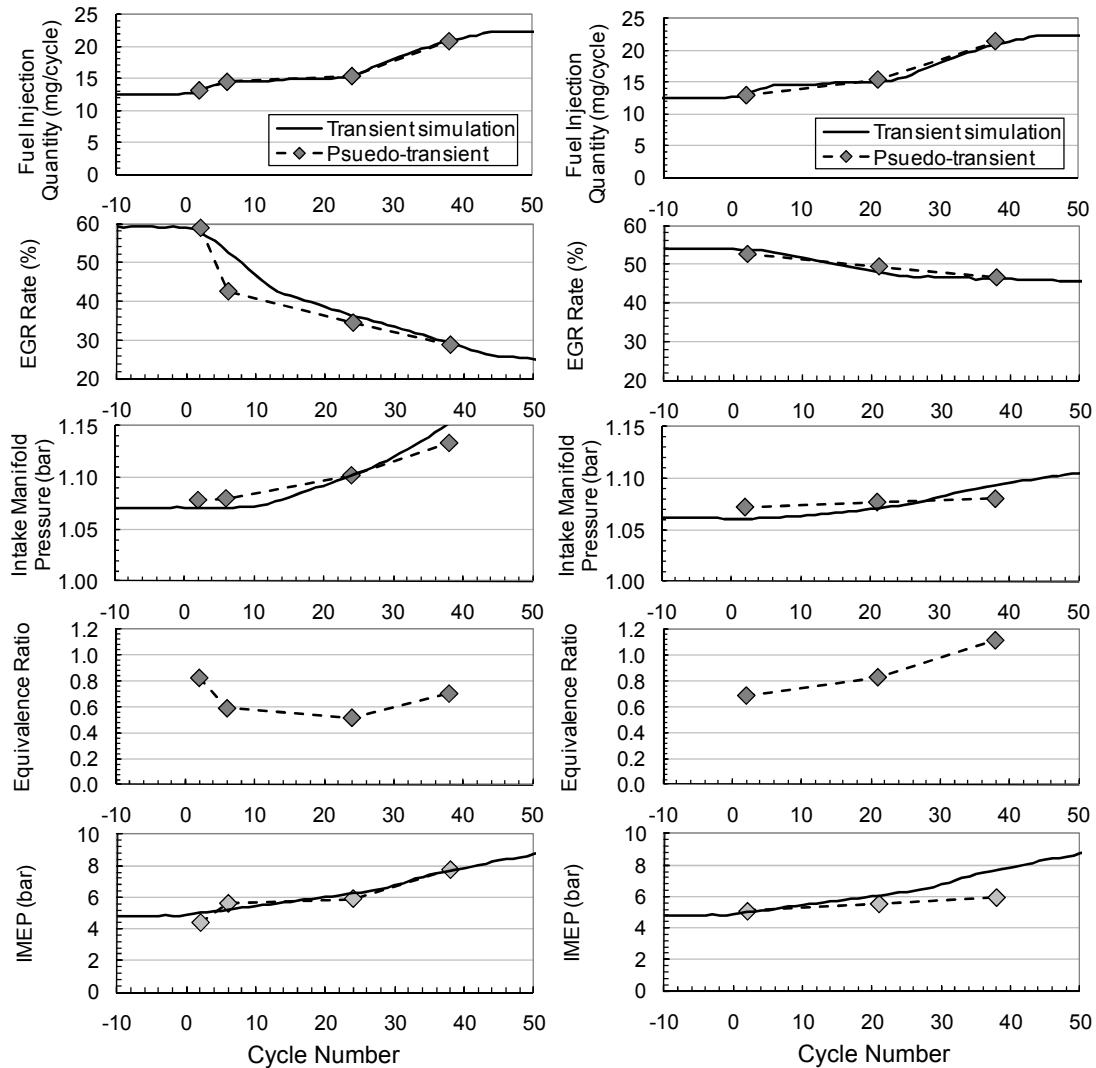


Figure 8.6 Engine operating parameters and performance for the pseudo-transient operating points during a load transient that involves a combustion mode (Left column: low EGR rate for conventional diesel; Right column: high EGR rate for conventional diesel)

For the 'high EGR' end-state case, the transient simulation demonstrated a smoother reduction in EGR rate and a slower increase in the boost pressure than the 'low EGR' end-state case, as shown in the right hand column of Figure 8.6. The high EGR rate at the end of the transient shifted the turbocharger into a lower-efficiency zone, causing a slower increase in the boost pressure. The oxygen based equivalence ratio increased during the transient process due to the low boost pressure and high level



of EGR. The combustion stayed in the LTC mode (as shown in right hand column of the Figure 8.7, with low NO<sub>x</sub> and low smoke emissions) until the fuel injection quantity was at 15.3 mg/cycle, the second pseudo-transient point of the transient route. When the fuel injection quantity was increased to 22 mg/cycle, the smoke emissions increased significantly, indicating that the combustion had transitioned into a high-EGR conventional diesel combustion mode. The high EGR rates throughout the transient route kept the NO<sub>x</sub> emissions at near-zero levels. Due to the relatively high equivalent ratios in this transient, THC and CO emissions were significantly higher than for the low EGR conventional diesel combustion transient route discussed previously and shown in the left hand column of the figure. However, efficiency was significantly lower.

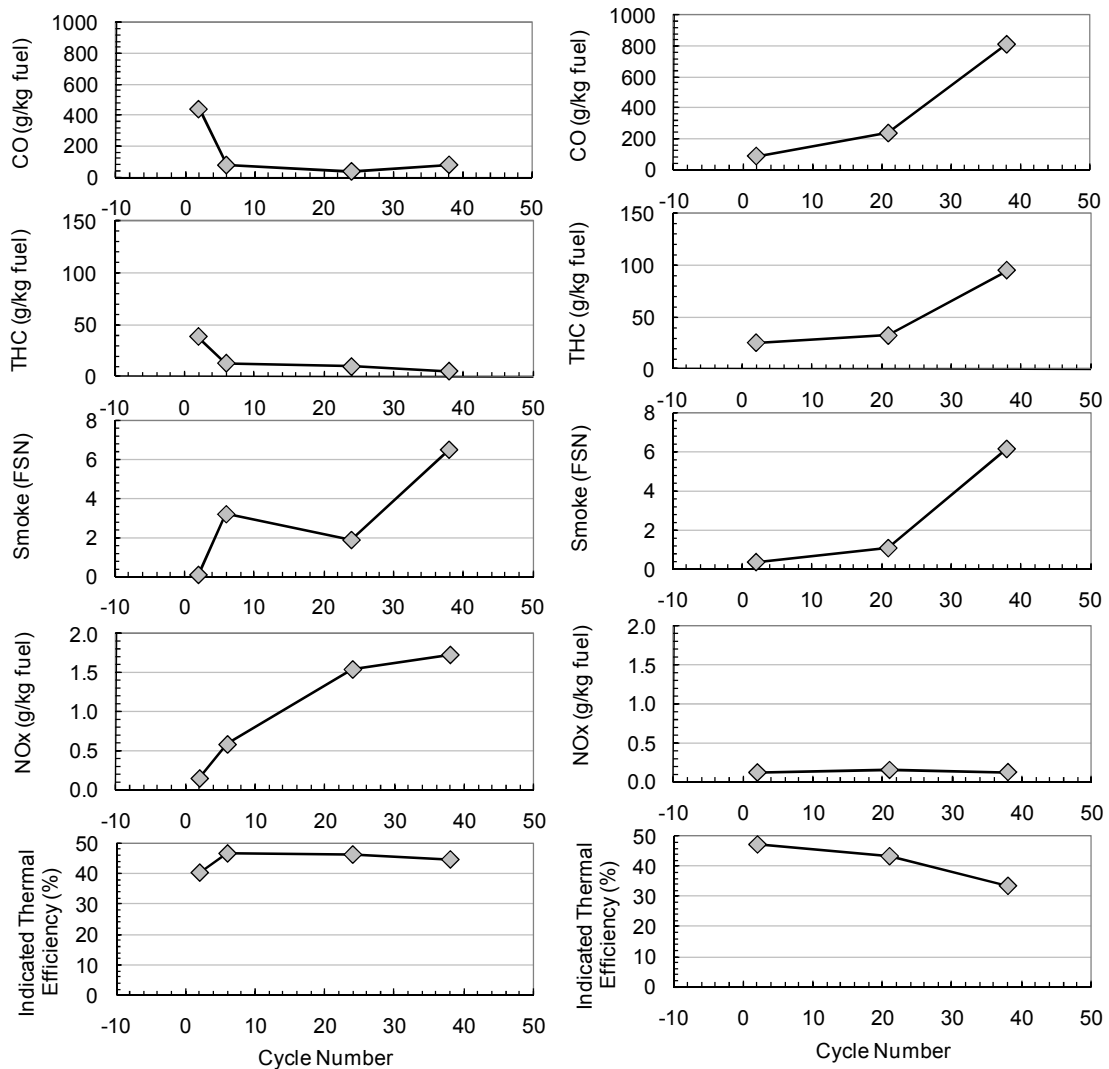


Figure 8.7 Emissions and efficiency of the pseudo-transient operating points during a load transient that involves a combustion mode (Left column: low EGR rate for conventional diesel; Right column: high EGR rate for conventional diesel)

The increase in IMEP was slower for the high EGR transient path than for the low EGR route described earlier. The low boost pressure and the high levels of EGR resulted in high equivalence ratio, leading to incomplete combustion, and hence reduced efficiency and lower engine power (for the same fuel injection quantity). This slow rate of power rise, due to the very low combustion efficiency, would significantly impair the engine's ability to follow the demanded transient. As the overall mixture was stoichiometric, a simple addition of more fuel would not generate a significant increase in power. As a result, different methods were investigated in an attempt to increase the engine power during the transient. The most feasible one was to assume that the boost pressure could be increased (either through a more advanced turbocharging system or optimisation for LTC operation). As a result, the high-EGR end point tests were repeated using increased boost pressures.

### **Boost pressure**

An increase in boost pressure for the pseudo-transient points 2 and 3 of the high-EGR transient route was successful in increasing the gross IMEP, as shown in Figure 8.8. The fuel injection timing was retarded for the high boost pressure cases to restrict the peak cylinder pressure rise rate and to maintain the combustion phasing around 5°CA ATDC. The ignition delay was reduced significantly with increased boost pressure, as shown by the heat release rates in Figure 8.9. The reduced global equivalence ratio by high boost pressure led to lower THC and CO emissions, while the NO<sub>x</sub> emissions were insignificantly affected, as shown in Figure 8.8. However, the smoke emissions were increased significantly by the high boost pressure. The reduction in ignition delay with the increased boost pressure likely led to higher local equivalence ratios due to less time available for mixing, and to higher combustion temperatures, both of which enhanced the soot formation process. The high EGR rate will have suppressed the soot oxidation, leading to the net increase in smoke number shown in Figure 8.8. Similar effects have been shown in the literature (Idicheria *et al.*, 2005).

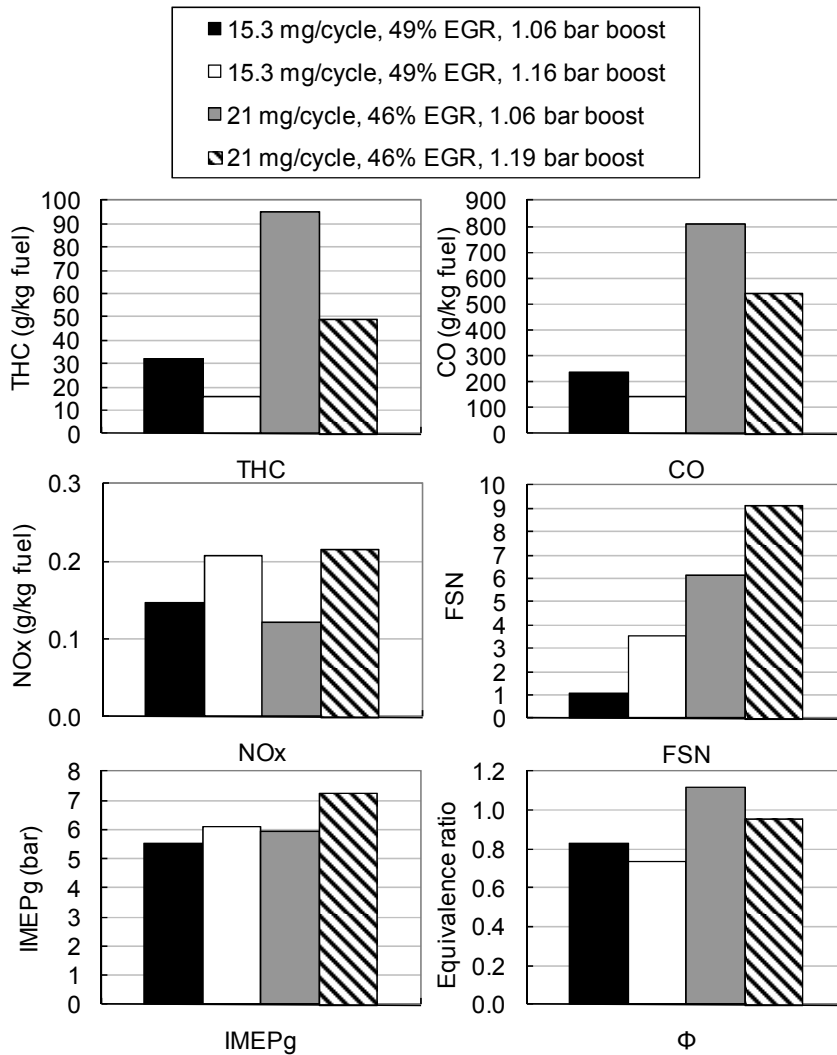


Figure 8.8 Effect of boost pressure on engine emissions and performance for the pseudo-transient points during a combustion mode shifting transient (15.3 mg/cycle, EGR 49%; 21 mg/cycle, EGR 46%)

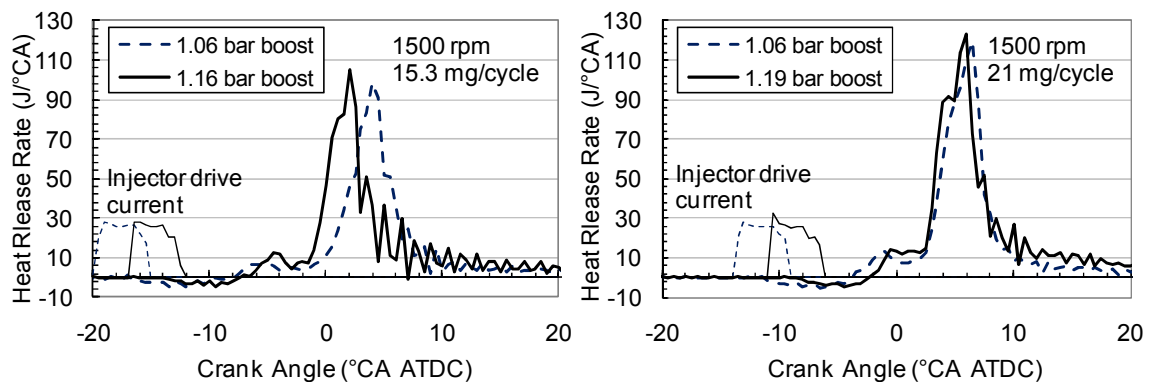


Figure 8.9 Effect of boost pressure on heat release rate for the pseudo-transient points (15.3 mg/cycle, EGR 49%; 21 mg/cycle, 46% EGR) of for points 2 and 3 of the combustion mode shift transient

The high fuelling pseudo-transient points from both the within-LTC transient (Section 8.3.1) and the combustion mode shift transients (Section 8.3.2) experienced high smoke emissions. Increasing the boost pressure resulted in increased smoke emissions, rather than reducing them as would have been expected for low EGR cases (Aoyagi *et al.*, 2006). These results demonstrate that improved boost pressure will not, on its own, make these transients more acceptable from an emissions viewpoint. To further investigate potential emissions-control techniques, a series of tests were carried out where the injection parameters and boost pressures were varied simultaneously. Because of the large number of tests required, these investigations were conducted at selected pseudo-transient points, as discussed in the experimental methodology section of this chapter (Section 8.2.3).

### **8.3.3 Effects of fuel injection parameters on high-EGR pseudo-transient points**

Reducing the smoke emissions from the pseudo-transient points was especially important for the higher load parts of the transient, given that these were the points with higher smoke emissions (as shown in Figures 8.4 and 8.7). Two injection process variables, fuel injection timing and pressure were investigated to identify the potential control strategies to reduce emissions. These two were selected on the grounds that they can respond quickly to demands from the engine ECU. The effects of these parameters were evaluated at different boost pressures. An operating condition which is close to the third transient point in the mode-shift transient (3) with the high EGR end-state (discussed in Section 8.3.2) was selected for this detailed assessment (1500 rpm, 20.3 mg/cycle, 1.08 bar boost, 46% EGR rate). This operating condition was selected because it exhibited high smoke emissions and low thermal efficiency in the baseline conditions, as shown in Figure 8.7. To cover the widest range of injection timings, the fuel injection timing was advanced until the cylinder pressure rise rate reached the 10 bar/°CA limit, and it was retarded until misfire started to occur. The fuel injection pressure was varied in the range of 800 bar to 1200 bar.

#### **Fuel injection timing**

Changes in the fuel injection timing and boost pressure significantly influenced the engine-out emissions. Retarded injection timing reduced the smoke emissions significantly for the high fuelling pseudo-transient point as shown in Figure 8.10. For the later fuel injection timings, increased boost pressure reduced the smoke

emissions further, while for the early fuel injection case, the higher boost pressure increased the smoke number. The NO<sub>x</sub> emissions were at low levels and were not significantly influenced by the boost pressure or the fuel injection timing. The THC and CO emissions were reduced for the high boost pressure cases. The increase in oxygen quantity during combustion improved the combustion efficiency. For the 12°CA ATDC fuel injection timing cases, the THC and CO emissions reached the minimum point, showing a trade-off with the smoke emissions. Both earlier and later fuel injection timing caused a significant increase in THC and CO emissions for both boost pressures, although the increase was much larger for the lower boost pressure case. As stated in Chapter 4, fuel impingement may contribute to the rise in emissions for early fuel injection timings. The increase in boost pressure led to a higher charge density, which will have reduced the fuel penetration length (Pickett *et al.*, 2009). This in turn may have reduced the contribution of fuel impingement to the increased THC and CO emissions. The increased oxygen content in the charge may also have improved the oxidation of the THC and CO formed by the impingement fuel.

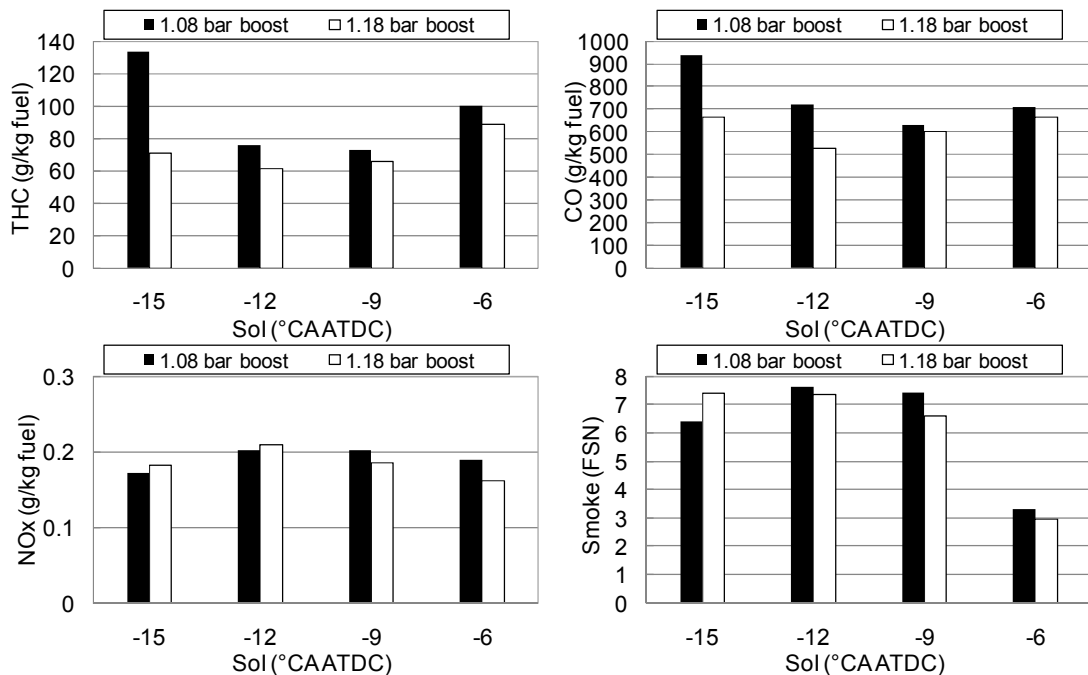


Figure 8.10 Effect of Sol and boost pressure on the pseudo-transient point emissions (20.3 mg/cycle, EGR 46%, fuel injection pressure 1200 bar)

The ignition delay was reduced and then increased with retarded fuel injection timing as shown in Figure 8.11. The trend of ignition delay correlates with the smoke emissions, following the trend that a short ignition delay leads to increased smoke emissions (Blanquart *et al.*, 2009; Heywood, 1988), as shown in Figure 8.10. An

increase in boost pressure reduced the ignition delay for all the fuel timings. The CA50 was delayed by the later fuel injection timing (as expected) and was advanced by increased boost pressure. The high boost pressure enhanced the combustion process, which in turn reduced the engine-out THC and CO emissions due to the increased oxygen availability.

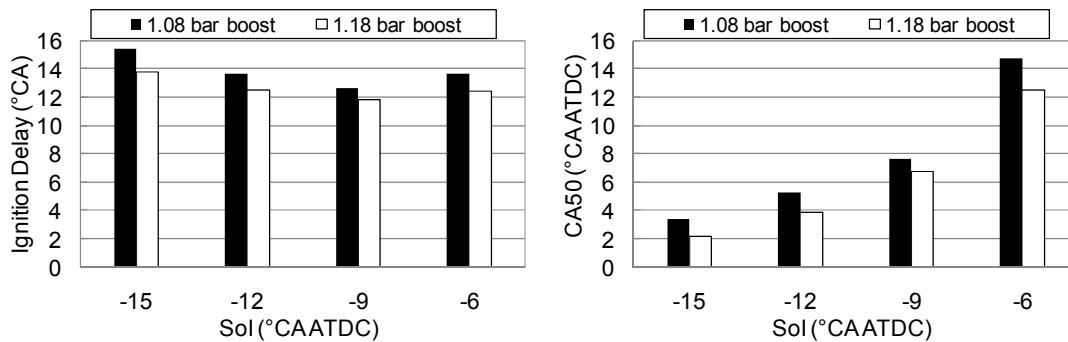


Figure 8.11 Effect of Sol and boost pressure on the pseudo-transient point ignition delay and CA50 (20.3 mg/cycle, EGR 46%, fuel injection pressure 1200 bar)

The advanced combustion phasing reduced combustion by-product emissions (improved combustion efficiency) for the higher boost pressure (Figure 8.10) and led to increased engine thermal efficiency, as shown in Figure 8.12. Therefore, for constant injected fuel mass, gross IMEP was increased in the higher boost pressure cases. This will lead directly to increased engine brake torque and a better ability to follow the demanded driving-cycle. However, the delay in fuel injection timing delayed the combustion phasing more significantly than the boost pressure could advance it, as shown in Figure 8.11. Thus, the increase in boost pressure compensated for only a part of the lost efficiency caused by the retarded fuel injection timing. As the results are based on gross-indicated values, and as the specific impact of the higher boost pressure on the exhaust back-pressure were not known, it is not possible to identify the exact effect on the pumping work of the higher boost pressure. This could have a further impact on the brake power output of the engine.

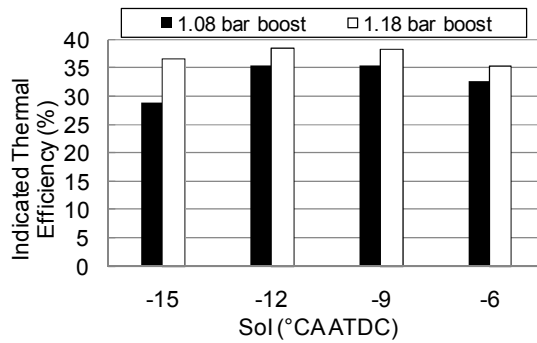


Figure 8.12 Effect of Sol and boost pressure on the pseudo-transient point indicated thermal efficiency (20.3 mg/cycle, EGR 46%, fuel injection pressure 1200 bar)

Under the low boost condition, retarded fuel injection timing delayed the combustion event and reduced the peak heat release rate significantly as shown in Figure 8.13. The increased ignition delay and reduced heat release rate indicate that the combustion process was relatively slow; this probably contributed to the reduced soot formation rate. An increase in boost pressure advanced the heat release profile and increased the peak heat release rate. However, the combustion phasing was still later and the peak heat release rate was lower than for the early fuelling case.

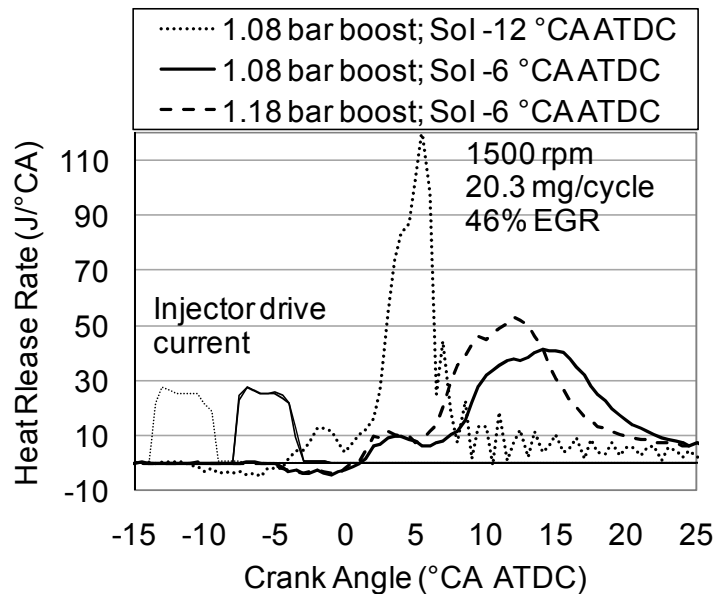


Figure 8.13 Effect of Sol and boost pressure on the pseudo-transient point heat release rate (20.3 mg/cycle, EGR 46%, fuel injection pressure 1200 bar)

### Fuel injection pressure

Fuel injection pressure showed less significant influence on smoke emissions than did the fuel injection timing. However, a combination of the reduced fuel injection pressure and increased boost pressure led to reduced smoke number, as shown in

Figure 8.14. The NOx emissions were insignificantly affected by the fuel injection pressure and boost pressure changes. An increase in fuel injection pressure led to reduced THC and CO emissions, and an increase in boost pressure reduced the emissions further. The increase in fuel injection pressure improved the fuel atomisation and mixing. This may have enhanced the combustion process with reduced THC and CO emissions. The reduced local equivalence ratio due to better mixing likely reduced the soot formation rate, while the enhanced combustion may have led to increased combustion temperature which could increase the soot formation rate. These competing effects resulted in reduced smoke number for the low fuel injection pressure high boost case, and increased smoke number for the high fuel injection pressure low boost case.

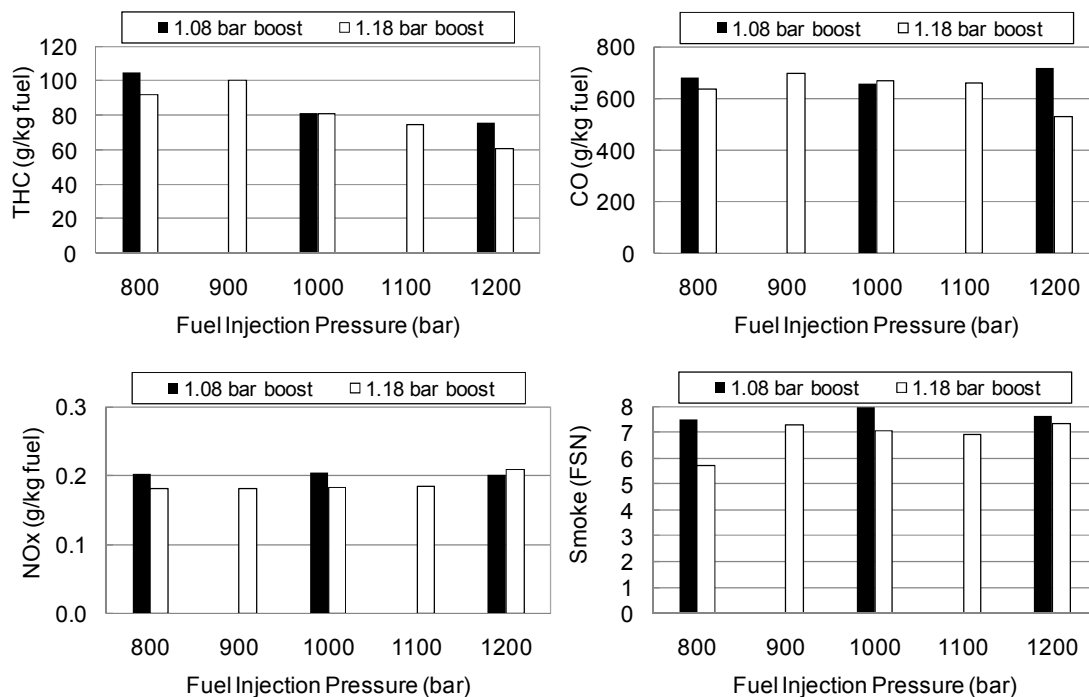


Figure 8.14 Effect of fuel injection pressure and boost pressure on the pseudo-transient point emissions (20.3 mg/cycle, EGR 46%, Sol -12°C ATDC)

Lower fuel injection pressure led to longer ignition delay and retarded combustion phasing as shown in Figure 8.15. The increased ignition delay and retarded combustion phasing led to longer mixing time and lower combustion peak heat release rate, both of which may have led to a reduction in soot formation rate. However, the extended ignition delay may have caused fuel over-mixing and led to higher THC emissions. The increase in boost pressure advanced the whole combustion process for the different fuel injection pressures. However, for the low injection pressure conditions, the ignition delay and CA50 showed less sensitivity to



the change of boost pressure. The poor fuel mixing due to the low fuel injection pressure may have reduced the effects of the boost pressure on advancing the combustion process.

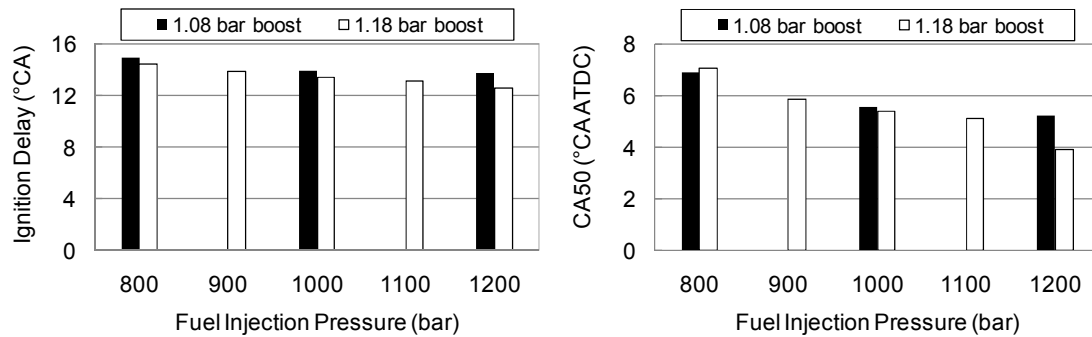


Figure 8.15 Effect of fuel injection pressure and boost pressure on the pseudo-transient point ignition delay and CA50 (20.3 mg/cycle, EGR 46%, Sol -12°CA ATDC)

The engine power output represented by gross IMEP was lower for the low fuel injection pressure cases. The retarded combustion phasing and reduced combustion efficiency shown in Figure 8.14 led to a reduction in thermal efficiency as shown in Figure 8.16. An increase in boost pressure advanced the combustion phasing and reduced the THC emissions, which resulted in improved combustion efficiency and hence higher thermal efficiency.

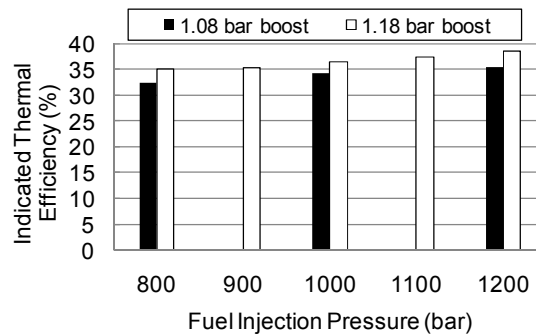


Figure 8.16 Effect of fuel injection pressure and boost pressure on the pseudo-transient point indicated thermal efficiency (20.3 mg/cycle, EGR 46%, Sol -12°CA ATDC)

Reduced fuel injection pressure delayed the combustion event and reduced the peak heat release rate, as shown in Figure 8.17. An increase in boost pressure may have resulted in a lower local equivalence ratio which reduced the soot formation rate. The improved availability of oxygen due to the lower global equivalence ratio led to a longer combustion duration as shown in the figure; it is expected that this would increase the soot oxidation rate, resulting in a reduction in net soot emissions.

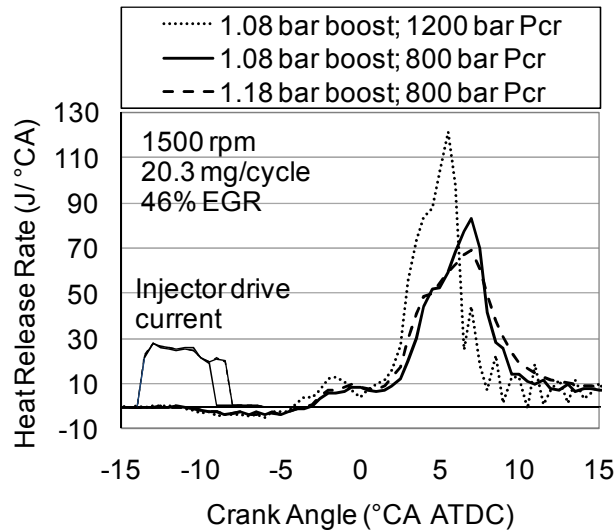


Figure 8.17 Effect of fuel injection pressure and boost pressure on the pseudo-transient point (20.3 mg/cycle, EGR 46%, Sol -12°CA ATDC) heat release rate (Pcr: fuel common rail pressure)

### 8.3.4 Effects of fuel injection parameters on low-EGR pseudo-transient point

As discussed in Section 8.3.2, the mode-crossing transient was conducted under both high- and low-EGR rate end states. The impacts of fuel injection parameters on the high-EGR end-state case were discussed in the preceding section. This section focuses on the impacts of these same parameters on an operating condition which is close to the fourth transient point in the low EGR transient route (Section 8.3.2) (1500 rpm, 21.5 mg/cycle, 1.18 bar boost, 32% EGR rate). This point was selected because the engine emitted high levels of smoke emissions under this pseudo-transient condition. As in the previous section, the fuel injection timing and pressure were varied for this case to evaluate their influence on the engine combustion and emissions. However, the intake manifold pressure was not varied due to the limited time and resources allocated. The range of fuel injection timings were based on the most advanced timing which the pressure rise rate was below the 10 bar/°CA limit, and the most retarded timing until misfire started to occur. This resulted in a range of injection timings from -3 to 3°CA ATDC. To be consistent with the results presented earlier in this thesis (Sections 4.33, 8.33), the fuel injection pressure was varied over a range from 800 bar to 1200 bar.

Retarding fuel injection timing from -3 to 3°CA ATDC reduced the smoke number from 8.1 FSN to 6.2 FSN, as shown in Figure 8.18. The NO<sub>x</sub> and CO were also reduced, while the THC emissions increased with the retarded fuel injection. The

ignition delay increased due to the retarded fuel injection timing. The CA50 was delayed more significantly than the delay in injection timing, as shown in Figure 8.19. This was a result of a longer ignition delay and slower combustion for the later fuel injection cases. The extended ignition delay and retarded combustion phasing resulted in reduced soot formation rate due to the improvement in mixing and the reduced combustion temperature. The late combustion event also led to reduced thermal efficiency as shown in Figure 8.20. This results in reduced engine brake torque and a higher fuel injection quantity demand to follow the driving-cycle. In this case, because the oxygen based equivalence ratio is relatively low, an increase in fuelling should result in higher power from the engine.

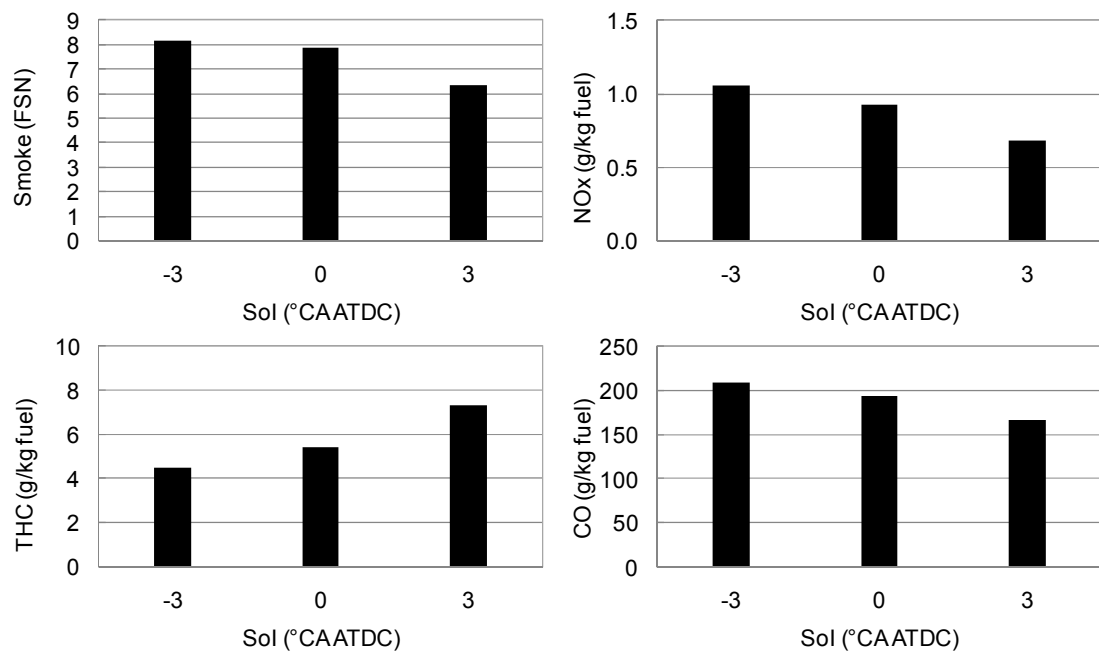


Figure 8.18 Effect of Sol on the low EGR pseudo-transient point emissions (21.5 mg/cycle, 32% EGR, fuel injection pressure 1200 bar, 1.18 bar boost)

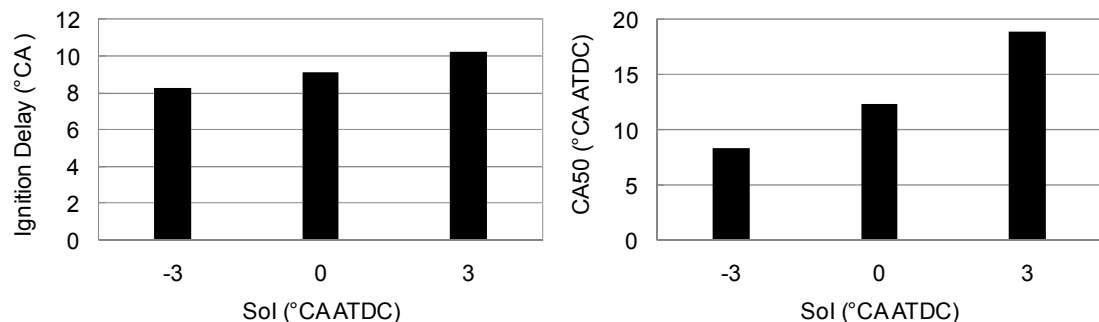


Figure 8.19 Effect of Sol on the low EGR pseudo-transient point ignition delay and CA50 (21.5 mg/cycle, 32% EGR, fuel injection pressure 1200 bar, 1.18 bar boost)

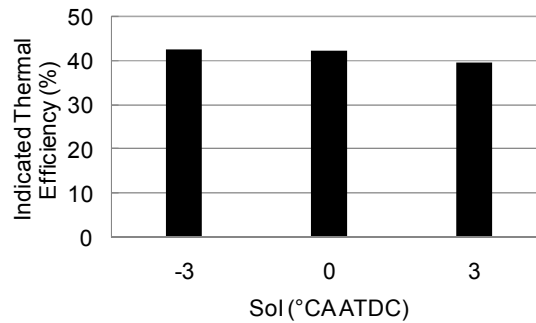


Figure 8.20 Effect of Sol on the low EGR pseudo-transient point indicated thermal efficiency (21.5 mg/cycle, 32% EGR, fuel injection pressure 1200 bar, 1.18 bar boost)

The 0°CA ATDC timing shows higher thermal efficiency with relatively lower emissions as shown in Figures 8.18 and 8.20. Thus this timing was used as the baseline point for the fuel injection pressure variations. In this case, the fuel injection pressure had an insignificant influence on smoke emissions, as shown in Figure 8.21. With increased fuel injection pressure, NO<sub>x</sub> and CO emissions were reduced, while the THC emissions reached a maximum at 1000 bar. An increase in fuel injection pressure led to reduced ignition delay and advanced combustion phasing as shown in Figure 8.22. The shorter ignition delay reduced the mixing time while the higher injection pressure improved the mixing intensity. These two features had opposite influences on soot formation and may have cancelled each other out, explaining why no significant difference in smoke emissions was observed. The thermal efficiency was increased by the high fuel injection pressures, because of the more advanced combustion phasing, as shown in Figure 8.23.

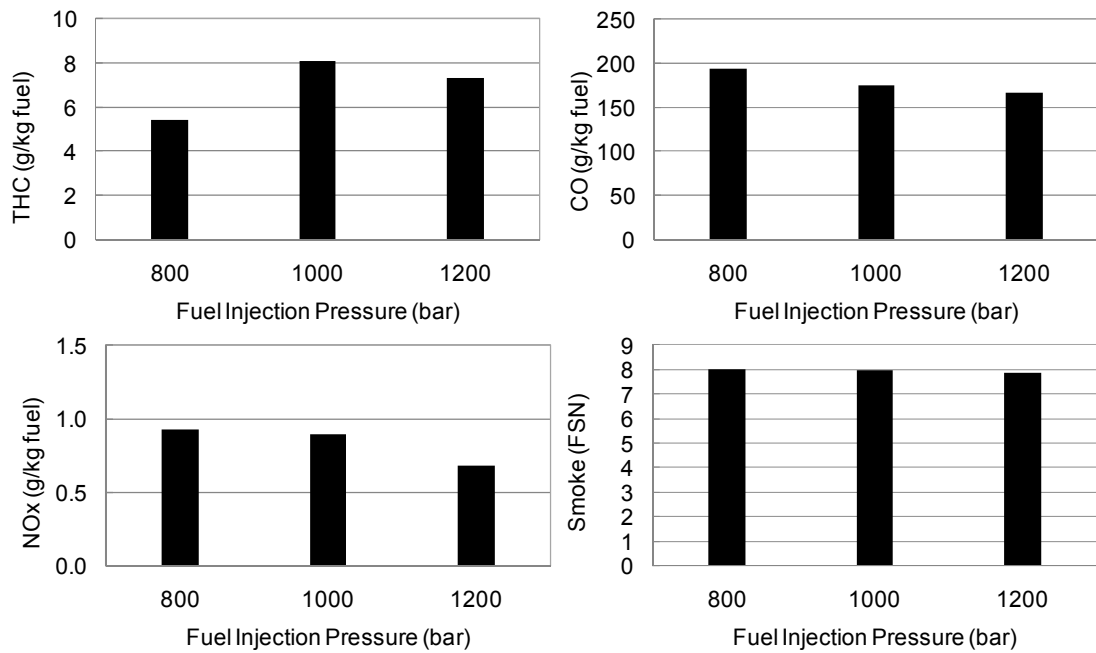


Figure 8.21 Effect of fuel injection pressure on the low EGR pseudo-transient point emissions (21.5 mg/cycle, 32% EGR, Sol 0°CA ATDC, 1.18 bar boost)

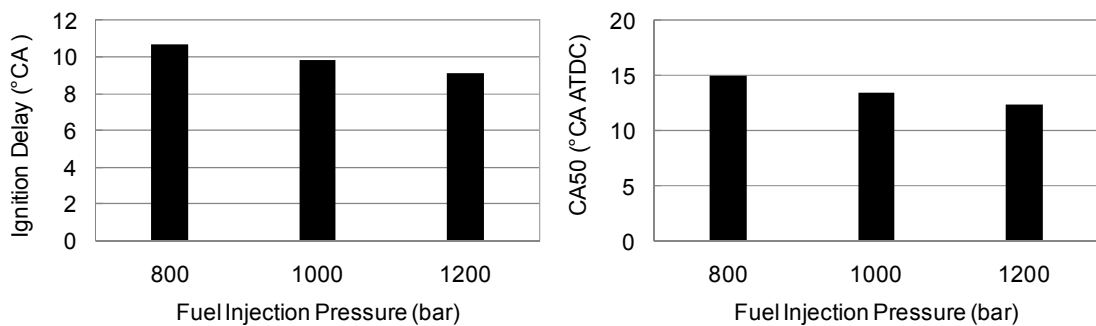


Figure 8.22 Effect of fuel injection pressure on the low EGR pseudo-transient point ignition delay and CA50 (21.5 mg/cycle, 32% EGR, Sol 0°CA ATDC, 1.18 bar boost)

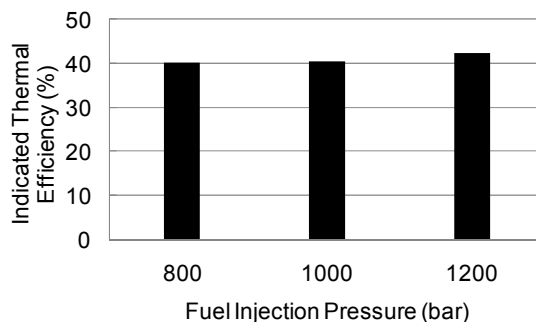


Figure 8.23 Effect of fuel injection pressure on the Low EGR pseudo-transient point indicated thermal efficiency (21.5 mg/cycle, 32% EGR, Sol 0°CA ATDC, 1.18 bar boost)

At this condition, fuel injection timing had a more significant influence on the heat release rate than the fuel injection pressure. Retarded fuel injection and reduced fuel injection pressure led to a later combustion event and a lower peak heat release rate

as shown in Figure 8.24. These resulted in a longer ignition delay and slower combustion progression, which reduced the smoke and NO<sub>x</sub> emissions as shown in Figures 8.18 and 8.21. The combustion phasing and emissions were more significantly influenced by the fuel injection timing than by the fuel injection pressure. This is consistent with the phenomenon shown in the heat release rate profiles. A reduction in fuel injection pressure from 1200 bar to 800 bar led to a 2.5 °CA delay in CA50, and a small reduction in smoke number. Retarding the fuel injection by 6 °CA led to a delay of the CA50 by 10.5 °CA, and a smoke number reduction of 1.9 FSN. This suggests that a delay in fuel injection timing will be a more effective measure to reduce the engine emissions for this pseudo-transient point. An increase in the fuel injection pressure could potentially somewhat compensate for the efficiency penalty induced by the later combustion phasing.

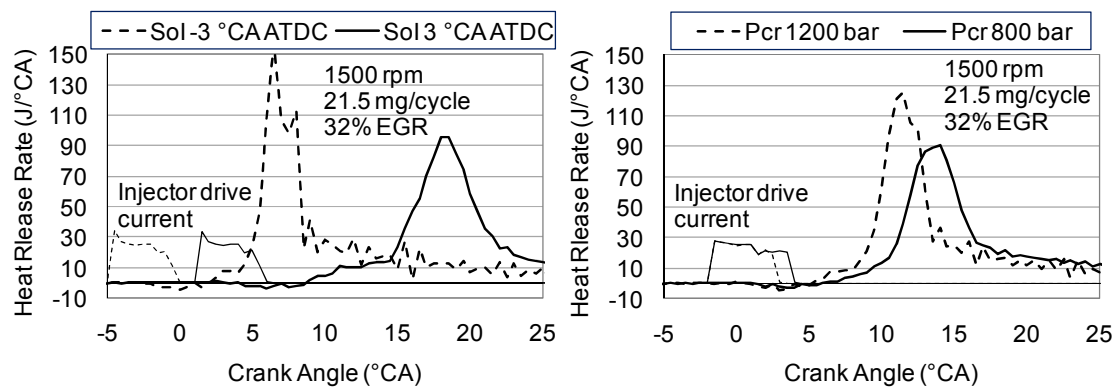


Figure 8.24 Effect of Sol and fuel injection pressure on the low EGR pseudo-transient point heat release rate (21.5 mg/cycle, 32% EGR, fuel injection pressure 1200 bar, Sol 0°CA ATDC, 1.18 bar boost) (Pcr - fuel common rail pressure)

## 8.4 Discussion

The transient events simulated in this study covered the largest load ramp for a representative engine in a vehicle following the NEDC driving-cycle for both within-LTC and combustion mode shift transients. The pseudo-transient points selected were able to represent the general operating conditions which a LTC-conventional diesel combustion 'dual-mode' engine will encounter during transient operation. The knowledge gained during the experimental study for the pseudo-transient points can be implemented on the other transient events as all the transient events have similar EGR valve and turbocharger behaviours.

With the conventional turbocharging system, the boost pressure was significantly affected by the high EGR rate of LTC. This was expected, given that the

turbocharger was not sized for such high EGR levels. The interactions between the close-coupled turbocharger control and the EGR rate control caused complicated fuel-air-ratio variations, as shown in the engine simulation results. These variations influenced the combustion and emissions as demonstrated on the single-cylinder research engine using the pseudo-transient test conditions. With the knowledge of diesel combustion characteristics with different levels of EGR reported in previous chapters, combustion strategies have been proposed to reduce the transient emissions. Retarded fuel injection timing can reduce the peak heat release rate and lead to low smoke emissions, and advanced combustion phasing can normally reduce the THC emissions unless fuel impingement or over-mixing occur. Fuel injection parameters and boost pressure can be used together to control the pseudo-transient operating conditions combustion and to reduce the emissions, as has been shown here.

Figure 8.25 shows a modified  $\Phi$ -T map based on the work of Akihama *et al.* (2001) that, as was used in Chapter 4 (Figure 4.33), illustrates the conceptual effects of engine operating parameters on soot and NOx emissions. The effects of engine operating parameter variations in LTC mode on local  $\Phi$ , T and smoke emissions are illustrated by the arrows. The trends are only to be used as a conceptual illustration based on qualitative analysis of the parameters. The starting points of the arrows in the figure were chosen arbitrarily to represent the local combustion zones which are presumed during different load LTC conditions. For low load LTC (Figure 8.25a), the combustion generally occurs within relatively low equivalence ratio and low temperature zones where the soot formation is insignificant. The variations in the operating parameters also show insignificant influence on soot formation. However, the changes in local equivalence ratio and combustion temperatures can significantly influence the engine efficiency and THC and CO emissions. For the intermediate load LTC (Figure 8.25b) the combustion tends to occur within relatively higher equivalence ratio and temperature zones where the soot formation rates tend to be higher. Variations in engine operating parameters may have more significant influence on soot emissions.

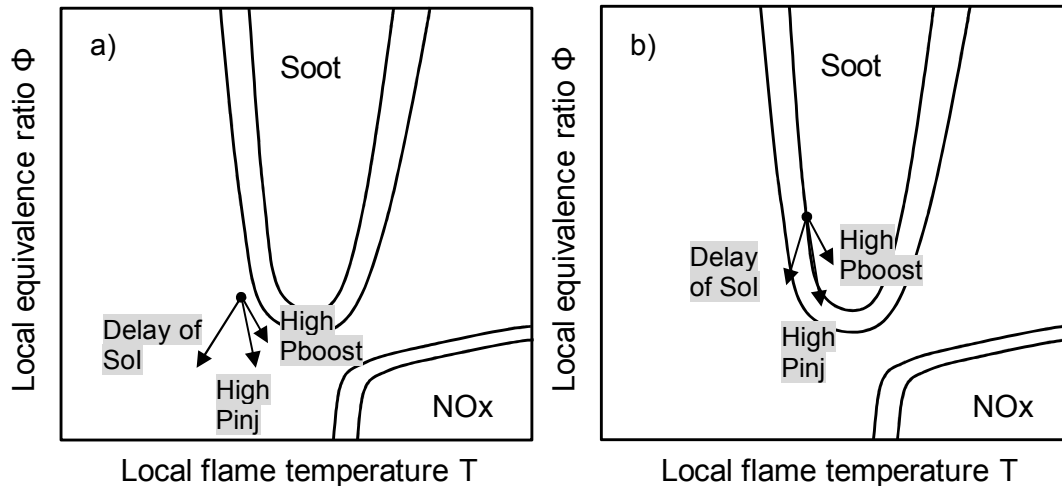


Figure 8.25 Conceptual effects of the variations in fuel injection timing (Sol), injection pressure (Pinj), boost pressure (Pboost) on  $\Phi$ , T and soot emissions (starting point, magnitudes and directions for illustration only) (a): low load condition; b): intermediate load condition)

An increase in boost pressure could increase the engine efficiency during the transient operation of a LTC-conventional diesel combustion ‘dual-mode’ engine. For the low fuelling stage (< 16 mg/cycle, ~6 bar gross IMEP) of the transients, an increase in boost pressure led to reduced global equivalence ratio as shown in Figure 8.25 and enhanced the THC and CO oxidation process while remaining within the LTC regime. Thus, it reduced the combustion by-product emissions without increasing NOx and smoke emissions due to the long ignition delay and low combustion temperature features of LTC. However, for the high fuelling part of the transient, an increase in boost pressure led to an increased oxygen-fuel-ratio and a reduced ignition delay. These features lead to higher combustion temperatures and higher rates of soot formation. NOx, on the other hand, remained low, indicating that combustion temperatures did not reach the levels required for significant NOx formation. Therefore, boost, on its own, is not the solution. However, it does tend to reduce the oxygen based equivalence ratio, which means that the operating regime is more efficient and stable.

Variable fuel injection control can be used to help improve the pseudo-transient operation of the engine. Retarding the combustion phasing can reduce the smoke emissions effectively for the high fuelling pseudo-transient operating conditions as shown in right hand column of Figure 8.25, although it does not reach the near-zero smoke levels of low-load LTC. The thermal efficiency lost due to the late combustion event can be recovered with increased boost pressure. Thus the implementation of a LTC regime may need a more advanced boost system than the stock turbocharger



system used in the base model (as used in this work) to provide rapid increases in pressure to cope with the transient controls.

High smoke emissions during the load transients were challenging due to the high equivalence ratio with increased fuel injection quantity for the constant combustion phasing based combustion control strategy. The reduction in EGR rate during load ramps made the smokeless diesel combustion difficult to achieve. Delay of the fuel injection timing reduced the intermediate load LTC combustion temperature and increased the ignition delay, which can significantly reduce the smoke emissions. However, the retarded fuel injection timing resulted in lower gross IMEP, hence a slow acceleration response of the vehicle. To ensure that the vehicle follows the driving-cycle, a higher fuel mass would need to be injected. This would result in a higher (global) equivalence ratio with a possible increase in smoke. The effects of this increase in equivalence ratio on performance and emissions were not investigated in this work, and will need further research.

Knowledge of the cycle-by-cycle intake charge pressure, temperature and EGR rate for the specific engine speed and load conditions during transients will enable the designated fuel injection strategies to be used to control the combustion process and emissions. However, the cycle resolved measurement of these parameters requires fast response sensors and may lead to a significant increase in cost for the engines. Model based fuel injection control, which takes the engine transient behaviour into account, with prediction of EGR rate and boost pressure may be used to improve the transient control of the LTC-conventional diesel combustion 'dual-mode' engine.

## **8.5 Conclusions**

This chapter has investigated the impacts of LTC on transient performance of a diesel engine using both a 1-D engine simulation and experimental engine research conducted at pseudo-transient test conditions. The results of this study lead to the following conclusions:

- 1) Within the LTC regime, the transients encountered insufficient intake charge boost pressure since the high pressure EGR system by-passed a significant part of the exhaust enthalpy, leading to a slow response and low isentropic efficiency of the turbocharger. The interactions between EGR control and boost pressure control during transients led to different combustion phenomenon for the pseudo-transient points from their steady-state counterparts of LTC or conventional diesel combustion.

2) The driving-cycle test data analysis showed that 100% of the four ECE driving-cycles and 70% of the EUDC driving-cycle (in time) has an engine load that should be achievable within the LTC operating region (fuel injection quantities  $< 20$  mg/cycle). Representative engine load transients within LTC and during combustion mode shifting were selected from the driving-cycle test data. These transients covered the majority of the load ramps which occurred during the NEDC driving-cycle test.

3) For the transients with continuously high levels of EGR (i.e., a transient within LTC or a mode-crossing transient with high EGR rates at the end of a transient), the boost pressure could not increase sufficiently rapidly with the stock turbocharger. However, for the transient process terminating in conditions with low EGR rate, the response of turbocharger was faster. Even in this case, a faster-response turbocharger would be beneficial.

4) Transient simulation of the engine using Ricardo WAVE was conducted to identify the pseudo-transient test conditions. Engine speed and fuel injection quantity were set to follow the driving-cycle test data, the EGR valve position followed the engine speed and fuel quantity based map, and the VGT vane position was controlled using a PID controller in the engine model with driving-cycle defined boost pressure targets. The critical operating points, which had large equivalence ratio discrepancies compared with the steady-state operating conditions, were selected as the pseudo-transient points for the experimental study.

5) Combustion at high fuelling pseudo-transient points ( $> 16$  mg/cycle) incurred high levels of smoke emissions for both within-LTC and combustion mode shifting transients. The THC and CO emissions were also high for the high EGR conditions. For the transient route terminating at low EGR rate conventional diesel combustion, the THC and CO emissions were lower, but both the NO<sub>x</sub> and smoke emissions were higher as compared to those from the high EGR rate route.

6) For the low fuelling pseudo-transient points ( $< 16$  mg/cycle), the combustion control was less challenging on emissions and efficiency. This suggests that restricting the LTC operational range to the fuelling conditions lower than the maximum achievable conditions could be beneficial from a transient response point of view.

7) For the transient terminating at the high EGR conventional diesel combustion, the high EGR rate led to significantly delayed turbocharger response. Thus, the increase in gross IMEP with fuel injection quantity was slow and the vehicle could not follow the driving-cycle demand. The high EGR rates and low boost pressure limited the engine power rise with low NO<sub>x</sub> emission, while the smoke number was increased significantly during the transient process. Because the equivalence ratio is near unity, it is unlikely that adding more fuel would significantly improve the engine power output. As a result, unless the air-system response can be improved, this high-EGR route is not suitable for this transient on the driving-cycle.

8) With increased boost pressure, the gross IMEP was increased and the THC and CO emissions were reduced for the pseudo-transient points. The NO<sub>x</sub> and smoke emissions were kept low for the low load (< 16 mg/cycle) pseudo-transient points. However, for the high fuelling (> 16 mg/cycle) points, the combustion was influenced by the increased boost pressure and resulted in increased smoke emissions.

9) An increase in boost combined with variations in fuel injection events enhanced the controllability of transients, especially for the high smoke pseudo-transient points. By retarding the fuel injection timing or by reducing fuel injection pressure, the smoke emissions were reduced with a thermal efficiency penalty. An increase in boost pressure at the same time reduced the penalty in fuel consumption without significantly affecting the smoke emissions.

This chapter has investigated the impacts of driving-cycle transients on the performance of a high-EGR LTC engine. The results have demonstrated the difficulties that a high-EGR engine will encounter and has demonstrated some strategies which can help to mitigate high emissions during a transient. The following chapter will summarize main conclusions from the thesis, integrating the steady-state, small-scale and large-scale transients investigated in this and the preceding chapters. Implications for engine developers from this study and further research opportunities are also suggested.

## Chapter 9 Conclusions and Further Work

The objective of this research was to improve the understanding of the diesel combustion with high levels of intake charge dilution through exhaust gas recirculation (EGR) under steady-state and pseudo-transient operating conditions. This objective has been addressed through studies where the EGR rate, fuel injection parameters, intake charge temperature and pressure were varied. The hypothesis of low temperature diesel combustion (LTC) by reducing local equivalence ratio ( $\Phi$ ) and flame temperature ( $T$ ) by high levels of EGR, variations in fuel injection parameters and intake charge conditions have been experimentally evaluated.

The following sections first provide a short discussion of the findings of this research, followed by a list of the major conclusions. The implication of these findings for engine development is then discussed. Finally, a discussion of potential further work is presented.

### 9.1 Discussion of Overall Results

Figure 9.1 shows a modified  $\Phi$ - $T$  map based on the work of Akihama et al (2001) that illustrates the conceptual effects of engine operating parameter variations on soot and NO<sub>x</sub> emissions. The figure indicates the general trends in NO<sub>x</sub> and soot emissions for the changes in local equivalence ratio and flame temperature and is used purely to help the discussion of the overall results. The effects of engine operating parameter variations in LTC mode on local  $\Phi$ ,  $T$  and smoke emissions are illustrated by the arrows. The trends are only to be used as a conceptual illustration based on qualitative analysis of the parameters. The starting points of the arrows in the figure were chosen arbitrarily to represent the local combustion zones which are presumed during different load LTC conditions. For low load LTC (Figure 9.1a), the combustion generally occurs within relatively low equivalence ratio and low temperature zones where soot formation is insignificant. The variations in the operating parameters also show insignificant influence on soot formation. However, for the intermediate load LTC (Figure 9.1b) the combustion tends to occur within relatively higher equivalence ratio and temperature zones where the soot formation rates tend to be higher than the low load condition. Variations in engine operating parameters may have a more significant influence on soot emissions. Details of the

effects of the individual parameters are described in more details in the following paragraphs.

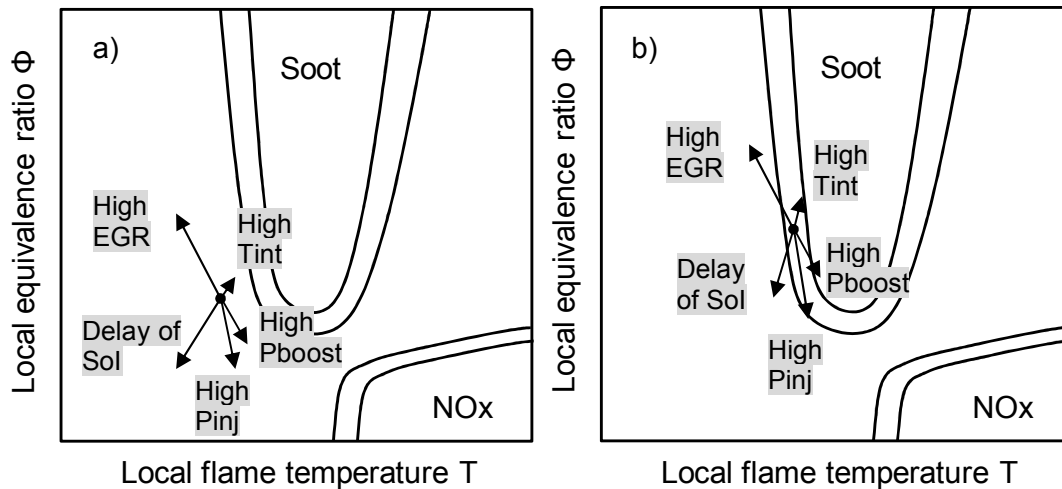


Figure 9.1 Conceptual effects of the variations in EGR rate, fuel injection timing (Sol), injection pressure (Pinj), boost pressure (Pboost) and intake charge temperature (Tint) on  $\Phi$ ,  $T$  and soot emissions (starting point, magnitudes and directions for illustration only) (a): low load condition; b): intermediate load condition)

Variations in EGR rate significantly influence the LTC combustion and emissions. The ignition delay increases with increasing EGR rate, since the low oxygen concentration in the charge limits the low temperature oxidation rate of the fuel and subsequently delays the high temperature combustion. The increased EGR rate leads to lower peak combustion temperatures and hence reduced peak heat release rate. NOx shows less sensitivity to changes in EGR rate under high-EGR LTC conditions as NO formation (by the thermal mechanism) has been effectively suppressed at the EGR ranges investigated in this research. The smoke emissions can be reduced by increased EGR rate due to the reduced combustion temperature which shifts the combustion towards the LTC region (bottom left hand side) of the  $\Phi$ - $T$  map even when the mixture is in a locally fuel-rich condition as shown in Figure 9.1. The THC and CO emissions increase with EGR rate due to bulk quenching and lower oxygen concentrations in the reaction zones, especially later in the cycle.

Fuel injection parameters also influence the LTC combustion and emissions. Retarded injection timing (delayed Sol, as illustrated in Figure 9.1) leads to the combustion event occurring later (typically in the expansion stroke), which results in reduced peak heat release rate and lower combustion temperatures. The delayed combustion reduces the smoke emissions further with the penalty of increased fuel consumption, THC and CO emissions. However, too early a fuel injection may cause

fuel impingement which also leads to increased THC and CO emissions. An increase in injection pressure improves the fuel mixing and advances the combustion phasing. The peak heat release rate is also increased by higher injection pressure. However, the injection pressure shows a less significant influence on smoke emissions than does the injection timing. The increased mixing intensity could have led to reduced soot formation in the combustion, while the enhanced combustion in return may have increased the combustion temperature which increases the soot formation rate in the LTC mode. The soot oxidation rates are expected to be insignificant due to the low oxygen concentration, especially in the later part of the combustion event where the temperature is also low. This poor oxidation is demonstrated by post fuel injection. Post fuel injection shows no benefit on the high EGR diesel combustion with high smoke emissions studied in this work. The low oxygen concentration in the charge limits the combustion of the fuel injected late in the combustion cycle and cannot improve the oxidation of the soot formed in the main fuel combustion.

Variability in engine fuel injection quantity, intake manifold temperature and engine speed show less significant influences on LTC combustion and emissions than does the EGR rate. The statistical study introduced in Chapter 7 showed that the only parameter for which a small variation has a significant impact on LTC combustion and emissions is the EGR rate. A more detailed comparison of the combustion under certain individual cases showed detectable differences in combustion between the different charge temperatures, as presented in Chapter 5.

Intake charge temperature has a complex influence on LTC combustion and emissions. The thermal throttling effects of high intake temperature reduce the oxygen quantity trapped in the combustion chamber, increasing the local equivalence ratio as shown in Figure 9.1. In LTC, the low oxygen content can lead to reduced combustion temperature and smoke emissions. However, the high intake charge temperature can also increase the combustion temperature. This, combined with the reduced oxygen-fuel-ratio due to thermal throttling effects could increase the formation rates of soot significantly. For the low load LTC cases (8 mg/cycle; ~3 bar gross IMEP), the smoke emissions were insignificantly influenced by the intake charge temperature. The relatively low equivalence ratio at these conditions showed little sensitivity to the thermal throttling effect. As well, the overall combustion temperature is lower for this case and the increase in the charge temperature does not shift the combustion into the smoke-rich zone in the  $\Phi$ -T map (illustrated in Figure 9.1). For the intermediate load conditions (16 mg/cycle), the combustion is

more likely to occur in a locally fuel-rich mode; and the overall combustion temperature is higher than that for the low load conditions. An increase in the intake charge temperature can lead to reduced ignition delay, resulting in a locally richer mixture, while also leading to higher combustion temperatures. This shifts the combustion into the smoke-rich zone in the  $\Phi$ -T map.

The transient simulation of an engine using a 1-D engine model indicates that, with the stock turbocharger, the boost pressure is insufficient for the engine running within LTC mode. Variations in EGR rate are also encountered in the transient processes. For a transient within a single LTC combustion mode, the slow response of the boost system can restrict the LTC operation to a low load range. For the higher load points, smoke emissions are increased significantly. An increase in boost pressure can increase the engine thermal efficiency and combustion efficiency without significantly influencing the NO<sub>x</sub> and PM emissions. For the transient during combustion mode shifting from LTC into conventional diesel combustion, the existence of high EGR in the transient cycles also leads to high smoke emissions as the engine load is increased beyond the range achievable with LTC. An increase in boost pressure for these high smoke conditions causes even higher emissions of smoke. This indicates that the combustion occurs in the low temperature part of the soot formation region in the  $\Phi$ -T map (Figure 9.1), where an increase in combustion temperature by the boost pressure increases the soot formation rates, but the investigated values may not be high enough to increase the soot oxidation rates proportionately. Retarded injection timing reduces the smoke emissions significantly for these cases. With increased boost pressures, the deterioration in combustion efficiency due to the late combustion event can be partially recovered.

## 9.2 Conclusions

This research has investigated the factors relating to LTC, exhaust back pressure, sensitivity and pseudo-transient operation of a research engine. This section summarises the major conclusions from the research.

1) EGR rate is the most important controlling parameter on LTC regime achieved using high levels of EGR. To reduce the engine-out NO<sub>x</sub> and smoke emissions simultaneously, increasing the EGR rate to a level where the PM formation terminates is an effective measure. However, the range of EGR levels where this can be achieved is limited by the high smoke (too low EGR) and combustion degradation (too high THC and CO emissions and reduction in engine thermal efficiency). Small

variations in EGR rate (within ~5%, i.e.  $60\% \pm 3\%$ ) demonstrate a significant influence on the LTC combustion and emissions. Changes in exhaust back pressure lead to variations in effective EGR rate and temperature by affecting the residual gas fraction. The ~4% effective EGR rate rise per bar of increase in exhaust back pressure, and the associated temperature rise due to the trapped hot exhaust gas also show detectable effects on LTC combustion and emissions.

2) The ignition delay of LTC can be affected by the engine operating parameters through varying the low temperature reaction (LTR) processes in the LTC combustion regime. LTC comprises three stages, starting with a cool flame reaction, followed by the negative temperature coefficient (NTC) regime and finally a partially-premixed main combustion process. Engine operating parameters (EGR rate, intake charge temperature, fuel injection timing and pressure) influence the charge composition, temperature and mixing intensity, which in turn affect the cool flame reaction rates. The occurrence and termination of the NTC processes are controlled by the charge temperature which is influenced by the heat released from the LTR process and the initial intake charge temperature. The termination of the NTC regime indicates the start of high temperature main combustion.

3) Engine transient simulation using a 1-D engine model suggests that during a load transient process of an engine running in LTC mode, the turbocharger responds to the transient command slowly and the EGR rate varies significantly. For transients with consistently high levels of EGR, the boost pressure does not increase sufficiently rapidly using the stock turbocharging system provided. This restricts the flexibility in LTC combustion control and optimisation. From transient simulation results, pseudo-transient operating points can be selected to represent the critical operating conditions during a transient operation of the engine. The critical operating parameters such as fuel injection quantity, EGR rate and boost pressure can be selected and implemented on the single-cylinder research engine to experimentally evaluate the combustion and emissions of the engine during a transient operation.

4) If the LTC operation is limited within a low load range (i.e.  $< 16$  mg/cycle,  $\sim 6$  bar gross IMEP), the pseudo-transient points within the LTC mode show less variation in the NO<sub>x</sub> and smoke emissions. An increase in boost pressure for these lower load transient points reduced the THC and CO emissions and increased engine efficiency, without affecting the NO<sub>x</sub> and smoke emissions significantly. However, for the higher load cases ( $> 16$  mg/cycle), the smoke emissions were very high, and higher boost pressure led to further increases in smoke. This is a result of higher PM formation



rates due to the increased combustion temperature in the high EGR combustion mode.

5) Engine transients during a combustion mode shift from LTC into higher load conventional diesel combustion encounter operating conditions with unfavourable values of EGR rate and boost pressure. Experimental results show that these operating conditions emit very high levels of smoke emissions. An increase in boost pressure itself cannot effectively reduce the smoke emissions, because the increased boost pressure leads to higher combustion temperatures which enhance soot formation as well as oxidation. The combustion is expected to occur at the high soot zone in the  $\Phi$ -T map and an increase in combustion temperature may shift the combustion to a higher soot zone as shown in Figure 9.1. For high EGR diesel combustion, the engine-out smoke emissions are mainly controlled by soot formation as the oxidation is expected to be insignificant due to the low oxygen content in the charge. Retarded fuel injection timing and low injection pressure can be used to reduce the smoke emissions with the penalty of increased THC and CO emissions and reduced efficiency. An increase in the boost pressure at this condition can recover part of these losses without significantly impacting the smoke emissions.

6) Small changes in engine speed, fuel injection quantity and intake charge temperature showed less significant influences on LTC combustion and emissions compared to EGR rate. The  $\pm 5\%$  variations in fuel injection quantity and engine speed and the  $\pm 10^\circ\text{C}$  change in intake manifold temperature had insignificant impacts on LTC combustion and emissions. However, a larger temperature variation ( $\pm 20^\circ\text{C}$ ) does influence the LTC combustion and emissions. An increase in the intake manifold temperature can reduce the THC and CO emissions for the low load LTC cases but increase these emissions at intermediate load LTC. The smoke emissions from the intermediate load LTC can also be increased by higher intake charge temperatures.

7) For LTC, the particle size distribution shows a smaller count median diameter and a higher total number than for operation at intermediate EGR conventional (non-LTC) diesel combustion conditions. The low smoke number measurement from LTC is a result of reduced particle size and possible changes in PM composition. The high dilution ratio in the intake charge leads to long ignition delays and low combustion temperatures which both suppress the particulate formation and oxidation. This is different from the conventional diesel combustion where both the formation and oxidation of particulates have a significant influence on the engine-out PM emissions.

With little oxidation, the formation rates of PM in LTC dictate the engine-out emissions.

8) Combustion stability deteriorates with high levels of EGR. Advanced combustion phasing improved the combustion stability with the combustion events occurring close to TDC. An increase in the intake charge temperature also improves the combustion stability for low load LTC conditions. The higher charge temperature leads to a thermal throttling effect that reduces the oxygen quantity (increases the local equivalence ratio) in the combustion and results in unstable combustion for intermediate load LTC cases.

9) Combustion phasing is controllable by adjusting fuel injection timing for LTC operation of the engine. The flexible LTC combustion phasing control due to the low peak cylinder pressure-rise-rate and low NO<sub>x</sub> emissions can be used to achieve increased engine thermal efficiency. However, for the intermediate load LTC, an equivalence ratio around unity results in low combustion efficiency which leads to higher fuel consumption.

10) Emissions of THC and CO are significantly higher for an engine running in LTC mode compared to running in conventional diesel mode. By adjusting the fuel injection timing and increasing the pressure, the THC and CO emissions can be reduced. However, levels still exceed acceptable values and therefore, aftertreatment systems for these emissions are expected to be required for engines operating using LTC techniques to meet emissions legislation.

### **9.3 Implications for Engine Developers**

The conclusions outlined in the previous section have significant implications for LTC diesel combustion system development. While not all the results are directly applicable to commercially-viable production engines, they do provide considerable guidance for diesel combustion system development.

The results indicate that an improvement in control accuracy in EGR rate is essential for LTC diesel combustion systems development. A control accuracy of five percent of the EGR rate (e.g. 60%±3%) will likely not be sufficient to both meet emissions standards and maintain acceptable engine stability. Once the EGR system is coupled with a turbocharging system, the interactions between these systems may amplify the influence of the variations in EGR rate and lead to unfavourable engine performance and emissions.

Aftertreatment systems for THC and CO are considered to be essential due to the increase of these emissions emitted from LTC combustion system. Diesel oxidation catalysts (DOC) could be an effective solution for the unburned emissions. However, the exhaust temperature and low oxygen concentration in the LTC exhaust need to be taken into account during the application of this technology (Jacobs *et al.*, 2008). Catalysts which can convert these emissions effectively under low exhaust temperature situation are in the process of development (Holroyd, 2008).

A larger number of small particles is generated from the test engine running within LTC mode than from the high smoke intermediate EGR combustion mode. Since the particle number is introduced in the Euro VI emissions legislation for light duty diesel vehicles, new control approaches may be needed to reduce the number of particulates in the exhaust gas. A DOC has been shown elsewhere to be able to reduce the SOF in the particulate matter emissions effectively. While the SOF ratio in PM emissions for LTC is expected to be high, the DOC specified for THC and CO emissions could be used to reduce the total particle number and mass. Further research is needed to validate this supposition.

Exhaust back pressure (EBP) due to the aftertreatment systems and turbocharging system need to be taken into account for the combustion control, particularly for the EGR rate control. A 4% increase in effective EGR rate with a one bar increase in EBP at a fixed intake manifold pressure was encountered for the research engine. As the EBP will change continuously, an EBP or estimation may be useful not only for the aftertreatment systems but also for the precise combustion control needed for LTC operation.

Currently, the application of LTC is limited to low and intermediate load conditions, and this project was not aimed at extending it. Thus, combustion mode shifting to conventional diesel combustion at high load must be handled carefully. The long response times of the EGR and turbocharging systems may cause the engine to operate under undesirable combustion conditions (that are not representative of either LTC or conventional diesel combustion) during the transients. Combustion control under these circumstances will almost certainly be challenging. Cylinder pressure based combustion control with intake oxygen concentration feedback/estimation is a possible solution to bridge the combustion modes smoothly. However, faster-response EGR systems and possibly a restriction on rate of load change when operating in LTC may be needed.

The phasing of the combustion event under high-EGR LTC is controllable using the injection timing. The combustion phasing can be changed by simply varying the fuel injection timing with generally low peak pressure-rise-rates. Thus, engine noise resulting from high peak cylinder pressure-rise-rate could be reduced with the implementation of LTC. The flexibility of efficiency optimisation through combustion phasing adjustment is also increased.

## **9.4 Further Work**

The study reported in this thesis provides insight into some of the aspects of LTC diesel processes with high levels of EGR. This section provides guidance for what aspects of future research might be pursued to achieve further reductions in emissions and improvements in engine efficiency.

The current work suggests that understanding of the in-cylinder conditions during the combustion event may reveal more details of the combustion process and the emission formation. An optical combustion study is currently being conducted in the research group to enhance the knowledge of LTC combustion and emissions formation process. The combustion temperature distribution and emissions formation zones will be identified with optical diagnostic tools.

The low temperature reaction/cool flame reaction before the main combustion event generates heat and produces intermediate radicals. How to control the heat release rate and the radical formation rates, and how to use them to influence the main combustion and emissions may be investigated in future work. With the understanding of the functions of the intermediate radicals, changes to the fuel properties could be used to influence the quantity of the specified radicals and to control the combustion and emissions.

High concentrations of THC and CO from previous cycles can join the combustion of subsequent cycles, either as residuals or through the EGR system. These may behave as additives to the freshly-injected diesel fuel. Their influence on the combustion and emissions can be investigated through changing the concentrations of these species in the EGR gas before they join the following combustion cycles.

Cylinder pressure based combustion control on an LTC diesel engine with the help of intake oxygen concentration measurement/prediction maybe an effective solution for the LTC combustion control and the engine transient control. The combustion control

strategies can be developed based on the understanding of the LTC combustion to realise smooth combustion mode shifting.

The composition of PM changes for different engine operating conditions. Understanding of the engine operating parameters, such as EGR rate, fuel injection parameters and intake charge temperature on PM composition would be useful for future exhaust aftertreatment system development and optimisation. It would also help to clarify the net benefits that could be expected from LTC operation. Particle size and number distribution under different LTC combustion conditions, and their sensitivity to other engine operating parameters, are also an important area for future research.

With improved understanding of diesel engine LTC operation and emissions, a practical implementation of this combustion regime becomes achievable. In this research, the critical control parameters in LTC combustion processes and emissions were identified. The characteristics of transient operation of a diesel engine running under LTC conditions for low and intermediate load conditions and conventional diesel mode for higher load conditions were also investigated. The engine combustion strategies during engine transients within LTC and combustion mode shifting from LTC to conventional diesel were evaluated. Retarded fuel injection timing with increased boost pressure was the most promising technique identified to control smoke emissions while retaining reasonable engine efficiency.

## **9.5 Closing Comments**

Future studies are expected to extend the understanding of the fundamentals of LTC, using techniques such as optical accessible combustion process to better understand the effects of low temperature reactions and the reactive species in EGR gases. Studies in advanced LTC engine control technologies, aftertreatment systems and the associated emissions properties will push the research to an area where a more realistic usage of LTC on diesel engines can be pursued. Overall, it is recommended that LTC research is continued, since it has significant future potential for diesel engine emissions control.

## References

- ACEA (2010). Trends in New Car Characteristics.
- Aizawa T, Kosaka H (2008). Investigation of Early Soot Formation Process in a Diesel Spray Flame via Excitation - Emission Matrix Using a Multi - Wavelength Laser Source. *International Journal of Engine Research* 9(1): 79-97.
- Akihama K, Takatori Y, Inagaki K, Sasaki S, Dean AM (2001). Mechanism of the Smokeless Rich Diesel Combustion by Reducing Temperature. *SAE Paper*: 2001-01-0655.
- Albrecht A, Corde G, Knop V, Boie H, Castagne M (2005). 1D Simulation of Turbocharged Gasoline Direct Injection Engine for Transient Strategy Optimization. *SAE Paper*: 2005-01-0693.
- Alriksson M, Denbratt IG (2006). Low Temperature Combustion in a Heavy Duty Diesel Engine Using High Levels of EGR. *SAE Paper*: 2006-01-0075
- Andreae MM, Cheng WK, Kenney T, Yang J (2007). On HCCI Engine Knock. *SAE Paper*: 2007-01-1858.
- Aoyagi Y, Osada H, Misawa M, Goto Y, Ishii H (2006). Advanced Diesel Combustion Using of Wide Range, High Boosted and Cooled EGR System by Single Cylinder Engine. *SAE Paper*: 2006-01-0077.
- APIS (2010). Overview of Nitrogen Oxides (NOx) Vol. 2010: [http://www.apis.ac.uk/overview/pollutants/overview\\_NOx.htm](http://www.apis.ac.uk/overview/pollutants/overview_NOx.htm).
- Arnold S, Groskreutz M, Shahed SM, Slupski K (2002). Advanced Variable Geometry Turbocharger for Diesel Engine Applications. *SAE Paper*: 2002-01-0161.
- Aronsson U, Andersson Ö, Egnell R, Miles PC, Ekoto IW (2009). Influence of Spray-Target and Squish Height on Sources of CO and UHC in a HSDI Diesel Engine During PPCI Low-Temperature Combustion. *SAE Paper*: 2009-01-2810
- Assanis DN, Filipi ZS, Fiveland SB, Syrimis M (2000). A Methodology for Cycle-By-Cycle Transient Heat Release Analysis in a Turbocharged Direct Injection Diesel Engine. *SAE Paper*: 2000-01-1185.
- Badami M, Mallamo F, Millo F, Rossi E (2003). Experimental investigation on the effect of multiple injection strategies on emissions, noise and brake specific fuel consumption of an automotive direct injection common-rail diesel engine. *International Journal of Engine Research* 4(4): 299-314.
- Bauer S, Zhang H, Pfeifer A, Wenz-lawski K (2007). Diesel Engine for Passenger Car and EU6: Entirely System Approach for Development of Fuel Injection System, Air/EGR Path and Emission Aftertreatment. *28 Internationales Wiener Motoren-symposium 2007*.
- Beatrice C, Avolio G, Bertoli C, Giacomo ND, Guido C, Migliaccio Mn (2007a). Critical Aspects on the Control in the Low Temperature Combustion Systems for

High Performance DI Diesel Engines. *Oil & Gas Science and Technology* **62**: 471-482.

Beatrice C, Avolio G, Guido C (2007b). Experimental Analysis of the Operating Parameter Influence on the Application of Low Temperature Combustion in the Modern Diesel Engines. *SAE Paper*: 2007-01-1839.

Benajes J, Lujan JM, Bermudez V, Serrano JR (2002). Modelling of Turbocharged Diesel Engines in Transient Operation. Part 1: Insight Into the Relevant Physical Phenomena. *Proceedings of the Institution of Mechanical Engineers, Part D: Journal of Automobile Engineering* **216**(5): 431-441.

Benajes J, Molina SA, Garcia JM (2001). Influence of Pre- and Post-Injection on the Performance and Pollutant Emissions in a HD Diesel Engine. *SAE Paper*: 2001-01-0526.

Black J, Eastwood PG, Tufail K, Winstanley T, Hardalupas Y, Taylor AMKP (2007). Diesel Engine Transient Control and Emissions Response During a European Extra-Urban Drive Cycle (EUDC). *SAE Paper*: 2007-01-1938.

Blanquart G, Pepiot-Desjardins P, Pitsch H (2009). Chemical Mechanism for High Temperature Combustion of Engine Relevant Fuels with Emphasis on Soot precursors. *Combustion and Flame* **156**(3): 588-607.

Bobba M, Musculus M, Neel W (2010). Effect of Post Injections on In-Cylinder and Exhaust Soot for Low-Temperature Combustion in a Heavy-Duty Diesel Engine. *SAE Paper*: 2010-01-0612.

Bobba MK, Genzale CL, Musculus MPB (2009). Effect of Ignition Delay on In-Cylinder Soot Characteristics of a Heavy Duty Diesel Engine Operating at Low Temperature Conditions. *SAE Paper*: 2009-01-0946

Bockhorn H, Geitlinger H, Jungfleisch B, Lehre T, Schon A, Streibel T, *et al.* (2002). Progress in Characterization of Soot Formation by Optical Methods. *Physical Chemistry* **4**: 3780–3793.

Boger T, Tilgner I-C, Shen M, Jiang Y (2008). Oxide Based Particulate Filters for Light-Duty Diesel Applications – Impact of the Filter Length on the Regeneration and Pressure Drop Behavior. *SAE Paper*: 2008-01-0485.

Boot M, Rijk E, Luijten C, Somers B, Albrecht B (2010). Spray Impingement in the Early Direct Injection Premixed Charge Compression Ignition Regime. *SAE Paper*: 2010-01-1501.

Buchwald R, Lautrich G, Maiwald O, Sommer A (2006). Boost and EGR System for the Highly Premixed Diesel Combustion. *SAE Paper*: 2006-01-0204

Burton JL, Williams DR, Glewen WJ, Andrie MJ, Krieger RB, Foster DE (2009). Investigation of Transient Emissions and Mixed Mode Combustion for a Light Duty Diesel Engine. *SAE Paper*: 2009-01-1347.

Busch S, Bohac SV, Assanis DN (2007). A Study of the Transition Between Lean Conventional Diesel Combustion and Lean, Premixed, Low-Temperature Diesel Combustion. *Proceedings of the ASME Internal Combustion Engine Division Fall Technical Conference*.

Cambustion (2010). Cambustion Products Introduction  
<http://www.cambustion.com/products> 2010.

Carlucci P, Ficarella A, Laforgia D (2003). Effects of Pilot Injection Parameters on Combustion for Common Rail Diesel Engines. *SAE Paper*: 2003-01-0700.

Chang K, Babajimopoulos A, Lavoie GA, Filipi ZS, Assanis DN (2006). Analysis of Load and Speed Transitions in an HCCI Engine Using 1-D Cycle Simulation and Thermal Networks. *SAE Paper*: 2006-01-1087.

Chen SK (2000). Simultaneous Reduction of NOx and Particulate Emissions by Using Multiple Injections in a Small Diesel Engine. *SAE Paper*: 2000-01-3084.

Choe S, Chang R, Jeon J, Violi A (2008). Molecular Dynamics Simulation Study of a Pulmonary Surfactant Film Interacting with a Carbonaceous Nanoparticle. *Biophysical Journal* **95**(9): 4102-4114.

Costa M, Siano D, Allocca L, Montanaro A, F.Bozza (2009). Light Duty Diesel Engine: Optimization of Performances, Noxious Emission and Radiated Noise. *SAE Paper*: 2009-2032-0105.

Costa M, Vaglieco BM, Corcione FE (2005). Radical Species in the Cool-flame Regime of Diesel Combustion: a Comparative Numerical and Experimental Study. *Experiments in Fluids* **39**: 512-524.

Crua C, Kennaird DA, Heikal MR (2003). Laser-induced Incandescence Study of Diesel Soot Formation in a Rapid Compression Machine at Elevated Pressures. *Combustion and Flame* **135**(4): 475-488.

Dec JE (1997). A Conceptual Model of DI Diesel Combustion Based on Laser-sheet Imaging. *SAE Paper*: 970873.

Desantes JM, Arregle J, Lopez JJ, Garcia A (2007). A Comprehensive Study of Diesel Combustion and Emissions with Post-injection. *SAE Paper*: 2007-01-0915.

Dhaenens M, Linden Gvd, Nehl J, Thiele R (2001). Analysis of Transient Noise Behavior of a Truck Diesel Engine. *SAE Paper*: 2001-01-1566.

DieselNet (2010). Emission Test Cycles-Summary of Worldwide Engine and Vehicle test cycles: DieselNet.

Eastwood PG, Morris T, Tufail K, Winstanley T, Hardalupas Y, Taylor AMKP (2007). The Effects of Fuel-injection Schedules on Emissions of NOx and Smoke in a Diesel Engine during Partial-premix Combustion. *SAE Paper*: 2007-24-0011.

Ehleskog R, Ochoterena R, Andersson S (2007). Effects of Multiple Injections on Engine-Out Emission Levels Including Particulate Mass from an HSDI Diesel Engine. *SAE Paper*: 2007-01-0910.

Ekoto IW, Colban WF, Miles PC, Park SW, Foster DE, Reitz RD, *et al.* (2009). UHC and CO Emissions Sources from a Light-Duty Diesel Engine Undergoing Dilution-Controlled Low-Temperature Combustion. *SAE International Journal of Engines* **2**: 411-430.



- EU (2006). *CO2 Reductions From Passenger Cars*. European Parliament
- EU (2009). *Regulation (EC) No 443/2009 of the European Parliament and of the Council*.
- EU (2007). Type approval of motor vehicles with respect to emissions from light passenger and commercial vehicles (Euro 5 and Euro 6) and on access to vehicle repair and maintenance information. In: *REGULATION (EC) No 715/2007 OF THE EUROPEAN PARLIAMENT AND OF THE COUNCIL*.
- Fang T, Lee C, Coverdill R, White R (2010). Effects of Injection Pressure on Low-sooting Combustion in an Optical HSDI Diesel Engine Using a Narrow Angle Injector. *SAE Paper*: 2010-01-0339.
- Filipi Z, Wang Y, Assanis D (2001). Effect of Variable Geometry Turbine (VGT) on Diesel Engine and Vehicle System Transient Response. *SAE Paper*: 2001-01-1247.
- Fischer S, Stein J-O (2009). Investigation on the Effect of Very High Fuel Injection Pressure on Soot-NOx Emissions at High Load in a Passenger Car Diesel Engine. *SAE Paper*: 2009-01-1930.
- Florchinger P, Zink U, Cutler W, Tomazic D (2004). DPF Regeneration-Concept to Avoid Uncontrolled Regeneration During Idle. *SAE Paper*: 2004-01-2657.
- Ford (2010). Diesel Engine Emissions during High-EGR Operation Quarterly Project Review Meeting (17-03-2010). Ford Dunton Technical Centre.
- Galindo J, Bermudez V, Serrano JR, Lopez JJ (2001). Cycle to Cycle Diesel Combustion Characterisation During Engine Transient Operation. *SAE Paper*: 2001-01-3262.
- Gardner T, Yetkin A, Shotwell R, Kotrba A, Gysling H, Mustafa Z, *et al.* (2009). Evaluation of a DPF Regeneration System and DOC Performance Using Secondary Fuel Injection. *SAE Paper*: 2009-01-2884.
- Gray AWB, Ryan TW (1997). Homogeneous Charge Compression Ignition (HCCI) of Diesel Fuel. *SAE Paper*: 971676.
- Green RM (2000). Measuring the Cylinder-to-Cylinder EGR Distribution in the Intake of a Diesel Engine During Transient Operation. *SAE Paper*: 2000-01-2866.
- Gurney D (2001). The Design of Turbocharged Engines Using 1D Simulation. *SAE Paper*: 2001-01-0576.
- Hagena JR, Filipi ZS, Assanis DN (2006). Transient Diesel Emissions: Analysis of Engine Operation During a Tip-In. *SAE Paper*: 2006-01-1151.
- Han M, Assanis DN, Bohac SV (2009). Sources of Hydrocarbon Emissions from Low-Temperature Premixed Compression Ignition Combustion from a Common Rail Direct Injection Diesel Engine. *Combustion Science and Technology* **181**(3): 496-517.
- Han M, Assanis DN, Jacobs TJ, Bohac SV (2008). Method and Detailed Analysis of Individual Hydrocarbon Species From Diesel Combustion Modes and Diesel Oxidation Catalyst. *Journal of Engineering for Gas Turbines and Power* **130**(4).

Hasegawa R, Yanagihara H (2003). HCCI Combustion in DI Diesel Engine. *SAE Paper*: 2003-01-0745.

He Y (2005). Development and Validation of a 1D Model of a Turbocharged V6 Diesel Engine Operating Under Steady-State and Transient Conditions. *SAE Paper*: 2005-01-3857.

Henein NA, Bahattachryya A, Schipper J, Kastury ASR, Bryzik W (2006). Effect of Injection Pressure and Swirl Motion on Diesel Engine-out Emissions in Conventional and Advanced Combustion Regimes. *SAE Paper*: 2006-01-0076

Heywood JB (1988). *Internal Combustion Engines Fundamentals*. edn. McGraw-Hill.

Hiereth H, Prenninger P (2006). *Charging of the Internal Combustion Engine*. edn. Springer Verlag: Vienna.

Hiroyuki Y, Kotaro S, Atsumu T, Yuichi G (2008). Transition from cool flame to thermal flame in compression ignition process. *Combustion and Flame* **154**(1-2): 248-258.

Holroyd JA (2008). Low Temperature Oxidation Catalyst Development and Applications. In: *American Filtration & Separation Society Annual Conference*. Valley Forge, PA.

Hountalas DT, Katsanos CO, Lamaris VT (2007). Recovering Energy from the Diesel Engine Exhaust Using Mechanical and Electrical Turbocompounding. *SAE Paper*: 2007-01-1563.

Hountalas DT, Kouremenos DA, Binder KB, Schwarz V, Mavropoulos GC (2003). Effect of Injection Pressure on the Performance and Exhaust Emissions of a Heavy-Duty Di Diesel Engine. *SAE Paper*: 2003-01-0340

Hsu BD (2002). *Practical Diesel-Engine Combustion Analysis*. edn. Society of Automotive Engineers: Warrendale.

Idicheria CA, Pickett LM (2005). Soot Formation in Diesel Combustion under High-EGR Conditions. *SAE Paper*: 2005-01-3834.

IPCC (2007). IPCC Fourth Assessment Report: Climate Change 2007 Vol. 2010.

Jacobs TJ, Assanis DN (2008). Characteristic Response of a Production Diesel Oxidation Catalyst Exposed to Lean and Rich PCI Exhaust. *Journal of Engineering for Gas Turbines and Power* **130**(4).

Jansons M, Brar A, Estefanous F, Florea R, Taraza D, Henein N, *et al.* (2008). Experimental Investigation of Single and Two-Stage Ignition in a Diesel Engine. *SAE Paper*: 2008-01-1071.

Johnson TV (2008). Diesel Emission Control in Review. *SAE Paper*: 2008-01-0069.

Johnson TV (2009). Diesel Emission Control in Review. *SAE Paper*: 2009-01-0121.

Johnson TV (2010). Review of Diesel Emissions and Control. *SAE Paper*: 2010-01-0301.

- Kang H, Farrell PV (2005). Experimental Investigation of Transient Emissions (HC and NOx) in a High Speed Direct Injection (HSDI) Diesel Engine. *SAE Paper*: 2005-01-3883.
- Kawano D, Suzuki H, Hajime Ishii, Goto Y, Odaka M, Murata Y, *et al.* (2005). Ignition and Combustion Control of Diesel HCCI. *SAE Paper*: 2005-01-2132.
- Kimura S, Aoki O, Kitahara Y, Aiyoshizawa E (2001). Ultra-Clean Combustion Technology Combining a Low-Temperature and Premixed Combustion Concept for Meeting Future Emission Standards. *SAE Paper*: 2001-01-0200.
- Kimura S, Aoki O, Ogawa H, Muranaka S, Enomoto Y (1999). New Combustion Concept for Ultra-Clean and High-Efficiency Small DI Diesel Engines. *SAE Paper*: 1999-01-3681.
- Kitamura T, Ito T, Senda J, Fujimoto H (2002). Mechanism of Smokeless Diesel Combustion with Oxygenated Fuels Based on the Dependence of the Equivalence Ratio and Temperature on Soot Particle Formation. *International Journal of Engine Research* **3**(4): 223-248.
- Kitamura Y, Mohammadi A, Ishiyama T, Shioji M (2005). Fundamental Investigation of NOx Formation in Diesel Combustion Under Supercharged and EGR Conditions. *SAE Paper*: 2005-01-0364.
- Koci CP, Ra Y, Krieger R, Andrie M, Foster DE, Siewert RM, *et al.* (2009). Detailed Unburned Hydrocarbon Investigations in a Highly-Dilute Diesel Low Temperature Combustion Regime. *SAE Paper*: 2009-01-0928.
- Kuo KK (2005). *Principles of Combustion*. Second edn. John Wiley & Sons: New Jersey.
- Ladommatos N, Abdelhalim S, Zhao H (1998a). Control of Oxides of Nitrogen from Diesel Engines Using Diluents while Minimising the Impact on Particulate Pollutants. *Applied Thermal Engineering* **18**(11): 963-980.
- Ladommatos N, Abdelhalim S, Zhao H (1998b). Effects of Exhaust Gas Recirculation Temperature on Diesel Engine Combustion and Emissions. *Proceedings of the Institution of Mechanical Engineers, Part D: Journal of Automobile Engineering* **212**(6): 479-500.
- Ladommatos N, Abdelhalim S, Zhao H (2000). The Effects of Exhaust Gas Recirculation on Diesel Combustion and Emissions. *Int. J. Engine Research* **1**: 107-126.
- Ladommatos N, Abdelhalim S, Zhao H, Hu Z (1998c). The Effects of Carbon Dioxide in Exhaust Gas Recirculation on Diesel Engine Emissions. *Proceedings of the Institution of Mechanical Engineers, Part D: Journal of Automobile Engineering* **212**(1): 25-42.
- Laguitton O, Crua C, Cowell T, Heikal MR, Gold MR (2007). The Effect of Compression Ratio on Exhaust Emissions from a PCCI Diesel Engine. *Energy Conversion and Management* **48**(11): 2918-2924.
- Langridge S, Fessler H (2002). Strategies for High EGR Rates in a Diesel Engine. *SAE Paper*: 2002-01-0961.

Lechner GA, Jacobs TJ, Chryssakis CA, Assanis DN, Siewert RM (2005). Evaluation of a Narrow Spray Cone Angle, Advanced Injection Timing Strategy to Achieve Partially Premixed Compression Ignition Combustion in a Diesel Engine. *SAE Paper*: 2005-01-0167.

Lee S, Reitz RD (2006). Spray Targeting to Minimize Soot and CO Formation in Premixed Charge Compression Ignition (PCCI) Combustion with a HSDI Diesel Engine. *SAE Paper*: 2006-01-0918.

Lee S, Shin D, Lee J, Sung N (2004). Soot Emission from a Direct Injection Diesel Engine. *SAE Paper*: 2004-01-0927.

Lefebvre A, Guilain S (2005). Modelling and Measurement of the Transient Response of a Turbocharged SI Engine. *SAE Paper*: 2005-01-0691.

Lehtoranta K, Matilainen P, Senbrygg J-M, Lievonen A, Kinnunen T-J, Keskinen J, *et al.* (2007). Particle Oxidation Catalyst in Light-Duty and Heavy-Duty Diesel Applications. *SAE Paper*: 2007-2024-0093.

Liebig D, Krane W, Ziman P, Garbe T, Hoenig M (2008). The Response of a Closed Loop Controlled Diesel Engine on Fuel Variation. *SAE Paper*: 2008-01-2471.

Maiboom A, Tauzia X, Hétet J-F (2009). Influence of EGR Unequal Distribution from Cylinder to Cylinder on NO<sub>x</sub>-PM Trade-off of a HSDI Automotive Diesel Engine. *Applied Thermal Engineering* **29**(10): 2043-2050.

Masoudi M, Zink U, Then P, Cash T, Thompson D, Heibel A (2000). Predicting Pressure Drop of Wall-Flow Diesel Particulate Filters -Theory and Experiment. *SAE Paper*: 2000-01-0184.

MECA (2001). *Emission Controls for Diesel Engines*. Manufacturers of Emission Controls Association.

Mendez S, Kashdan JT, Bruneaux G, Thirouard B, Vangraefschepe F (2009). Formation of Unburned Hydrocarbons in Low Temperature Diesel Combustion. *SAE Int. J. Engines* **2**(2): 205-225.

Michailidis AD, Stobart RK, McTaggart-Cowan GP (2010). Fuel-line Stationary Waves and Variability in CI Combustion during Complex Injection Strategies. In: ASME 2010 Internal Combustion Engine Division Fall Technical Conference. San Antonio, Texas, USA.

Millo F, Ferraro CV, Bernardi MG, Barbero S, Pasero P (2009). Experimental and Computational Analysis of Different EGR Systems for a Common Rail Passenger Car Diesel Engine. *SAE Paper*: 2009-01-0672.

Minami T, Yamaguchi I, Shintani M, Tsujimura K, Suzuki T (1990). Analysis of Fuel Spray Characteristics and Combustion Phenomena Under High Pressure Fuel Injection. *SAE Paper*: 900438.

Molina S, Payri F, Benajes J, Pastor JV (2002). Influence of the Post-Injection Pattern on Performance, Soot and Nox Emissions in a HD Diesel Engine. *SAE Paper*: 2002-01-0502.

- Montgomery DC (2009). *Design and Analysis of Experiments*. Seventh edn. Wiley.
- Morgan R, Gold M, Laguitton O, Crua C, Heikal M (2003). Characterization of the Soot Formation Processes in a High Pressure Combusting Diesel Fuel Spray. *SAE Paper*: 2003-01-3086.
- Muench J, Leppelt R, Dotzel R (2008). Extruded Zeolite Based Honeycomb Catalyst for NO<sub>x</sub> Removal from Diesel Exhaust. *SAE Paper*: 2008-01-1024.
- Musculus MPB (2006). Multiple Simultaneous Optical Diagnostic Imaging of Early-Injection Low-Temperature Combustion in a Heavy-Duty Diesel Engine. *SAE Paper*: 2006-01-0079.
- Naidja A, Krishna CR, Butcher T, Mahajan D (2003). Cool Flame Partial Oxidation and Its Role in Combustion and Reforming of Fuels for Fuel Cell Systems. *Progress in Energy and Combustion Science* **29**(2): 155-191.
- Nakayama S, Ibuki T, Hosaki H, Tominaga H (2008). An Application of Model Based Combustion Control to Transient Cycle-by-Cycle Diesel Combustion. 2008-01-1311.
- Narayanaswamy K, Rutland CJ (2006). A Modeling Investigation of Combustion Control Variables During DI-Diesel HCCI Engine Transients. *SAE Paper*: 2006-01-1084.
- Navratil J, Macek J, Polasek M (2004). Simulation of a Small Turbocharged Gasoline Engine in Transient Operation. *SAE Paper*: 2004-01-0995.
- Neely GD, Sasaki S, Yiqun Huang, Leet JA, Stewart DW (2005). New Diesel Emission Control Strategy to Meet US Tier 2 Emissions Regulations. *SAE Paper*: 2005-01-1091.
- Nieuwstadt MJV, Kolmanovsky IV, Moraal PE (2000). Coordinated EGR-VGT Control for Diesel Engines: an Experimental Comparison. *SAE Paper*: 2000-01-0266.
- Nitu B, Singh I, Zhong L, Badreshany K, Henein NA, Bryzik W (2002). Effect of EGR on Autoignition, Combustion, Regulated Emissions and Aldehydes in DI Diesel Engines. *SAE Paper*: 2002-01-1153.
- Oberdorster G, Ferin J, Lehnert BE (1994). Correlation between Particle Size, in Vivo Particle Persistence, and Lung Injury. *Environmental Health Perspectives* **102**: 173-179.
- Oberdorster G, Sharp Z, Atudorei V, Elder A, Gelein R, Lunts A, *et al.* (2002). Extrapulmonary Translocation of Ultrafine Carbon Particles Following Whole-body Inhalation Exposure of Rats. *Journal of Toxicology and Environmental Health, Part A* **65**(20): 1531 - 1543.
- Ogawa H, Li T, Miyamoto N (2007). Characteristics of Low Temperature and Low Oxygen Diesel Combustion with Ultra-high Exhaust Gas Recirculation. *International Journal of Engine Research*. **8**: 365-378.
- Olivier C, António P, Stephane J (2005). Detailed Chemistry-based Auto-ignition Model Including Low Temperature Phenomena Applied to 3-D Engine Calculations. *Proceedings of the Combustion Institute* **30**(2): 2649-2656.

- Osada H, Aoyagi Y, Shimada K, Goto Y, Suzuki H (2010). Reduction of NO<sub>x</sub> and PM for a Heavy Duty Diesel Using 50% EGR Rate in Single Cylinder Engine. *SAE Paper*: 2010-01-1120.
- Otobe T, Grigoriadis P, Sens M, Berndt R (2010). Method of Performance Measurement for Low Turbocharger Speeds. In: 9th International Conference on Turbochargers and Turbocharging. London: IMechE.
- Page VJ, Garner CP, Hargrave GK, Versteeg HK (2002). Development of a Validated CFD Process for the Analysis of Inlet Manifold Flows With EGR. *SAE Paper*: 2002-01-0071.
- Park C, Kook S, Bae C (2004). Effects of Multiple Injections in a HSDI Diesel Engine Equipped with Common-rail Injection System. *SAE Paper*: 2004-01-0127.
- Payri F, Benajes J, Galindo J, Serrano JR (2002). Modelling of Turbocharged Diesel Engines in Transient Operation. Part2: Wave Action Models for Calculating the Transient Operation in a High Speed Direct Injection Engine. *Proceedings of the Institution of Mechanical Engineers, Part D: Journal of Automobile Engineering* **216**(6): 479-493.
- Payri F, Luján J, Climent H, Pla B (2010). Effects of the Intake Charge Distribution in HSDI Engines. *SAE Paper*: 2010-01-1119.
- Pickett LM, Kook S, Williams TC (2009). Transient Liquid Penetration of Early-Injection Diesel Sprays. *SAE Paper*: 2009-01-0839.
- Pickett LM, Siebers DL (2004). Soot in Diesel Fuel Jets: Effects of Ambient Temperature, Ambient Density, and Injection Pressure. *Combustion and Flame* **138**(1-2): 114-135.
- Pilling MJ (1997). *Low - Temperature Combustion and Autoignition*. edn, vol. Volume 35. Elsevier.
- Rakopoulos CD, Giakoumis EG (2009a). *Diesel Engine Transient Operation - Principles of Operation and Simulation Analysis*. edn. Springer.
- Rakopoulos CD, Mavropoulos GC (2009b). Effects of Transient Diesel Engine Operation on Its Cyclic Heat Transfer: an Experimental Assessment. *Proceedings of the Institution of Mechanical Engineers, Part D: Journal of Automobile Engineering* **223**(11): 1373-1394.
- Risberg P, Kalghatgian G, Angstrom H-E, Wahlin F (2005). Auto-ignition Quality of Diesel-like Fuels in HCCI Engines. *SAE Paper*: 2005-01-2127.
- Ross PJ (1996). *Taguchi Techniques for Quality Engineering*. Second edn. McGraw-Hill.
- Sarangi AK, McTaggart-Cowan GP, Garner CP (2010). The Effects of Intake Pressure on High EGR Low Temperature Diesel Engine Combustion. *SAE Paper*: 2010-01-2145.
- Serrano JR, Arnau FJ, Dolz V, Piqueras P (2009a). Methodology for Characterisation and Simulation of Turbocharged Diesel Engines Combustion during Transient

Operation. Part 1: Data Acquisition and Post-processing. *Applied Thermal Engineering* **29**(1): 142-149.

Serrano JR, Climent H, Guardiola C, Piqueras P (2009b). Methodology for Characterisation and Simulation of Turbocharged Diesel Engines Combustion during Transient Operation. Part 2: Phenomenological Combustion Simulation. *Applied Thermal Engineering* **29**(1): 150-158.

Shirakawa T, Miura M, Itoyama H, Aiyoshizawa E, Kimura S (2001). Study of Model-based Cooperative Control of EGR and VGT for a Low-temperature, Premixed Combustion Diesel Engine. *SAE Paper*: 2001-01-2006.

Shutty J, Czarnowski R (2009). Control Strategy for a Dual Loop EGR System to Meet Euro 6 and Beyond. In: *2009 Directions in Engine-Efficiency and Emissions Reduction Research (DEER) Conference*. Dearborn, Michigan.

Siewert RM, Krieger RB, Huebler MS, Baruah PC, Khalighi B, Wesslau M (2001). Modifying an Intake Manifold to Improve Cylinder-to-Cylinder EGR Distribution in a DI Diesel Engine Using Combined CFD and Engine Experiments. *SAE Paper*: 2001-01-3685.

Simescu S, Fiveland SB, Dodge LG (2003). An Experimental Investigation of PCCI-DI Combustion and Emissions in a Heavy-Duty Diesel Engine. *SAE Paper*: 2003-01-0345.

Simescu S, III TWR, Neely GD, Matheaus AC, Surampudi B (2002). Partial Pre-Mixed Combustion with Cooled and Uncooled EGR in a Heavy-Duty Diesel Engine. *SAE Paper*: 2002-01-0963.

Smith OI (1981). Fundamentals of Soot Formation in Flames with Application to Diesel Engine Particulate Emissions. *Prog Energy Combust Sci* **7**: 275–291.

Su W, Lin T, Pei Y (2003). A Compound Technology for HCCI Combustion in a DI Diesel Engine Based on the Multi-Pulse Injection and the BUMP Combustion Chamber. *SAE Paper*: 2003-01-0741.

Tan P-q, Deng K, Lu J-x (2004). Analysis of Particulate Matter Composition from a Heavy-duty Diesel Engine. *Proceedings of the Institution of Mechanical Engineers, Part D: Journal of Automobile Engineering* **218**(11): 1325-1331.

Tao T, Xie Y, Dawes S, Melscoet-Chauvel I, Pfeifer M, Spurk PC (2004). Diesel SCR NOx Reduction and Performance on Washcoated SCR Catalysts. *SAE Paper*: 2004-01-1293.

Taylor CF (1985). *The Internal Combustion Engine in Theory and Practice*. edn, vol. 1. The M.I.T. Press.

Tennison P, Lambert C, Levin M (2004). NOx Control Development with Urea SCR on a Diesel Passenger Car. *SAE Paper*: 2004-01-1291.

Theis JR, Ura J, McCabe R (2010). The Effects of Sulfur Poisoning and Desulfation Temperature on the NOx Conversion of LNT+SCR Systems for Diesel Applications. *SAE Paper*: 2010-01-0300.

- Thring RH (1989). Homogeneous-Charge Compression-Ignition (HCCI) Engines. *SAE Paper*: 892068.
- Tomazic D, Pfeifer A (2002). Cooled EGR - A Must or an Option for 2002/04. *SAE Paper*: 2002-01-0962.
- Tree DR, Svensson KI (2007). Soot Processes in Compression Ignition Engines. *Progress in Energy and Combustion Science*, **33**(3): 272-309.
- Vitek O, Macek J, Polasek M, Schmerbeck S, Kammerdiener T (2008). Comparison of Different EGR Solutions. *SAE Paper*: 2008-01-0206.
- Wahlin F, Cronhjort A (2004). Fuel Sprays for Premixed Compression Ignited Combustion - Characteristics of Impinging Sprays. *SAE Paper*: 2004-01-1776.
- Walter B, Gatellier B (2002). Development of the High Power NADITM Concept Using Dual Mode Diesel Combustion to Achieve Zero NOx and Particulate Emissions. *SAE Paper*: 2002-01-1744.
- Wang J (2007). Hybrid Robust Control for Engines Running Low Temperature Combustion and Conventional Diesel Combustion Modes. *SAE Paper*: 2007-01-0770.
- Wang Y (2006). *Introduction to Engine Valvetrains*. edn. SAE.
- Warnatz J, Maas U, Dibble RW (1999). *Combustion - Physical and Chemical Fundamentals, Modeling and Simulation, Experiments, Pollutant Formation*. Second edn. Springer: Berlin.
- Watson N, Janota MS (1984). Turbocharging the Internal Combustion Engine.
- Westbrook CK (2000). Chemical Kinetics of Hydrocarbon Ignition in Practical Combustion Systems. *Proceedings of the Combustion Institute* **28**(2): 1563-1577.
- Wijetunge RS, Brace CJ, Hawley JG, Vaughan ND, Horrocks RW, Bird GL (1999). Dynamic Behavior of a High Speed Direct Injection Diesel Engine. *SAE Transactions—Journal of Engines* **108**: Paper No. 1999-01-0829.
- Wilhelmsson C, Vressner A, Tunestål P, Johansson B, Särner G, Aldén M (2005). Combustion Chamber Wall Temperature Measurement and Modeling During Transient HCCI Operation. *SAE Paper*: 2005-01-3731.
- Williams AM, Garner CP, Binner JGP (2008). Analysis and optimization of gel-cast ceramic foam diesel particulate filter performance. *Proceedings of the Institution of Mechanical Engineers, Part D: Journal of Automobile Engineering* **222**(11): 2235-2247.
- Williams AM, Garner CP, Harry JE, Hoare DW, Mariotti D, Ladha KS, *et al.* (2009). Low Power Autoselective Regeneration of Monolithic Wall Flow Diesel Particulate Filters. *SAE Paper*: 2009-01-1927.
- Wirojsakunchai E, Schroeder E, Kolodziej C, Foster DE, Schmidt N, Root T, *et al.* (2007). Detailed Diesel Exhaust Particulate Characterization and Real-Time DPF Filtration Efficiency Measurements During PM Filling Process. *SAE Paper*: 2007-01-0320.



Woods M, Kamo R, Bryzik W (2000). High-Pressure Fuel Injection for High-Power Density Diesel Engines. *SAE Paper*: 2000-01-1186.

Xi J, Zhong BJ (2006). Soot in Diesel Combustion Systems. *Chemical Engineering & Technology* **29**(6): 665-673.

Xu L, Graham G, McCabe R, Hoard J, Yang J (2008). The Feasibility of an Alumina-Based Lean NOx Trap (LNT) for Diesel and HCCI Applications. *SAE Paper*: 2008-01-0451.

Yamada H, Goto Y, Tezaki A (2006). Analysis of Reaction Mechanisms Controlling Cool and Thermal Flame with DME Fueled HCCI Engines. *SAE Paper*: 2006-01-3299.

Yao M, Zheng Z, Liu H (2009). Progress and Recent Trends in Homogeneous Charge Compression Ignition (HCCI) Engines. *Progress in Energy and Combustion Science* **35**(5): 398-437.

Yokomura H, Kouketsu S, Kotooka S, Akao Y (2004). Transient EGR Control for a Turbocharged Heavy Duty Diesel Engine. *SAE Paper*: 2004-01-0120.

Yun H, Reitz RD (2007). An Experimental Investigation on the Effect of Post-Injection Strategies on Combustion and Emissions in the Low-Temperature Diesel Combustion Regime. *Journal of Engineering for Gas Turbines and Power* **129**(JANUARY 2007).

Yun H, Reitz RD (2005a). Combustion Optimization in the Low-temperature Diesel Combustion Regime. *International Journal of Engine Research* **6**(5): 513-524.

Yun H, Sellnau M, Milovanovic N, Zuelch S (2008). Development of Premixed Low-Temperature Diesel Combustion in a HSDI Diesel Engine. *SAE*: 2008-01-0639.

Yun H, Sun Y, Reitz RD (2005b). An Experimental and Numerical Investigation on the Effect of Post Injection Strategies on Combustion and Emissions in the Low-Temperature Diesel Combustion Regime. *ASME Internal Combustion Engine Division 2005 Spring Technical Conference*.

Zhan R, Huang Y, Khair M (2006). Methodologies to Control DPF Uncontrolled Regenerations. *SAE Paper*: 2006-01-1090.

Zhang L (1999). A Study of Pilot Injection in a DI Diesel Engine. *SAE Paper*: 1999-01-3493.

Zhao F, Asmus TW, Assanis DN, Dec JE, Eng JA, Najt PM (eds) (2003). *Homogeneous Charge Compression Ignition Engines*. SAE.

Zheng M, Tan Y, Reader GT, Asad U, Han X, Wang M (2009). Prompt Heat Release Analysis to Improve Diesel Low Temperature Combustion. *SAE Paper*: 2009-01-1883.

Zhong L, Singh IP, Han J, Lai M-C, Henein NA (2003). Effect of Cycle-to-Cycle Variation in the Injection Pressure in a Common Rail Diesel Injection System on Engine Performance. *SAE Paper*: 2003-01-0699.

## Appendices

### **Appendix A1 Design of Intake and Exhaust Surge Tanks**

A Ricardo WAVE model was created based on the single-cylinder research engine to simulate the performance of the test engine. Different size surge tanks were simulated to evaluate the influence of the surge tank design on the intake and exhaust flow pulsations. The relative size of surge tanks was based on the engine displacement volume ( $V_d$ ); 100, 50, 25 and 0 times of the  $V_d$  were selected for the simulation. Figure A1.1 shows the effects of the surge tank size on the pressures in the inlet pipe upstream of the surge tank, intake manifold, exhaust manifold and exhaust pipe downstream of the exhaust surge tank for 2500 rpm and 1500 rpm conditions.

The introduction of surge tanks significantly reduced the pulsations in the intake and exhaust systems. An increase in the tank size led to lower pulsations in the pipes both downstream and upstream of the tanks. However, the damping effects of the tanks become marginal when the size of the tanks reaches 50 times of the engine displacement volume. Thus, surge tanks of 50 times of the engine displacement volume were selected for the engine.

Measurements of the intake and exhaust manifold pressures with and without surge tanks are compared and shown in Figure A1.2. The results indicate that with the intake surge tank, the pressure drop during the intake stroke in the intake manifold was reduced. The existence of intake surge tank reduced the negative pressure in the intake manifold caused by intake stroke. However, the exhaust manifold pressure was increased, especially during the exhaust stroke. The exhaust back pressure valve installed downstream of the exhaust surge tank has increased the flow resistance in the exhaust system; this could be the cause of the increased exhaust pressures. The increased pressure pulsations during the combustion and expansion strokes are of the results of the surge tanks, as there are no gases flows across the engine during these strokes. For the non-surge tank case, there would be very little flow in the manifolds during both the intake and exhaust valves are closed. When the surge tanks are installed, they tend to create some flows in the manifolds during the non-gases-exchange period and lead to the increased pressure pulsations.

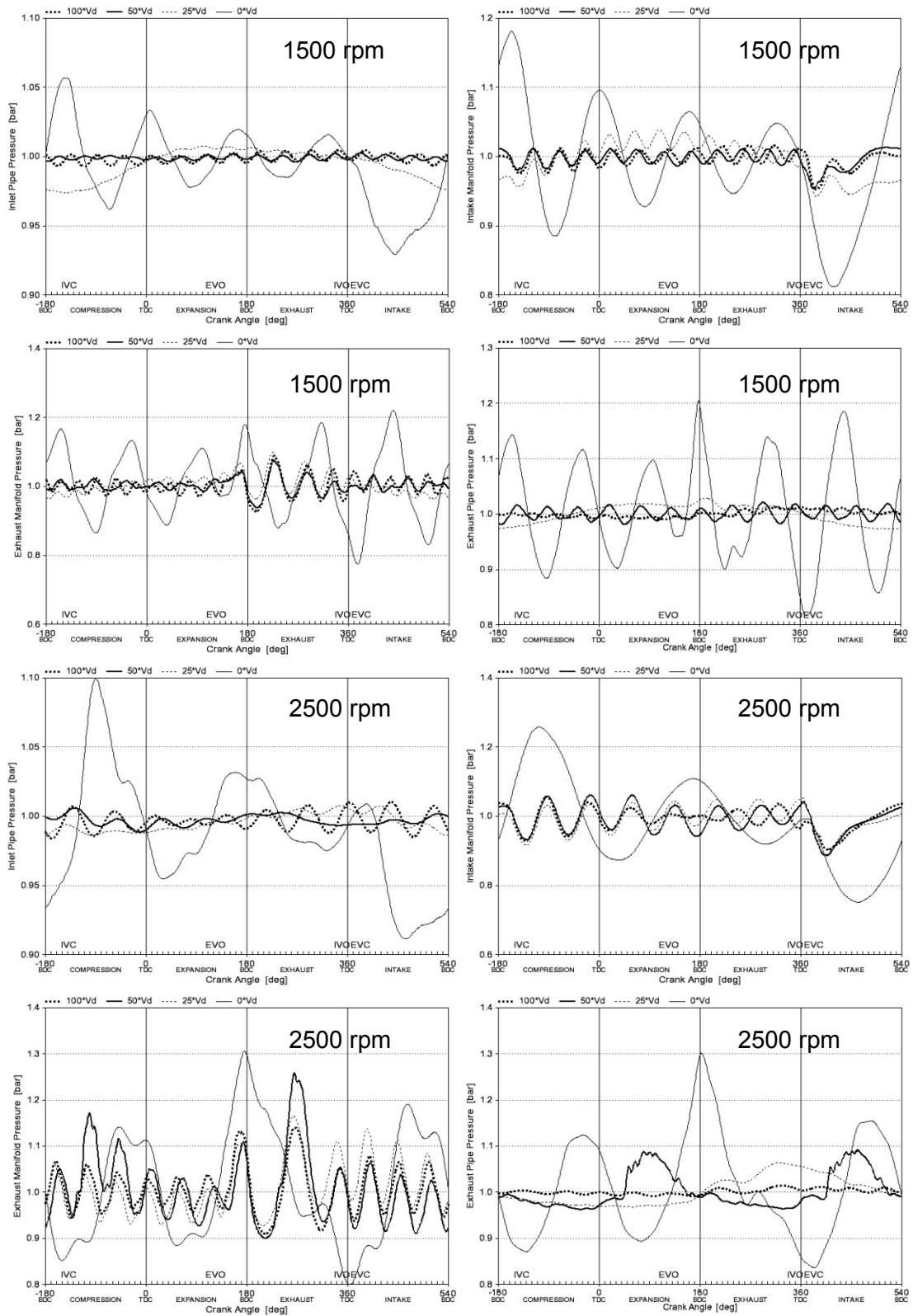


Figure A1.1 Simulation results of the effects of surge tanks size on the pressure pulsations in the intake and exhaust system

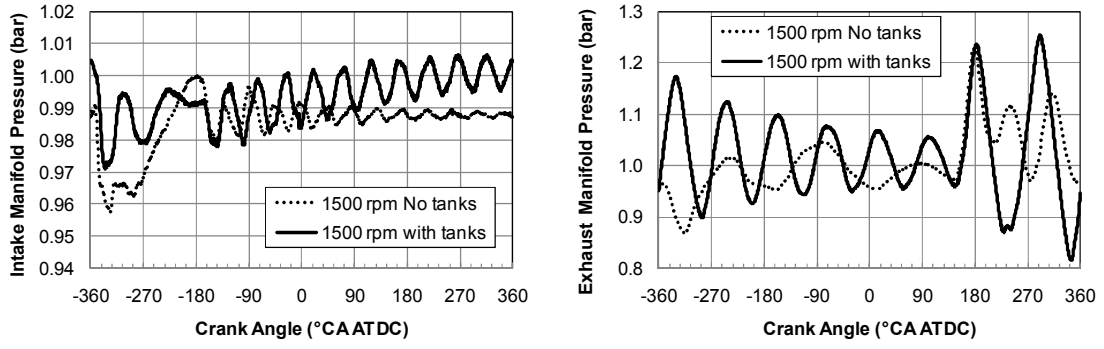


Figure A1.2 Effects of surge tanks on the pressure pulsations in the intake and exhaust manifolds

## **Appendix A2 Engine Instrumentation**

Table A2.1 Engine instrumentation list

Equipment	Measurement	Range	Resolution	Stated accuracy	Manufacturer
AVL 733 Dynamic Fuel Meter	Fuel flow rate	0- 125 kg/hr	0.01 kg/h	0.12%	AVL
Air flow meter	Air mass flow	10-140 kg/h	0.1 kg/h	5%	Cole-Parmer
AVL 364C angle encoder	Crank shaft angle	360-7200 pulse/rev	0.05 °CA		AVL
AVL QC34C	Cylinder pressure	0-250 bar	19.54 pC/bar	±0.2%	AVL
KISTLER 4045A5	Absolute pressure	0-5 bar	100 mv/bar	±0.3%	KISTLER
Omegadyne PX219-060G10V, PX219-060GI transducers	Gauge pressure	0-4.1 bar		±.5%	Omega
AVL SL31D-2000 High Pressure Transducer	Fuel pipe pressure	0-2000 bar	4.5x10 <sup>3</sup> mV/V /MPa	± 0.5 %	AVL
K-type Thermal couple	Temperature	0-899°C	0.1°C		Omega
RTD	Temperature	-30 -350°C	0.1°C		Omega
DAQ Chassis cDAQ9172	Modular Chassis				National Instruments
NI 9211	Thermal couple				National Instruments
NI 9217	RTD				National Instruments
NI 9215	High speed Voltage	±10V			National Instruments
NI 9205	Voltage	±10V			National Instruments
NI 9208	Current	4-16 mA			National Instruments
NI 9401	Digital IO				National Instruments

## Appendix A3 Emissions measurement equipment

Table A3.1 Emissions measurement equipment specifications

Equipment	Measurement	Range	Resolution	Stated Accuracy	Operating Condition
AVL 415 Smoke Meter	Filter Smoke Number	0-10 FSN	0.01 FSN	±3% of measurement value	-100 to 400 mbar abs; T ≤ 600°C
Horiba MEXA7100 HEGR	NO <sub>x</sub>	0-10 ~ 500, 1k ~ 10k ppm	≤ 2.0% FS	σ ≤ ±0.5 FS%	0.5 L/min
	CO <sub>2</sub>	0-0.5 ~ 20 vol%	≤ 1.0% FS	min(σ ≤ ±1.0FS%, σ ≤ ±2.0RS%)	0 to 30 kPa abs. pressure for normal lines, -66.7 to 0 kPa for EGR line; 2 L /min
	CO	0-50 ~ 5k ppm	≤ ±0.5% FS	min(σ ≤ ±1.0 FS%, σ ≤ ±2.0 RS%)	3 L/min
	HC	0-10 ~ 500, 0-1k ~ 50k ppmC1	≤ 1.0% FS	σ ≤ ± 0.5% FS	0.5 L/min 113°C or 191°C
	O <sub>2</sub>	0-1-25 vol%	≤ 1.0% FS (O <sub>2</sub> ≥ 5 vol%), ≤ 2.0% FS (O <sub>2</sub> ≤ 5 vol%)	σ ≤ ± 0.5% FS	0.7 L/min
Horiba MEXA 584L	CO	0-10 vol%	0.01 vol%	0.01 vol% or 1.7 RS%	
Cambustion DMS500	Particle size distribution	5–1000 nm			≤ 1.5 bar gauge pressure
Cambustion NDIR500	CO <sub>2</sub>	0-5-25 vol%	0.01 vol%	±2% FS	5 L/min
	CO	0-5-15 vol%	0.01 vol%	±2% FS	5 L/min

FS – full scale; RS - reading scale

## **Appendix A4 Residual Gas Fraction Measurement and Prediction\***

### ***A4.1 Introduction***

During internal combustion engine operation, incomplete gas exchange results in some combustion products being retained in the combustion chamber during the subsequent cycle. The higher temperatures and charge dilution effects of these residual gases can influence the engine combustion behaviour and emissions formation (Heywood, 1988).

Traditionally, diesel engines trap relatively small fractions of exhaust gas and have higher tolerance to residual gas compared with spark ignition engines, due to their throttle-free design, high compression ratio and overall lean combustion processes (Heywood, 1988). However, with the introduction of advanced engine technologies, such as exhaust gas recirculation (EGR, especially when using exhaust/intake throttling to drive the exhaust gas into the intake manifold) and exhaust aftertreatment systems, the difference between intake and exhaust pressures has been increased (Masoudi *et al.*, 2000; Williams *et al.*, 2008). Furthermore, when a diesel engine is operated with high levels of EGR, such as those found in 'low temperature combustion' modes (Beatrice *et al.*, 2007; Ogawa *et al.*, 2007), combustion stability can be very sensitive to changes in residual gas fraction (RGF).

Species such as carbon dioxide (CO<sub>2</sub>), nitric oxide (NO), and unburned hydrocarbons (HC) can be used as tracers to detect the concentration of trapped exhaust gas (Cho *et al.*, 2001; Davis *et al.*, 2008; Ford *et al.*, 1999; Francqueville *et al.*, 2006). However, the formation of NO and HC depends on engine operation conditions, such as speed, load, intake temperature and charge dilution. The absolute values of the gases concentrations also are relatively low. CO<sub>2</sub>, however, is the most stable and has the highest concentration in the exhaust gases and hence it is an ideal candidate for determining RGF.

---

\* Part of the work presented in this section was presented at the SAE Powertrains, Fuels and Lubricants Meeting, June 2009, Florence, ITALY. S. Cong, G. P. McTaggart-Cowan and C. P. Garner. Measurement of Residual Gas Fraction in a Single Cylinder HSDI Diesel Engine through Skip-firing. SAE paper 2009-01-1961.

The residual gas generally comes from two sources. The first is due to the clearance and crevice volumes at TDC. The quantity of this part of the residual gas is dictated by the engine geometry and the clearance and crevice volume pressure and temperature. Some of this residual gas may be expelled into the intake manifold at the start of the intake stroke, in cases where the in-cylinder pressure at this point is higher than the intake manifold pressure. The other part of the residual gas comes from the reverse flow of exhaust gas from the exhaust manifold into the combustion chamber during the intake stroke while exhaust valves are still open; i.e. during the valve overlap period.

Measuring of the RGF is normally carried out by in-cylinder gas sampling (Cho *et al.*, 2001; Davis *et al.*, 2008; Ford *et al.*, 1999), in which case the RGF is the ratio of the compression and exhaust concentrations. However, in-cylinder sampling probes are difficult to install, furthermore, the in-cylinder combustion products are not homogeneously distributed (Francqueville *et al.*, 2006; Liu *et al.*, 2004), and hence the location of the sampling probe can influence the result. Exhaust manifold gas sampling techniques, however, do not need complicated sampling systems and avoid the measurement errors due to the distribution of exhaust gas in the combustion chamber. This study proposes and evaluates a method for determining RGF using exhaust manifold gas sampling techniques in conjunction with skip-firing a diesel engine.

#### **A4.2 Research apparatus**

Table A4.1 lists the engine operating conditions. The engine was operated at 1500 and 3000 rpm and at 3 and 6 bar gross indicated mean effective pressure (IMEP). To evaluate the effects of exhaust back pressure on the RGF and engine combustion, three different exhaust throttle plates were used to restrict the exhaust gas flow. These plates had orifices of 18, 15, or 12 mm diameter drilled in them centrally, and were mounted in the exhaust pipe 60 mm downstream of the exhaust port. Combined with the unthrottled 35 mm diameter pipe, four sets of data for each operating condition were collected and compared.

In this work, the exhaust back pressure (EBP) was calculated by time-averaging the exhaust manifold pressure during the exhaust-valve open period. The maximum EBP achieved was less than 2.2 bar with 12 mm throttle diameter at 3000 rpm 6 bar IMEP operation condition.



Table A4. 1 Engine operating conditions

Engine speed (rpm)	1500	1500	3000	3000
IMEP (bar)	3	6	3	6
SoI (CAD ATDC)	-3	-3	-11.25	-11.25
Fuel injection pressure (bar)	500	600	700	900
Exhaust Throttle Plate Orifice Diameters diameter (mm)	35	18	15	12

#### **CO and CO<sub>2</sub> emissions analyzer**

Non-Dispersive Infra-Red (NDIR) detectors are the industry standard method of measuring the concentration of carbon oxides (CO and CO<sub>2</sub>). Each constituent gas in a sample will absorb some infrared light at a particular frequency. By directing an infrared light beam through a sample cell (containing CO or CO<sub>2</sub>), and measuring the amount of infrared light absorbed by the sample at the necessary wavelength, an NDIR detector is able to measure the volumetric concentration of CO or CO<sub>2</sub> in the sample (Sutela *et al.*, 2001).

A Combustion NDIR500 fast CO and CO<sub>2</sub> analyzer was used to measure the transient CO<sub>2</sub> concentration in the exhaust manifold. It had a response time of < 8 ms for a 10% to 90% of full scale change and non-linearity was less than ±2% full scale (Sutela *et al.*, 2001). The sampling probe was fixed 25 mm from the exhaust port, with its head located in the centre of the exhaust flow stream. The sampling rate was set to 1000 samples per second for the tests.

#### **Novel RGF measurement method**

The concept of the RGF measurement through exhaust manifold gas sampling with skip-firing was illustrated in Figure 6.1. The CO<sub>2</sub> concentration measured near to the exhaust port gives the concentration of CO<sub>2</sub> formed in the previous combustion cycle. If the fuel injection is stopped, there will be no fuel injection or combustion in the subsequent cycle, and the exhaust gas from this skip-fired cycle is, therefore, the mixture of the trapped residual gases and fresh intake air. This is defined in Equation (1), with [CO<sub>2</sub>]<sub>f</sub> representing the firing cycle CO<sub>2</sub> concentration, [CO<sub>2</sub>]<sub>rg</sub> representing the first motoring cycle CO<sub>2</sub> concentration and [CO<sub>2</sub>]<sub>amb</sub> representing the ambient CO<sub>2</sub> concentration as measured after 5 non-firing cycles (value ~0.03%).

$$\text{RGF(\%)} = \frac{([\text{CO}_2]_{\text{rg}} - [\text{CO}_2]_{\text{bg}})}{([\text{CO}_2]_{\text{f}} - [\text{CO}_2]_{\text{amb}})} \times 100\% \quad (1)$$

where  $[CO_2]_f$  is the last firing cycle  $CO_2$  concentration;  $[CO_2]_{rg}$  is the first skip-firing cycle  $CO_2$  concentration;  $[CO_2]_{amb}$  is the ambient  $CO_2$  concentration.

Examples of exhaust gas  $CO_2$  concentration measurements during successive skip firing cycles were shown in Figure 6.2. There is a delay between exhaust valves opening (EVO) and detection of the  $CO_2$  concentration at the sensor. The initial part of the  $CO_2$  reading during the early part of the cycle is discarded due to large pressure oscillations in the exhaust manifold which cause the measured  $CO_2$  values to be inaccurate. The  $CO_2$  emitted from the first motoring cycle during the skip fire event originates from the trapped combustion products from the previous firing cycle. These two effective  $CO_2$  measurements are averaged separately and used to determine the residual gas fraction, as defined above.

### A4.3 Results

The method of RGF measurement was tested on the single-cylinder research engine at different operation conditions. Each of the operating conditions was repeated for 10 successive skip-firing events and the variability in the calculated value was found to be virtually constant for every operation condition. Figure A4.1 shows the RGF measurement results vs. EBP at different engine operating conditions with the standard (unthrottled) exhaust system. The 95% confidence intervals are used as error bars in the plotted data, which are less than 2.5%. As the figure shows, the RGF was more sensitive to operating condition than EBP.

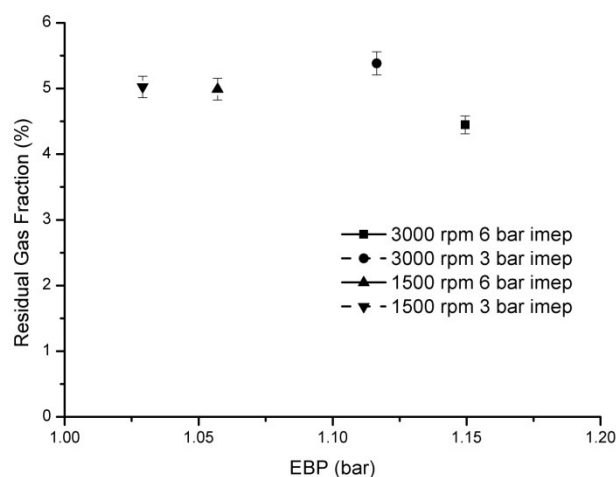


Figure A4.1 RGF measurement results without throttling in the exhaust system vs. exhaust back pressure

The influence of exhaust throttling on exhaust back pressure is shown in Figure A4.2. The EBP here is the average of the absolute exhaust manifold pressure during the exhaust-valve open period (from EVO to EVC). As expected, the exhaust back pressure increased with the reduction of the throttle diameter. At higher speed and load operating conditions the back pressure increased more for a given orifice diameter, due to the higher gas flow rates in the system.

Figure A4.3 shows that the RGF increased linearly with exhaust back pressure (EBP). The slope between the RGF and EBP increase was approximately 4% per bar. At the same engine speed, the lower load operating condition cases had higher RGF measurements; this was due to the different exhaust temperatures for the different loads. At lower load conditions, the exhaust temperatures were lower (by approximately 170°C) than at high load at the same speed and hence the exhaust gas densities were higher. For a similar volume of exhaust gas trapped in the cylinder, the higher the density of the gas the higher the RGF.

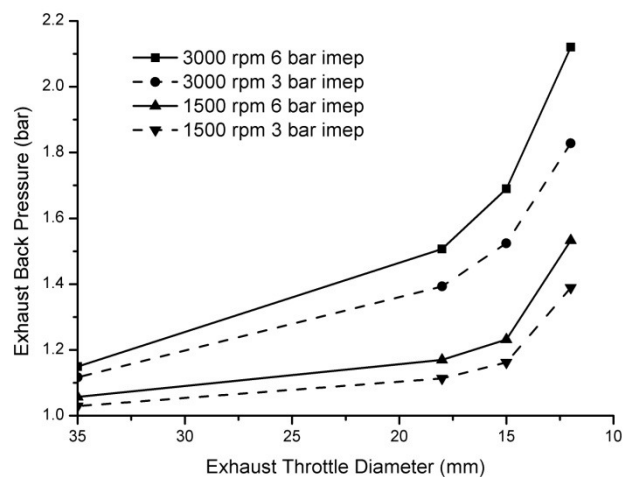


Figure A4.2 Exhaust back pressure vs. throttle diameter

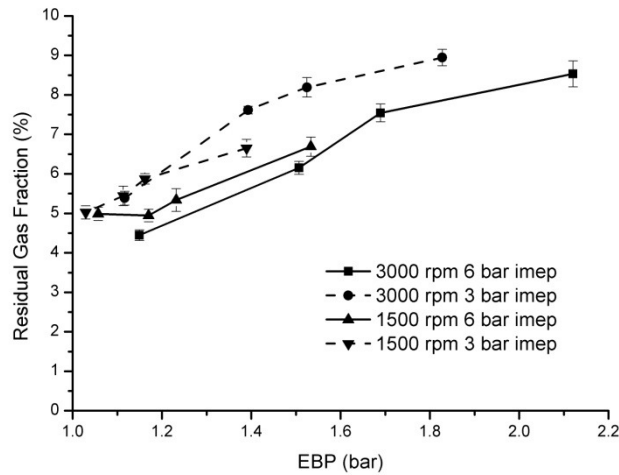


Figure A4.3 RGF vs. exhaust back pressure

The back-flow of exhaust gas into the combustion chamber and intake manifold during the valve overlap period played an important role on the high RGFs at high EBP situations. In Figure A4.4, the intake manifold, in-cylinder and exhaust manifold pressures during the intake stroke of the 3000 rpm 6 bar IMEP case are compared for the unthrottled and throttled (12 mm orifice) conditions. With throttling, the in-cylinder pressure was elevated by the exhaust back pressure during the exhaust stroke. During the valve overlap period, both the exhaust and in-cylinder pressure were higher than the intake manifold pressure. This resulted in a back-flow of exhaust gas into the intake manifold, which caused an increase in the intake manifold pressure, as shown in the figure. The exhaust gas in the intake manifold was re-inducted into the cylinder before the intake valves closed, contributing to the increased RGF.

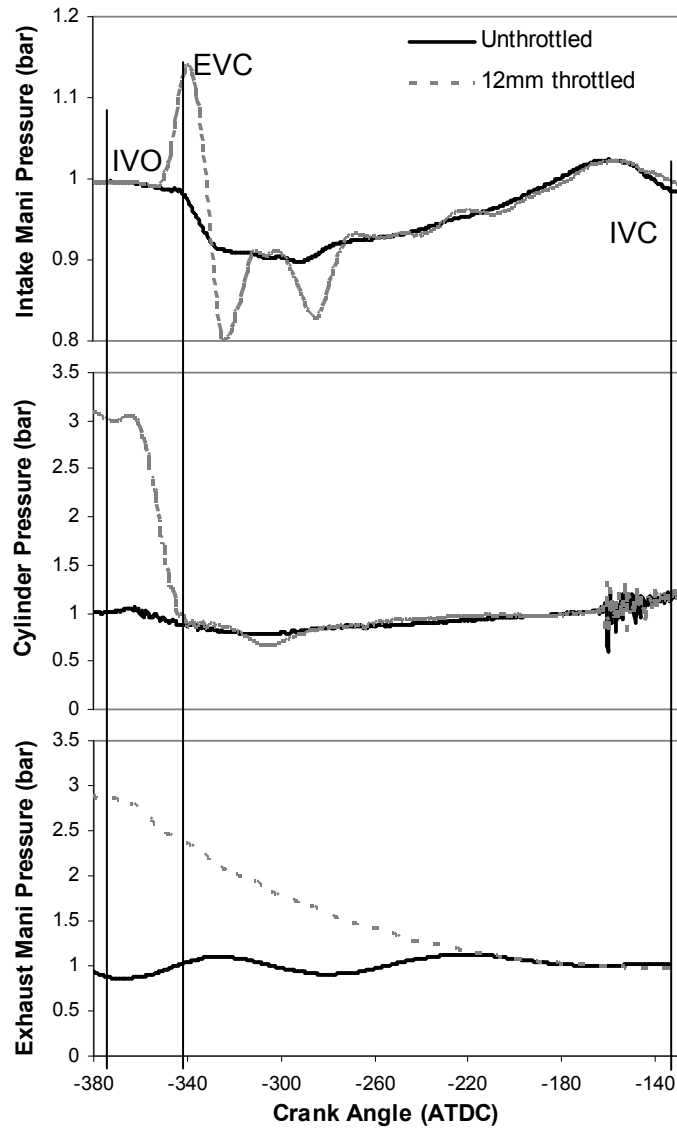


Figure A4.4 Effect of exhaust throttling on intake manifold (top), in-cylinder (middle) and exhaust manifold (bottom) pressures (absolute) during the intake valve opening period at 3000 rpm, 6 bar IMEP

#### A4.4 Comparison of model predicted RGFs with experimental results

A 1-D engine model built using Ricardo WAVE was adopted to simulate the performance of the single cylinder engine. In the model, the environment conditions were set to the ambient pressure and temperature measured during the engine tests. The piping geometry was modelled equivalent to the research engine, including surface roughness and estimated heat transfer coefficients. Experimentally-determined valve lift profiles and flow coefficients were used to simulate the gas exchange processes. The heat release profiles obtained from experiments were fed into the model for the combustion process simulation. Different throttle plates were

simulated using the 'Orifice' component by changing the junction diameters at the proper position in the model.

Intake manifold pressures were compared between the model prediction and measurements to verify the model. The model predictions agree reasonably well with the measurements, as shown in Figure A4.5.

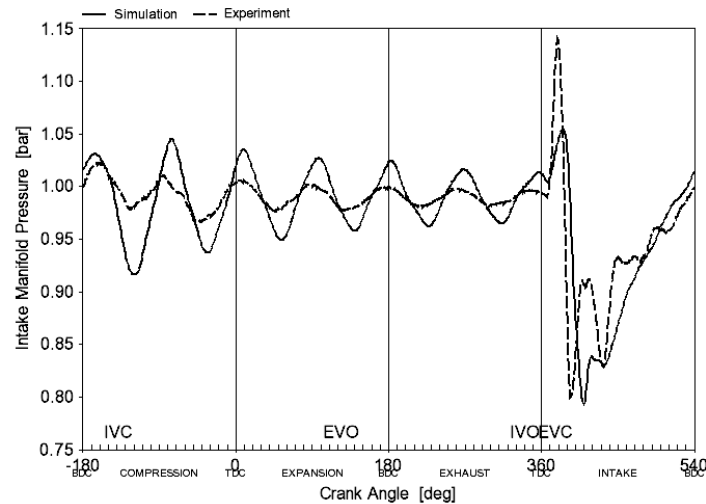


Figure A4.5 Comparison of intake manifold pressure between engine model prediction and measurement at 3000 rpm 6 bar IMEP condition with 12 mm orifice diameter throttling in exhaust

Figure A4.6 shows the comparison of the experimental and simulation results of RGF vs. EBP for both the 3000 rpm operating conditions. The simulation and the measurement results show similar slopes for EBPs lower than 1.8 bar. The fact that measured RGFs are higher than the predictions in this EBP range is thought to be due to the volume between the exhaust valve and the sampling probe. The exhaust gas trapped in this volume biases the measurement of the first motoring cycle CO<sub>2</sub> concentrations. A shorter distance between the exhaust valve and sampling probe could help to overcome this problem. For the smallest throttle diameter (EBP over 1.8 bar), the measurement RGFs were lower than the simulated ones, due to the high EBP causing larger pressure fluctuations, which influenced the NDIR sampling chamber. This meant that only a relatively short period of 'effective' CO<sub>2</sub> concentrations (shown in Figure 6.2) was available for measurement, reducing the accuracy and potentially biasing these high back-pressure results. However, over the range of back-pressures likely to be encountered in a conventional application, the simulation and experimental results show strong similarities: this suggests that either method could be used in future experiments to provide an estimate of the effect of a change of EBP on RGF.

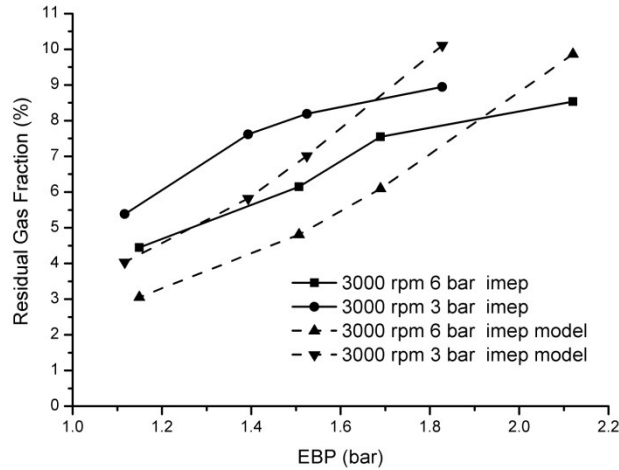


Figure A4.6 Comparison of RGFs between model predictions and measurement results at 3000 rpm cases

The contributions of different sources of RGF have been calculated through post-processing the simulation results, as shown in Figure A4.7. During the early stage of the valve overlap period, the cylinder pressure was higher than both intake and exhaust pressures and there was backflow from the cylinder to the intake manifold, as well as flow from the cylinder to the exhaust. As the intake valve opened, the cylinder pressure dropped; once it was lower than the exhaust pressure, back-flow from the exhaust to the cylinder occurred until the exhaust valve closed. The combustion products that flowed back to the intake manifold were re-induced later during the intake stroke. As expected from the analysis of the intake, exhaust, and in-cylinder pressures in Figure A4.4, the back-flow of exhaust gas from the exhaust to the cylinder and to the intake manifold played important roles in the observed increase in RGF with increased back pressure.

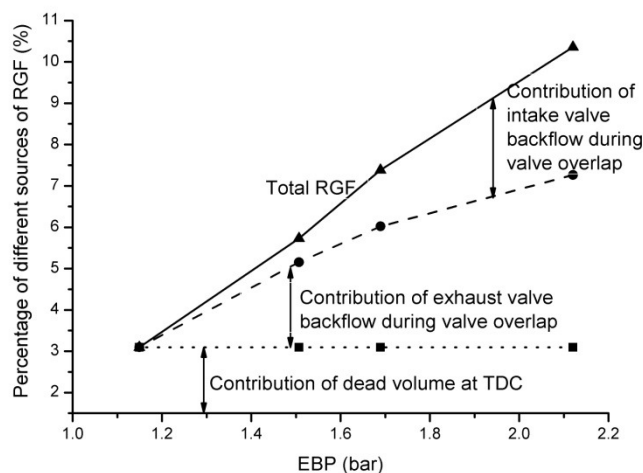


Figure A4.7 Breakup of the sources of RGF for 3000 rpm 6 bar IMEP operating condition

#### **A4.5 Discussion**

RGF in conventional diesel engines is often treated as negligible due to its small effect on the combustion processes. However, with the application of advanced engine combustion techniques and aftertreatment systems, the exhaust back pressure is unavoidably increased, which consequently increases the pumping work and the RGF. When the RGF is increased sufficiently, it influences the ignition delay and combustion phasing.

The method of RGF measurement presented in this paper is based on a naturally-aspirated engine. Theoretically, the method is applicable to a boosted multi-cylinder engine as well.

Advanced engine combustion patterns such as HCCI and low temperature combustion (LTC) are more sensitive to the charge thermal condition and composition. Thus, the variance in RGF needs to be considered carefully for its thermal and dilution effects on the combustion behaviour. So, an accurate measurement of RGF that does not involve in-cylinder sampling is essential to understand the combustion processes better.

#### **A4.6 Conclusions**

A novel method of diesel engine residual gas fraction measurement has been proposed in this work that uses exhaust manifold CO<sub>2</sub> concentration measurements during skip firing processes. The conclusions are as follows:

- 1) Throttling the exhaust flow at constant intake pressure demonstrates that the RGF is almost linearly related to the EBP values. The rate of increase in RGF with EBP is independent of engine speed, but depends on load.
- 2) Increasing the EBP at constant intake manifold pressure results in significant back-flow of the burned gases into the intake manifold due to the higher in-cylinder pressure at IVO. Back-flow from the exhaust to the intake during the valve overlap also contributes to the increased RGF.
- 3) At low load operating conditions, the increasing exhaust throttling increases RGF more than at high load conditions. This is due to the higher density of the residual gases at these conditions, due to the lower post-combustion temperatures.



#### **A4.7 References**

Beatrice C, Avolio G, Guido C (2007). Experimental Analysis of the Operating Parameter Influence on the application of Low Temperature Combustion in the Modern Diesel Engines. *SAE Paper*: 2007-01-1839.

Cho H, Lee K, Lee J, Yoo J, Min K (2001). Measurements and Modeling of Residual Gas Fraction in SI Engines. *SAE Paper*: 2001-01-1910.

Davis PW, Peckham MS (2008). Cycle-by-Cycle Gasoline Engine Cold Start Measurement of Residual Gas and AFR Using a Fast Response CO&CO<sub>2</sub> Analyzer. *SAE Paper*: 2008-01-1649.

Ford R, Collings N (1999). Measurement of Residual Gas Fraction using a Fast Response NO Sensor. *SAE Paper*: 1999-01-0208.

Francqueville Ld, Thirouard B, Ricordeau V (2006). Measurement of Residual Gas Fraction Using IR Absorption. *SAE Paper*: 2006-01-3337.

Heywood JB (1988). *Internal Combustion Engines Fundamentals*. edn. McGraw-Hill.

Liu Y, Ali A, Reitz RD (2004). Simulation of Effects of Valve Pockets and Internal Residual Gas Distribution on HSDI Diesel Combustion and Emissions. *SAE Paper*: 2004-01-0105.

Masoudi M, Zink U, Then P, Cash T, Thompson D, Heibel A (2000). Predicting Pressure Drop of Wall-Flow Diesel Particulate Filters -Theory and Experiment. *SAE Paper*: 2000-01-0184.

Ogawa H, Li T, Miyamoto N (2007). Characteristics of Low Temperature and Low Oxygen Diesel Combustion with Ultra-high Exhaust Gas Recirculation. *Int. J. Engine Res.* **8**: 365-378.

Sutela C, Hands T, Collings N (2001). Intake Manifold Burned Gas Backflow Measurements. *Proceedings. JSAE Annual Congress* **36-01**: 9-12.

Williams AM, Garner CP, Binner JGP (2008). Analysis and Optimization of Gel-cast Ceramic Foam Diesel Particulate Filter Performance. *Proceedings of the Institution of Mechanical Engineers, Part D: Journal of Automobile Engineering* **222(11)**: 2235-2247.